Film condensation heat transfer of low integral-fin tube.

Masuda, Hiroshi

FILM CONDENSATION HEAT TRANSFER
ON
LOW INTEGRAL-FIN TUBE

BY

HIROSHI MASUDA

THESIS SUBMITTED FOR THE DEGREE OF

DOCTOR OF PHILOSOPHY

TO THE UNIVERSITY OF LONDON

DEPARTMENT OF MECHANICAL ENGINEERING

QUEEN MARY COLLEGE

UNIVERSITY OF LONDON

JULY 1985

ABSTRACT

For condensation on horizontal low-finned tubes, the dependence of heat-transfer performance on fin spacing has been investigated experimentally for condensation of refrigerant 113 and ethylene glycol. Fourteen tubes have been used with inside diameter 9.78 mm and working length exposed to vapour 102 mm. The tube had rectangular section fins having the same width and height (0.5 mm and 1.59 mm) and with the spacing between fins varying from 0.25 mm to 20 mm. The diameter of the tube at the fin root was 12.7 mm. Tests were also made using a plain tube having the same inside diameter and an outside diameter equal to that at the root of the fins for the finned tubes. All tests were made at near atmospheric pressure with vapour flowing vertically downward with velocities of 0.24 m/s and 0.36 m/s for refrigerant 113 and ethylene glycol respectively. Optimum fin spacings were found at 0.5 mm and 1.0 mm for refrigerant 113 and ethylene glycol respectively. In earlier experiments for steam using the same tubes, the optimum fin spacing was found to be 1.5 mm. Maximum enhancement ratios of vapour-side heat-transfer coefficient (vapour-side coefficient for a finned tube / vapour-side coefficient for a plain tube, for the same vapour-side temperature difference) were 7.5, 5.2 and 3.0 for refrigerant 113, ethylene glycol and steam respectively.

Enhancement phenomena have also been studied theoretically. Consideration has been given to a role of surface tension forces on the motion and configuration of condensate film. On the basis of this study, several semi-empirical equations, to predict heat-transfer performance, have been obtained. These are considered to represent recent reliable data (present and other recent works) satisfactorily.

ACKNOWLEDGEMENTS

The author is deeply indebted to Dr. J.W.Rose, who initiated the project, for his supervison, guidance and helpful advice during the course of this work.

Thanks must also go to Dr. M.Nigtingale for his generous guidance in usage of the computer program for "curve fitting".

Thanks are due to the technicians of the Mechanical Engineering Department, in particular to Mr. M.Greenslade whose positive involvement in this project is gratefully acknowledged.

The author also wishes to thank all his colleagues in the mechanical Department for the helpful and friendly atmosphere which they generated.

The generosity of Mitsubishi Electric Corp. in granting sabbatical leave is gratefully acknowledged.

LIST OF CONTENTS

LIST OF SYMBOLS

A_b	Surface area of interfin space on tube surface
A_f	Surface area of fin flanks
A_p	total surface area
A_s	Cross-sectional area of test section in the apparatus
$\tilde{a}$	Constant for 'Sieder-Tate type' equation
$\tilde{b}$	Constant for 'Nusselt type' equation
c_{p_c}	isobaric specific heat-capacity of coolant at T_c
c_p	isobaric specific heat-capacity of condensate at T^*
d_i	inside tube diameter
d_r	outside tube diameter of plain tube and diameter at the fin root of finned tube
E	Enhancement ratio of vapour-side heat-transfer coefficient for the same temperature difference
E_{cal}	calculated enhancement ratio
E_{obs}	Enhancement ratio determined from experimental data
g	specific force of gravity
h	fin hieght, R_o-R_r
h_o	height of liquid "wedge" on fin flank measured from base of tube
h_{fg}	specific enthalpy of evaporation
k	thermal conductivity of condensate
k_c	thermal conductivity of coolant
k_t	thermal conductivity of tube material
L	average vertical height of fin flank
ℓ	length of condensation tube exposed on vapour
LMTD	overall log-mean temperature difference
m_c	mass flow rate of coolant
m_v	mass flow rate of vapour
Nu_c	coolant-side Nusselt number, $Qd_r/\Delta T_c k_c = Q_i d_i/\Delta T_c k$
Nu_v	vapour-side Nusselt number, $Qd_r/\Delta Tk$

p	pitch of fin
P	pressure of vapour
P_c	pressure in condensate film
Pr_c	coolant Prandtl number
$Psat(T)$	saturation pressure at T
Q	heat flux based on outer surface, $Q/\pi d_r \ell$
Q_c	heat-transfer rate to coolant
Q_h	power input to boiler
Q_i	heat flux based on inner surface, $Q_c/\pi d_i \ell$
Q_{loss}	thermal loss from the apparatus
r	radius of liquid "wedge"
R_e	coolant Reunold number, $u_c \rho_c d_i/\mu_c$
R_r	radius at fin root
R_w	thermal resistance in tube wall
t	fin thickness
T_c	coolant mean temperature, $(T_{in}+T_{out})/2$
T_{in}	inlet coolant temperature
T_{out}	outlet coolant temperature
T_s	coolant saturation temperature
T_v	vapour temperature
T_w	outside wall temperature
T_{wi}	inside wall temperature
T^*	mean condensate temperature, $2/3\ T_w + 1/3\ T_v$
U	overall heat-transfer coefficient, Q/LMTD
u	component of condensate flow velocity
u_c	coolant velocity
v	component of condensate flow velocity
v_v	vapour velocity
w	component of condensate flow velocity
W_s	mass fraction of non-condensing gas

x length in x-coordinate deirction

X_e length of liquid "wedge" on tube surface between fins

y length in y-coordinate direction

z length in z-coordinate direction

Greek symbols

α heat-transfer coefficient

α_b heat-transfer coefficient given by Nusselt equation for horizontal plain tube

α_f heat-transfer coefficient for fin flank

α_L heat-transfer coefficient given by Nuuselt equation for vertical plain plate, heat-transfer coefficient for flooded region in Owen et al. [42] theory

α_t heat-trasfer coefficient for fin top

α_c coolant-side heat-transfer coefficient

α_v vapour-side heat-transfer coefficient

δ condensate film thickness

ΔT vapour-side temperature difference, $T_v - T_w$

ΔT_c coolant-side temperature difference, $T_{wi} - T_c$

ξ area ratio of finned tube to plain tube

η fin efficiency

θ a half angle of fin tip

μ viscosity of condensate at T^*

μ_c viscosity of coolant at T_c

μ_w viscosity of coolant at T_{wi}

ρ condensate density at T^*

ρ_c coolant density at T_c

σ surface tension of condensate at T^*

σ_c surface tension of coolant at T_s

ϕ angle from top of tube

ϕ_f angle from top of tube at which interfin space becomes full of condensate

LIST OF FIGURES

* CHAPTER 4

LIST OF TABLES

CHAPTER 1 INTRODUCTION

1. Introduction

Condensation on finned tubes is a complex phencmenon involving surface tension-influenced three-dimensional flow of the condensate film. Evaluation of the effective surface heat-transfer coefficient, either theoretically or by correlation of experimental data, is complicated on account of the large number of variables involved.

For horizontal finned tubes, Beatty and Katz [29] performed experiments using different geometries of tubes and fins and found that the enhancement of vapour-side heat transfer, relative to a smooth tube, achieved values higher than the corresponding surface area increase due to finning. They also proposed a theoretical expression based on the Nusselt analysis for the tube in the interfin space and for the vertical fin surfaces. Since then several experimental works have broadly supported their observation. However other data including recent studies at Queen Mary College, and particularly data for steam, agreed less well with the prediction of the Beatty and Katz model.

Later theoretical studies, following Gregorig [7], have considered the effect of surface tension on the motion of the condensate film. More recently attention has been drawn to the effect of "flooding" between fins on the lower part of tube also due to surface tension. Several models including these phenomena have been proposed. However there is as yet no satisfactory model for predicting the heat-transfer performance of finned tube.

Reliable experimental data, from investigations in which the important variables are systematically studied, are of vital importance to the development of a successful model. In the present work, experiments have been conducted in which refrigerant 113 (R-113) and ethylene glycol have been condensed on fourteen horizontal finned tubes having the same diameter, fin height and thickness. The fin spacing varied from 0.25 mm to 20 mm. For comparison, data were also obtained using a plain tube with diameter equal to that at the fin root for the finned tube. The heat flux and vapour-side temperature difference were determined for a range of coolant flow rates. The velocity of the vapour, which flowed vertically downwards on the tubes, was also determined. Care was taken to achieve high experimental accuracy and, in particular, to avoid errors due to the presence in the vapour of non-condensing gases or to the occurrence of dropwise condensation.

For both fluids, the heat-transfer enhancement was found significantly to exceed that which might have been expected on grounds of increase in surface area due to finning. For both fluids an optimum fin spacing was found in the range tested. The enhancement ratios (finned tube heat-transfer coefficient divided by that of the plain tube) were higher for the lower surface tension fluid (R-113) and the optimum fin spacing was smaller for this fluid. These trends are in good accord with earlier data for steam, where the condensate has a higher surface tension than ethylene glycol and the enhancement ratio was lower.

Theoretical studies, and attempts to correlate the data using dimensional analysis, have also been carried out as part of the present investigation, with the objective of providing improved expressions for predicting the heat-transfer performance of horizontal finned tube. Theoretically-based equations have been obtained which are considered to represent the more recent reliable data (present and other recent data) more satisfactorily than earlier models.

CHAPTER 2 LITERATURE SURVEY

2. Literature survey

2.1 Methods of heat-transfer augmentation in condensation

Substantial efforts to achieve higher condenser performance and reduced size, i.e. space occupied and weight, for the same duty, have been made in recent years. Techniques for heat-transfer augmentation on the vapour side have been categorised into two groups, i.e. active and passive techniques. Active techniques require an external agency, such as electric or acoustic field, or vibration, while passive ones employ special condensing surface geometries or additives. So far, the passive techniques have recieved most attention because of their lower cost and the complexity of active techniques.

Dropwise condensation (a passive technique) offers the prospect of highest heat-transfer enhancement. For condensation of steam, the vapour-side heat-transfer coefficient can exceed that of film condensation by a factor of around 20. However, this passive enhancement technique has not been used industrially to any significant extent owing to the difficulty of ensuring in practice that the dropwise mode persists throughout the lifetime of the condenser. Moreover, dropwise condensation can only be obtained with a few high-surface tension fluids.

Since for filmwise condensation, the dominant thermal resistance is that of the condensate film, a surface geometry which promotes reduced film thickness will provide heat-transfer enhancement. For this purpose, many kinds of surface geometries have been used.

Before discussion in detail of the use of low-fin tubes, enhancement techniques with other surface geometries are briefly reviewed.

(1) <u>non-wetting strips</u> :

Brown and Martin (1971) [1] made an analytical study of condensation on a vertical plain surface with vertical non-wetting ptfe strips. They concluded that the thining of the condensate film near the ptfe surface could lead to vapour-side heat-transfer coefficient 2 to 5 times higher than the values of the Nusselt prediction for the same heat flux. The enhancement was dependent on the liquid contact angle with the ptfe and the thermal conductivity of the metal.

Cary and Mikic (1973) [2] analysed the same problem using a different model. They suggested that the enhancement might be due to the Marangoni effect; the liquid surface tension for the thinner condensate film near the ptfe-metal interface, being lower than elsewhere owing the higher temperature, causes the secondary flow. The analysis predicted up to about 80 % increase in heat-transfer coefficient for the same heat flux.

Glicksman et al.(1973) [3] performed condensation tests for steam on a horizontal copper tube , 12.7 mm in diameter, fitted with non-wetting ptfe tapes, 3.2 mm wide and 0.16 mm thick. For helically wound strips, the results showed a maximum increase in heat-transfer coefficient by 35 % over that for the plain tube for the same vapour-side temperature difference for wrapping with pitch/diameter=3. For a single axial strip positioned along the bottom of the tube, The maximum increase 50 % was observed.

(2) <u>Roughness</u> :

Nicol and Medwell (1965) [4] theoretically investigated heat-transfer enhancement due to a closely-knurled surface roughness for a condensate film flowing down a vertical surface. The flow was divided into three regions:- an hydraulically smooth regime, a transition regime and a fully developed rough regime. Theory showed that the benefit of roughness was characterized by the "roughness Reynolds number". They conducted experiments condensing steam on a vertical tube, 50 mm in diameter and 1.8 m in length, with several different surface roughnesses varying in height up to 0.5 mm. Thermocouples located in the tube wall were used to determine the surface temperature. Ratios of local surface heat-transfer coefficient for the knurled surface to the plain tube ranged from 1.4 to 4.2. The experimental results offered suport for their theory. Despite the large enhancement reported no follow-up work on such surfaces has been apparently undertaken.

Webb [5] reported that Notaro (1979) [6] investigated an enhancement technique which consisted of an array of small diameter metal particles 0.25 to 1.0 mm high bonded to the condensing surface, covering 20 to 60 % of the tube surface. The tests were made for steam using 6 m long vertical tube having 50 % of area covered by 0.5 mm diameter particles. The vapour-side heat-transfer coefficient was reported to be 17 times higher than that predicted by the Nusselt equation. There has been, however, no report of suport for Notaro's results so far.

(3) <u>Vertical fluted tube</u> :

Gregorig (1954) [7] suggested a method of using surface tension forces to enhance laminar film condensation on a vertical surface. It was noted that the combination of convex and concave condensate surface as shown in Fig.2-1 would establish a suface-tension-induced pressure gradient, drawing the condensate from the convex into the concave region, and in consequence, a thin film would be formed on the convex surface. Gregorig's analysis gave the surface profile for which the film thickness over the convex surface would be uniform.

Following [7], other investigators [8,9,10,11,12,13] have made theoretical studies along the same general lines aimed at predicting optimum surface profiles.

Carnavos (1965) [14] gave experimental data for steam using internally and externally fluted tube, nominal 81 mm O.D. and 3 m high. Enhancement ratios of vapour-side heat-transfer coefficient of around 5 were obtained for the same heat flux.

Cooper and Rose [15] reported that Combs (1978) [16,17] performed experiments for ammonia, R-11, R-21, R-22, R-117, R-114, R-115 and R-600 using three fluted tubes with outside-diameter of 8.26 mm, 9.75 mm and 12.7 mm and with 48, 24 and 60 flutes respectively. For comparison, a plain tube with outside diameter of 7.98 mm was used. It was found in all cases that fluted tubes were significantly better than the plain tube in heat transfer. The ratio of heat transfer for fluted tubes to that of the plain tube for the same heat flux was in range of 4 to 7 in the case of ammonia and for other fluids, in the range of 2 to 7. These values exceeded the surface area increase due to the fluting.

(4) <u>vertical wire</u> :

Thomas (1968) [18] found that similar enhancenent to that provided by vertical fluted surfaces, could be obtained by loosely attached vertical wires spaced on a vertical surface. Seven wires with different sizes, including two different shapes (cylindrical and rectangular) were tested on a vertical tube which was 12.7 mm O.D. and 1.08 m long. The rectangular shape wires were found to increase the condensation rate by a factor of more than 9, somewhat greater than circular cross-section wire. A simple correlating equation for the vapour-side heat-transfer coefficient was given.

Rifert and Leont'ev (1976) [19] performed experiments using cylidrical cross-section wires with different diameters. It was found that the enhancement ratios ranged 3 to 6 and that augmentation decreased with increasing heat flux. A theoretical approach, in which the condensate film flow between wires was governed by gravity and surface tension forces, was also made.

Thomas et al. (1979) [20] performed condensation tests for anmonia on a helically-wire-wrapped smooth vertical tube. The measured vapour-side heat-transfer coefficient was found to be approximately 3 times higher than that predicted by the Nusselt equation.

(5) <u>Other fin types</u> :

Arai et al. [21] investigated experimentaly a "saw-toothed" fin (shown in Fig.2-2) having a notch depth approximately 40 % of the fin height and small thickness at the fin tips. The commercially available surface, known as "Thermoexcel-C", having 13.8 fins/cm and 1.2 mm in height was found to give 50 % increase of condensation rate for R-113, as compared with the same fin geometry but without the grooved fin tips.

Webb and Gee (1979) [22] concluded that significant enhancement could be achieved with "spine-fins" having a three-dimensinal configuration shown in Fig.2-3. The resulting analytical prediction, based on Nusselt theory, indicated a reduction of fin material of about 60 % for equal condensing duty when considering R-11 and R-22 as working fluids. Webb, Keswani and Rudy (1983) [23] performed experiments condensing R-12 on spine fins extended on a vertical plate, with fins 1.0 mm high and 0.3 mm square in a uniformly-spaced square array with a surface density of 15137 fins per square meter. The heat-transfer performance was found to be 3 times higher than that predicted by the Nusselt equation. Webb et al.[23] also gave an analytical model which included the effect of surface tension force and agreed with their experimental data to within 10 %.

Nader (1978) [24] gave a theoretical solution for condensation on a plane-sided vertical fin attached to a horizontal tube at its lower end. The interaction of conduction within the fin and condensation on the fin surface was considered in the model.

Patanker and Sparrow (1979) [25] analysed film condensation on a vertical fin attached to a vertical plate or a vertical tube. Their model also included conduction within the fin. In the model, temperature variation across the thickness of fin was neglected but those along the width and the height of the fin were considered. It was concluded that the heat transfer on the fins would be significantly lower than that predicted by the Nusselt model, i.e. an isothermal fin model.

Mori et al. (1979) [26,27] investigated experimentally the vertical finned plates using R-113 with the plates of 50 mm or 25 mm height and 50 mm width having equilateral triangular fins of 0.87 mm height and 1.0 mm or 0.5 mm pitch. It was found that the heat flux based on the projected area of the test surface were 5 times higher than that predicted by the Nusselt equation. The analytical model was made for three types of the finned plates shown in Fig.2-4. The surface tension forces were assumed to play an important role in withdrawing the condensate on the fin tips and flanks into the groove. It was stated that the triangular and wavy fins performed similarly, while the flat bottom groove gave the best heat-transfer performance. Further, the higher performance was given by the smaller tip angle, i.e parallel sided-fins gave the highest heat-transfer coefficient. Mori et al. (1980) [28] later investigated the effect of the flat bottom groove. Experiments were conducted simulating the film flow in the groove, shown in Fig.2-5, using ethanol. The measurements of the distribution of film thickness were made by utilizing the reflection of striped light beams on the liquid surface. It was found that the film was thinned locally, as shown in Fig.2-5. Flow visualization using aluminum powder indicated that liquid between edges was withdrawn into the wedge. These phenomena were analysed with a physical model in which the surface forces as well as gravity governed the film flow. Good agreement was found with the experimental data. It was mentioned that there would exist an optimum fin spacing for the flat bottom groove.

2.2 Horizontal low-fin tubes

Low integral-finned tubes have found wide commercial acceptance for condensation on horizontal tubes. These tubes permit higher condensation rates than plain tubes and this may yield advantage in reducing the size, weight and cost of the condensers. Finning increases the effective area for heat transfer and can provide a substantially higher heat-transfer coefficient. Augmentation of heat transfer due to finning has been supported by many experimental works. However, the enhancement mechanism is still not fully understood, despite significant research effort in recent years.

2.2.1 Experimental works of horizontal low-fin tube

Beatty and Katz (1948) [29] performed condensation tests on horizontal tubes with six different fluids:- methyl chloride, sulphur dioxide, R-22, propane, n-butane, and n-pentane using seven different finned tubes, and one plain tube. The dimensions of finned tubes are given in the Table 2-1. Preliminary observations were made to determine the range of temperature and pressure over which satisfactory measurements were possible. In all cases, the mean temperature of condensing vapour was maintained constant with range of 37 °C to 76 °C. Duplicate runs were made at each coolant velocity to assess possible effect of non-condensing gases. During operation, visual observations were made through the sight glasses. Since the vapour-side heat-transfer coefficients were determined by using the "Wilson plot" method, measurements for each tube were made at four or five different coolant rates. Only one fluid (R-22) was used with the plain tube, so that there is no direct measurement of enhancement for the other fluids, except by comparing with theoretical values given by the Nusselt theory. Table 2-1 shows the results of measurements for R-22. It is seen that the heat-transfer enhancement ratios for the finned tubes are larger than increase of surface area due to finning.

Katz et al. (1948) [30] investigated condensation on six finned tubes in a vertical row for R-12, n-butane, acetone and water using a finned tube which had fins of 15.6 mm in root diameter, 1.56 mm in fin height and 0.48 mm in the average fin thickness. The fin density was 15 fins per inch. The same procedure as described in [29] was made. Measurements were made at five coolant flow rates. The vapour-side heat-transfer coefficient was determined by the "Wilson plot" method. It was found that the average vapour-side heat-transfer coefficient was only 10 % below that of the top tube except water, where dropwise condensation was observed and no decrease in heat-transfer coefficient was found. Comparison was made with the Beatty and Katz [29] prediction (described in the next section) modified using Nusselt's model for tubes in a vertical raw. The prediction underestimated the average vapour-side heat-transfer coefficient for all tubes by a factor of 1.25 to 1.5.

Pearson and Withers (1969) [31] performed experiments for R-22. The water-cooled condenser (" 40 tons capacity ") had 60 copper tubes of length 1.8 m. Tests were carried out using finned tubes with 26 fins per inch and with 19 fins per inch. In both cases the root diameter was 15.8 mm, the fin height and thickness were 1.42 mm and 0.31 mm. Data were obtained at two levels of condenser duty, around 167 kW and 111 kW, and several runs at each duty level covered a range of water flow and inlet water temperature. The apparatus was operated to maintain a constant condenser pressure such that the saturation temperature was 58 °C+0.5 K. Care was taken to purge air from the system. The data were analized by a "modified Wilson plot" method. It was stated that the heat-transfer rate was 25 % higher for the tubes with high density. It was reported that the Beatty and Katz model (described in the next section) predicted the experimental results satisfactorily.

Mills et al. (1975) [32] performed experiments on a single tube with 36 threads per inch American standard screw thread cut on 0.75 in outside diameter tube. The effect of tube material was investigated using tubes of copper, brass and cupro-nickel. Thermocouples located in the tube wall were employed to determine the surface temperature. The measurements were made with steam under saturation conditions at temperatures between 301 K to 327 K. Vapour-side temperature differences were found between 1 K and 10 K. The enhancement ratios were between about 2.5 and 5.5 for the same vapour-side temperature difference. The enhancement was found to increase with the thermal conductivity of the tube metal. The highest enhancement ratios occured at lowest temperature differences. At the highest temperature differences, more typical of practical steam condensers, the enhancement ratio was around 2.5 to 3.0 (see table 2-2).

Carnavos (1980) [33] conducted experiments condensing saturated R-11 vapour at 35 °C on twelve different single horizontal copper tubes, including a plain tube, and low-fin tubes, as well as a fluted tube, a pin-fin tube and a pin-fluted tube. The choice of R-11 as the working fluid was based on the ability to operate close to atomospheric pressure to permit positive venting and exclusion of non-condensing gases during operation. Operation was in the reflux mode without continuous venting of vapour. At the maximum heat flux of 40 kW/m^2, the approach velocity of the vapour to the tube was 0.022 m/s and condensation was considered to be unaffected by vapour shear. Noncondensing gases were considered to be at a statisfactorily low level when the vapour temparature, as determined by a thermometer located above the condensing tube, and the saturation temperature at test section pressure, were within 0.25 K. Comparison of heat flux between tubes was made for the same overall logarithmic mean temperature difference. Only two different values were used for each tube by employing two different coolant temperatures. The condensing heat-transfer coefficients were also shown as a function of the vapour-side temperature difference. The results are given in Table 2-3 (as rearranged by Cooper and Rose [15]). The fluted tube (N-2) appeared to be best with enhancement ratios of 5.6 and 4.6 at vapour-side temperature differences of 2.5 K and 4 K respectively. For this tube, which has an area ratio of 2.15, the enhancement is significantly greater than the increase of surface area. The data for low-fined tubes tested with fin spacing between 0.36 mm and 0.59 mm indicate that wider fin spacing gives better performance. However, it should be noted that the fin height and thickness were different for different tubes.

Honda et al. (1983) [34] conducted experiments condensing R-113 and methanol on three different low-fin tubes and a saw-tooth-shaped fin tube fitted with wall thermocouples at angles from top of 0°, 90°, 135° and 180°. Care was taken to ensure that the apparatus was leak tight. Prior to the experiment, non-condensing gas was removed from the vapour loop by a vacuum pump. During the experiments, the pressure was kept above atmospheric. Agreement between the saturation temperature at the measured vapour pressure and the measured vapour temperature were within 0.1 K. The saturation vapour temperature was kept between 321 K and 334 K for R-113 and between 338 K and 349 K for methanol. The maximum value of the enhancement of vapour-side heat-transfer coefficient for the same temperature difference was 9.0 for R-113 and 6.1 for methanol. Table 2-4 shows their results at vapour-side temperature difference of 5 K. In addition, the measurements of the distribution of temperature in the tube wall and the film thickness at the middle point between fins in circumferential direction were made. It was found that the temperature and film thickness varied significantly around the tube. In the cases of the film thickness the rate of increase became rather sharp at a particular angle around the tube.

Yau, Cooper and Rose (1983) [35,36,37] conducted the experiments with condensation of steam on horizontal finned tubes. Thirteen tubes were used with rectangular section fins having the same width 0.5 mm and height 1.59 mm (*) and with fin spacing, 0.5, 1, 1.5, 2, 4, 6, 8, 10, 12, 14, 16, 18 and 20 mm. For comparison, tests were made using a plain tube having the same inside diameter 9.78 mm and an outside diameter equal to that at the root of fins for the finned tubes, i.e. 12.7 mm. All tests were made at near

(*) note that 1.0 mm was missreported for the fin height in [35].

atmospheric pressure, with vapour flowing vertically downwards with velocities of about 0.5, 0.7, and 1.1 m/s. Care was taken to expel the non-condensing gases and to avoid dropwise condensation. The mass fraction of non-condensing gas (taken to be air) as estimated from the pressure and temperature measurements was ±0.005, i.e. zero to within the precision of the determination. The maximum enhancement of vapour-side heat-transfer coefficient for the same heat flux (500 kW/m^2)was found to be around 3.6 for the tube with a fin spacing of 1.5 mm. The enhancement ratio increased with decreasing fin spacing from 20 mm to 1.5 mm but decreasing for fin spacing less than 1.5 mm.

Wanniarachchi et al. (1984) [38,39] performed tests at atmospheric pressure and at 11 kPa using single finned tubes, 1 mm in fin height and 1 mm in fin thickness, and a plain tube. The fin spacings used were 0.5, 1.0, 1.5, 2.0, 4.0 and 9.0 mm. The diameter at the root of fins was 19.0 mm and the internal diameter was 12.7 mm. The tubes were tested under vertical downwards steam flow with a velocity of approximately 1 m/s when operating at atomospheric pressure, and 2 m/s when operating at 11 kPa. The Gibbs-Dalton ideal-gas mixture relations were used to compute the non-condensing gas (assumed to be air) concentration. The computed air concentration was estimated as in [35,36,37] be within 0.5 %; i.e. zero to within the accuracy of measurements. The maximum enhancement ratios of the vapour-side heat-transfer coefficient for the same heat flux (*) (1000 kw/m^2 and 350 kw/m^2) were around 5.5 and 3.5 at atmospheric and lower pressure respectively and occured at a fin spacing of 1.5 mm as found by Yau et al. [35,36,37] for tube diameter 12.7 mm. All of the finned tubes showed heat-transfer enhancement in excess of area increase due to finning. The finned tube with the smallest fin-spacing (0.5 mm) gave a performance increase at least equal to the area increase due to finning despite the fact that the fins were almost all flooded with condensate.

Georgiadis (1984) [40] examined in more detail the effect of fin thickness and height using a total of 21 tubes with 5 fin spacings, 5 fin thicknesses and 2 fin heights as detailed in Table 2-5. The apparatus used was the same as that of Wanniarachchi et al. [38]. It was found that the heat-transfer enhancement for the same heat flux was primarily dependent on fin spacing. It was not strongly dependent on the fin thickness for the same fin spacing. For a given fin spacing and thickness increase in fin height (giving an area increase of about 50 %) increase the vapour-side heat transfer coefficient by only about 20 %.

(*) note that the heat flux was not achieved with the plain tube and the stated enhancement ratios are based on extrapolations.

Concluding remarks

As indicated above, many investigations have found that the enhancement ratios of vapour-side heat-transfer coefficient on finned tubes are higher than the increase of area due to finning. It should be noted however that the enhancement has been evaluated with different criteria. For example, Beatty and Katz [29], Mills [32], Carnavos [33] and Honda et al. [34] used enhancement values for the same vapour-side temperature difference. Yau et al. [36,37], Wanniarachchi et al. [38] and Georgiadis [40] evaluated them for the same heat flux. Care should be taken to define the enhancement, since the enhancement ratios are significantly different between two criteria as well as depending on the values of temperature difference and heat flux at which they are evaluated.

Heat transfer on finned tubes may be affected by many parameters, such as configuration of fins, properties of the condensing fluids and vapour velocity. In many studies, experiments were performed with non-systematic change of variables, e.g. fin spacing, height and thickness. Beatty and Katz [29], Carnavos [33] and Pearson and Withers [31] all used several fluids and tubes but more than one of the geometric variables were changed as the same time as the fluid. More recently Yau et al. [35,36,37], Wanniarachchi et al. [38] and Georgiadis [40] have used fewer fluids but have made a systematic study of fin dimensions from which it has become clear that fin spacing is the most important geometric variable .

2.2.2 Condensate retention

Katz et al. (1948) [30] investigated the retention of liquid between fins. Measurements under static conditions (without condensation occuring) were made using acetone, carbon tetrachloride, aniline and water with ten different finned tubes (not detailed in [30]). Results showed the portions of tubes covered by retained liquid in the range of 15 % to 90 %. However, by examining their heat-transfer data, it was concluded that the increase of retention was not reflected in decrease in heat transfer and that static liquid retention was no criterion for judging heat-transfer performance during condensation.

Recent studies have verified that condensate is retained between fins at the lower part of the tube due to surface tension forces as shown in Fig.2-6, while the conensate film elsewhere is thinned by the surface tension forces.

Rudy and Webb (1981) [41] investigated the retention angle problem using water, R-11 and n-pentane with various fin spacings. They performed experiments under "dynamic" conditions (with condensation occuring) and under "static" condition (without condensation but with liquid remaining on the tube after "dynamic" experiments). The liquid retention angles were measured by sighting through a cathetometer. Little difference between "static" and "dynamic" values was found (see Fig.2-7).

Sadesai, Owen and Smith (1982) [42] attempted to analyse the retention angle portion using a static force balance between surface tension forces and gravity. Using reasoning which is not entirely clear, they obtained the expression:

$$\phi_f = \cos^{-1}\left(\frac{4\sigma}{\rho g d_o b} - 1\right) \qquad (2\text{-}1)$$

The above equation was compared with experimental data [30,40] and good agreement was found.

Honda et al. (1983) [34] performed experiments condensing of R-113 and ethanol on finned tubes which were observed visually under both "dynamic" and "static" conditions. As in Rudy et al. [41], little difference was found between the two conditions. They also made a detailed theoretical study of the problem. The physical model and coordinates used are shown in Fig.2-6. The following force balance equations for the static condition were given:-

$$\rho g z - \frac{\sigma}{r_o} = 0 \qquad (2\text{-}2)$$

$$-\frac{\sigma}{r} + \rho g y \cos\phi = -\frac{\sigma}{r_o} \qquad (2\text{-}3)$$

$$\text{where} \quad z = R_o + (R_b + \delta_o)\cos\phi \qquad (2\text{-}4)$$

The radius of curvature r is given by:

$$r = \frac{(1+(dy/dx)^2)^{3/2}}{(d^2y/dx^2)} \qquad (2\text{-}5)$$

The boundary conditions are given as follows:-

$y=0$ and $dy/dx=0$ at $x=0$

$r=r_0=\infty$ at $\phi=\pi$

The radius of curvature was solved numerically (no detail in [34]). It was mentioned that the profile of condensate surface between the fins at its intersection with a radial plane at any angular position agreed closely with a circular arc for the tube and fin geometries used in practice. The found result for the so-called retention angle was the same as that given by Owen et al. [42] (see eq.(2-1)). Comparisons with their own experimental data and that of Rudy et al. [41] and Katz et al. [30] were good. It should be noted that careful study of the Honda et al. theory (see Chapter 5) reveals that the found result is only valid when $b \leq 2h$, where b and h are fin spacing and height.

Yau et al. (1983) [37] also conducted experiments to observe retention angles. Measurements were made only under "static" conditions using water, R-113 and ethylene glycol with finned tubes whose fin height was 1.59 mm and fin spacing varying between 0.5 mm to 20 mm. Good agreement with eq.(2-1) was found for fin spacing less than 4 mm (note that is within the range of $b<2h$).

Rudy et al. (1984) [43] analysed the same problem using an apparently simpler but rather obscure different model and obtained:

$$\phi_f = \cos^{-1}\left(\frac{2\sigma(L-t_b)}{d_o \rho g(ph-A_p)} - 1\right) \qquad (2\text{-}6)$$

where L is wetted perimeter of fin cross section,

t_b is thickness of fin at the root,

p is pitch,

h is fin height,

Ap is profile area of fin over fin cross section.

Concluding remarks

Earlier, Katz et al. [30] measured the retention angle under "static" conditions, but no analysis was made. For reasoning no effect of the condensate retention on heat-transfer performance, this problem had been neglected..

Recently, Rudy and Webb [40] performed experiments under "dynamic" and "static" conditions. It was found that there was little difference between the two conditions and that heat-transfer performance could be affected by the liquid retention. Later Honda et al. [34] also performed experiments under the two conditions and results have supported Rudy et al. conclusion.

Owen et al. [41] proposed an equation to give the retention angle, but the physical model was obscure. On the other hand Honda et al. [34] made a detailed theoretical study with force balances for the static conditions and the same expression as Owen et al. was finally given. Rudy et al. [42] analysed the same problem with a different physical model and a similar expression to that of Honda et al. was proposed.

Yau et al. [36] performed experiments under static conditions with wide range of fin spacings, 0.5 mm to 20 mm. Good agreement with the Honda et al. expression was found for $b<2h$.

2.2.3 Theoretical studies of low finned tubes

The first theoretical prediction was made by Beatty and Katz [29] in 1948. Their model was based on the Nusselt theory for a vertical plate and a horizontal tube and did not include surface tension forces. The total heat transfer was considered as the sum of the heat-transfer rate on the unfinned portion of tube and on the vertical faces of fins. This lead to a composite heat-transfer coefficient based on an equivalent surface area Ap expressed by:

$$\alpha_{BK} = \frac{A_b}{A_p}\alpha_b + \eta\frac{A_f}{A_p}\alpha_L \qquad (2\text{-}7)$$

where A_p is the unfinned surface area of the tube,

A_f is the surface area of fin sides,

$A_p = A_b + \eta A_f$ and η is the fin efficiency.

α_b and α_L are given by Nusselt theory;

for horizontal tube:

$$\alpha_b = 0.728\left(\frac{k^3\rho^2 g h_{fg}}{\mu\Delta T d_r}\right)^{1/4} \qquad (2\text{-}8)$$

for a vertical plate:

$$\alpha_L = 0.943\left(\frac{k^3\rho^2 g h_{fg}}{\mu\Delta T\ L}\right)^{1/4} \qquad (2\text{-}9)$$

where L is the average height of fin side given by:

$$L = \frac{\pi(d_o^2 - d_r^2)}{4d_o} \qquad (2\text{-}10)$$

Substitution of eqs.(2-8) to (2-10) in eq.(2-7) gives:

$$\alpha_{BK}=\alpha_b(d_r/d_{eq})^{1/4} \qquad (2\text{-}11)$$

where the equivalent diameter d_{eq} is given by:

$$\left(\frac{1}{d_{eq}}\right)^{1/4} = \frac{0.943}{0.728}\frac{A_f}{A_p L^{1/4}} + \frac{A_b}{A_p d_r^{1/4}} \qquad (2\text{-}12)$$

The theoretical expression correlated their experimental data (see in section 2.2.1) on average by about ±5 %.

In 1954, Gregorig [7] predicted the effect of surface tension on a fluted surface (see Fig.2-8). Though this work is not specifically related to horizontal low-fin tubes, it has formed the basis of subsequent analyses and is therefore reviewed briefly. Surface tension gives rise to pressure gradients in the condensate due to the varying curvature of the condensing surface. The pressure gradient produces a thin film of condensate over the convex part of the surface. Gregorig demonstrated both analytically and experimentally the benefits to be gained from fluting a vertical condenser surface. The effect of gravity on the condensate flow was neglected in comparison to that of the surface tension forces, so that the flow was two-dimensional. The condensate flow was assumed laminar. The force momentum balance equation was given by:

$$\frac{dp}{ds} = -3\mu\frac{v}{\delta^2} \qquad (2\text{-}13)$$

where the pressure gradient due to surface tension was given by:

$$\frac{dp}{ds} = \sigma\frac{d}{ds}(r^{-1}) \qquad (2\text{-}14)$$

The mass and energy balance equations were given by:

$$m = \rho v \delta \qquad (2\text{-}15)$$

$$\frac{dm}{ds} = \frac{k\Delta T}{h_{fg}} \frac{1}{\delta} \qquad (2\text{-}16)$$

where r is radius of curvature of condensate film,

v is average velocity of condensate flow,

m is mass flow rate per length of film,

s is distance along the profile.

Fig.2-8 shows the coordinates and parameters used in the calculation.

The above equations lead to the following expressions:-

$$\frac{1}{r} = -\int \frac{3\mu m}{\delta^3 \sigma \rho} ds \qquad (2\text{-}17)$$

$$m = \int \frac{k\Delta T}{h_{fg}\delta} ds \qquad (2\text{-}18)$$

In addition, the film thickness was geometrically defined as:

$$\delta = \int_0^s (\theta - \psi) ds \qquad (2\text{-}19)$$

$$\text{where} \quad \theta = \int_0^s R^{-1} ds$$

$$\psi = \int_0^s r^{-1} ds$$

The set of formulae (2-17) to (2-19) were numerically integrated and solved for the film thickness in terms of distance along the surface for a given profile of a fluted surface. Substituting eq.(2-18) into eq.(2-17) leads to:

$$\frac{1}{r} = -\frac{3\mu k\Delta T}{h_{fg}\sigma\rho}\int_0^s\int_0^s \frac{ds}{\delta}\ \frac{ds}{\delta^3} + C \qquad (2\text{-}20)$$

On the basis of the above equation, Gregorig proposed a surface profile which would give a constant film thickness over the convex arc of length S_1. Since $\alpha = k/\delta$, Gregorig's surface will yield a constant heat-transfer coefficient over the entire convex surface. When the film thickness is independent of s, the above equation leads to:

$$\frac{1}{r} = -\frac{3s^2}{2B\delta^4} + C \qquad (2\text{-}21)$$

where $B = \dfrac{\sigma\rho g h_{fg}}{\mu k\Delta T}$

A finite radius r_o at the crest of the flute was assumed. At the termination of the convex surface $s=S_1$, $1/r=0$ were given (see Fig.2-8). The film thickness and heat-transfer coefficient for the convex surface are given by:

$$\delta = \left(\frac{3}{2B}\, r_o S_1^{\,2}\right)^{1/4} \qquad (2\text{-}22)$$

$$\alpha_{GR} = \frac{k}{\delta} = \text{constant} \qquad (2\text{-}23)$$

Karkhu and Borovkov (1971) [44] investigated the effect of surface tension force on a horizontal tube with trapezoidally-shaped fins. Fig.2-9 shows their physical model. The vapour-side surface was divided into two parts: the fin flank on which the condensation occured and the fin spacing into which the condensate was pulled by surface tension forces. It was considered that the condensate motion on the fin flank was driven by the surface tension forces due to the varying surface curvature. The fin trough was considered to serve as the drainage path and not contributing to the heat transfer. The momentum balance for condensate flow along the fin flank is given by:

$$\frac{1}{\mu}\frac{\partial P}{\partial x} + \frac{\partial^2 u}{\partial z^2} = 0 \qquad (2\text{-}24)$$

with the boundary conditions:-

$u=0$ at $y=0$

$\frac{\partial u}{\partial y}=0$ at $y=\delta$

In addition, the pressure gradient was assumed to be uniform over the fin flank and approximated as:

$$\left|\frac{\partial P}{\partial x}\right| \simeq \frac{\Delta P}{\Delta x} \simeq \frac{\sigma\cos\theta}{r_t(h-\Delta)} \qquad (2\text{-}25)$$

where r_t was approximated by:

$$r_t = b(1+\tan\theta) \qquad (2\text{-}26)$$

Equ.(2-24) may be then solved. The average velocity and film thickness were given by:-

$$u=-\frac{\delta^2}{3\mu}\frac{\partial P}{\partial x} = \frac{\sigma\delta^2\cos\theta}{3\mu(h-\Delta)(1+\tan\theta)b} \qquad (2\text{-}27)$$

$$\delta \doteq \left\{\frac{4\mu k\Delta T\ (1+\tan\theta)(h-\Delta)bx}{\sigma\rho h_{fg}\cos\theta}\right\}^{\frac{1}{4}} \qquad (2\text{-}28)$$

For the trough, laminar gravity-driven circumferential flow was analysed. The velocity distribution normal to the base of the trough was given by:

$$u^* = \frac{\rho\sin\psi}{\mu}\left\{(a+\Delta\tan\theta)y-\frac{y^2}{2}\right\} \qquad (2\text{-}29)$$

In the above equation, shear stress at the fin flank surface was considered but that at the surface of tube was neglected. The flow rate of condensate in the trough is then given by:

$$G_\psi = \frac{\rho^2 h^4 \sin^3\theta}{12\mu} \sin\psi (z+m)^4 \qquad (2\text{-}30)$$

$$z = \frac{\Delta}{h} \qquad m = \frac{a}{h\tan\theta}$$

and the mass balance gives:

$$\frac{dG_\psi}{R_r d\psi} = \rho u \delta \qquad (2\text{-}31)$$

A combination of eq.(2-30) and (2-31) leads to:

$$\frac{dz}{d\psi} = 2.8H \frac{(1-z)^{\frac{1}{2}}}{(z+m)^3 \sin\psi} - \frac{z+m}{4\tan\psi} \qquad (2\text{-}32)$$

$$H = \frac{\sigma^{1/4} \mu^{1/4} k^{3/4} d_r \Delta T^{3/4}}{\rho^{7/4} h_{fg}^{3/4} b^{1/4} h^{3.5} \sin^3\theta (1+\tan\theta)^{1/4}}$$

with the boundary condition;

$$\frac{\partial z}{\partial \psi} = 0 \quad \text{at } \psi = 0$$

Eq.(2-32) was numerically solved for Z. Since the condensate level in the trough is determined by condensation on the flank, the local condensation rate can be found from the rate of increase of depth of the trough with angle around the tube.

One empirical expression, based on the above a theoretical work, was made using parameters appearing in eq.(2-32). It was mentioned that the effective area for heat transfer was limited within ψ=150°, since there was a sharp rise of submergence in the fin spacing at around $\psi=150^\circ$. According to this observation, it was assumed that $\psi=150^\circ$ was the boundary of the region in which the condensation occured. The depth of submergence up to $\psi=150^\circ$ was expressed by:

$$z_b = 1.6(2.8H)^{0.2}(1-0.35(2.8)^{-0.3}m) \qquad (2-33)$$

The flow rate at $\psi=150^\circ$, i.e total condensation rate on the fin flank was given by substituting Z_b into Z in eq.(2-30) to give:

$$G_\psi = G_\psi(z_b)$$

Therefore the average heat-transfer coefficient over total surface area was given by:

$$\alpha = \frac{G_\psi h_{fg}}{(a+b+h/\cos\theta)\pi R_0 \Delta T} \qquad (2-34)$$

This expression was said to correlate their experimental data for water and R-113 to within ±5 % (details of these experiments are not described in [44]).

A more obscure model, covering evaporation and condensation on a horizontal triangular finned tube was developed by Edward et al. (1973) [45]. Their analysis for a horizontal grooved tube was composed of two seperate parts, one dealing with fluid flow in the grooves and the other with heat transfer. The condensate flow around tube was considered to be driven by gravity and "capillary pressure" due to surface tension. The heat transfer was treated seperately as a conduction process in two adjacent phases of the fin and condensate. However, the flow and heat-transfer performance are unconnected and their treatment seems to include incompatible assumption. No comparison with available experimental data was made.

Hirasawa et al. (1979) [27] have analysed three types of vertical fin plates (as described in section 2.1 and shown in Fig.2-4). In their model, the gravitational forces in the region 1 and 2 were assumed to be negligibly smaller than those due to surface tension. While, it was assumed that the flow in the region 3 was governed only by gravity and the curvature of liquid surface was approximated by a circular arc. The following assumptions for the condensate profile were made:-

1) In the region 1, the condensate on the leading edge forms a parabola.
2) In the region 2, the assumption of zero gravity leads to:

$$\frac{\sigma}{3\mu}\frac{d}{dy}\left[\delta^3\frac{d}{dy}\left\{\frac{d^2\delta}{dy^2}/\left(1+(d\delta/dy)^2\right)^{3/2}\right\}\right]=\frac{k\Delta T}{\rho h_{fg}\delta} \qquad (2\text{-}35)$$

3) In the region 3, the liquid velocity component of the horizontal direction is neglected, so that the force balance is given by:

$$\mu\left(\frac{\partial^2 u}{\partial y^2}+\frac{\partial^2 u}{\partial z^2}\right)+\rho g=0 \qquad (2\text{-}36)$$

A numerical solution was used which iterative procedures to match the slope of the liquid surface at the junction of region 1 and 2, and region 2 and 3.

The reliability of the model was checked by comparing the computed results with experimental data. Experiments were made using R-113 with the triangular finnned plate of 0.5 mm in pitch and 0.43 mm in fin height. Good agreement was found. It was concluded from the calculation that fins with a sharp leading edge, i.e. triangular fins, would give thinner condensate films than smoothly crested fins in region 1 but that the opposite was truefor region 2. These opposite effects gave the same heat transfer for the both types of fin. On the other hand, the flat bottomed grooves, for the same pitch and height as those of triangular fins, gave higher heat-transfer performance. Further, parallel-sided fins (i.e. zero tip angle) gave the highest heat transfer, e.g. those with 0.5 mm pitch and 0.87 mm height gave 10 times higher heat transfer for R-113 (based on the surface of plain plate) than a plain plate.

Hirasawa et al. (1980) [28], further, investigated the film flow on a plain surface with vertical fins having the parallel sides. The following expression was for the film thickness in the trough between the fins (see Fig.2-5):

$$\frac{\rho g}{3\mu}\frac{\partial \delta^3}{\partial x}+\frac{\sigma}{3\mu}\frac{\partial}{\partial y}\delta^3\frac{\partial}{\partial y}\left[\frac{\frac{\partial^2\delta}{\partial y^2}}{\{1+(\frac{\partial\delta}{\partial y})^2\}^{3/2}}\right]=\frac{k(T_v-T_w)}{\rho h_{fg}\delta} \quad (2\text{-}37)$$

where x is measured vertically downward,

y is measured horizontally and parallely to the base of the trough.

The profile of film in the vicinity of the fin root was assumed to be parabolic and having an area satifying the mass balance. Initial calculation without condensation but with constant mass flow from the top was compared with experiment results as described in section 2.1. Good agreement was found. Then the calculation was carried out for the case of condensation of R-113 at T_v=323 K and T_v-T_w =10 K with fins having height 0.9 mm. It was concluded that the heat-transfer coefficient increased as the fin spacing decreased but there seemed to exist an optimum spacing which would give a maximum heat-transfer coefficient.

Borovkov (1980) [46] modified his previous theory by assuming that for the condensate flow in the trough, the shear stress at the tube wall was more significant than that at the fin side (note the opposite assumption was used previously [43]). The mean velocity was then given by:

$$u^* = \frac{h^2 \rho \sin\psi}{3\ \mu} z^2$$

The condensate flow in the trough at the angle $\psi=150^\circ$ was given by:

$$G_\psi = \rho u^* \frac{a\Delta}{\cos\psi} \qquad (2\text{-}38)$$

The following differential equation was obtained for flow in the trough:

$$\frac{dz}{d\psi} = 0.47F_i \frac{(1-z)^{\frac{1}{2}}}{z^2 \sin\psi} - \frac{z}{3\tan\psi} \qquad (2\text{-}39)$$

$$F_i = \frac{\sigma^{1/4}\mu^{3/4}k^{3/4}dr\Delta Ts^{3/4}\eta^{3/4}\cos^{3/4}\theta}{ab^{1/4}h_{fg}^{3/4}h^{2.5}\rho^{3/4}(1+\tan\theta)^{1/4}} \qquad (2\text{-}40)$$

It was stated that the relation between the depth of film on the tube surface at $\psi=150^\circ$ and the nondimensional parameter F_i, as given by numerical solution of eq.(2-39), was represented within 15 % for several fluids and finned tube geometries by the following expression:

$$Z_b = 2.0\ F_i^{1/3} \qquad (2\text{-}41)$$

Hence, the mean heat-transfer coefficient for a finned tube based on surface of the smooth tube having the same diameter as that at the fin root, i.e. d_r, was expressed by:

$$\alpha = \frac{2G_\psi h_{fg}}{d_r s \Delta T} \qquad (2\text{-}42)$$

Since G_ψ is the total flow rate at $\psi=150^\circ$ given by eq.(2-38) using Z_b in eq.(2-41) (i.e. total condensate rate on the fin flank), the average heat-transfer coefficient was given by:

$$\alpha_{BO} = 1.7\frac{\rho^2 h_{fg} a h^3}{\mu\Delta T d_r s\cos\theta}F_i \qquad (2\text{-}43)$$

where $s=2(a+b+h\tan\theta)$

Owen et al. (1983) [42] developed a similar model to that of Beatty and Katz [29] but included consideration of the retention angle. For the upper part of the tube ($0<\phi<\phi_f$), where ϕ_f is the retention angle, the Beatty and Katz model was adopted. For the flooded part, parallel heat-transfer paths were considered for the fins and the condensate between fins. The average heat transfer coefficient was then written as:

$$\alpha_{OW} = \frac{\phi_f}{\pi}\alpha_{BK} + (1-\frac{\phi_f}{\pi})\ \alpha_L \qquad (2\text{-}44)$$

where $\alpha_L^{-1} = \alpha_{eff}^{-1} + \alpha_c^{-1}$

$$\alpha_c = 0.728\left(\frac{\rho^2 g h_{fg} k^3}{\mu \Delta T d_o}\right)^{1/4}$$

$$\alpha_{eff} = k_{eff}/h$$

$$k_{eff} = (1-bN)k_t + bNk \qquad N \text{ is density of fin}$$

This model were said to predict experimental data by Beatty and Katz, Pearson and Carnavos (see section 2.2) within ±30 %. It may be noted, however, that α_{Bk} and α_L are expressed on the basis of different areas and may not be simply ccmbined as in eq.(2-44). To correct eq.(2-44), the second term of the right hand side in eq.(2-44) should be multiplied by $\left(\frac{d_r}{d_{eq}}\right)^{1/4}$.

Rudy and Webb later (1983) [47] employed the Karkhu and Borovkov aproximation of the uniform pressure gradient on the fin flank resulting from surface tension, and gave the following relation for pressure gradient:

$$\frac{dP}{dx} \approx \frac{\sigma}{h}\left(\frac{1}{r_t} - \frac{1}{r_b}\right) \qquad (2\text{-}45)$$

where r_t and r_b are radius of condensate film at fin tip and fin bottom.

The radii values were approximated (see Fig.2-10) by:

$$r_t = t/2 \qquad r_b = -b/2 \qquad (2\text{-}46)$$

$$\therefore \qquad \frac{dP}{dx} = \frac{2\sigma}{h}\left(\frac{1}{b} + \frac{1}{t}\right) \qquad (2\text{-}47)$$

The film on the fin flank was then treated by the Nusselt model except that the gravity term was omitted and the pressure gradient in eq.(2-45) was included. This led to the following equation for the heat-transfer coefficient:

$$\alpha_f = 0.943\left(\frac{k^3 \rho h_{fg}}{\mu \Delta T}\right)^{1/4}\left\{2\frac{\sigma}{h^2}\left(\frac{1}{b}+\frac{1}{t}\right)\right\}^{1/4} \qquad (2\text{-}48)$$

Heat transfer in the flooded region was neglected and the total heat transfer was considered as the sum of that on the fin flank and that in the trough for unflooded region. The average heat-transfer coefficient over the total surface was given by:

$$\alpha_{RU} = \left(\frac{A_b}{A_p}\alpha_b + \eta\frac{A_f}{A_p}\alpha_f\right)\frac{\phi_f}{\pi} \qquad (2\text{-}49)$$

where α_b and α_f are given by eq.(2-8) and eq.(2-48).

Adamek (1983) [12] gave a convenient method for investigating the optimum shape for flutes on a vertical fluted tube. The Gregorig method [7] predicts the

heat-transfer coefficient for a specific flute profile. Adamek considered the following family of suitable interface profile:

$$\kappa(s)=r^{-1}=r_0^{-1}-as^n \qquad 0<n<\infty \qquad (2\text{-}50)$$

$$=as^n-r_0^{-1} \qquad -1<n<0$$

The angle ω, between the tangent at the condensate surface at distance s and at the top of flute, varies from zero at the crest to ω_1 at the end of the convex part of the surface $s=S_1$ (see Fig.2-11). The element length along the condensate surface, ds, is given by:

$$ds=r\,d\omega \quad \text{or} \quad d\omega=r^{-1}ds \qquad (2\text{-}51)$$

so that, for the condensate surface profile considered, the following expression is given:

$$\int_0^{S_1}\kappa(s)ds=\frac{1}{r_0}S_1-\frac{a}{n+1}S_1^{n+1}=\omega_1 \qquad 0<n<\infty \qquad (2\text{-}52)$$

$$=\frac{a}{n+1}S_1^{n+1}-\frac{1}{r_0}S_1=\omega_1 \qquad -1<n<0$$

The momentum and energy balances as given by Gregorig are then used to obtain:

$$\delta(s)=(\kappa')^{-1/3}\left(4\int_0^S c(\kappa')^{1/3}ds+c_0\right)^{\frac{1}{4}} \qquad (2\text{-}53)$$

At the transition from the convex to the concave surface, $1/r=0$. Hence:

$$\frac{1}{r_0}=aS_1^n \qquad (2\text{-}54)$$

where $$a=\omega_1\left(\frac{n+1}{n}\right)S_1^{-(n+1)} \qquad 0<n<\infty$$

$$=-\omega_1\left(\frac{n+1}{n}\right)S_1^{-(n+1)} \qquad -1<n<0$$

so that, the film thickness is given by:

$$\delta(s)=\{\frac{12}{B\omega_1}\frac{S_1^{n+1}s^{2-n}}{(n+1)(n+2)}\}^{\frac{1}{4}} \qquad (2\text{-}55)$$

$$B=\frac{\sigma\rho g h_{fg}}{\mu k \Delta T}$$

The flute profile is found by subtracting the film thickness given by eq.(2-55) from the interface profile given by eq.(2-50). The mean heat-transfer coefficient over the convex surface is finally given by:

$$\alpha_{AD}=2.149k(B\omega_1(n+1)(n+2)^{-3}S_1{}^{3})^{\frac{1}{4}} \qquad (2\text{-}56)$$

The optimum combination of ω_1, n and S_1 in the above equation gives the highest heat-transfer coefficient over the convex surface. Following numerical investigations using the above technique, Adamek suggested that a sharp leading edge would lead to high heat-transfer coefficients.

More recently, Rudy and Webb (1984) [43] adopted Adamek's [12] expression for obtaining the heat-transfer coefficient on the fin side and the model of parallel heat transfer paths for the fins and condensate for the flooded region. The following equation for the heat-transfer coefficient was given:

$$\alpha_{RD}=(\frac{A_b}{A_p}\alpha_h+\eta\frac{A_f}{A_p}\alpha_f)\frac{\phi_f}{\pi}+\frac{A_b}{A_p}\alpha_L(1-\frac{\phi_f}{\pi}) \qquad (2\text{-}57)$$

where α_L is found by numerically solving the two dimensional conduction problem for fin and condensate in the flooded region matching the heat flux at the fin-condensate boundary. α_f is given by Adamek's model. α_h is predicted by the Nusselt theory for the interfin space with modification to accord for the additional condensate from the fin flanks:

$$\alpha_h = 1.514\left(\frac{k^3 \rho^2 g}{\mu^2 Re}\right)^{1/3} \qquad (2\text{-}58)$$

$$Re = \frac{4m}{\mu(p-t)} \qquad (2\text{-}59)$$

To obtain α_h, iteration was carried out until mass flow rate in m is equal to the sum of the condensation rates on fin flank m_f and in the trough m_h given by:

$$m_f = \frac{\eta \alpha_f A_f \Delta T}{h_{fg}} \qquad (2\text{-}60)$$

$$m_h = \frac{\alpha_h A_p \Delta T}{h_{fg}} \qquad (2\text{-}61)$$

Adamek's expresion is suitable only for fin profiles as described in the above section. Rudy and Webb later made an approximation to adopt Adamek's expression to trapezoidal cross-sectional fins giving moderate values of n in eq.(2-56). Flook (1985) [48] reported that this model under-estimated the heat-transfer coefficients given by Georgiadis [40] for steam by a factor of around 40 %.

Honda et al. (1984) [49] has given what is probably the most realistic approch to date. Fig.2-12 shows the physical model in which the cross section of the fin was composed of straight portions at the tip and side, and a round corner at the tip. The condensate on the fin surface was driven by combined gravity and surface tension forces into the fin root and liquid between fins was drained by gravity. Thus the surface of the fin was divided into two parts; i.e. a thin film region on upper part of the fin surface and thick film region at the fin root. For analysis of the film flow, the following assumptions were made;

1) The wall temperature is uniform through the fin.

2) The condensate flow is laminar.

3) The condensate film thickness is small so that the inertia terms in the momentum equation and the convection terms in the energy equation can be neglected.

4) Circumferancial flow can be neglected in comparison with radial flow.

5) The fin height is substantially smaller than the tube radius.

Then the motion for the condensate film along the fin top and flank was given by the following equation:

$$\frac{\rho g}{3\mu}\frac{\partial \delta^3}{\partial x}f_x - \frac{\sigma}{3\mu}\frac{\partial}{\partial x}\left[\delta^3 \frac{\partial}{\partial x}\left(\frac{1}{r}\right)\right] = \frac{k(T_v - T_w)}{\rho h_{fg}\delta} \qquad (2\text{-}62)$$

where f_x is the x component (radial) of "nomalized gravity", i.e. $f_x = \cos\phi\cos\theta$ for fin flank and $f_x = 0$ for fin top, r is the radius of curvature of the liquid-vapour interface, and δ is condensate film thickness. The local film thickness on the fin was calculated by using a numerical implicit finite difference scheme. The average Nusselt number (pitch as representative length) over fin side was respectively defined as:

$$Nu_p = 2\int_0^X (1/\delta)dx \qquad (2\text{-}63)$$

Approximate expression for Nu_p in both unflooded and flooded regions were derived based on the results of the numerical analysis. The overall average Nusselt number Nu_d was written in relevant parameters for the u(unflooded) and f(flooded) regions to give the following approximate result:

$$Nu_d = \frac{Nu_u \eta_u (1-\widetilde{Tw}_u)\widetilde{\phi}_f + Nu_{df}\eta_f (1-\widetilde{Tw}_f)(1-\widetilde{\phi}_f)}{(1-\widetilde{Tw}_u)\widetilde{\phi}_f + (1-\widetilde{Tw}_f)(1-\widetilde{\phi}_f)} \qquad (2\text{-}64)$$

where Nu_{du} and Nu_{df} are Nusselt number based on the average condensate different temperature differences for the flooded and unflooded regions, T_{wu} and T_{wf}, since experiments [34] have shown that the wall temperature changes considerably with angle, as a result of large difference in heat-transfer coefficient between the unflooded and flooded regions.

Nu_{du} was expressed as a combination of values for surface-tension-force-controlled condensation $(Nu_{du})_s$ and gravity-controlled condensation $(Nu_{du})_g$:

$$Nu_{du}=\{(nu_{du})_g^3+(Nu_{du})_s^3\}^{1/3} \qquad (2\text{-}65)$$

This approximate expression was justified by consideration of the numerical solutions. For $(Nu_{du})_g$, the Beatty and Katz model(see eq.(2-1)) was used. $(Nu_{du})_s$ is related to Nu_{pu} , such that:

$$(Nu_{du})_s=Nu_{pu}\frac{(d_o+d_r)}{2p} \qquad (2\text{-}66)$$

For the flooded region, the effect of gravity was neglected and Nu_{df} (with outer diameter d_o as the representative length) so that:

$$(Nu_{du})_f=Nu_{pf}\frac{d_o}{p} \qquad (2\text{-}67)$$

replaced Nu_{pf}. η_u and η_f are the fin efficiences. $\tilde{T}_{wu}$ and $\tilde{T}_{wf}$ are dimensionless average temperature differences at the fin root given by $\tilde{T}=(T-T_c)/(T_v-T_c)$ where Tc is coolant temperature. ϕ_f is angle of flooded point from the top of tube and $\tilde{\Phi}_f=\phi_f/\pi$. The values of T_{wu} and T_{wf} were determined by solving the considering heat trarsfer from vapour to coolant. It was assumed that the coclant-side heat-transfer coefficient was constant and average (constant) values were used for the vapour-side coefficient for the unflooded and flooded regions. Circumferential conduction in the wall between the two regions was neglected so that the temperature drops across the wall for the two regions were found on the basis of uniform radial conduction. The heat balance equations for the unflooded and the flooded region then yield differential equation for T_w as function of ϕ:

$$\eta_i Nu_{di} \frac{k}{k_t} - \{\eta_i Nu_{di} \frac{k}{k_t} + (\frac{1}{2} \ln(\frac{d_r}{d_i}) + \frac{1}{Nu_c} (\frac{k_t}{k_c})^{-1}\} T_w' = -\frac{4t}{\pi^2 d_r} \frac{d^2 T_w}{d\phi^2}$$

(2-68)

where Nu_{dc} is the Nusselt number for inner surface of the tube and i indicates u (unflooded) or f (flooded). The boundary and compatibility conditions are:

$dT_w/d\phi=0$ at $\phi=0$ and 1

$(T_w)_u=(T_w)_f$, $(dT_w/d\phi)_u=(dT_w/d\phi)_f$ at $\phi=\phi_f$

Honda's model was found to predict most of available data within 20%, Beatty and Katz's [29] and Owen's [41] predictions were less good, and Rudy's model [46] predicted most data satisfactorily except for steam.

While Honda's model appears to have been generally satisfactory, it must be noted that numerical computer solution is required to obtain Nu even in their approximate model. A further defect is that the circumferancial flow of condensate and heat transfer in the trough are neglected. (In a private communication, Honda has indicated that he has modified his model to include heat transfer in trough and has reported that this gave better agreement with the present author's data.)

<u>Concluding remarks</u>

Several theoretical models have been attempted. In outline:-

1. Beatty and Katz [29], 1948. This is basically a Nusselt type of approach combining gravity flow on a horizontal tube and flow on a vertical plane surface. Surface tension forces were not included.

2. Karkhu and Borovkov [44], 1971, and Borovkov [45], 1980. This approch attempted to include surface tension drainage forces but involved several unsubstantiated assumption and approximation.

3. Owen et al.[42], 1981. This approch is similar to the Beatty and Katz model but takes account of heat transfer through flooded region using parallel paths through fin and flooded interfin space. (Note Owen's final result is incorrect but readily is modified.)

4. Rudy and Webb [47], 1983. This approach employed the assumption of (2) (uniform pressure gradient on finflank) but also included retention of

condensate on a lower part of tube. Heat transfer through flooded part of the tube was neglected.

5. Rudy and Webb [43], 1984. This approch adopts Adamek [12] model for treating the fin flank. For flooded region, two-dimensional conduction analysis is used. Numerical solution is needed to determine the average heat-transfer coefficient.

6. Honda et al [49], 1984. This is a complex approch for both flooded and unflooded part of tube. Numerical solution of the momentum and energy equations for condensate film on fin flank including surface tension and gravity forces. These are summarised by approximate formulae but the final result required additional numerical solution to take account of temperature variation of the tube wall between the flooded and un-flooded regions.

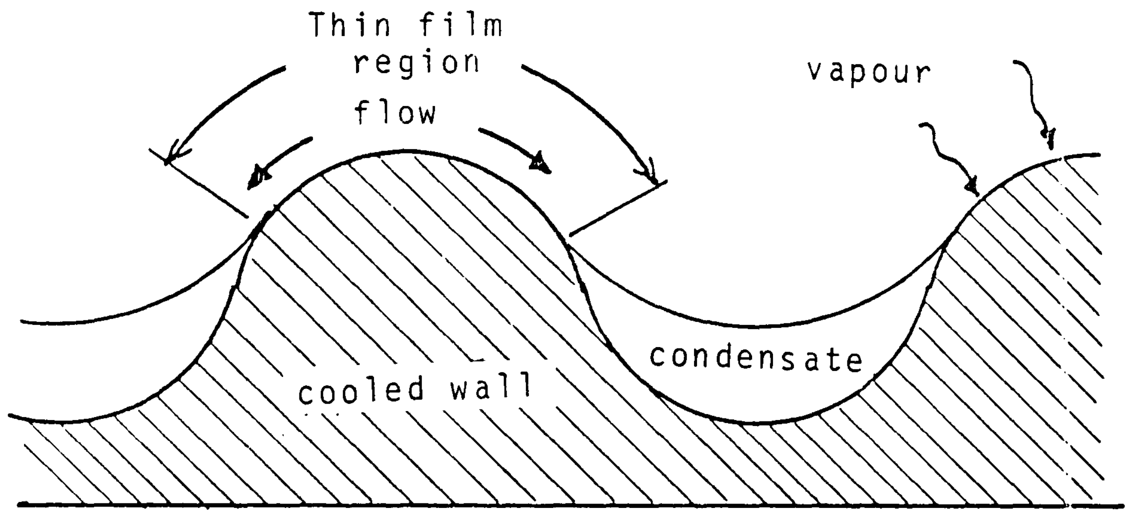

Fig. 2-1 Cross section on fluting condensing surface reproduced from Gregorig [7]

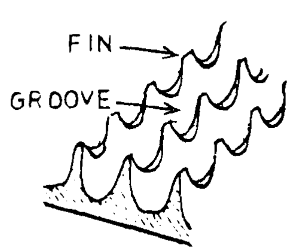

Fig. 2-2 "Saw-toothed" fins, so called "Thermoexcel-C" reproduced from [21]

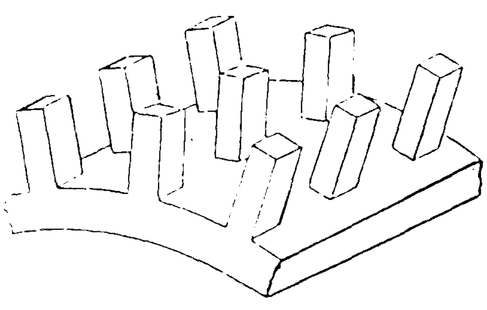

Fig.2-3 "Spine-fins reproduced from [22]

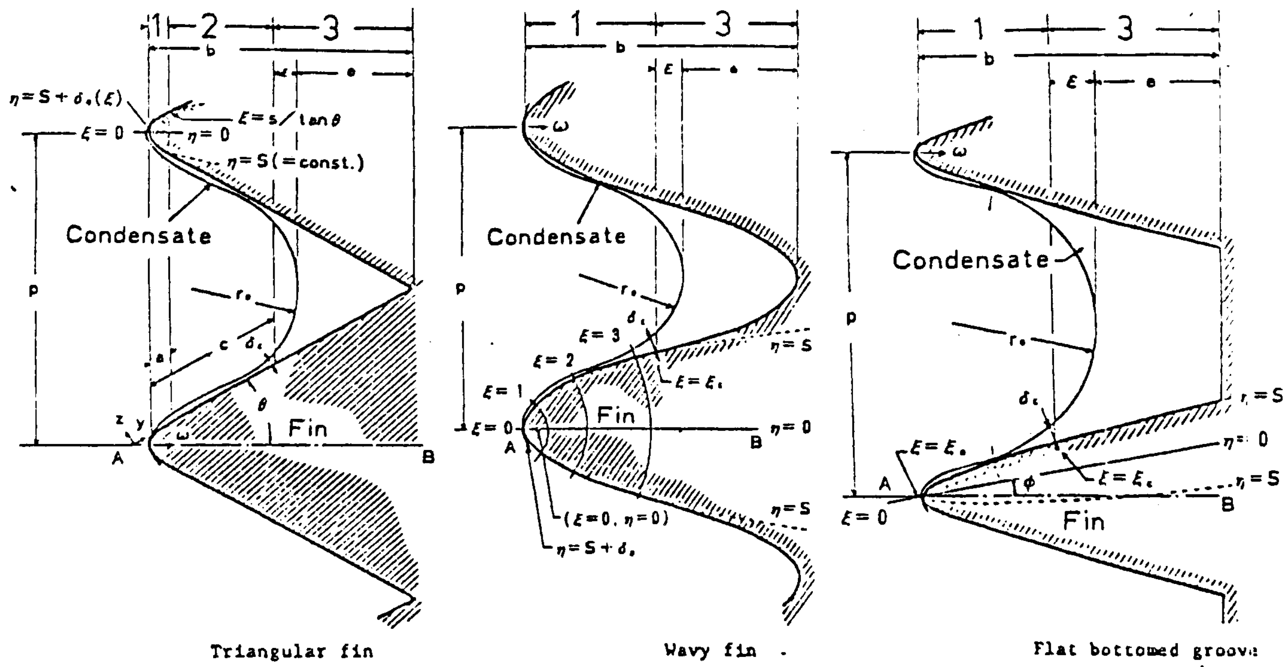

Fig.2-4 Three types of fins investigated by Mori et al. reproduced from [26,27]

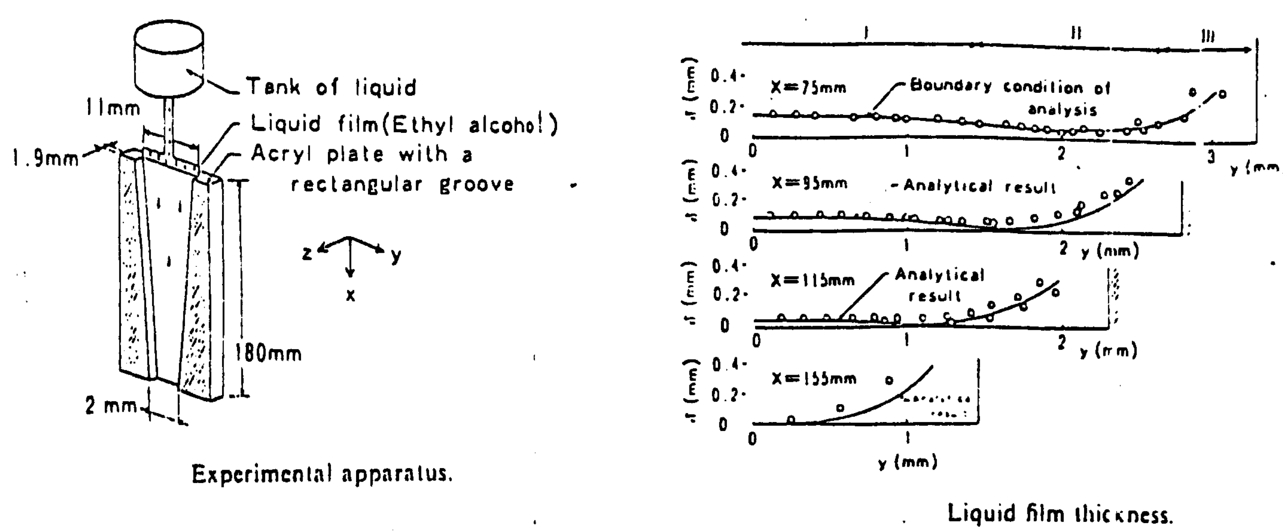

Fig.2-5 Experiments performed by Mori et al. on effect of surface tension forces over vertical finned plate. (reproduced from [28])

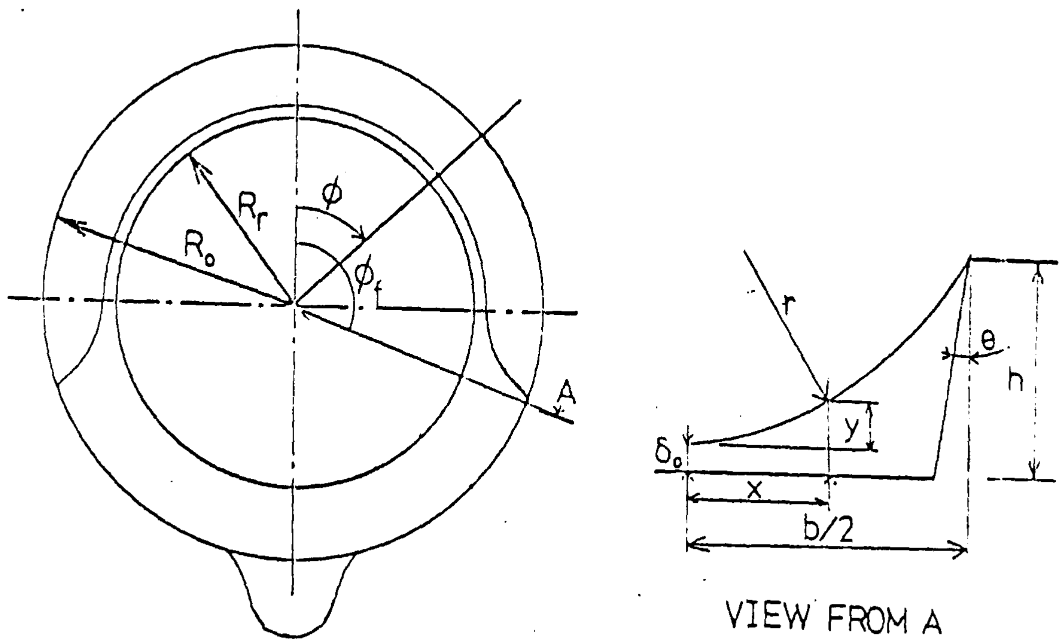

Fig.2-6 Condensate retention. General view and coordinate system used by Honda et al. [34]

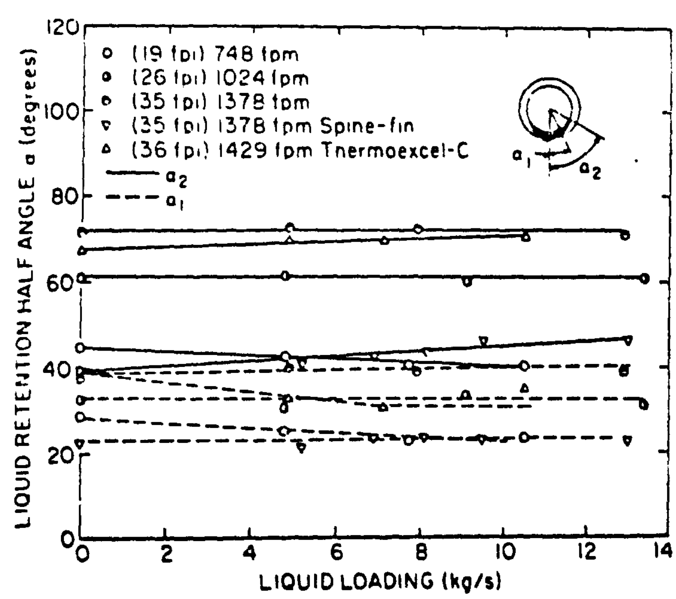

Fig.2-7 Experimental results of condensate retention under "static" and "dynamic" conditions conducted by Rudy et al. [41]

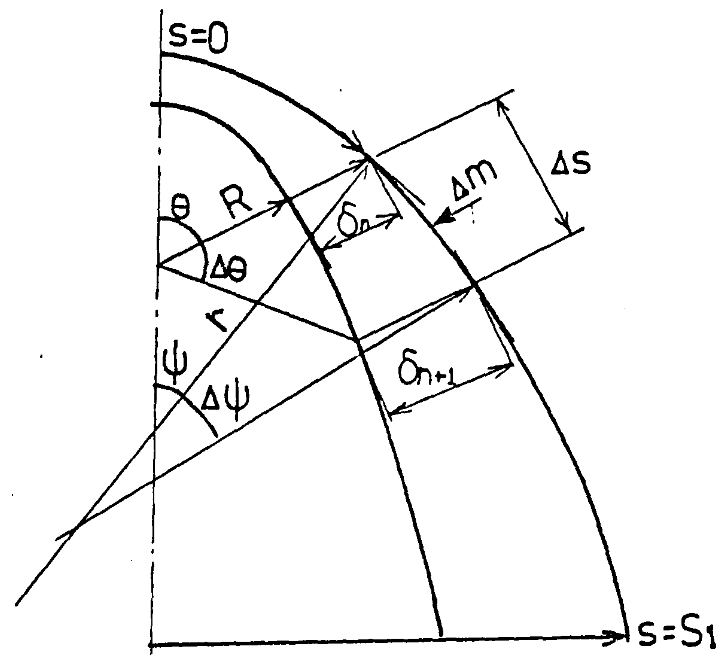

Fig.2-8 Physical model and coordinate system of Greogorig's fluted surface [7]

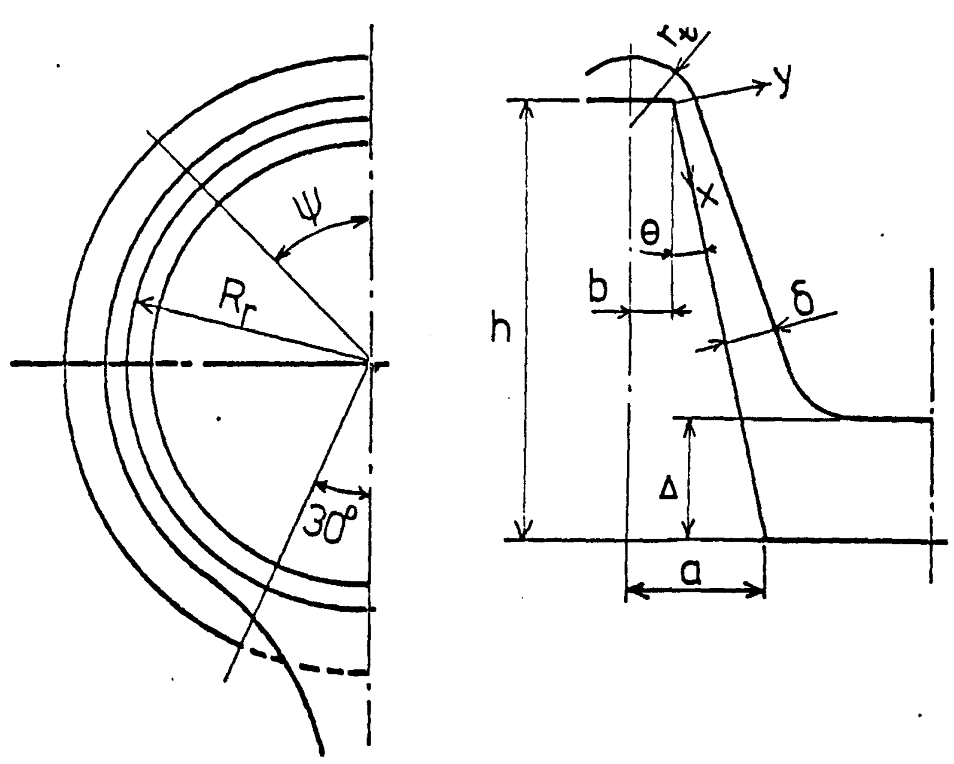

Fig.2-9 Physical model and coordinate system of finned tube studied by Karkhu and Borovkov [44]

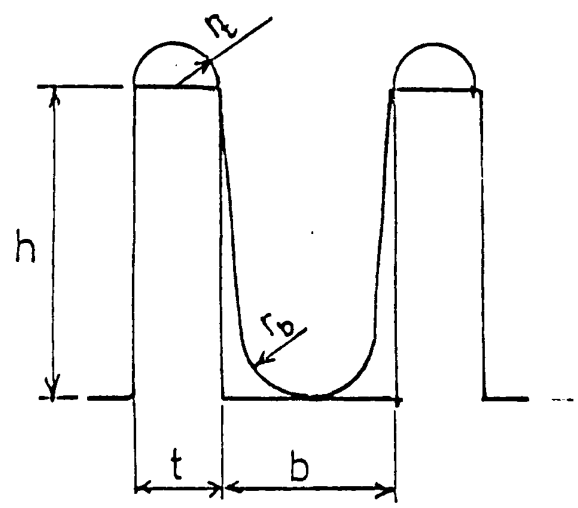

Fig.2-10 Parameters and approximations in Rudy et al. model [47]

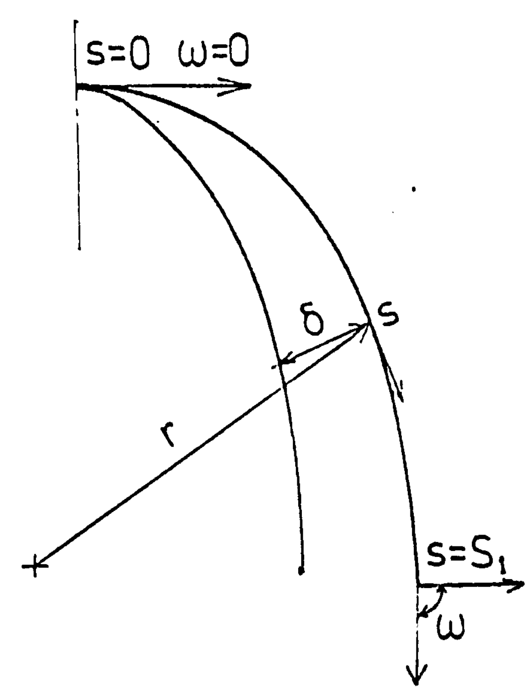

Fig.2-11 Physical model and coordinate system of "Gregorig type" condensation surface studied by Adamek [12]

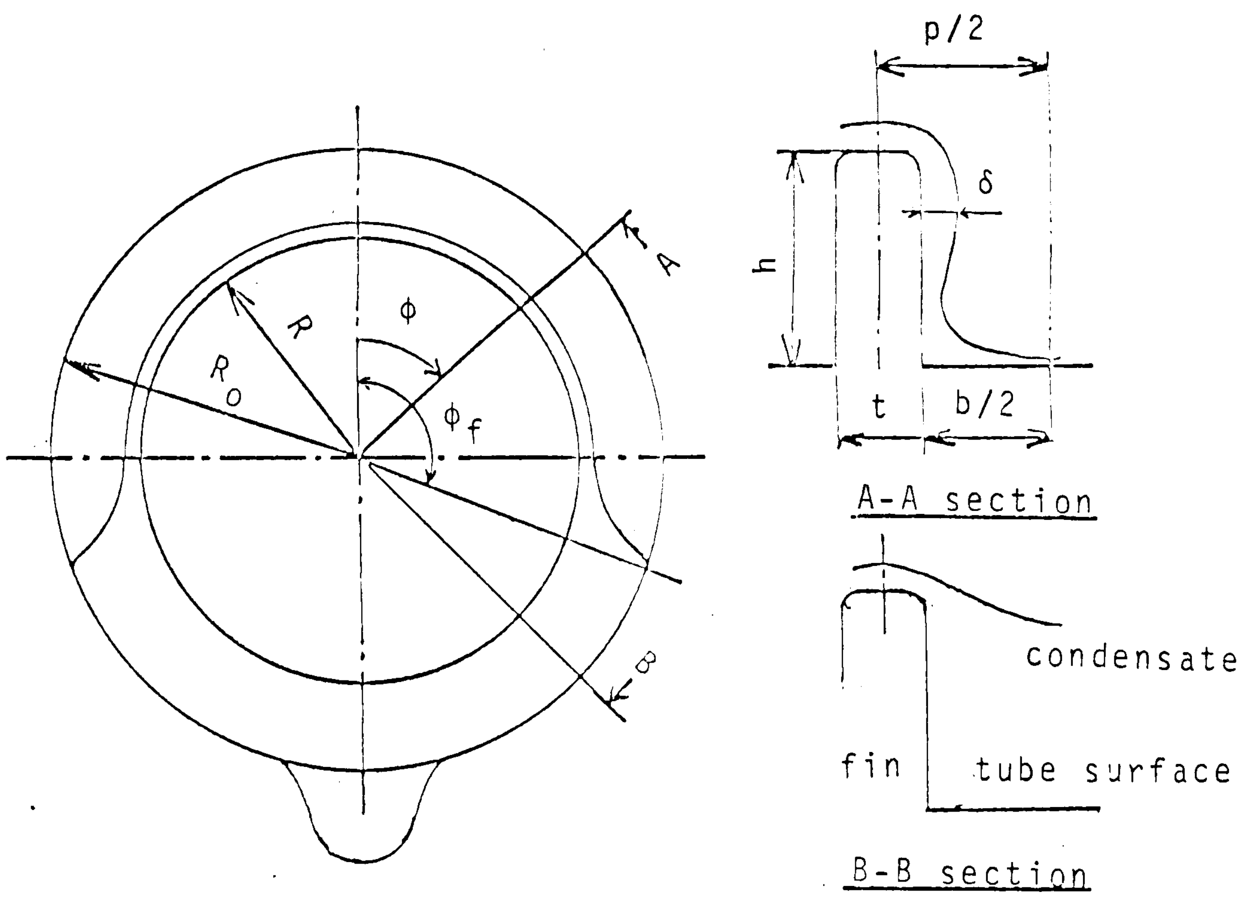

Fig.2-12 Physical model and coordinate system of condensation on finned tube studied by Honda et al. [49]

Table 2-1 Dimensions and enhancement performance of smooth and finned tubes (reproduced from Beatty and Katz [29])

Tube Number		1	2	3	4	5	6	7
Fluid					R-22			
root diamter	d_r/mm	15.87	19.05	19.51	19.51	19.23	19.51	19.51
pitch	p /mm	1.645	-	3.676	3.708	3.89	3.681	3.676
fin spacing	b /mm							
fin thickness top		0.33	plain	0.33	0.737	0.406	0.33	0.533
bottom		0.584		0.94	0.94	1.04	0.94	0.94
fin hight	h /mm	1.437		8.66	3.45	7.42	8.15	6.17
area ratio		1.9	1.0	5.39	2.38	4.66	4.32	4.03
vapour temp.	T_v/K	339	359	358	359	359	359	360
temp. difference	/K	36	36	35	36	36	36	33
Enhancement ratio of heat transfer		3.38		8.68	4.07	6.8	6.57	7.01

Table 2-2 Data for condensation of saturated steam from Mills et al. [32] (reproduced by Cooper and Rose [15])

tube material	T_{sat}/K	ΔT/K	$Q\times10^{-5}$ W/m^2	$Q/Q_{plain\ tube}$
Copper	313.2	5.5	2.151	3.746
	318.2	8.2	2.200	2.839
	307.1	2.2	1.106	3.829
	316.2	10.0	2.234	2.485
Brass	310.0	1.1	1.024	5.965
	305.6	3.3	1.475	3.768
	301.0	6.0	0.940	1.534
	326.6	8.8	2.626	3.214
Cuppro-Nickel	309.2	1.3	0.478	2.454
	309.4	3.0	1.263	3.465
	316.3	4.8	1.383	2.568
	323.6	6.7	1.702	2.556

Table 2-3 Dimensions and enhancement performance of finned tubes (reproduced from Carnavos [33])

Tube code		W-1	W-2	HC	HP	N-2	FC-2
		fins		pin	fins	flute	pin flute
Fluid				R-11			
root diameter	d_r/mm	14.3	15.7	15.5	15.8	11.8	14.3
pitch	p /mm	0.943	0.621	0.725	0.820	0.794	0.704
fin spacing	b /mm	0.587	0.367	0.446	0.566	-	-
fin thickness	t /mm	0.356	0.254	0.279	0.254	-	-
fin hight	h /mm	1.32	0.914	1.04	0.787	0.508	0.89
area ratio		3.53	3.75	-	2.79	2.18	-
vapour temp.	T_v/K			308			
Enhancement ratio of heat transfer							
ΔT	2.5 K	5.2	4.6	4.0	4.6	5.6	4.2
	4.5 K	4.04	3.65	3.17	3.65	4.57	3.48

Table 2-4 Dimensions and enhancement performance of finned tubes (reproduced from Honda et al. [34])

Tube code		B	C	D	B	C	D
Fluid			R-113			Methanol	
root diameter	d_r/mm	15.77	17.05	17.09	15.77	17.05	17.09
pitch	p /mm	0.98	0.64	0.50	0.98	0.64	0.50
fin spacing	b /mm	0.71	0.46	0.39	0.71	0.46	0.39
fin thickness	t /mm	0.27	0.18	0.11	0.27	0.18	0.11
fin higth	h /mm	1.46	0.92	1.13	1.46	0.92	1.13
area ratio		3.84	3.68	5.48	3.84	3.68	5.48
vapour temp.	T_v/K		328			341	
temp difference	/K		5			5	
Enhancement ratio of heat transfer		6.36	8.31	9.08	5.01	5.44	5.05

Table 2-5 Geometry of finned tubes used in Gerogiadis tests [40]

Fin spacing mm	Fin Thickness mm	Fin Height mm
0.5, 1.0, 1.5, 2.0, 4.0	1.0	1.0
0.5, 1.0, 1.5, 2.0, 4.0	0.75	1.0
0.5, 1.0, 1.5, 2.0, 4.0	0.5	1.0
1.0, 1.5, 2.0, 4.0	1.0	2.0
1.0	1.5	1.0
1.25	1.25	1.0

CHAPTER 3 EXPERIMENTAL STUDY

3 Experimental study

3. 1. Apparatus and procedure

The apparatus is shown in Fig 3-1. Vapour was generated from subcooled working fluid (R-113 and ethylene glycol) in the stainless steel boiler which was fitted with four electric immersion heater, providing a total power of 16 kW, and a transparent level-indicating tube. The heater specification is shown in Table 3-1. Note that the apparatus was rearranged for experiments using ethylene glycol so that its specification is different from that for water in [35,36,37] and R-113 in present study. The condenser tube was located in the test section on which a pyrex glass window was located to view the condenser tube. Details of the test section are shown in Fig 3-2. Cooling water was passed through the condenser tube via a float-type flow meter. The test condenser tube and the inlet and outlet ducts were well insulated from the body of the test section and from the environment with nylon66 and ptfe components. The vapour flowed vertically downwards over the condenser tube. Condensate from the tube and uncondensed vapour were led to the auxillary condenser and all the condensate was returned by gravity to the boiler. The boiler, vapour supply duct and the test section were thermally well insulated from the surroundings.

Before test runs

The apparatus was first run for around an hour to expel air and to achieve steady operating conditions. The condenser tube was visually inspected to comfirm that film condensation prevailed. That the isothermal immersion of the thermocouples was adequate was checked by withdrawing the junctions by 1 or 2 cm. No change in the thermo-emf was found.

During operation, the inlet temperature of the coolant (water), the inlet-to-outlet temperature difference, the vapour temperature in the test section and the temperature of condensate returning to the boiler were measured with copper-constantan thermocouples which fitted tightly in a closed copper tubes. The thermo-emfs were measured by a digital voltmeter with a precision 1 μV. All tests were carried out at slightly above atmospheric pressure. The pressure in the test section was measured with a liquid(condensate) manometer.

3.2 Tubes tested

The test condenser tubes were of copper with internal diameter 9.78 mm and effective length, i.e.length exposed to vapour, of 102 mm. The outside diameter at the root of fins was 12.7 mm. The fins in all cases had the same rectangular cross section. The fin height and width were 1.59 mm and 0.5 mm respectively. Fin spacings of 0.25, 0.5, 1.0, 1.5, 2, 4, 6, 8, 10, 12, 16, 18 and 20 mm were used. Details of the tubes are given in Table 3-2 and illustrated in Fig.3-3.

To ensure film condensation, the tube and ptfe bushes were first thoroughly cleaned. The tubes and ptfe bushes were first wiped using a clean cloth. After rinsing with distilled water, they were then cleaned by immersing, for a few minutes, in a mixture of 200 g sodium dichromate and 100 cm^3 concentrated sulphuric acid in 2 ℓ of distilled water. While immersed, the tube was agitated to ensure that all air bubbles were removed so that the solution came into contact with all parts of the surface. The tubes were then rinsed with distilled water and dried with a clean cloth. The tube and bushes were finally rinsed with the working fluid.

3.3. Determination of the experimental parameters

3.3.1. Pressure

The test section pressure was obtained adding the observed gauge pressure to the barometer pressure.

3.3.2 Input power

The power input to the boiler was determined using the following eqation:

$$Q_h = \Sigma(V_i^2/R_i) \qquad (3\text{-}1)$$

where Q_h is the total input power, V_i is potential drop across and R_i is the resistance of heater i. Since the resistances of the heaters were known (see Table 3-1), Q_h was determined by recording the potential drop across the heaters indicated by a voltmeter. For the R-113 tests only one heater was used at main potential. For the ethylene glycol tests, the three heaters were also used at main potential.

3.3.3 Temperature

The various temperatures were determined by using the thermocouple calibration formula [35]:

$$T= A_1+A_2e+A_3e^2+A_4e^3 \tag{3-2}$$

A_1=273.1

A_2=2.5518496x10^{-2}

A_3=-6.6119645x10^{-7}

A_4=2.6750257x10^{-11}

where e is the emf/μV and T is the thermodynamic temperature /K. In the case of measuring the potential drop between the coolant at inlet to and outlet from the condenser tube, the temperature drop was calculated by the following eqation:

$$\Delta T = \left(\frac{dT}{de}\right)_{e=e_m} \Delta e \qquad (3-3)$$

where $\left(\frac{dT}{de}\right)_{e=e_m}$ is obtained by differentiating

eq.(3-2) and $e_m = e_1 + \Delta e/2.$ (3-4)

where ΔT is temperature increase, Δe is potential increase, e_1 is inlet thermoemf.

3.3.4 Parameters for the coolant

The mean coolant velocity was found from the continuity eqation:

$$u_c = V_c / A_i \qquad (3-5)$$

where V_c is volume flow rate given by the float-type flow meter. A_i is the internal cross sectional area of the tube. The mass flow rate of the coolant was calculated by:

$$m_c = V_c \rho_c \qquad (3-6)$$

The coolant Reynolds number was found by:

$$Re = \rho_c u_c d_i / \mu_c \qquad (3-7)$$

and the coolant Prandtl number was determinded by:

$$Pr_c = \mu_c c_{p_c} / k_c \qquad (3\text{-}8)$$

The properties, μ_c kinematic viscosity, ρ_c density, c_{p_c} specific heat capacity and k_c thermal conductivity, were evaluated at the mean coolant temperature T_c, i.e;

$$T_c = (T_{in}+T_{out})/2 \qquad (3\text{-}9)$$

where T_{in} is the coolant inlet temperature and T_{out} is that at outlet.

3.3.5 Heat transfer rate

The heat transfer rate to the coolant was found from:

$$Q_c = m_c c_{p_c} (T_{out} - T_{in}) \qquad (3\text{-}10)$$

The heat fluxes for the outside and inside surfaces are given by:

$$Q = Q_c / (\pi d_r \ell) \qquad (3\text{-}11)$$

$$Q_i = Q\ (d_r / d_i) \qquad (3\text{-}12)$$

where d_i is the inside diameter and d_r is the outside diamter for the plain tube and the diameter at the fin root for the finned tubes.

3.3.6 Overall heat-transfer coefficient

The overall heat-transfer coefficient is given by:

$$U = Q\ /LMTD \qquad (3\text{-}13)$$

where Q is give by eq.(3-12) and LMTD (log mean temperature difference) is given by:

$$LMTD = \frac{T_{out} - T_{in}}{\ln\left(\frac{T_v - T_{in}}{T_v - T_{out}}\right)} \qquad (3\text{-}14)$$

where T_v is the vapour temperature.

3.3.7 Vapour mass flow rate

The vapour mass flow rate and hence vapour velocity at the test section were obtained from the input power to the boiler by applying a steady flow energy balance between the boiler inlet and the test section. A correction for the relatively small thermal losses from the apparatus was incorporated. The losses were established in preliminary tests in which the minimum power required to provide vapour at the test section was determined [35]. The following equation was used for the "heat loss":

$$\frac{Q_{loss}}{W} = 8.328\left(\frac{T_v - T_a}{K}\right) \qquad (3\text{-}15)$$

where T_v is the vapour temperature and T_a is the ambient temparature. A steady flow enegy balance between test section and boiler inlet gives:

$$Q_h - Q_{loss} = m_v(c_p\ (T_v - T_r) + h_{fg}) \qquad (3-16)$$

where m_v is the mass flow rate of the vapour, c_p is the condensate isobaric specific heat capacity, and h_{fg} the specific enthalpy of evaporation. The vapour velocity is then given by:

$$v_v = m_v/(\rho_v A_s) \qquad (3-17)$$

where A_s is the cross-sectional area of test section.

3.3.8 Mass fraction of non-condensing gases

The mass fraction of non-condensing gases present in the test section was estimated from the pressure and temperature mesurements using the ideal-gas mixture laws and assuming saturation conditions, i.e:

$$W_s = \frac{P - P_{sat}(T_s)}{P - (1 - \frac{M_v}{M_g}) P_{sat}(T_s)} \qquad (3-18)$$

where P is the observed pressure of gas-vapour mixture, i.e. the pressure in the test section. $P_{sat}(T_s)$ is the liquid-vapour eqiulibrium (saturation) pressure of the vapour. M_v is relative molecular mass of the vapour. M_g is relative molecular mass of non-condensing gas.

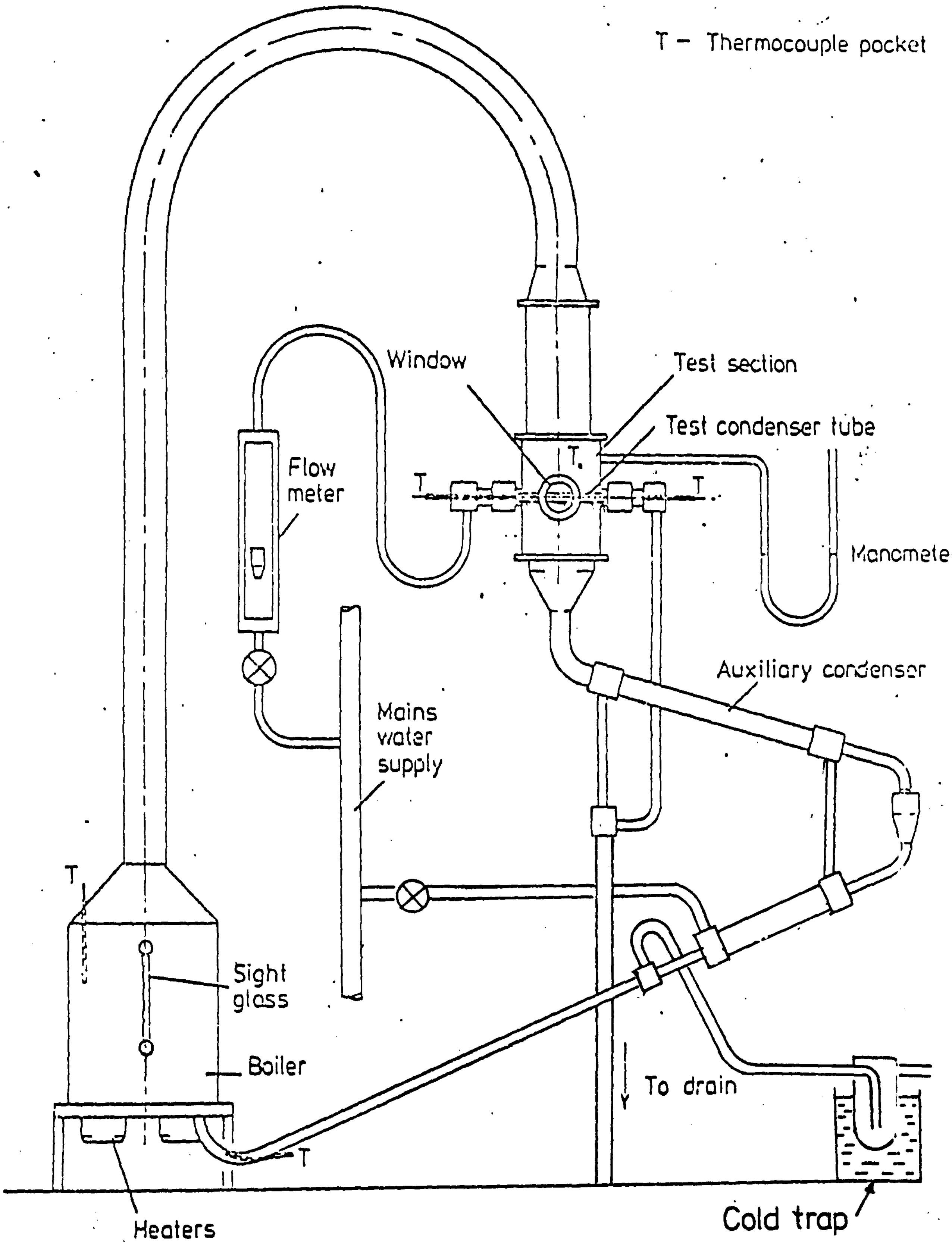

Fig.3-1 Line diagram of apparatus

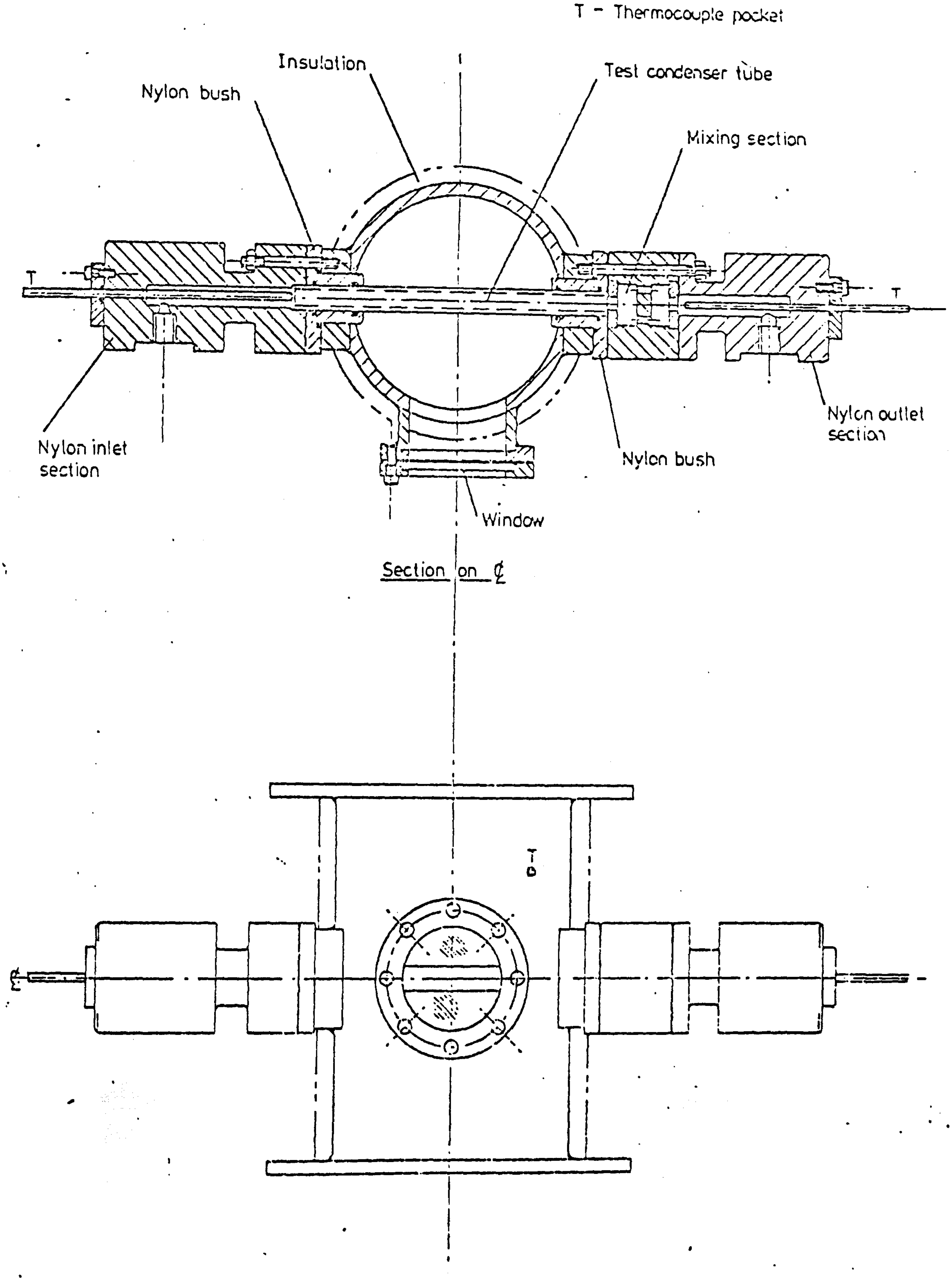

Fig.3-2 Line diagram of test section

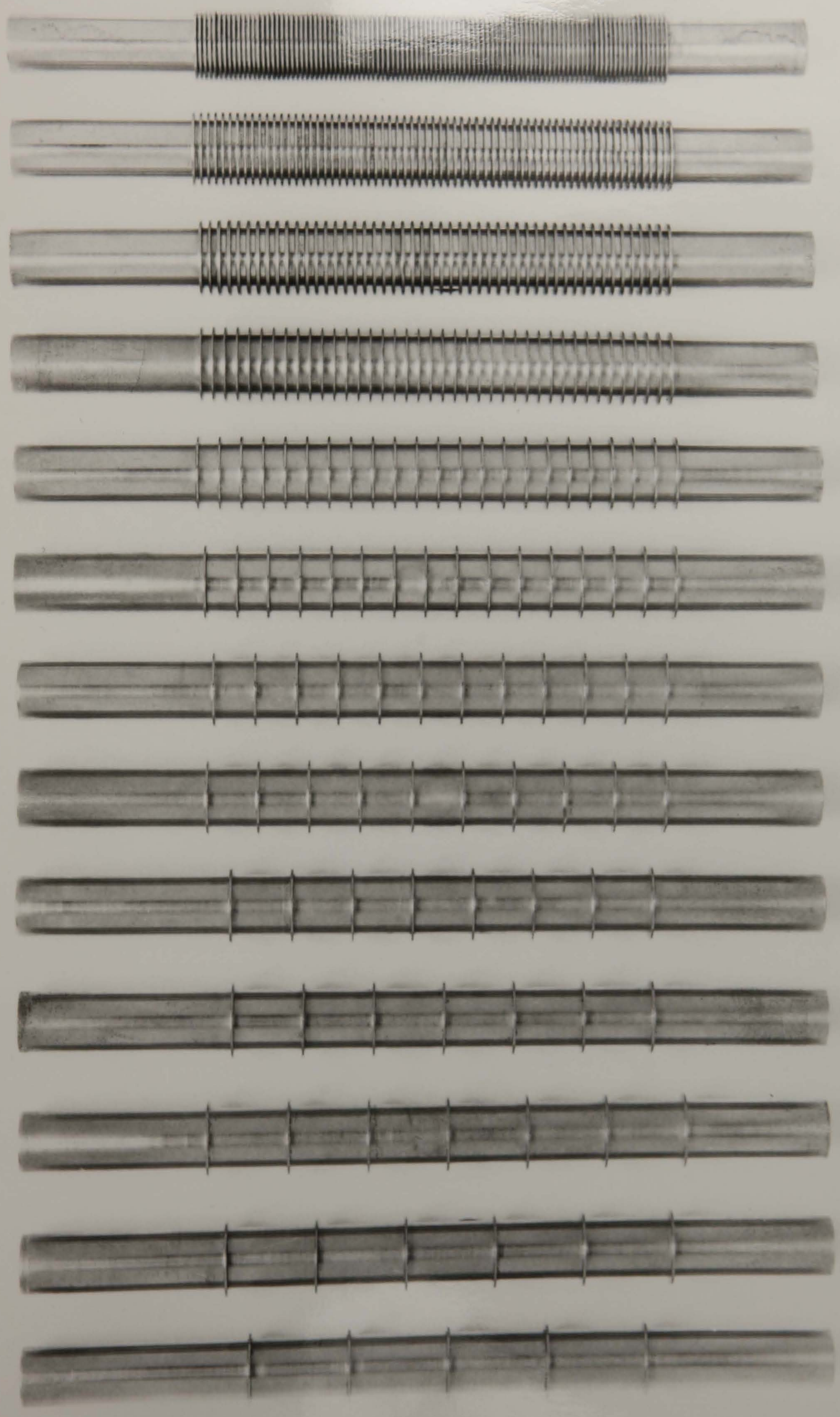

Fig. 3-3 Condenser tubes tested

Table 3-1 Heater resistances

Heater	1	2	3	4	
R/Ω	10.84	19.25	10.83	18.6	: Yau wt al. 35,36,37 present work for R-113
	18.0	11.2	17.0	11.8	: present work for ethylene glycol

Table 3-2 Geometry of condenser tubes used in present work

d_i = 9.78 mm
d_r = 12.7 mm
h = 1.59 mm
t = 0.5 mm

$\frac{b=p-t}{mm}$	Area ratio	$\frac{b=p-t}{mm}$	Area ratio
0.25	5.92	8.0	1.40
0.5	4.67	10.0	1.33
1.0	3.43	12.0	1.29
1.55	2.82	14.0	1.25
2.0	2.45	16.0	1.22
4.0	1.80	18.0	1.18
6.0	1.54	20.0	1.15

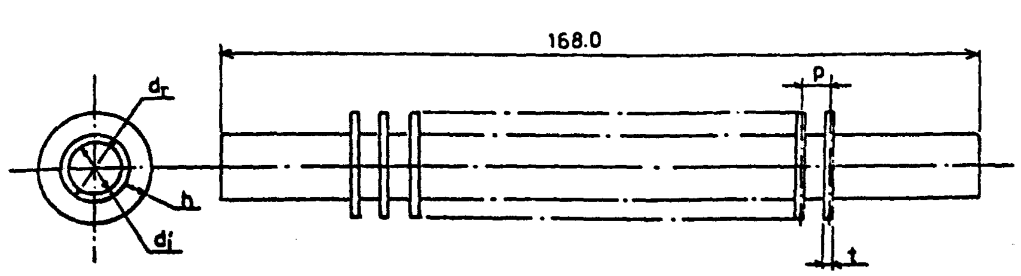

CHAPTER 4 RESULTS

4. Results

4.1 Determination of the vapour-side temperature

The tube wall temperature was not measured directly during experiments, because of difficulty of fitting a thermocouples in the walls of 13 finned tubes. Further the distortion of the isotherms in the tube wall and the thermal resistance caused by presence of wall thermocouples introduces additional uncertainty in the measured heat-transfer coefficients.

In an earlier investigation for steam [35,36,37], the coolant-side heat-transfer coefficient was at first evaluated by employing thermocouples in the wall of the smooth tube. The following "Sieder-Tate type" equation correlated the coolant-side heat transfer very closely:

$$Nu_c = 0.03\ Re_c^{0.8} Pr_c^{1/3} (\mu_c/\mu_w)^{0.14} \qquad (4\text{-}1)$$

The vapour-side wall temperature of the finned tubes in [35] was found by subtracting coolant-side (from eq.(4-1)) and wall resistances, on the basis of uniform radial conduction, from the measured overall thermal resistance given by:

$$U^{-1} = \frac{LMTD}{Q} \qquad (4\text{-}2)$$

The tube wall was regarded as extending to the root of fins so that the effect of fins and condensate are lumped together in the vapour-side heat-transfer coefficient.

In the present investigation, it was found for R-113 that results determined using eq.(4-1) as indicated above were not entirely satisfactory. Fig.4-1 shows the relation between heat flux and vapour-side temperature difference for the tube with fin pitch 1.0 mm. It can be seen that, when adopting eq.(4-1) for the coolant side, the heat flux seems to approach a finite value at zero temperature difference. It is thought that eq.(4-1) (determined using data for condensation of steam on an instrumented tube) may be less appropriate for other condensing fluids owing to differences in the relative magnitudes of the circumferential variation in tube wall temperature. When the vapour-side resistance dominates (e.g. R-113), the temperature profile is relatively flat [49,50], while when the coolant-side resistance dominates or when the coolant and vapour-side resistances are of similar magnitude, a strong variation in wall temperature results from the variation of the condensate film thickness around the tube.

In this investigation, an alternative calculation method has been used. In outline, the method is to select suitable function involving unknown "disposable" constants, to express the coolant-side and vapour-side temperature drops in terms of the relevant parameters. For a given run (tests at several coolant flow rates for a particular tube), the constants are determined by minimizing the sum of squares of residuals (difference between calculated and measured values of the vapour-to-coolant temperature difference). Details of the procedure are described below.

For coolant-side heat transfer, a Sieder-Tate type equation was used:

$$Nu_c = \tilde{a}\ Re^{0.8} Pr^{1/3} (\mu_c/\mu_w)^{0.14} \qquad (4\text{-}3)$$

where $\tilde{a}$ is an unknown to be found. The temperature difference between coolant and tube inside surface is then given by:

$$T_{wi} - T_c = \frac{Q d_i}{Nu_c k_c} \qquad (4\text{-}4)$$

The temperature difference between outside (i.e. at fin root diameter) and inside surface of tube was found by considering uniform radial conduction through a tube wall, i.e:

$$T_{wo} - T_{wi} = \frac{Q\ d_r}{2k_t} \ln\left(\frac{d_r}{d_i}\right) \qquad (4\text{-}5)$$

In the previous study [35,36,37], it was found that the Q-ΔT curves were fitted closely by equation of the form $Q=C\Delta T^n$. For the finned tubes in [35,36,37] values of n between 0.64 and 0.86 were found with no systematic dependence on fin spacing. The fits were negligibly less good when using a value of 0.75 (with appropriate values of the constant n) throughout. In the present work, a "Nusselt type" equation was employed for vapour-side heat transfer:

$$Nu_v=\tilde{b}\left(\frac{\rho^2 g h_{fg} d_r^3}{k\mu\Delta T}\right)^{\frac{1}{4}} \qquad (4-6)$$

where $\tilde{b}$ is an unknown constant to be found.

This is thought to be an improvement on the equation $Q=C\Delta T^{3/4}$ in that it should account for property variation in an approximate way, even though it does noy include surface tension whose effect would be incorporated in $\tilde{b}$. Eq.(4-6), if strictly valid, would indicate that eq.(4-6) has the advantage that it enables an "enhancement ratio" $Nu/Nu_{plain}=\tilde{b}/\tilde{b}_{plain}$ would be independent of Q or ΔT.

The temperature difference between vapour and wall is then given by:

$$T_v-T_{wo}=\frac{Qd_r}{Nu_v k} \qquad (4-7)$$

All values except the "disposable" constants $\tilde{a}$ and $\tilde{b}$ are determined experimentally, so that the overall temperature difference between vapour and coolant may be expressed as a linear equation:

$$\Delta T_{obs}=aC_1+bC_2+C_3+\varepsilon \qquad (4\text{-}8)$$

where C_1, C_2 and C_3 are given by properties, the heat flux and the tube dimensions, $a=\hat{a}^{-1}$ and $b=\tilde{b}^{-4/3}$ and ε is the deviation of ΔT.

In the eqs.(4-3) to (4-8), μ_w was evaluated at T_{wi}, hfg at T_v, coolant properties at the arithmetic mean of the coolant inlet and exit temperatures, and the condensate properties at:

$$T^{*}=(1/3)T_v+(2/3)T_{wo} \qquad (4\text{-}9)$$

Values of a and b (and hence $\hat{a}$ and $\tilde{b}$) are then found by the "least squares method", such that:-

$$\frac{\partial}{\partial a}\sum(\Delta T_{obs}-\Delta T_{cal})^2=0 \qquad (4\text{-}10)$$

$$\frac{\partial}{\partial b}\sum(\Delta T_{obs}-\Delta T_{cal})^2=0 \qquad (4\text{-}11)$$

Eqs.(4-10) and (4-11) lead to the following equations:

$$a\sum C_1^2+b\sum C_2C_1+\sum C_3C_1=\sum \Delta T_{obs}C_1 \qquad (4\text{-}12)$$

$$a\sum C_1C_2+b\sum C_2^2+\sum C_3C_2=\sum \Delta T_{obs}C_2 \qquad (4\text{-}13)$$

which may be solved for a and b.

In order to evaluate the properties at the temperatures (initially unkown) indicated above the following iterative procedure was adopted:-

(1) The tube inner and outer wall temperature are set initially to be equal to the coolant inlet temperature

(2) The coolant viscosity μ_W and condensate properties are calculated at the wall temperature and the temperature given by eq.(4-9).

(3) Then constants C_1 , C_2 and C_3 are calculated and first estimates $\tilde{a}$ and $\tilde{b}$ are obtained from eqs.(4-12) and (4-13).

(4) New values of inner and outer wall temperatures are given by eqs.(4-3) and (4-5) with the first estimate of $\tilde{a}$.

This procedure repeated until the variance (ABS(new value - old value)/ new value) between new and old values of both a and b became less than 5×10^{-4} . Properties are reevaluated at each step at the new temperatures. It was comfirmed that essentially the same values of $\tilde{a}$ and $\tilde{b}$ were obtained when a smaller convergence test value was used.

The reliability of this method was examined by using it also with earlier smooth-tube data for steam [35,36,37]. The constant $\tilde{a}$ was found to be 0.0298 by the method described above. This may be compared with 0.03 as given by experiments using the instrumented plain tube in [35,36,37]. Evidently, in the case of steam the present method gives essentially the same vapour-side temperature drop as that found when using eq.(4-1) for the coolant side.

Fig.4-1 illustrates the fact that more reasonable results are found for R-113 using this technique than when using $\tilde{a}$=0.03 for all tests as in [35,36,37]. For each individual data points at a particular coolant flow rate , the vapour-side temperature difference was found by subtracting the coolant-side temperature drop (as given by eqs.(4-3) and (4-4) with the determined value of $\tilde{a}$) and that across the wall (as given by equation (4-5)) from the measured overall temperature differences. The line through the data in Fig.4-1 is given by eq.(4-6) with $\tilde{a}$=0.041. Values of $\tilde{a}$ and $\tilde{b}$ of all test are in Table 4-1. It may also be noted (as will be seen later) that the present data agreed with other recent result for R-113 [52] fcr similar fin geometry.

A similar data analysis procedure has been used by Nobbs [53] and described as a "modified Wilson plot" method.

4.2 Experimental results for R-113

All tests were carried out at one particular input power, giving a vapour velocity at approach to the test condenser tube of 0.24 m/s.

Data for which the coolant-temperature rise corresponded to a thermo-emf less than 15 μV were judged to be of marginal accuracy (precision of measurement 1 μV) and are not reported. The discarded data are mainly those with the plain tube and tubes with large fin spacing for the higher coolant velocities.

Fig.4-2 shows the overall heat-transfer coefficient versus coolant velocity. To avoid confusion the lower overall heat-transfer coefficients for b>2 mm and the higher values for b≤2 mm are shown separately. It may be seen that the overall heat-transfer coefficient increased with decreasing fin spacing for b=19.5 mm to 0.5 mm, but the value at b=0.25 mm was slightly less than that at b=0.5 mm, i.e. an optimum fin spacing exists. The increase of coolant-side heat-transfer coefficient, with increasing coolant velocity, leads to the observed increase in total overall heat-transfer coefficient with coolant velocity.

Since the enhancement is much higher at the higher fin density, the vapour-side performance is shown in Figs.4-3 and 4-4 only for the tubes with $b \leq 2$ mm and, for comparison, for the plain tube. The lines are given by eq.(4-6) with the determined values of $\tilde{b}$ (see table 4-1) and the condensate properties evaluated using eq.(4-9) with a mean (over all data) vapour temperature of T_v=321 K. The good agreement with the Nusselt theory for the plain tube and with the recent data of Honda [52] for a finned tube with similar geometry (see Fig.4-5) lends support to the reliability of the data and method of processing. It may be seen that significant enhancement is obtained with all finned tubes, the best being that with fin spacing b=0.5 mm.

4.3 Experimental results for ethylene glycol

As in the case of R-113, all tests were carried out with the same heater power which gave a vapour velocity at approach to the test condenser tube of 0.36 m/s.

In this case the coolant temperature rise corrsponded to a thermo-emf greater than 15 μV so that no data points were discarded as in the case of R-113. However, as will be seen later, at low coolant flow rates, boiling occured on the inside surface of the condenser tube. In these circumstance there is considerable doubt as to the form of the coolant-side correlation, and no attempt has been made to determine vapour-side coefficient.

Fig.4-6 shows the overall heat-transfer coefficient versus coolant velocity. It can be seen that the overall heat-transfer coefficient did not, in general, increase monotonically with coolant velocity. As will be explained, this behaviour was due to boiling at the coolant-side wall at low coolant velocity due to the fact for ethylene glycol the vapour temperature is around 200 °C at atmospheric pressure. When the wall temperature becomes higher than the saturation temperature of the coolant (water), nucleate boiling may occur at the wall, even though the mean temperature of coolant is less than the saturation temperature.

The following equation has been given in [54] for the wall temperature, at which the surface boiling occurs:

$$T_{wi} = T_s + \left\{ \frac{8 \sigma T_s \upsilon_g}{k_c h_{fg}} Q \right\}^{\frac{1}{2}} \qquad (4-14)$$

where the coolant properties are evaluated at the saturation temperature.

Fig.4-7 shows apparent (i.e. as calculated by the procedure outline in section 4.2) vapour-side results for ethylene glycol. Also shown is the vapour-side temperature difference, at which the boiling occurs, according to eq.(4-14). Evidently, in the presence of local surface boiling the Sieder-Tate type equation (see eq.(4-3)) will no longer adequately represent the coolant-side heat transfer. The appearance of Fig.4-7 may be explained as follows. At high coolant velocity where the coolant side temperature drop is small (high ΔT) the wall temperature is low and no boiling occurs. As the coolant velocity is decreased (Q and hence ΔT decreasing) the wall temperature rises until eventually boiling occurs according to eq.(4-14). Under these conditions the coolant-side heat-transfer becomes more dominated by boiling than by the single-phase correlation used in determining these data.

The line on Fig.4-7 indicating onset of boiling was determined using eq.(4-14) as follows. Assuming the saturation temperature of coolant T_s to be 100 °C, the inner wall temperature is evaluated by eq.(4-14) for a given heat flux. The wall outer temperature at the fin root is then given by eq.(4-5). The vapour-side temperature difference is found subtracting the wall outer temperature found from the measured vapour temperature. The change in behaviour of the curves are clearly in good agreement and testifies to the validity of the explanation. Obviously the data to the left of this line are invalid. Since we do not have a suitable form of coolant-side correlation for the boiling region, these data cannot be used to determine the vapour-side temperature difference.

Fig.4-8 shows the overall heat-transfer coefficient versus coolant velocity, omitting the data points for which ΔT was less than that for which eq.(4-14) predicts onset of boiling as indicated above. The fin spacing which gave maximum heat-transfer coefficient was b=1.0 mm. For the plain tube and tubes with relatively large fin spacing the overall heat-transfer coefficient varies only slightly with coolant velocity since, in this case, the heat-transfer resistance is dominated by the vapour side. Thus with increasing in coolant velocity the coolant-side resistances leading to a decrease in overall resistance and consequently increase of condensation rate. The increase in condensation rate, however, leads to an increase in the vapour-side resistance and consequently to a higher overall resistance.

The vapour-side heat transfer is shown in Fig.4-9 and Fig.4-10. In these figures, lines are given by eq.(4-7) using a mean vapour temperature T_v=472 K. Again, it is seen that the best tube was that with b=1.0 mm and the plain tube data are in good agreement with Nusselt theory.

4.4 Evaluation of heat-transfer enhancement

4.4.1 Overall coefficient enhancement

Before considering the more useful concept of vapour-side enhancement, it is of interest to examine the overall coefficient enhancement at a given coolant velocity. In the present investigation, the overall coefficient was the directly-measured quantity while the vapour-side coefficients invoked additional assumptions or approximations as given above. Since for R-113 reliable plain tube data were only obtained for relatively low coolant velocity, direct comparison can only be made at the same coolant velocity for relatively low values. Alternatively, the approximate representatives of the vapour and coolant-side heat transfer indicated in the previous section may be used with the experimental data to provide an approximate relation between heat flux and vapour and coolant conditions (T_v, u_c and T_{in}). Using eqs(4-3) and (4-6) for Nu_c and Nu_v with the values found for $\hat{a}$ and $\tilde{b}$, we may obtain the overall coefficient from:

$$U^{-1}=\alpha_c^{-1}+R_w+\alpha_v^{-1} \tag{4-15}$$

$$\alpha_c=Nu_c k_c/d_i$$

$$R_w=d_i/(2k_t \ln(d_r/d_i))$$

$$\alpha_v=Nu_v k/d_r$$

So that for given values of T_v, u_c and T_{in} and appropriate iterative procedure to obtain the liquid properties as indicated in section 4.2, we may obtain U.

Fig.4-11 shows enhancement ratio of overall heat-transfer coefficient of finned tubes to that of plain tube for R-113 and ethylene glycol. For comparison the earlier data of Yau et al [35,36,37] for the same tubes have also been analysed in this way and the results are indicated in Fig.4-11. The coolant velocity used in the calculation is 4 m/s and coolant inlet temperature is 293 K. The vapour temperatures are respectively 321 K for R-113, 472 K for ethylene glycol and 373 K for steam (mean of the experimental values used). The maximum enhancement ratio occurs at fin spacing of 0.5 mm, 1.0 mm and 1.5 mm for R-113, ethylene glycol and steam respectively. These maximum values are 5.1, 4.3 and 1.6 for R-113, ethylene glycol and steam respectively. These results are indicative of the overall enhancement that can be obtained for water-cooled finned condenser tubes but the particular values relate to the present coolant-side conditions (inlet temperature, velocity and inside diameter).

4.4.2 Vapour-side enhancement

In earlier investigations, enhancement ratios (vapour-side coefficient for finned tube / vapour-side coefficient for plain tube) have been given either for the same ΔT or for the same Q and at the same specified value of one of these parameters. The fact that both finned and plain tube data have been found in the present investigation to be adequately represented by eq.(4-6) enables specification of enhancement ratios independent of the values of ΔT and Q. Thus:

for the same ΔT: $$\frac{\alpha}{\alpha_{plain}} = \frac{\tilde{b}}{\tilde{b}_{plain}} \qquad (4\text{-}16)$$

for the same Q: $$\frac{\alpha}{\alpha_{plain}} = \left(\frac{\tilde{b}}{\tilde{b}_{plain}}\right)^{4/3} \qquad (4\text{-}17)$$

In the present work we give enhancement ratios (E) for the same values of ΔT, and take value of $\tilde{b}_{plain}$ of 0.74 and 0.78 for R-113 and ethylene glycol respectively as given by the plain tube data. Additionally, the same processing procedure was adopted for the earlier data [35,36,37] for steam. For the plain tube this gave values of $\tilde{b}$ of 0.907, 0.846 and 0.804 for vapour velocities of 1.1, 0.73 and 0.52 m/s respectively. The excess of $\tilde{b}$ over 0.728 indicates the effect of vapour shear stress.

Fig.4-12 shows the vapour-side enhancement ratio versus the fin spacing. As fin spacing decreases, the enhancement ratio at first increases. For fin spacings less than 4 mm the enhancement ratios exhibit maxima, which occured at around 0.5 mm for R-113, around 1.0 mm for ethylene glycol and 1.5 mm for steam. For smaller fin spacing, the enhancement ratio drops sharply for R-113 and ethylene glycol. It may be noted that enhancement ratios were significantly larger than the area ratio, except at the lowest fin spacing and for steam.

There was a moderate difference between the enhancement ratios for R-113 and ethylene glycol for fin spacing larger than 4 mm, although the R-113 data were clearly larger than those of ethylene glycol. Enhancement ratios for steam were smaller than those for the other fluids but differences between the values for the three fluids became smaller for fin spacing more than 8 mm. For fin spacing less than 4 mm, the difference is more significant. The largest enhancements are 7.5 at a fin spacing of 0.5 mm for R-113 and 5.2 at a fin spacing of 1.0 mm for ethylene glycol and 3.0 at a fin spacing of 1.5 mm for steam. Note that for steam only the data for a vapour velocity of 1.1 m/s have been plotted. The enhancement ratios for the other velocities used in [35,36,37] are closely similar.

4.5 Comparison with the earlier theoretical models

Comparisons with the models presented by Beatty and Katz [29], Owen et al.[41] and Rudy et al.[46] are made for the present results for $b \leq 2$ mm. Fig.4-13 shows comparisons for R-113. There are large discrepancies and, in all cases, systematic dependence on fin spacing; the quantity $\alpha_{cal}/\alpha_{obs}$ increases, for all three models, with decreasing fin spacing. The most satisfactory model is that of Rudy et al. which underesimates the heat-transfer coefficient by about 40 % at fin spacing 2 mm and overestimates by about 25 % at fin spacing 0.25 mm, the data for the intermediate fin spacings being predicted within these limits.

Fig.4-14 shows comparisons for ethylene glycol. The models of Beatty and Katz, and Owen et al. overpredict for the higher fin densities, b=0.25 mm and 0.5 mm, but underpredict for lower fin density. For example, vapour-side heat-transfer coefficients at a fin spacing 0.25 mm are overpredicted by a factor of 2.5 (not included in Fig.4-14) by the Beatty and Katz model and by a factor of 1.8 by the Owen et al. model. On the other hand, the Rudy et al. model underestimates the heat transfer for the high fin density. The Rudy et al. model does not include heat transfer in flooded region, so that for completly flooded case, i.e. for a fin spacing 0.25 mm, zero heat transfer would be predicted. For fin spacings 1.0, 1.5 and 2.0 mm, the Rudy et al. model gives good predictions.

Fig.4-15 shows comparisons for steam data. All models overpredict the heat transfer coefficient. The Beatty and Katz model overestimates by between 20 and 250 % (not indcluded in Fig.4-15). The Owen et al. model predicts by about 10 % at b=1.5 mm and by about 25 % at b=2.0 mm. Again the Rudy et al. model would give zero heat transfer for b=0.25 mm and 0.5 mm because of the neglect of heat transfer for the completely flooded tubes ($b \leq 0.5$ mm). For the other tubes, the Rudy et al. model overestimates by 20 % to 90 %.

It is apparent that none of the above simpler models represents the data adequately, i.e. they do not predict the correct dependence on geometry (fin spacing) and fluid properties. Comparison with the more complex theory of Honda et al.[49], requiring extensive numerical procedures, have not made. However, provisonal calculations supplied by Honda [52] indicated that this model gives the correct general dependence on fin spacing and that it underestimated the present vapour-side heat-transfer coefficient for R-113 by between 15 and 35 %. For ethylene glycol the data were said to be underestimated by up to 25 % for all tubes except that with b=0.5 mm. In this case the model overestimated by 25 %. For steam data of Yau et al. [35,36] the model was said to overpredict the vapour-side heat transfer by up to 25 %, except at b=2.0 mm where it overestimated by 60 %.

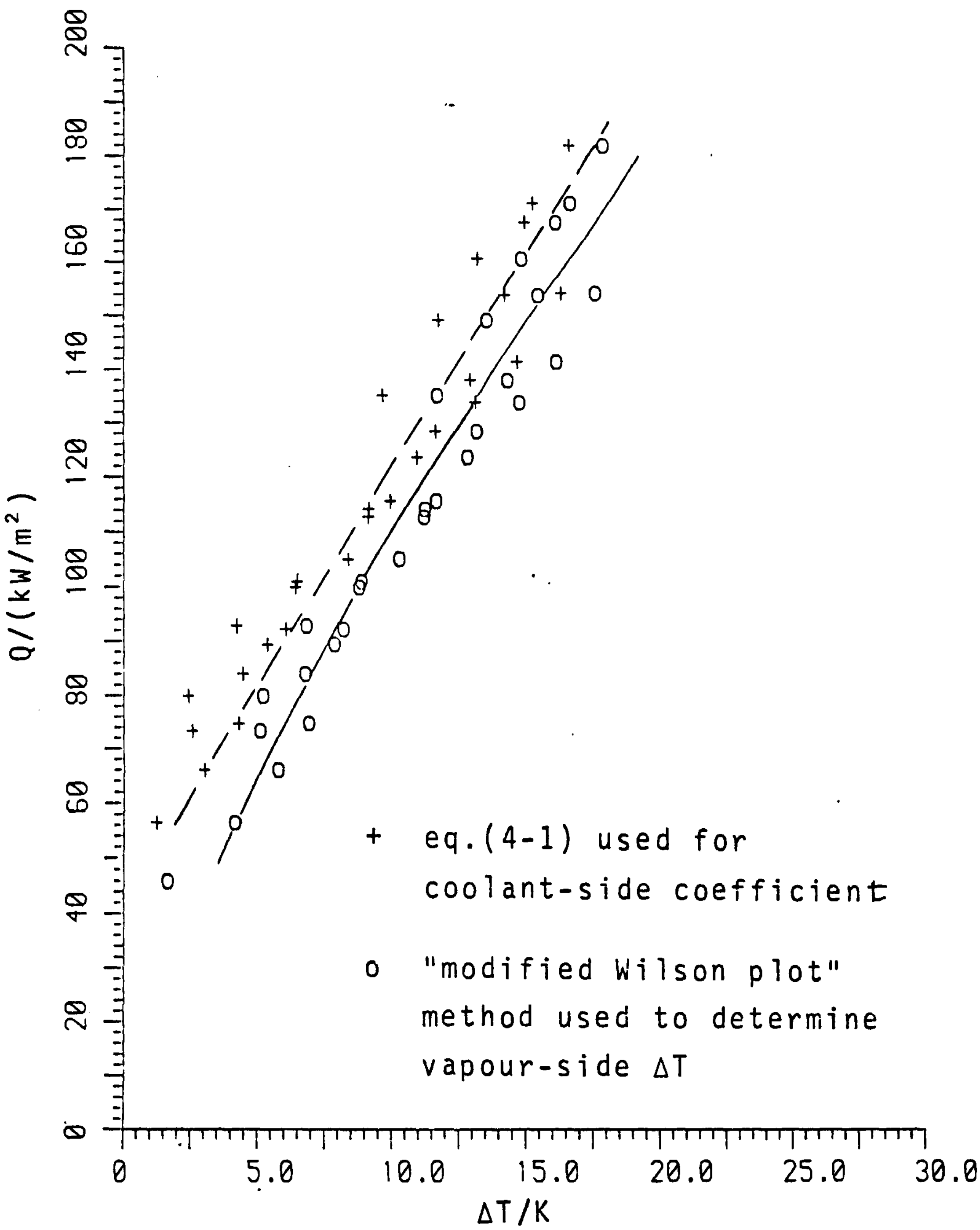

Fig.4-1 Comparison between vapour-side condensation of R-113 on finned tube (pitch=1.0 mm) evaluated by different methods

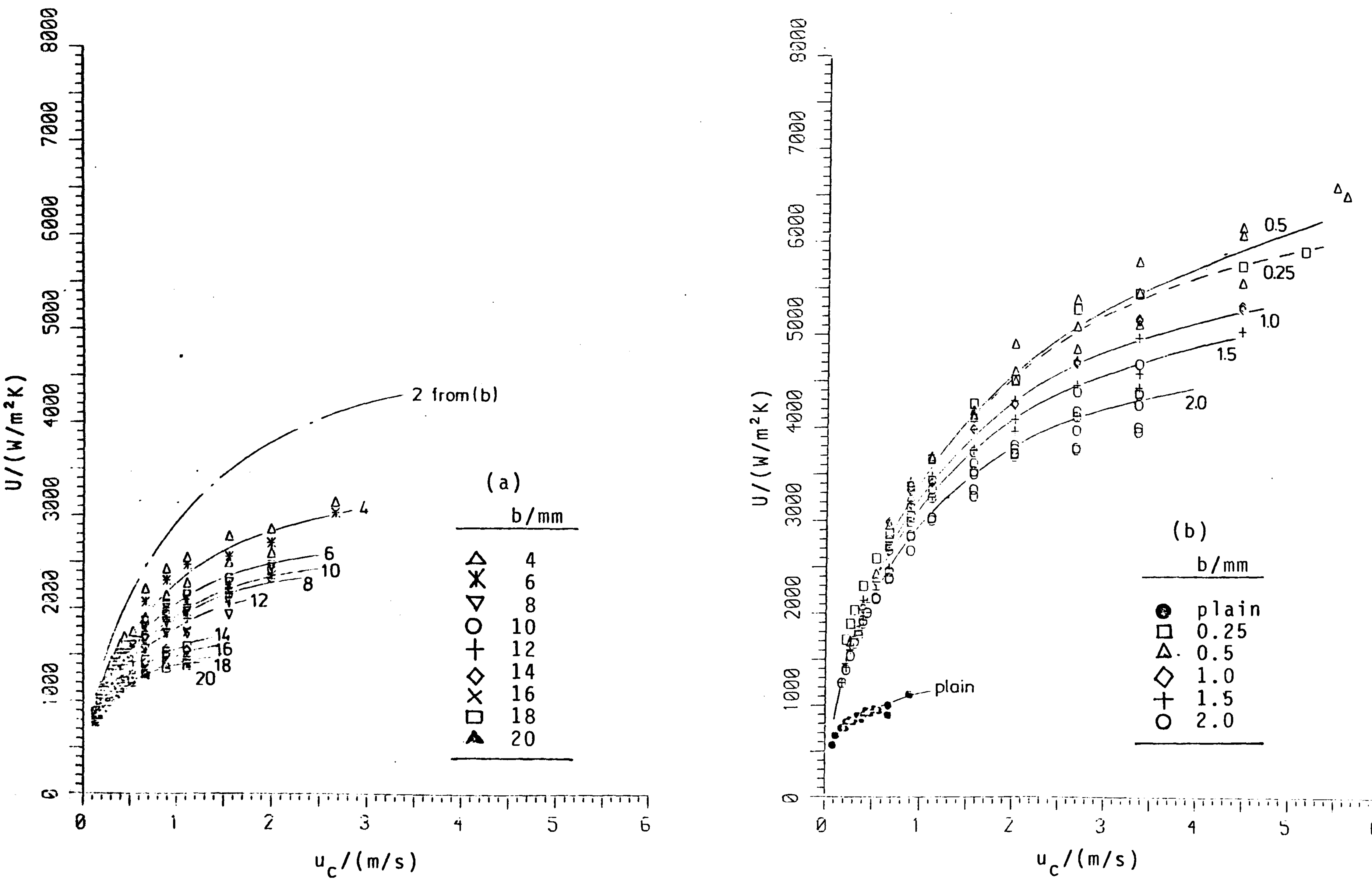

Fig.4-2 Overall heat-transfer vs coolant velocity coefficient for R-113

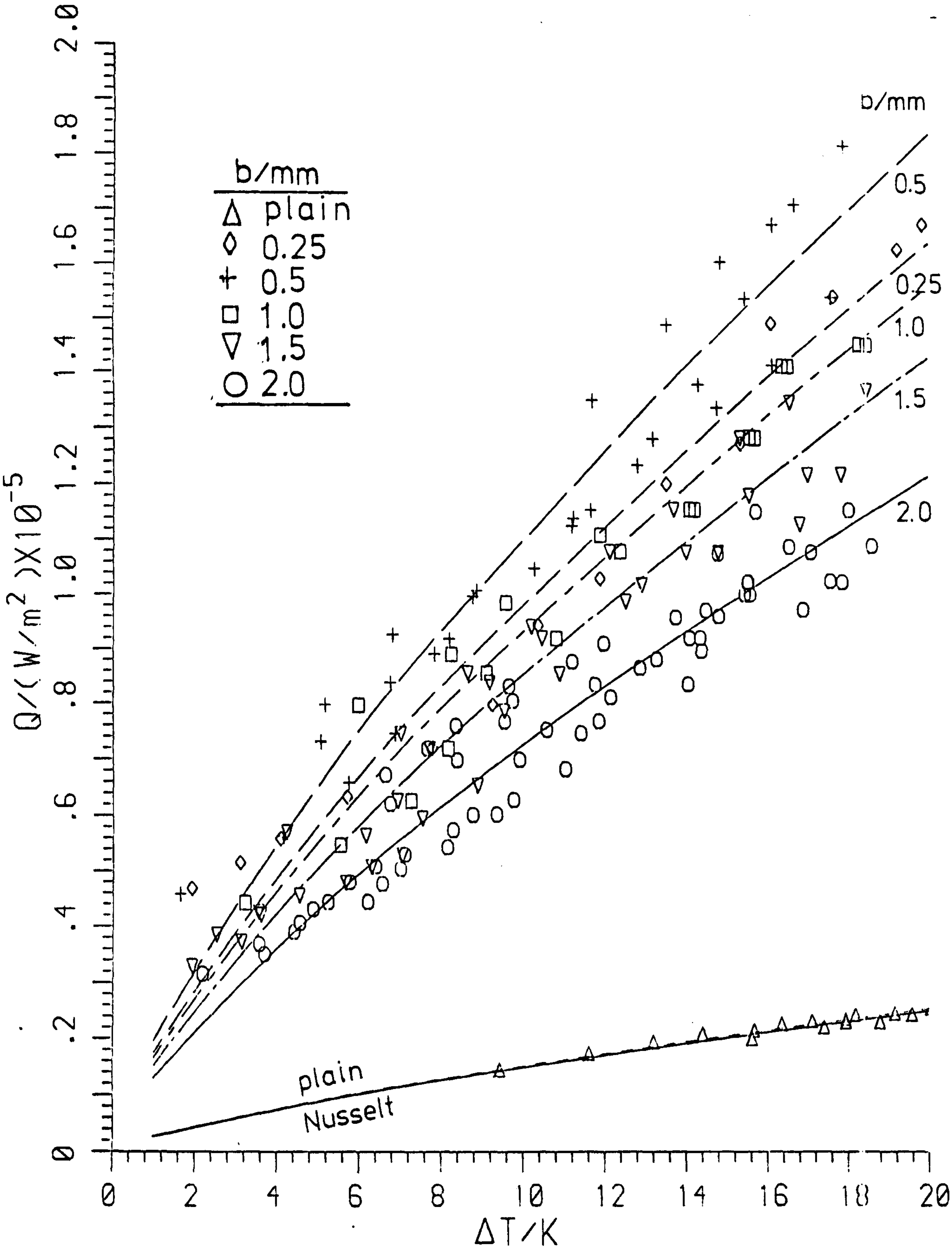

Fig.4-3 Heat flux vs vapour-side temperature difference for R-113

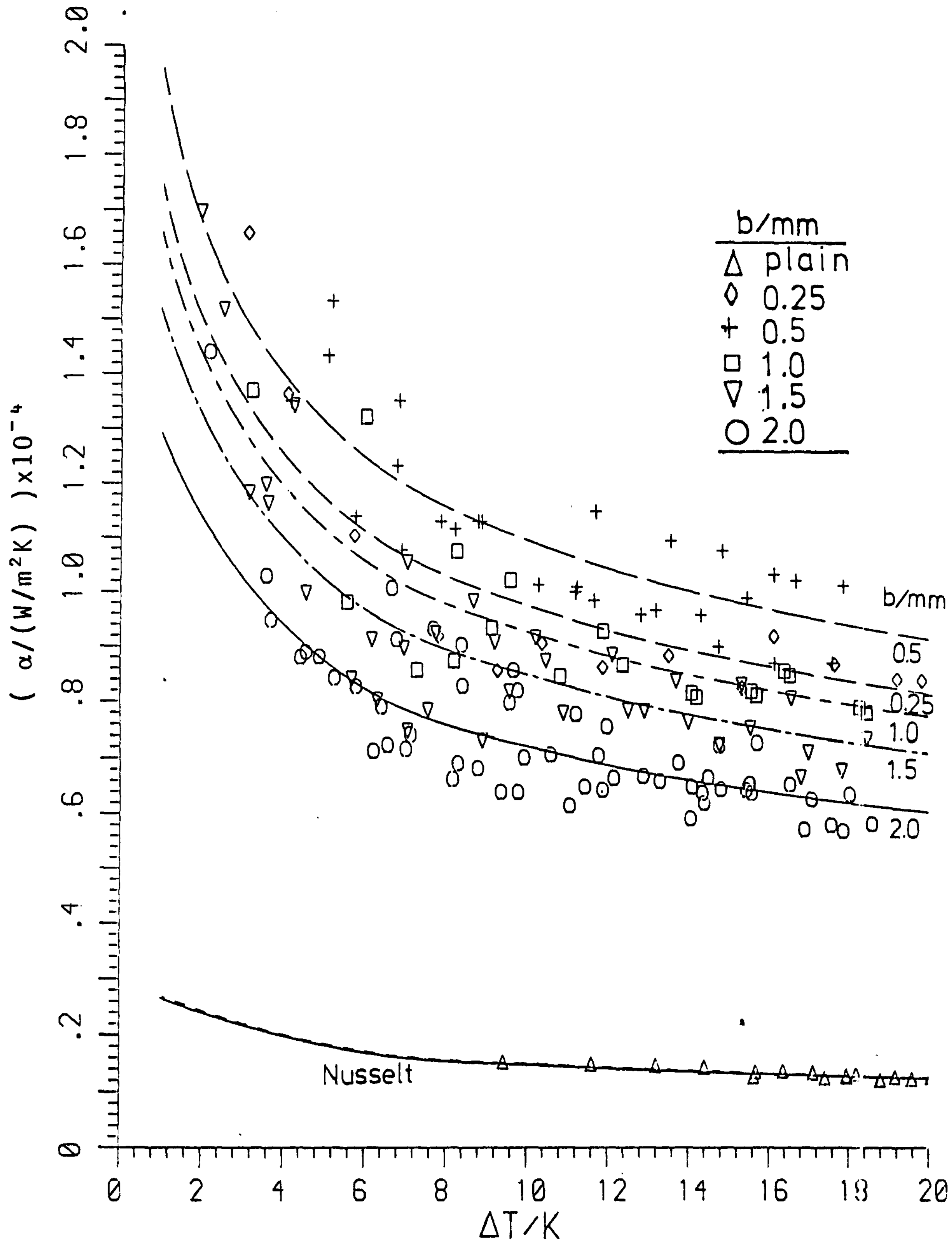

Fig.4-4 Realation between vapour-side heat-transfer coefficient and temperature difference for R-113

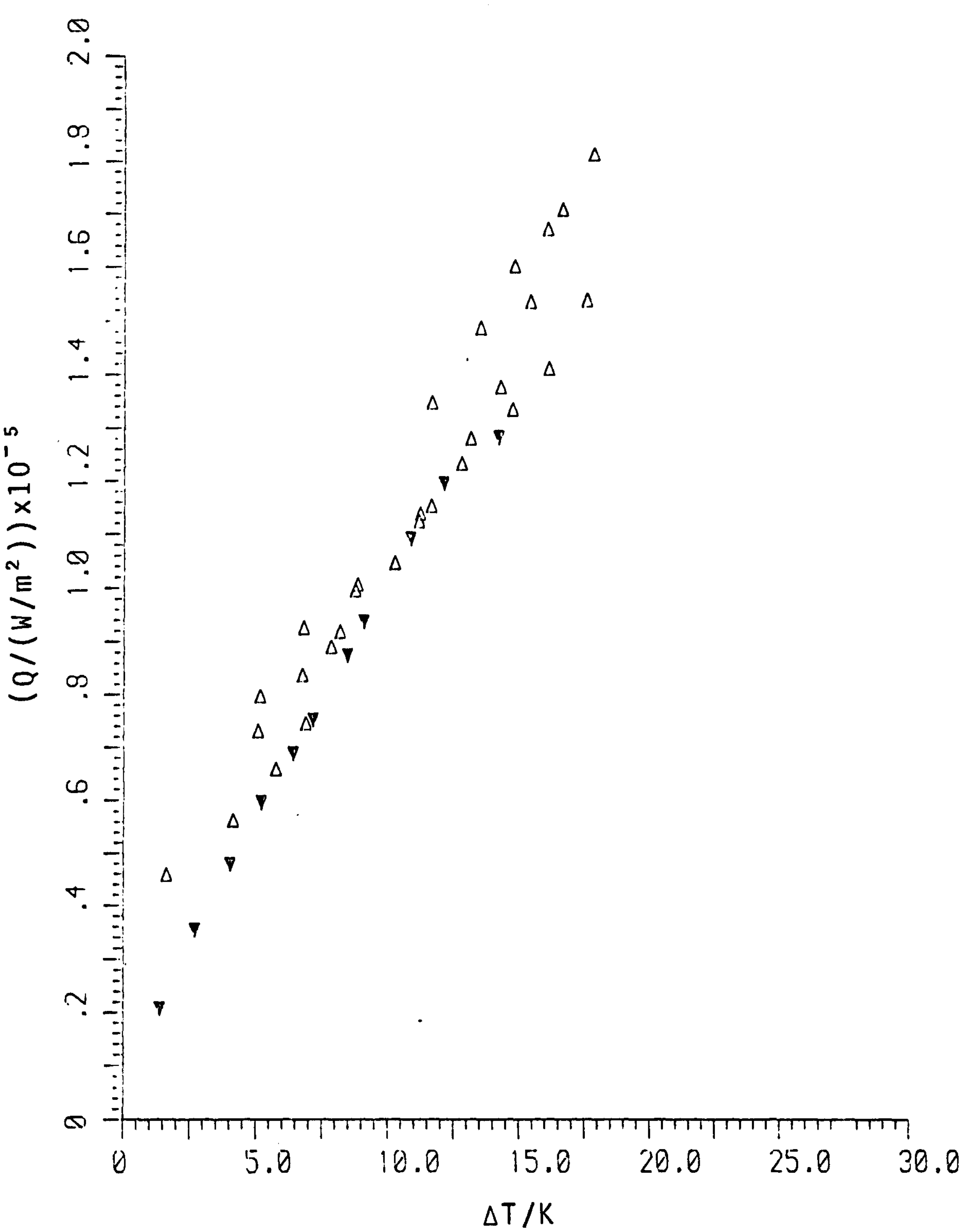

Fig 4-5 Condensation of R-113. Comparison of present results with those of Honda [52] for similar tube and fin geometries.

dimension /mm	d_r	p	b	h	t
Δ QMC data	12.7	1.0	0.5	1.59	0.5
▼ Honda	15.77	0.98	0.47	1.46	0.51

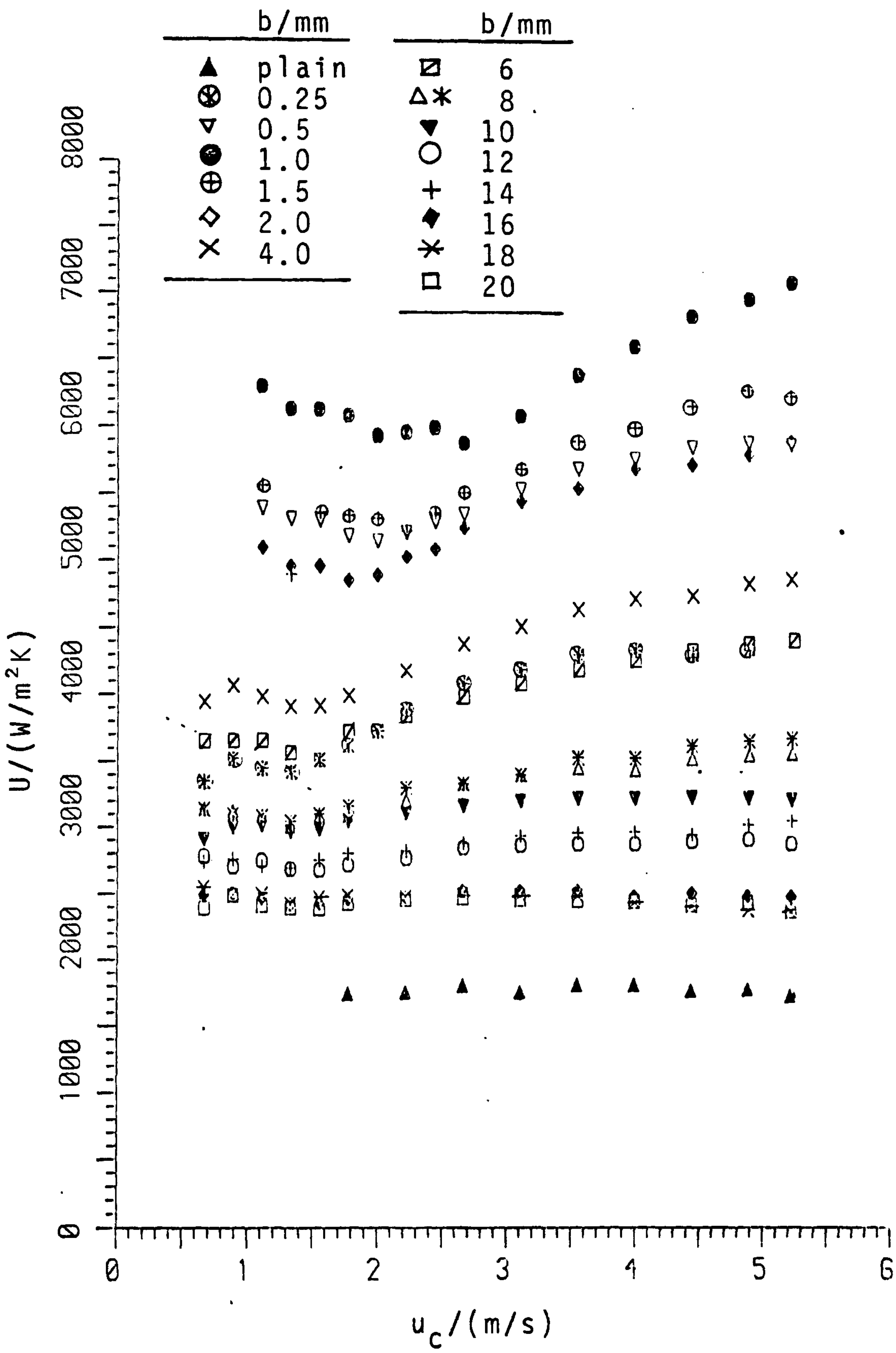

Fig.4-6 Overall heat-transfer coefficient vs coolant velocity for ethylene glycol

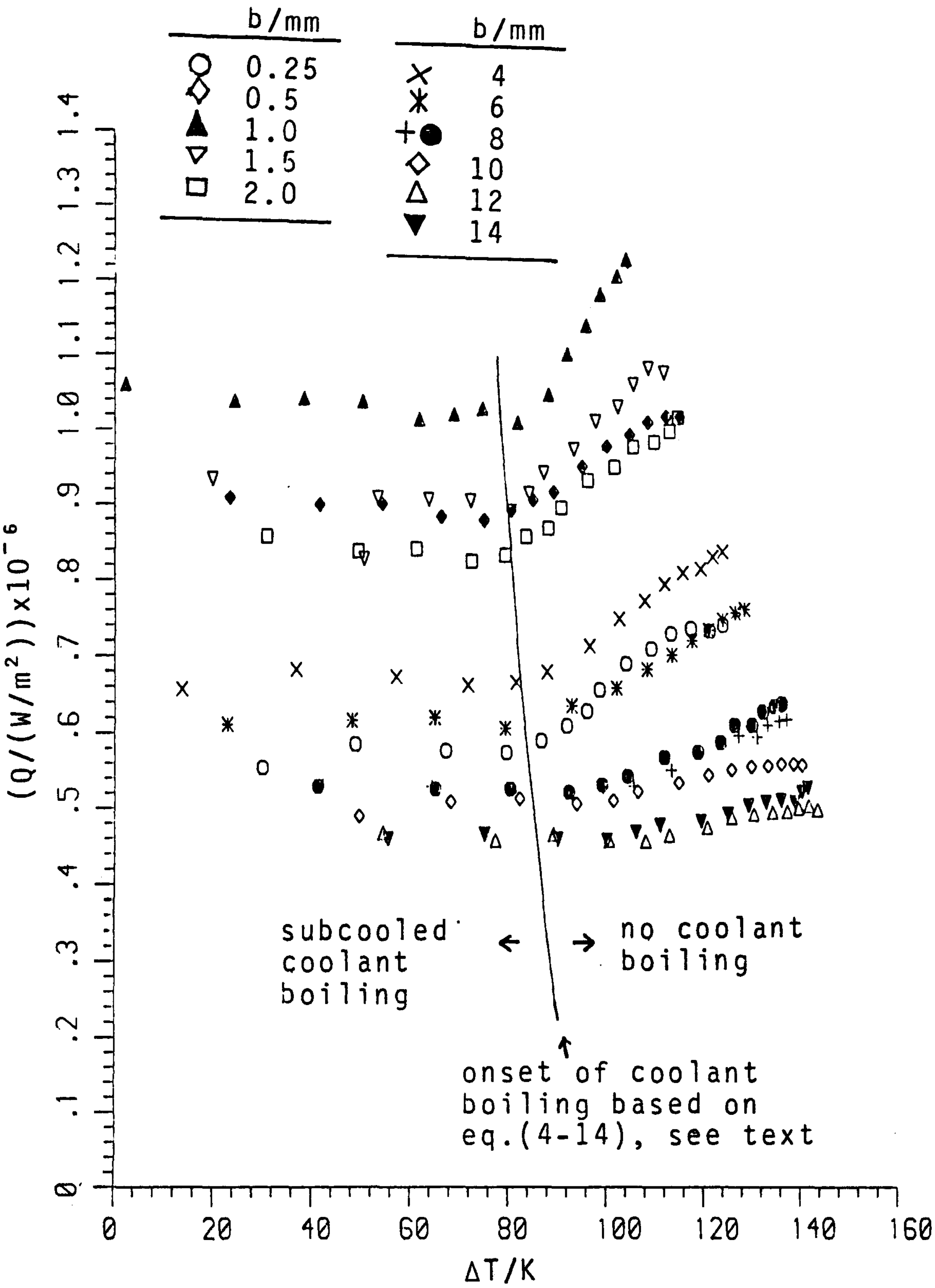

Fig.4-7 Heat flux vs vapour-side temperature difference for ethylene glycol

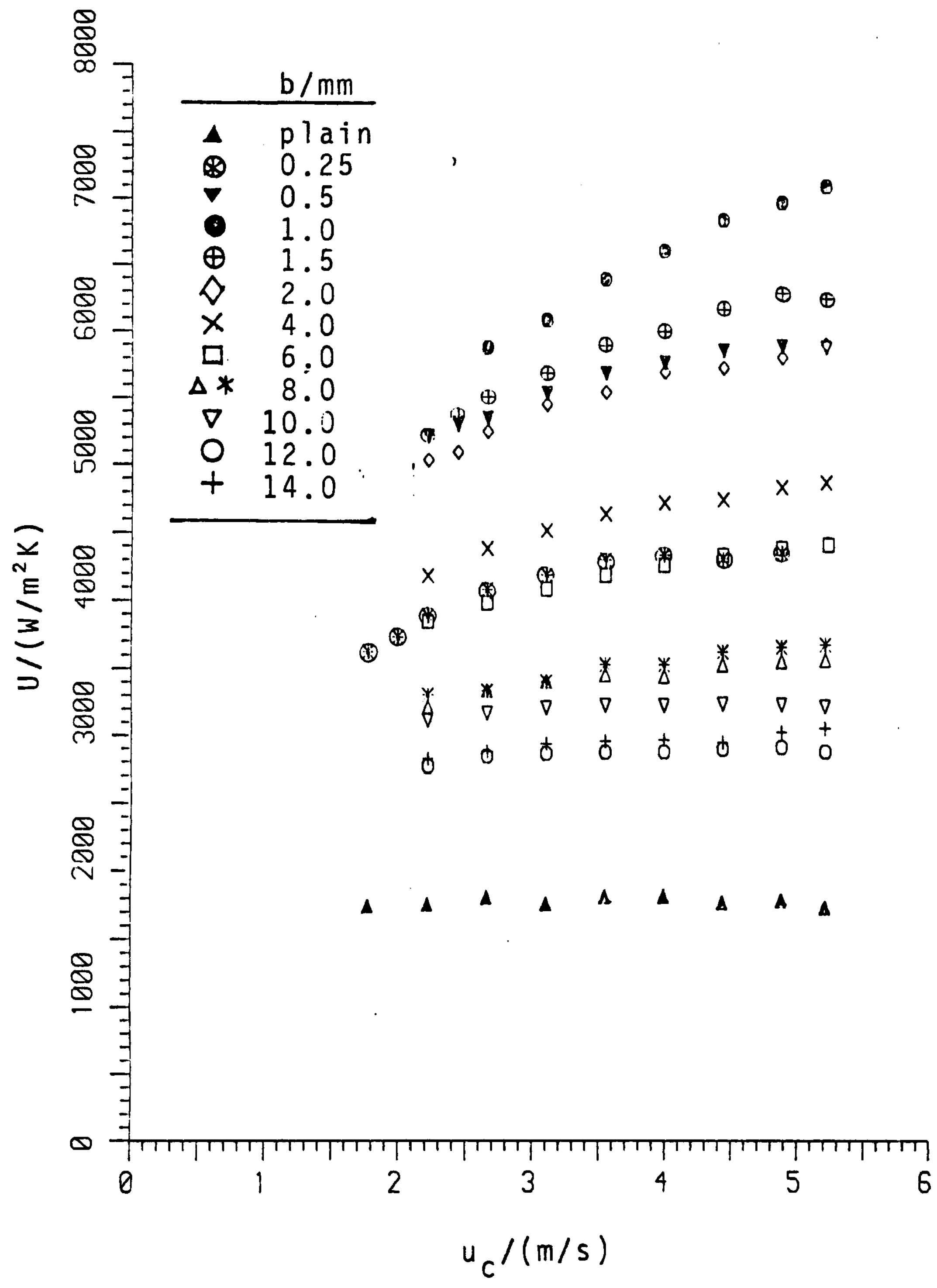

Fig.4-8 Overall heat-transfer coefficient vs coolant velocity for ethylene glycol used in determination of vapour-side coefficient

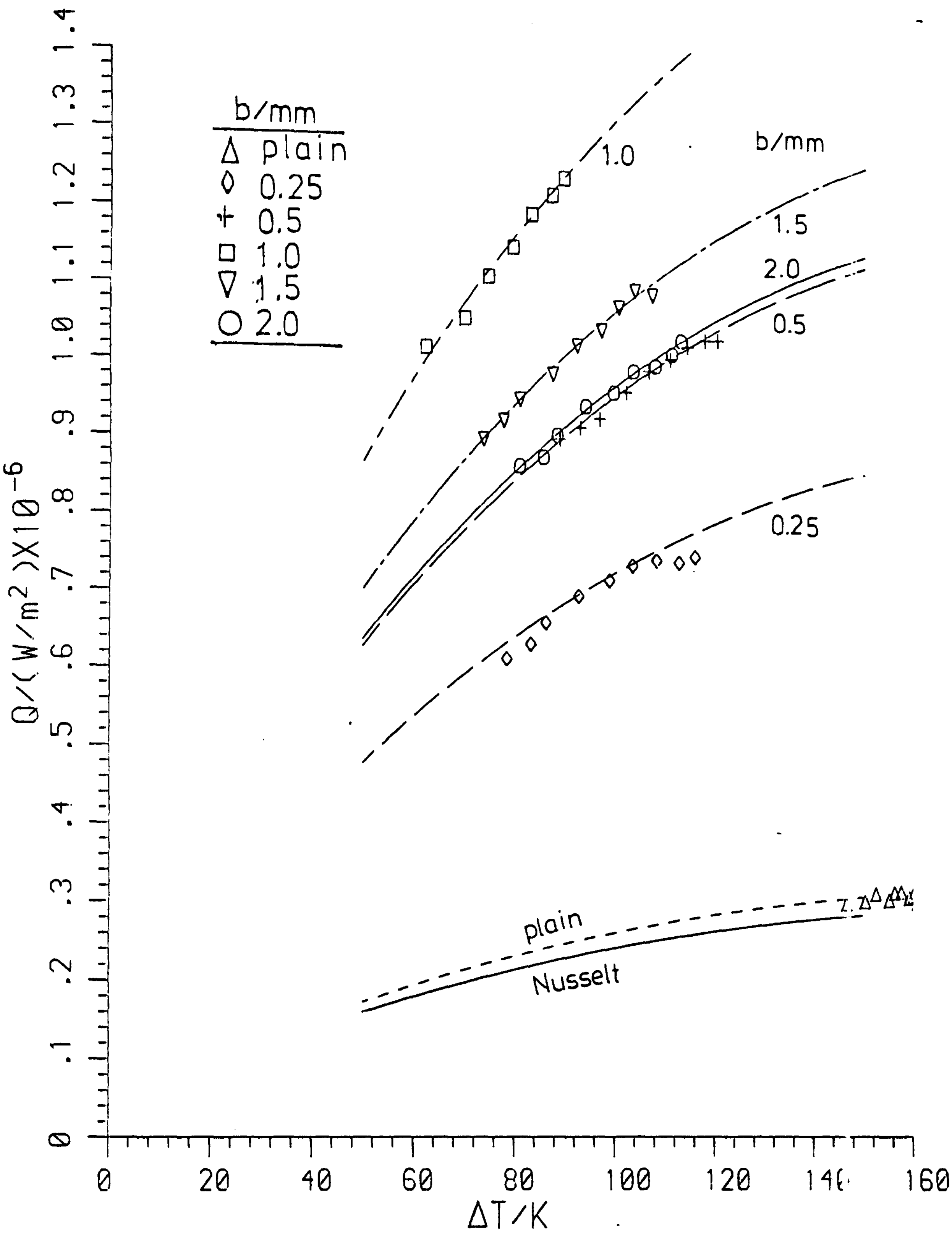

Fig.4-9 **Heat flux vs vapour-side temperature difference for ethylene glycol**

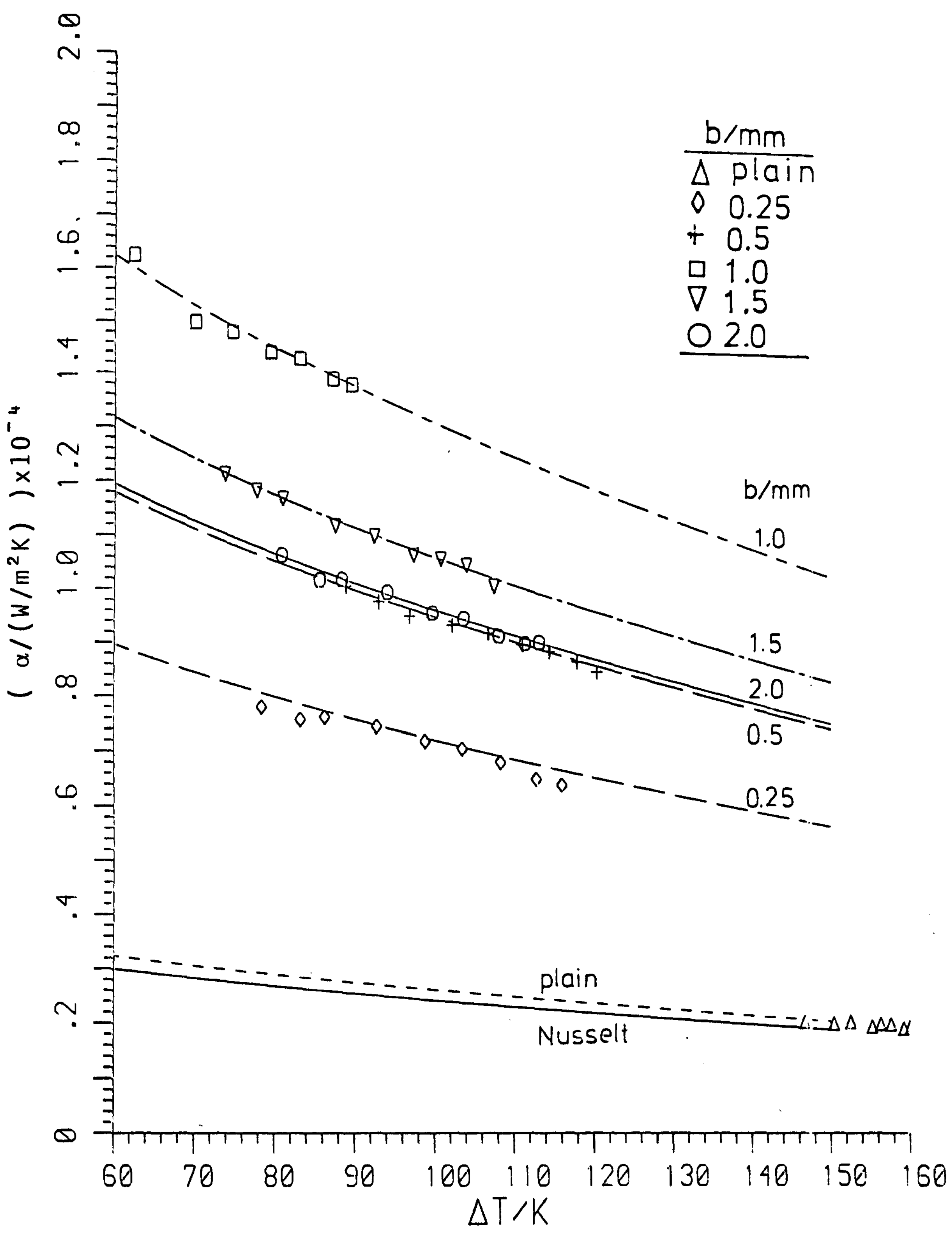

Fig.4-10 Relation between vapour-side heat-transfer coefficient and temperature difference for ethylene glycol

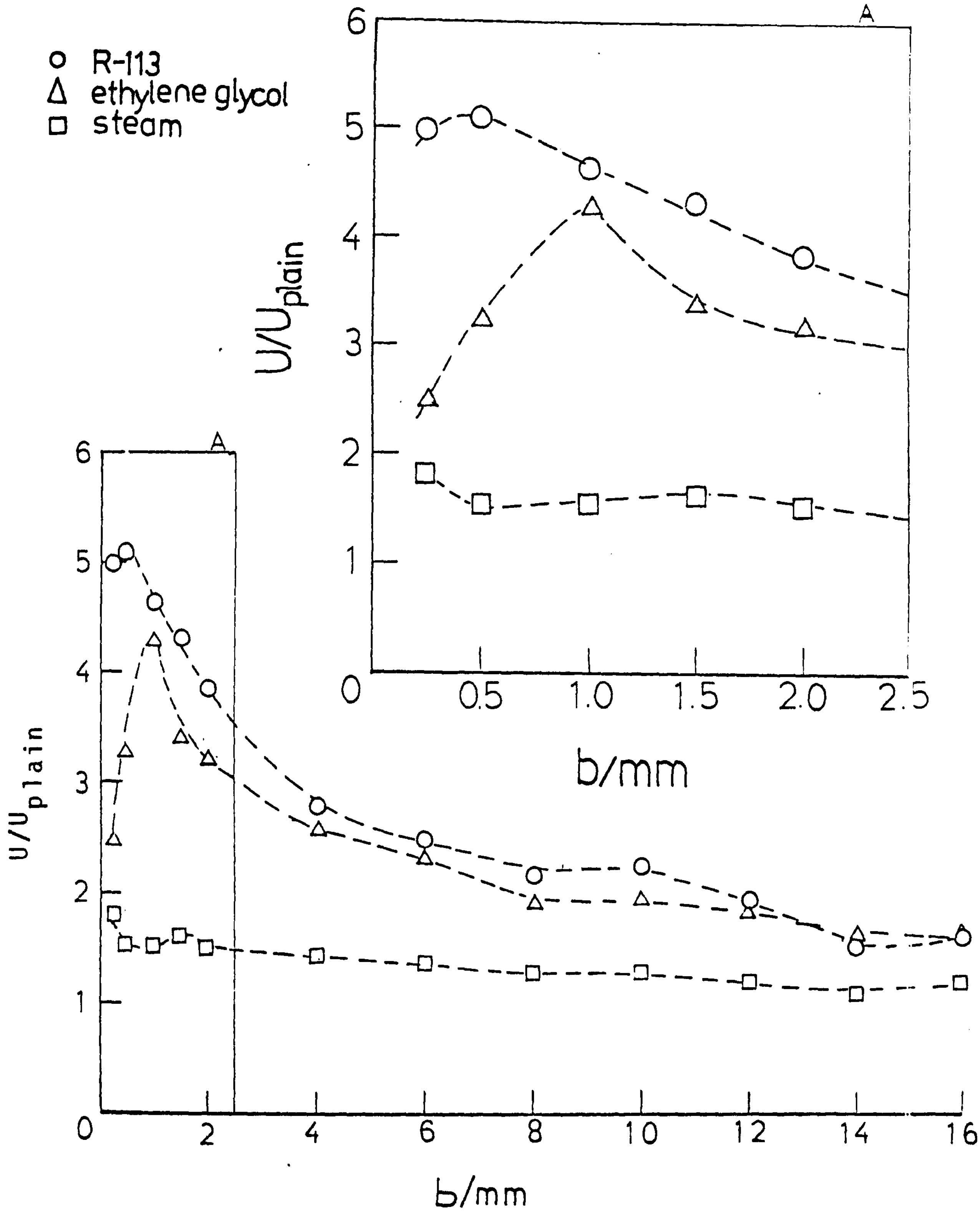

Fig.4-11 Enhancement ratios of overall heat-transfer coefficient at coolant velocity of 4 m/s.

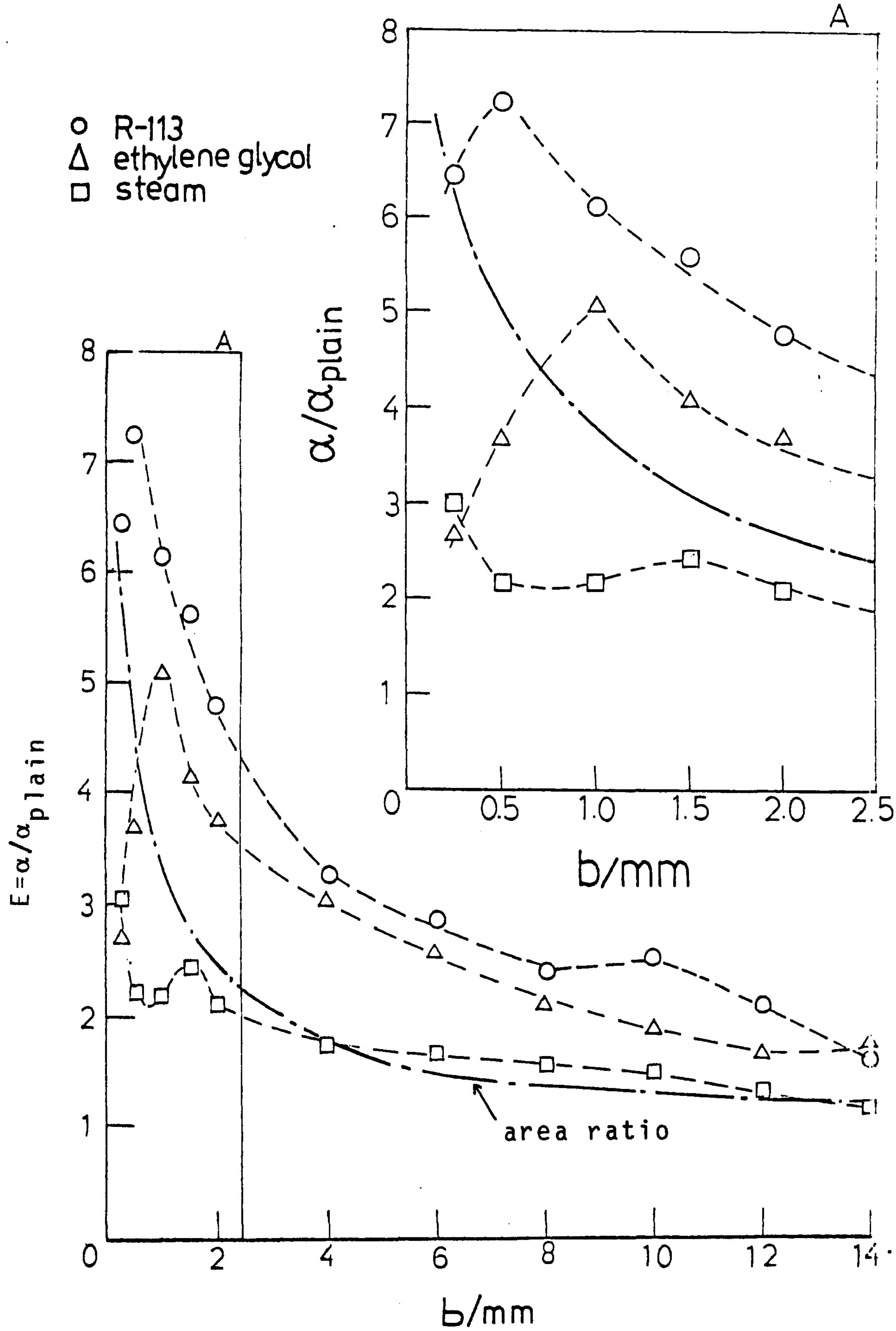

Fig.4-12 Enhancement ratios of vapour-side heat-transfer coeffifcient for the same vapour-side temperature difference.

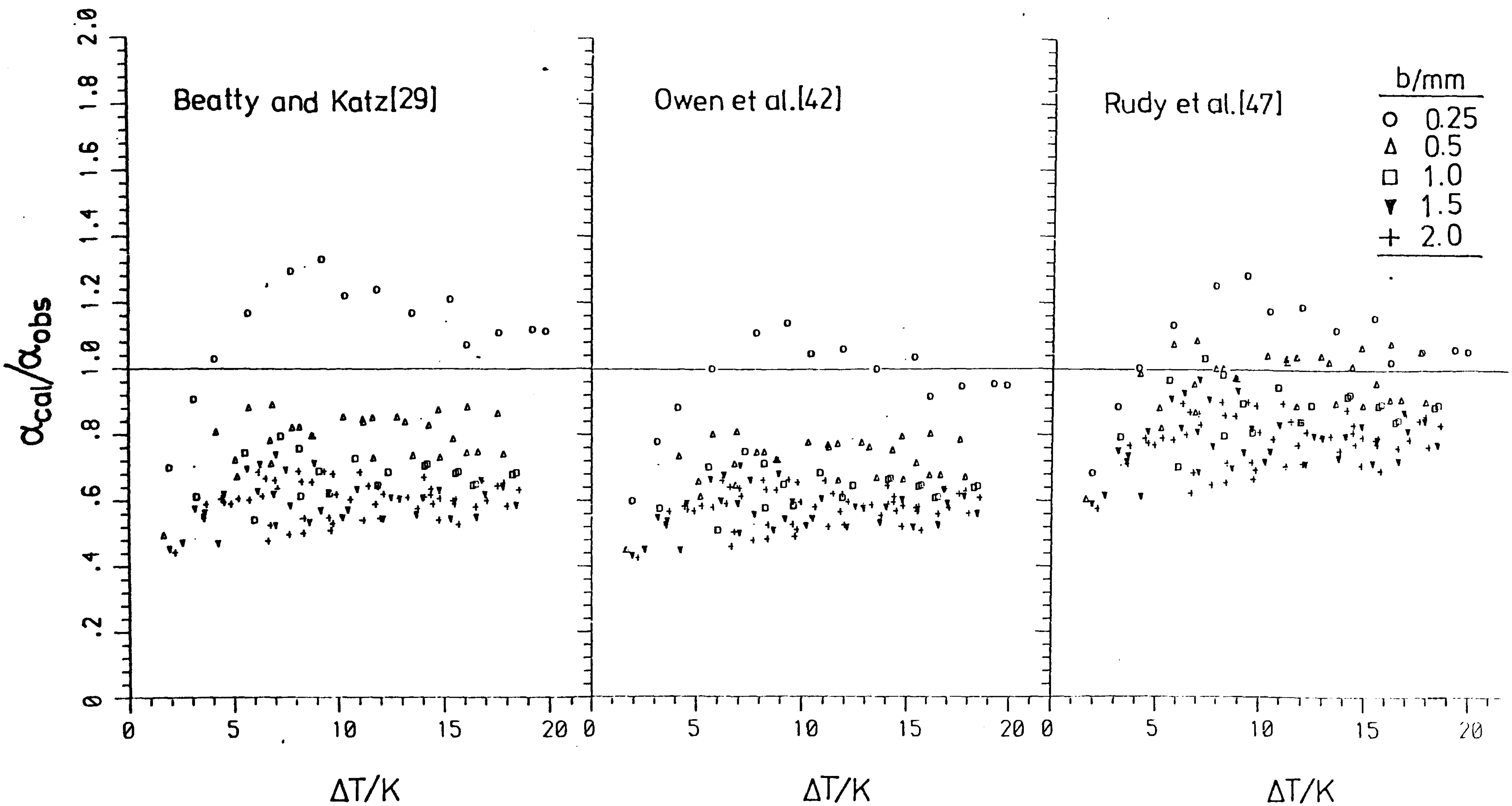

Fig.4-13 Comparison of present data for R-113
with earlier theoretical models

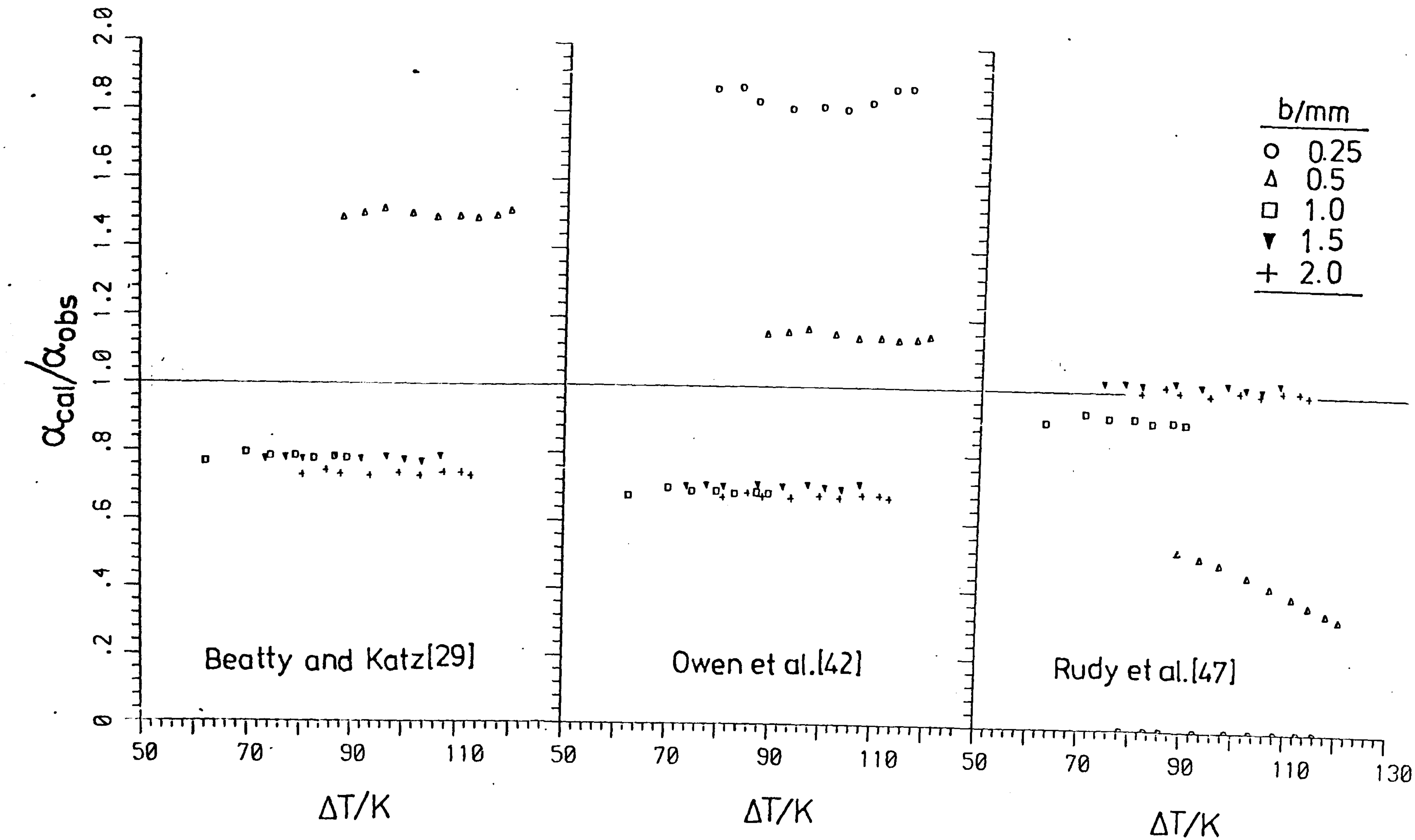

Fig.4-14 Comparison of present data for ethylene glycol with earlier theoretical models

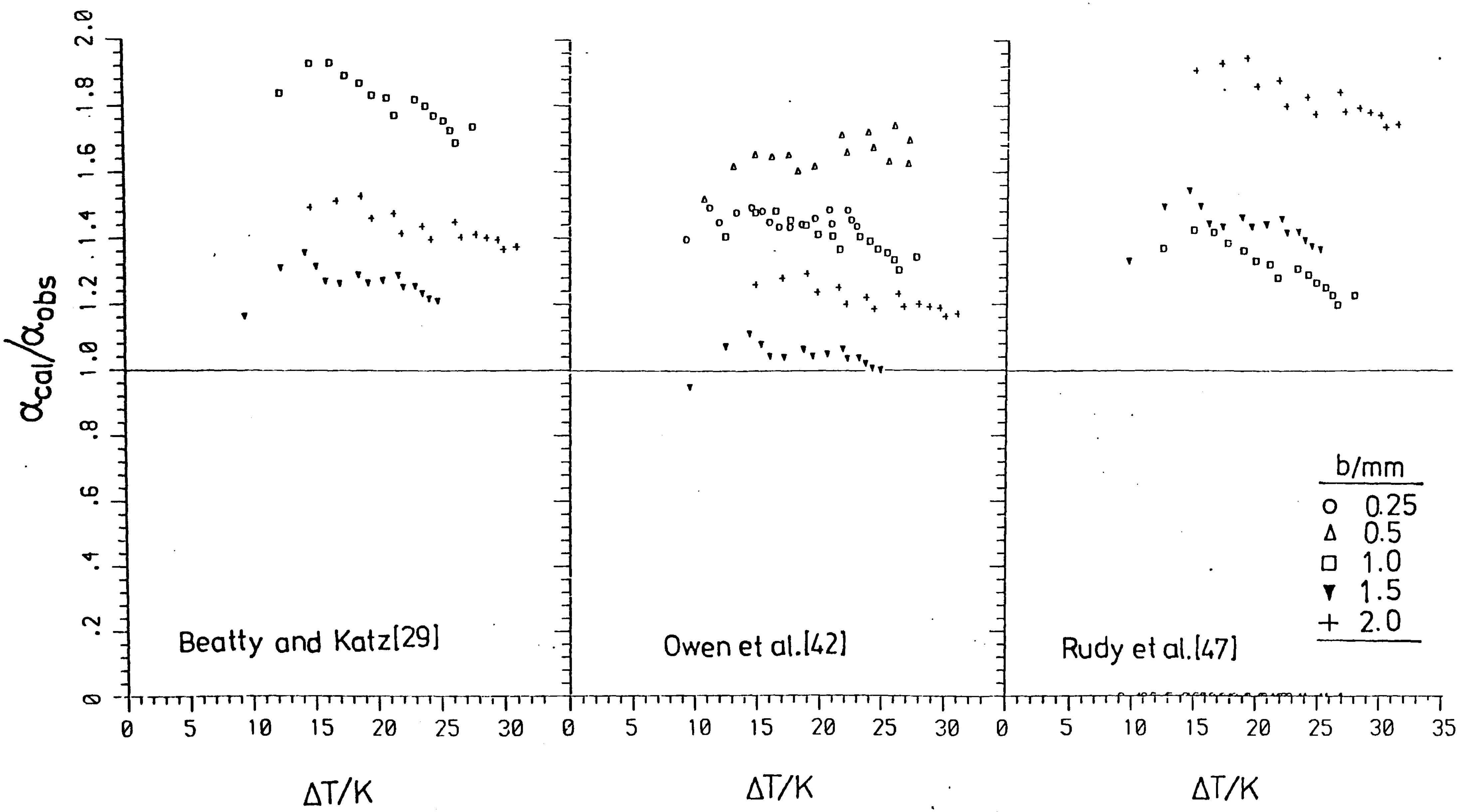

Fig.4-15 Comparison of Yau et al.[35,36,37] steam data with the earlier theoretical models

Table 4-1 Values of $\tilde{a}$ and $\tilde{b}$ determined by modified "Wilson Plot" method

pitch/mm	R-113 $\tilde{a}$	R-113 $\tilde{b}$	ethylene glycol $\tilde{a}$	ethylene glycol $\tilde{b}$
0.0	0.0412	0.740	0.0486	0.781
0.75	0.0410	4.78	0.0248	2.18
1.0	0.0341	5.36	0.0333	2.86
1.5	0.0358	4.55	0.0237	3.95
2.0	0.0350	4.16	0.0274	3.20
2.5	0.0352	3.54	0.0288	2.90
4.5	0.0331	2.42	0.0252	2.38
6.5	0.0317	2.14	0.0239	2.14
8.5	0.0328	1.79	0.0231	1.71
10.5	0.0322	1.88	0.0421	1.45
12.5	0.0341	1.56	0.0347	1.30
14.5	0.0380	1.19	0.0259	1.39
16.5	0.0340	1.30	-	-
18.5	0.0382	1.13	-	-
20.5	0.0364	1.07	-	-

CHAPTER 5 ANALYSIS

5. Analysis

5.1. Introduction

For condensation on the horizontal finned tubes there are no models which can predict all available experimental data satisfactorily, though some progress has been made towards understanding the phenomena involved. Recent investigations have concentrated on surface tension forces which cause condensate retention between fins on the lower part of tubes (adverse effect) and on the film-thinning effect on the upper surfaces (beneficial effect) as described in Chapter 2.

In this chapter, the liquid retention problem is studied in detail and the static configuration of retained liquid over the whole tube is analysed theoretically. Initially the heat-transfer problem was approached using dimensional analysis. Constants, in the semi-empirical equations developed, were determined by "fitting" experimental data for three fluids and five fin spacings. These results led to the unexpected conclusion that surface tension had a negative effect on heat tansfer for the upper "unflooded" part of the tube. Theoretical studies, described in this chapter, provide a physical explanation for this phenomenon as well as alternative predictive equations.

5.2 Determination of the static configuration of retained liquid

The fact that liquid is retained in the interfin space surface has been observed and the "retention" angle was measured by Rudy et al. [41], Honda et al. [34] and Yau et al. [37], as described in section 2.3. The fact that there is little difference in the "retention" angle between observations under "dynamic", i.e. condensing, conditions and "static" conditions has been also reported by Rudy et al. and Honda et al. As reviewed in section 2.3, Honda et al.[34] have given a force balance for static conditions leading to a second order differential equation describing the liquid meniscus at the position where this just reaches the top of the fin, i.e. the position of "complete flooding". Honda et al. solved numerically this equation for the film thickness in the radial cross section at the "retention" angle, i.e. at which the interfin spacing is completely flooded and the film reaches the fin tip. On the basis of this solution a simple equation which gives the "retention" angle was proposed.

As noted above Honda et al. concentrated their attention on the location of "flooding". However, as will be seen in the analysis which follows, liquid is also retained higher on the surface in the form of a "wedge" between the fin flanks and the tube surface, which gets smaller with height on the tube, as illustrated in Fig.5-1.

Liquid filling interfin spacing in the lower part of the tube (E) rises around the tube. The radii of the curvature of liquid surface become gradually smaller and film thicknesses at the middle point become thinner as liquid rises from E to D. At the upper part above the "retention" angle ϕ_f, liquid does not reach the top of fin flank (B,C) and eventually it separates into two parts adjacent to opposite fin flanks (B).

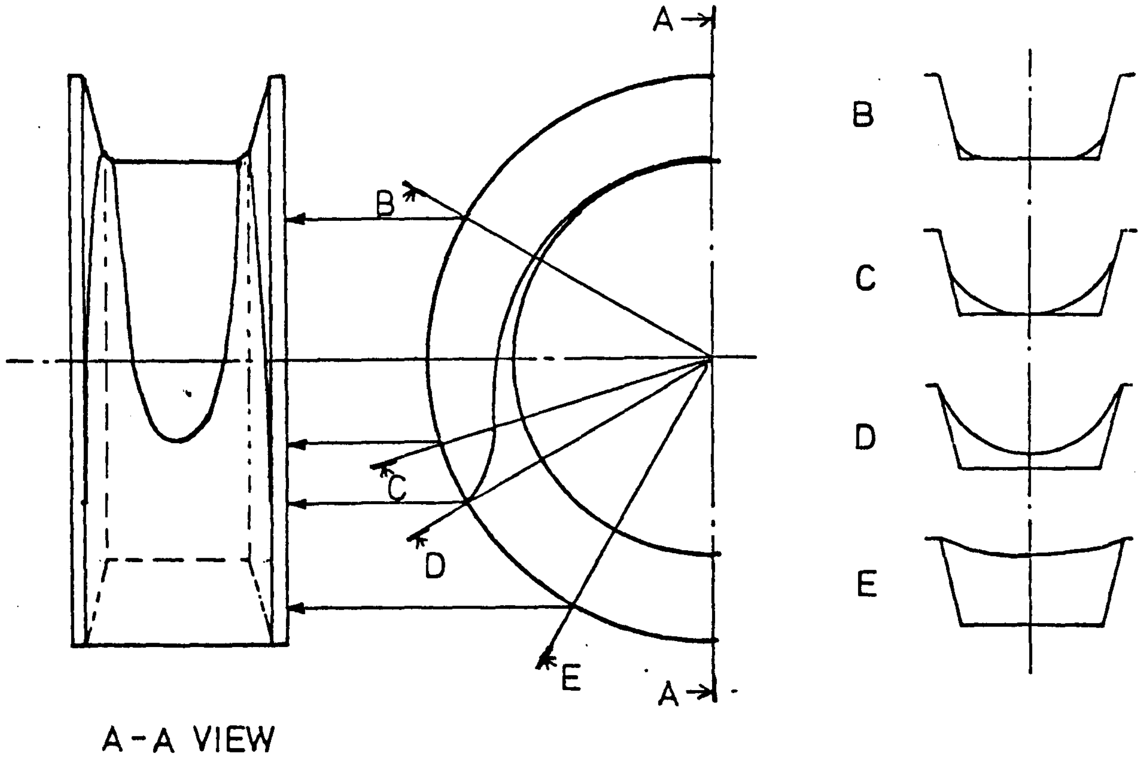

Fig.5-1 The static configuration of retained liquid on finned tube

In this section we adopt the force balances given by Honda et al. [34] in order to determine the meniscus shape for the general case. Honda et al. have given the following expression for the force balances of retained liquid, i.e:-

$$\rho g z - \frac{\sigma}{r_0} = 0 \tag{5-1}$$

$$-\frac{\sigma}{r} + \rho g y \cos\phi = -\frac{\sigma}{r_0} \tag{5-2}$$

$$r = \frac{(1+(dy/dx)^2)^{3/2}}{(d^2y/dx^2)} \tag{5-3}$$

$$z = R_0 + (R_r + \delta_0)\cos\phi \tag{5-4}$$

Fig.5-2 shows the physical model and the coordinate scheme for the cases of B and C in Fig.5-1, where x is the distance measured along the tube from the point of contact of the liquid with the tube surface, y is the height of the meniscus in the radial direction, z is the height of the liquid above the base of the tube ($\phi=\pi$) at x=0, y=0, r is the radius of curvature of the meniscus and r_0 and r_e are values of r at x=0 and $x=X_e$ respectively.

Fig.5-3 shows the situation between C and D (see Fig.5-1) where d_0 is the radial distance from the tube surface to the meniscus, x is measured from the mid-point between fins and y is measured radially outward from point δ_0.

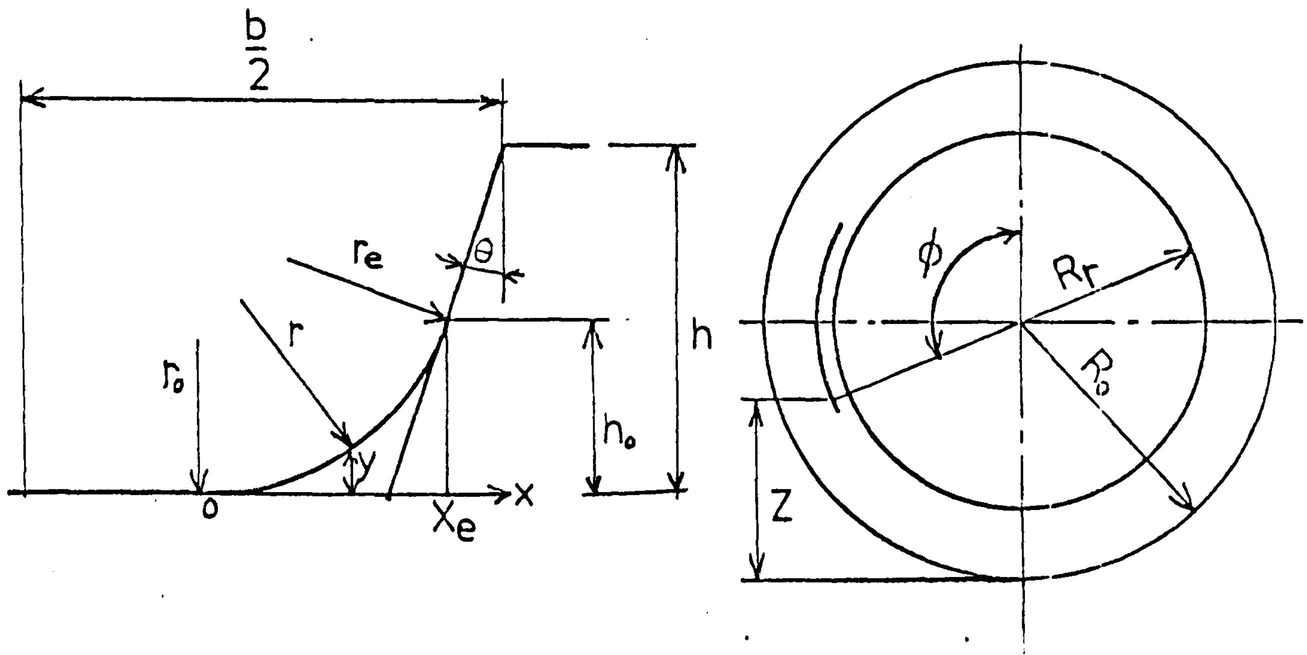

Fig.5-2 Physical model and coordinate system for static configuration of retained liquid at position B, see Fig 5-1

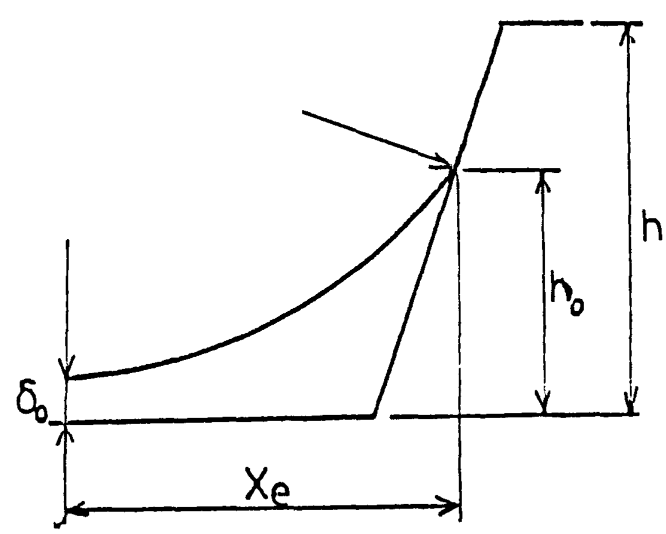

Fig.5-3 Physical model and coordinate system for static configuration of retained liquid at position between C and D, see Fig.5-1

As shown in Fig.5-2, r is a radius of curvature of the condensate "wedge" at the bottom of fins. At the starting point of the curvature, ie $x=0$, $r=r_o$ and $\delta=\delta_0$. The varying radial outward distance y reaches $y=h_0-\delta_0$ and contacts the fin flank with zero contact angle. Combination of eqs.(5-1) to (5-4) gives:

$$\frac{1}{r} = \frac{\rho g}{\sigma} y\cos\phi + \frac{1}{r_0} \tag{5-5}$$

$$\frac{y''}{(1+y'^2)^{3/2}} = \frac{\rho g}{\sigma}(z+y\cos\phi) \tag{5-6}$$

For calculation, the following parameters are defined:

$$Y=z+y\cos\phi \tag{5-7}$$

$$D=\frac{dy}{dx} \tag{5-8}$$

$$D\frac{dD}{dy}=\frac{d^2y}{dx^2} \tag{5-9}$$

Therefore, eq.(5-6) may be rewritten as:

$$\frac{DdD}{(1+D^2)^{3/2}} = \frac{\rho g}{\sigma} Y dy \tag{5-10}$$

where $dy=dY/\cos\phi$

so that,

$$\frac{DdD}{(1+D^2)^{3/2}} = \frac{\rho g}{\sigma\cos\phi} Y^2+C \tag{5-11}$$

Integration of the above equation leads to:

$$\frac{1}{\sqrt{1+D^2}} = -\frac{\rho g}{2\sigma\cos\phi} Y^2 + C \tag{5-12}$$

with the boundary conditions:-

$$D=\cot\theta \quad \text{and } y=h_o-\delta_o \quad \text{at } x=X_e$$
$$D=0 \quad \text{and } y=0 \quad \text{at } x=0$$

Putting these boundary conditions in eq.(5-12) we obtain:

$$\sin\theta=-\frac{\rho g}{2\sigma\cos\phi}\,Y_e^2+C \qquad (5\text{-}13)$$

$$1=-\frac{\rho g}{2\sigma\cos\phi}\,Y_o^2+C \qquad (5\text{-}14)$$

where

$$Y_e=R_o+(R_r+\delta_o)\cos\phi+(h_o-\delta_o)\cos\phi$$
$$Y_o=R_o+(R_r+\delta_o)\cos\phi$$

Eliminating the constant between eqs.(5-13) and (5-14) leads to:

$$1-\sin\theta=-\frac{\rho g}{2\sigma\cos\phi}(Y_o^2-Y_e^2) \qquad (5\text{-}15)$$

where

$$Y_o^2-Y_e^2=-2(h_o-\delta_o)\cos\phi(R_o+(R_r+\delta_o)\cos\phi-(h_o-\delta_o)\cos^2\phi$$

Therefore, the height h_o which condensate reaches is found by:

$$1-\sin\theta=\frac{\rho g}{2\sigma}[2(h_o-\delta_o)\{R_o+(R_r+\delta_o)\cos\phi\}+(h_o-\delta_o)^2\cos\phi] \qquad (5\text{-}16)$$
$$\simeq\frac{\rho g}{\sigma}(h_o-\delta)(R_o+R_r\cos\phi) \qquad (5\text{-}17)$$

$$\therefore \qquad h_o-\delta_o=\frac{\sigma(1-\sin\theta)}{\rho g(R_o+R_r\cos\phi)} \qquad (5\text{-}18)$$

We now determine the meniscus profile, i.e. the radial "height" of film at any x. Eliminating the constant between eqs.(5-12) and (5-14) leads to:

$$\frac{1}{\sqrt{1+D^2}} = -\frac{\rho g}{2\sigma\cos\phi}(Y^2-Y_0^2)+1 \qquad (5\text{-}19)$$

The above equation is now solved for D, i.e:

$$D=\frac{dy}{dx}=\pm\frac{\sqrt{2A-A^2}}{1-A} \qquad (5\text{-}20)$$

where

$$A=\frac{\rho g}{2\sigma\cos\phi}(Y^2-Y_0^2)$$

$$=\frac{\rho g}{2\sigma}y(2z+y\cos\phi)$$

$$\simeq\frac{\rho g}{\sigma}\,y(R_0+R_r\cos\phi)$$

From eq.(5-18), y varies from 0 to $h_0-\delta_0$, so that A varies from 0 to $(1-\sin\theta)<1$. Note that this satisfies the requirement that eq.(5-20) has real roots. Since $dy/dx>0$, the positive sign in eq.(5-20) is taken.

Now:

$$dA=\frac{\rho g}{\sigma}(R_0+R_r\cos\phi)dy$$

$$=B\,dy$$

where $B=\frac{\rho g}{\sigma}(R_0+R_r\cos\phi)$

so that

$$dy=dA/B$$

Therefore, eq.(5-20) may be rewritten as:

$$\frac{1-A}{\sqrt{2A-A^2}}\,\frac{dA}{B} = dx \qquad (5\text{-}21)$$

Defining:

$$K^2=2A-A^2 \qquad (5\text{-}22)$$

$$2K\,dK=2(1-A)dA$$

i.e.:

$$\frac{dK}{B} = dx$$

Integration of the above equation leads to:

$$K=Bx+C \tag{5-23}$$

where

$$C=0 \quad \text{for } y=0 \text{ at } x=0$$

Then

$$K=(2By-B^2y^2)^{\frac{1}{2}}=Bx \tag{5-24}$$

so that

$$2By-B^2y^2-B^2x^2=0 \tag{5-25}$$

$$y=\frac{1}{B} \pm \sqrt{B^{-2}-x^2}$$

Differentiating the above equation leads to:

$$\frac{dy}{dx}=\pm(B^{-2}-x^2)^{-\frac{1}{2}}(-2x) \tag{5-26}$$

As described earlier, dy/dx>0, so that the negative sign in eq.(5-26) is used. From eq.(5-18), the extent of the condensate "wedge" along the interface space:

$$X_e=\sqrt{\{\frac{2}{B}-(h_0-\delta_0)\}(h_0-\delta_0)} \tag{5-27}$$

$$=\frac{\cos\theta}{B}$$

In the case of $\theta=0$, as in the present work:

$$h_0-\delta_0 = X_e = \frac{\sigma}{\rho g(R_0+R_r\cos\phi)} \tag{5-28}$$

Now, the radius of curvature of liquid surface in the wedge is given in eq.(5-5), i.e:

$$\frac{1}{r} = \frac{\rho g}{\sigma} Y \tag{5-29}$$

The radius at the end point of curvature and the starting point, r_e and r_o, are given respectively by:

$$\frac{1}{r_e}=\frac{\rho g}{\sigma}Y_e=\frac{\rho g}{\sigma}(R_o+(R_r+h_o)\cos\phi) \qquad (5\text{-}30)$$

$$\frac{1}{r_o}=\frac{\rho g}{\sigma}Y_o=\frac{\rho g}{\sigma}(R_o+(R_r+\delta_o)\cos\phi) \qquad (5\text{-}31)$$

Eqs.(5-25),(5-30) and (5-31) indicate that the profile of the liquid surface in the wedge is parabolic, and the curvature changes smoothly with radii r_o, r and r_e. For the low-finned tube, $R_o \simeq R_r$, so that the curvature of liquid surface can be regarded as a circular arc.

5.3 Condensate retention angle

The "retention" angle, ϕ_f, is defined as the angle measured from the top of the tube to the position at which liquid film between fins reaches the fin tip (see Fig.5-4), i.e. where h_o is equal to the fin height h. Therefore h_o in eq.(5-16) is substituted by h.

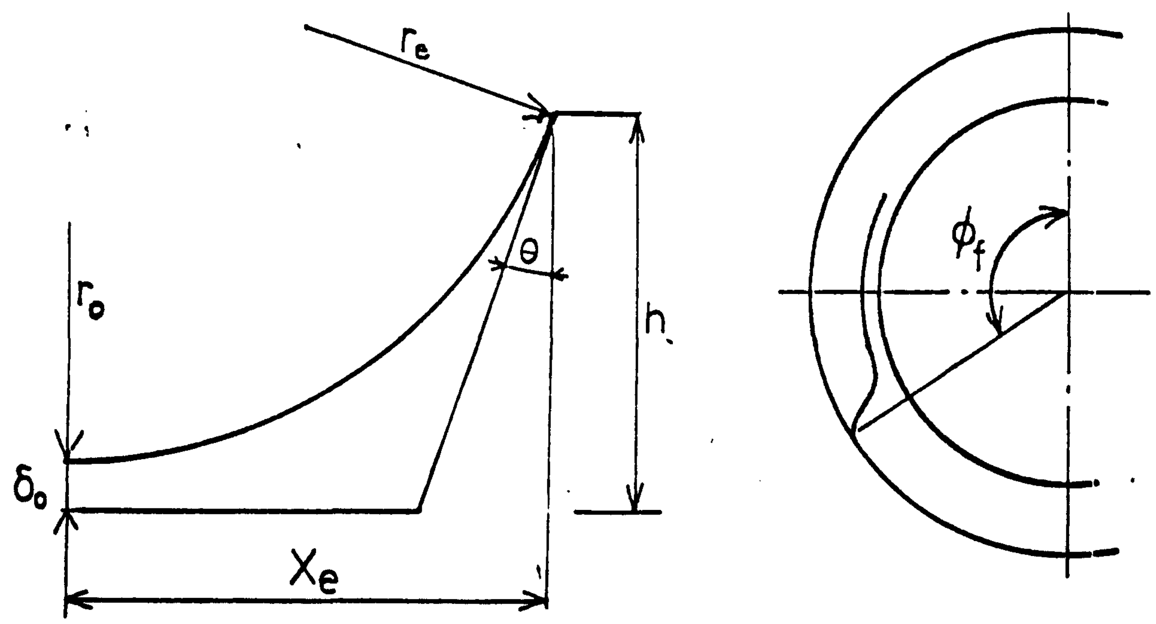

Fig.5-4 Physical model and coordinate system for static configuration of retained liquid at position D (i.e. "flooding" point) when b<2hcosθ/(1-sinθ)

Then:

$$1-\sin\theta=\frac{\rho g}{2\sigma}[2(h-\delta_o)\{R_o+(R_r+\delta_o)\cos\phi_f\}+(h-\delta_o)^2\cos\phi_f]$$

Hence, the retention angle ϕ_f is given by:

$$\cos\phi_f=\{\frac{\sigma(1-\sin\theta)}{\rho g R_o(h-\delta_o)}-1\}/(1-\frac{h-\delta_o}{2R_o}) \qquad (5-32)$$

For the case where $\delta_o>0$ (note we can also define a "flooding" as the retention angle for widely-spaced fins where $\delta_o=0$, by the condition that $h_o=h$ as will be considered next) the approximation that the meniscus is a circular arc of radius r leads to:

$$h-\delta_o=\frac{b}{2}\,\frac{(1-\sin\theta)}{\cos\theta} \qquad (5-33)$$

Substitute of eq.(5-34) in eq.(5-32) leads to:

$$\cos\phi_f=(\frac{2\sigma\cos\theta}{\rho g R_o b}-1)/\{1-\frac{b}{4R_o}\frac{(1-\sin\theta)}{\cos\theta}\} \qquad (5-34)$$

For predicted low-finned tubes, it is often the case that:

$$b\,\frac{1-\sin\theta}{\cos\theta}\leq 2h$$

which leads to:

$$\cos\phi_f=\frac{2\sigma\cos\theta}{\rho g R_o b}-1 \qquad (5-35)$$

as obtained by Honda et al. [34].

For widely space fins where $\delta_o=0$ (see Fig.5-5) the circular arc approximation gives:

$$b > 2h \frac{\cos\theta}{1-\sin\theta}$$

Hence:

$$\cos\phi_f=\left(\frac{\sigma(1-\sin\theta)}{\rho g R_o h} - 1\right)/\left(1-\frac{h}{2R_o}\right) \qquad (5\text{-}36)$$

Eq.(5.36) indicates that ϕ_f is no longer dependent on fin spacing b.

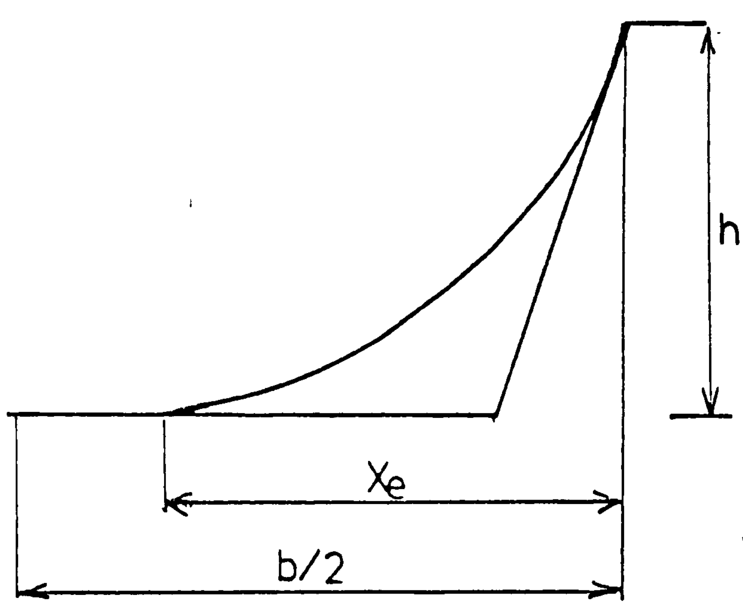

Fig.5-5 Physical model and coordinate system for static configuration of retained liquid at "flooding" point when b>2hcosθ/(1-sinθ)

Liquid retention measurement [55] have been made for R-113, ethylene glycol and water using rectangular cross-section fins Fig.5-6 shows comparisons of the experimental data and lines calculated by eq.(5-35) and (5-36). Good agreement was found for b<2h. As the spacing increased beyond 2h, the retention angle changed little. This trend may be explained by eq.(5-36). Experimental results are detailed in Table 5-1.

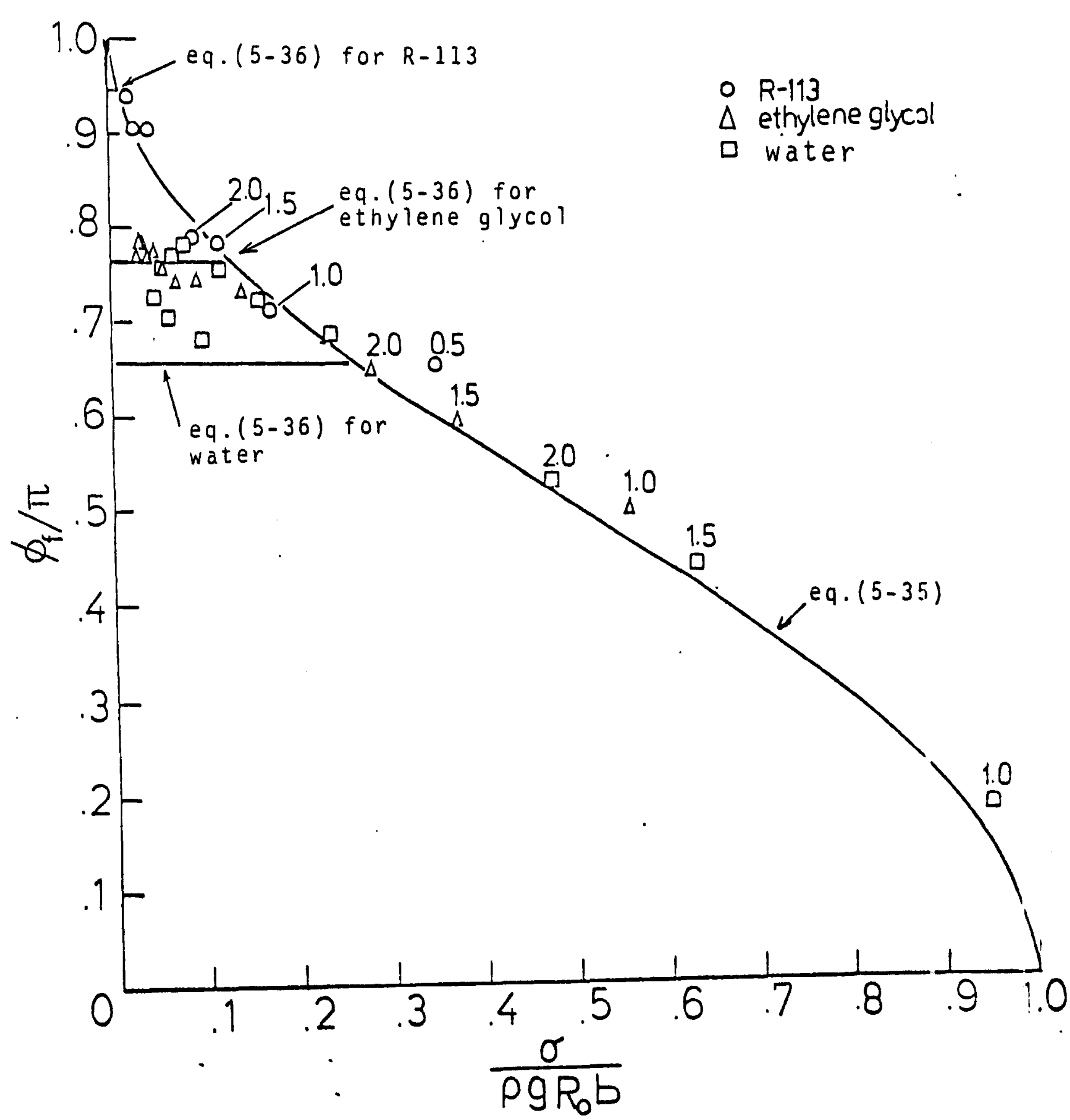

Fig.5-6 Experimental results [55] and comparison with theoretical predictions by eqs.(5-35) and (5-36)

5.4 Heat transfer analysis

5.4.1 Introduction

In this section we discuss attempts to obtain a relatively simple equation to predict heat-transfer performance. An approach based on dimensional analysis and an approximate theoretical treatment are given. In both cases the heat-transfer surface is divided into two areas by the "retention" angle ϕ_f, as described in the former section. The heat flux on the tubes may be written by:

$$Q = Q_{0-\phi_f}\,\xi\left(\frac{\phi_f}{\pi}\right) + Q_{\phi_f-\pi}\,\xi\left(1-\frac{\phi_f}{\pi}\right) \tag{5-37}$$

where Q is heat flux based on the nominal surface equal to that of plain tube with diameter d_r,

$Q_{0-\phi_f}$ and $Q_{\phi_f-\pi}$ are heat fluxes for the the "unflooded" and "flooded" regions,

ξ is the ratio of area of the finned tube to that of plain tube,

and ϕ_f is found from eq.(5-35).

5.4.2 Dimensional analysis

(1) Basic expression for heat transfer

We suppose the average condensate film thickness on a particular surface may be written :

$$\delta=f(\rho g,\sigma,L,\mu,V) \qquad (5\text{-}38)$$

where σ is surface tension, ρ is density of condensate, μ is viscosity of condensate, V is volume flux of condensate and L is geometrical dimension as before.

The π-theorem then suggest a relationship between three dimensionless parameters. Keeping surface tension and gravity separately, we consider:

$$\frac{\delta}{L} = g\left(\frac{\mu V}{\sigma}, \frac{\mu V}{\rho g L^2}\right) \qquad (5\text{-}39)$$

and, in addition, we have:

$$V=Q/h_{fg}\rho \qquad (5\text{-}40)$$

$$Q=k\Delta T/\delta=V\rho h_{fg} \qquad (5\text{-}41)$$

For convenience we suppose eq.(5-39) may be witten:

$$\frac{\delta}{L} = C\left(\frac{\mu V}{\sigma}\right)^{\alpha}\left(\frac{\mu V}{\rho g L^2}\right)^{\beta} \qquad (5\text{-}42)$$

where C , α and β are constants. Substituting eq.(5-40) and (5-41) into eq.(5-42) gives:

$$\frac{k\Delta T}{Q}\ \frac{1}{L} = C\left(\frac{\mu Q}{\sigma\rho h_{fg}}\right)^{\alpha}\left(\frac{\mu Q}{\rho^2 g h_{fg} L^2}\right)^{\beta} \qquad (5\text{-}43)$$

The above equation may be rearranged in non-dimensional form, thus:

$$Nu=\frac{QL}{k\Delta T}=C_o\left(\frac{h_{fg}\rho\sigma L}{\mu k\Delta T}\right)^{n}\left(\frac{h_{fg}\rho^2 g L^3}{\mu k\ \Delta T}\right)^{m} \qquad (5\text{-}44)$$

where

$$C_o = \frac{1}{C}\ \frac{1}{\alpha+\beta+1}$$

$$n = \frac{\alpha}{\alpha+\beta+1}$$

$$m = \frac{\beta}{\alpha+\beta+1}$$

For a plain tube we have:

$$Nu_{plain} = C_1\left(\frac{h_{fg}\rho g d_r^3}{\mu k \Delta T}\right)^{\frac{1}{4}} \qquad (5\text{-}45)$$

Nusselt theory would give $C_1=0.728$. The present plain tube data at low vapour velocity gave value of 0.74 and 0.78 for R-113 and ethylene glycol respectively. Yau et al. [35,36] data for steam were represented by 0.907, 0.846 and 0.804 for vapour velocities of 1.1, 0.7 and 0.5 m/s respectively.

The enhancement ratio (for finned tube and plain tube with the same ΔT) is given by:

$$\frac{Q}{Q_{plain}} = \frac{C_0}{C_1}\left(\frac{h_{fg}\rho\sigma L}{\mu k \Delta T}\right)^n \left(\frac{h_{fg}\rho^2 g}{\mu k \Delta T}\right)^{m-\frac{1}{4}} L^{3m-1} d_r^{\frac{1}{4}} \xi \qquad (5\text{-}46)$$

The present experimental results and those of Yau et al., the enhancement ratio is essentially independent of ΔT, in which case eq.(5-46) would suggest:

$$-n-(m-\frac{1}{4})=0$$

Eq.(5-55) is then simplified as:

$$\frac{Q}{Q_{plain}} = K\left(\frac{\sigma}{\rho g L^2}\right)^n \left(\frac{d_r}{L}\right)^{\frac{1}{4}} \xi \qquad (5\text{-}47)$$

At this point we note that eq.(5-47) has two unknown constants K and m and that we have yet to specify the appropriate value of L. For the unflooded region we now apply eq.(5-47) to the fin flank, when we take L=h, and to the interfin space, when we take L=b. For the top of fin we ignore surface tension effects. Moreover, for the flooded region we neglect effects of surface tension and suppose that the enhancement may be written as a constant (to be found) multiplied by the finned-to-plain tube area ratio. On basis of those assumption, the enhancement ratio (E) for the whole tubes is given by:

$$E = K_1 \frac{t}{b+t} + K_2 \left(\frac{\sigma}{\rho g b^2}\right)^n \left(\frac{d_r}{b}\right)^{1/4} \frac{b}{b+t} +$$

$$K_3 \left(\frac{\sigma}{\rho g h^2}\right)^n \left(\frac{d_r}{h}\right)^{1/4} \frac{2h}{b+t} \frac{\phi_f}{\pi} + K_4 \xi \left(1-\frac{\phi_f}{\pi}\right) \qquad (5\text{-}48)$$

where K_1, K_2, K_3, K_4 and n are constants.

If the Nusselt theory were applied for the fin top in the unflooded region, we would have $K_1 = \{(d_r+2h)/d_r\}^{3/4} \approx 1$ for low-fin tube. Also we expect $K_4 < 1$.

(a) <u>Determination of the constants</u>

We now employ the present results and those of Yau et al. [35,36] to determine the values of K_1, K_2, K_3 and K_4 so as to minimize the sum of squares of relative residual, i.e. we minimize $\{(E_{cal}-E_{obs})/E_{obs}\}^2$. Note that K_1, K_2, K_3 and K_4 are involved in a linear manner and can be found by a straight-forward "least-squares" procedure, while an iterative minimization technique is needed for n. The procedure followed is to iterate on n and at end iteration to determine the best values of K_1, K_2, K_3 and K_4 by "least squares". The computer program "NONLIN" (see Appendix E) was used for this problem.

It was considered more appropriate to minimize relative residuals that absolute residuals, i.e. $(E_{cal}-E_{obs})$, since the range of E was different for the three fluids considered. As assessment of the "goodness of fit" was give by the standard deviation as:

$$SD=\{\Sigma(E_{cal}/E_{obs}-1)^2/(n_d-n_c-n_s)\}^{\frac{1}{2}}$$

where n_d is number of experimental data points,

n_c is number of linear constants and

n_s is number of non-linear constants.

The experimental data used for this analysis are listed in Table 5-2.

(b) Results and comparisons

The results of the curve fit described above are shown in Table 5-3. The low (negative) value of n would suggest that surface tension is not important (apart from its role in the determination of θ_f). However, K_1 and K_3 are unreasonable. This result is no doubt due to "overfitting", i.e. the data are not adequate to determine five canstants.

Supposing heat transfer to the fin top in the unflooded region to be of minor importance, we set $K_1=0$ and redetermine the other constants. The results of this procedure are given in Table 5-4. It is seen that the standard deviation is reduced and the constants are of moderate magnitude. Unexpected n is negative, indicating that surface tension has a detrimental effect on heat transfer in the unflooded region.

The negative value of n was at first considered unacceptable and, keeping $K_1=0$, n was set arbitrary to a positive value of 0.25 and the other constants redetermined. Table 5-5 shows that, in this case, the standard deviation of the fit was doubled and K_2 became negative in our attempt to indicate a detrimental effect of surface tension. We are therefore forced to the conclusion that, if the data are reliable and if the above approach is soundly based, surface tension has a negative effect on heat transfer in the unflooded region and the value of the constants considered most appropriate are then given in Table 5-4, i.e.:

$$n=0.275 \quad K_1=0 \quad K_2=1.17 \quad K_3=1.4 \quad K_4=0.48$$

Fig.5-7 shows the comparison with experimental data for this case. In all three cases the maximum enhancement given by eq.(5-48) occurs at approximately the correct fin spacing. Only in the case of ethylene glycol the errors are significant with maximum value by about 26 %.

(2) Modified approach

As already described in section 5.2, the "wedge", i.e. the thick film formed at the fin root, will clearly constitute a region of high thermal resistance, so that this region will reduce the effective surface on the fin flank and in the interfin space. Here we treat this in an approximate way be taking an average "wedge radius" given by:

$$\bar{r} = \frac{1}{\phi_f} \int_0^{\phi_f} r \, d\phi \qquad (5\text{-}49)$$

As noted in section 5.2, r can be treated as constant at a given angle ϕ and given by:

$$\frac{1}{r} \simeq \frac{\rho\, g}{\sigma} R_0 (1+\cos\phi) \qquad (5\text{-}50)$$

so that:

$$\bar{r} = \frac{1}{\phi_f} \frac{\sigma}{\rho g R_0} \int_0^{\phi_f} \frac{d\phi}{1+\cos\phi} \qquad (5\text{-}51)$$

$$= \frac{\sigma}{\rho g R_0} \frac{\tan(\phi_f/2)}{\phi_f}$$

For the unflooded region, the "wedge" may be considered to extend to the height of $\bar{r}$ on the fin flank and along the interfin space to a distance $\bar{r}$. Therefore the effective space for heat transfer over the fin flank and interfin space will be reduced by $(1-\bar{r}/h)$ and $(1-2\bar{r}/b)$ respectively.

Regarding the surface covered by the wedge to be adiabatic eq.(5-48) became:

$$E=\{K_1\frac{t}{b+t}+K_2\left(\frac{\sigma}{\rho g b^2}\right)^n\left(\frac{d_r}{b}\right)^{1/4}\frac{b-2\bar{r}}{b+t}$$

$$+K_3\left(\frac{\sigma}{\rho g h^2}\right)^n\left(\frac{d_r}{h}\right)^{1/4}\frac{2(h-\bar{r})}{b+t}\}\frac{\phi_f}{\pi}+K_4\left(1-\frac{\phi_f}{\pi}\right) \quad (5\text{-}52)$$

Note that in eq.(5-52) where $2\bar{r}/b>1$ the interfin space along tube surface (in the unflooded region) is covered entirely by the wedge. In this case the second term in the expression for E, i.e. eq.(5-52), is zero, i.e. the term of $(1-2\bar{r}/b)$ should be set to zero when negative.

Determination of constants, Results and comparisons

Curve fits were now carried out as described above in correction with eq.(5-48). As before all five constants were regarded as disposable. The results are given in Table 5-6. As in the former case, K_1 took an unreasonable value (large and negative). This is no doubt due to "overfitting". We again set $K_1=0$ and redetermine the remaining constants. As previously, the constants (see Table 5-7) take reasonable values and n is small and negative showing a weak (but deleterious) effect of surface tension. As before n was arbitrarily set to +0.25 where, as indicated in Table 5-8, the standard deviation significantly increased. Finally, since in table 5-7 n was quite close to zero it was therefore worth setting n=0 to give an appreciably simple final result. Table 5-9 shows that the remaining constants and the standard deviation were not greatly changed.

Fig.5-8 shows the comparison with experimental data for this case. As in the case of Fig.5-7, the only significant deviation are for ethylene glycol, where the fit is somewhat improved. It may be noted that the graphical representation of eq.(5-52) with the constants give in Table 5-7 (i.e small negative value of n) is essentially the same as Fig.5-8.

(3) Concluding remarks

It is noteworthy that, comparing eqs.(5-48) and (5.52), and using the constans found when K_1 was set to zero:-

(a) The allowance for the adiabatic condensate "wedge" (eq.(5-52)) lead to an improved fit (i.e. smaller standard deviation) and to a value of n closer to zero. Note : n=0 implies no effect of surface tension forces in the unflooded region.

(b) Eq.(5-48), with constants given by table 5-4, accounts for surface tension empirically. Eq.(5-52) includes a theoretically-based correction while eq.(5-52) give almost the same results. For n=0, the simpliest equation may be written as:

$$E=\{K_2(\frac{b}{b+t})(1-\frac{2\bar{r}}{b}) + K_3(\frac{2h}{b+t})(1-\frac{\bar{r}}{h})\}\frac{\phi_f}{\pi} + K_4\xi(1-\frac{\phi_f}{\pi}) \quad (5\text{-}53)$$

where $K_2=3.51$, $K_3=2.99$ and $K_4=0.473$.

(c) It is of interest to note that in all of the curve fits for both eqs.(5-48) and (5-52) the constant K4 for the "flooded region" was little changed having a value of about 0.47 in all cases. This may reflect the fact that the approximate, somewhat arbitrarily, treatment for the flooded region may be a good approximation to the truth.

Further development of this approach must await new data for other fluids and fin geometries.

5.4.3 Theoretical analysis

The following assumption are employed:-

1) There exist no non-condensing gases and vapour is saturated.

2) Wall surface temperature is uniform .

3) For vapour speed is slow or zero so that the viscous shear force of the vapour on the condensate film is negligible.

4) The condensate film is thin, so that the inertia and convection terms are negligible.

Moreover, we restrict our attention to plain parallel-side fins (as used in the present experimental investigation).

(1) Theoretical expression

(a) Differential equation for the film thickness on the fin flank

Fig.5-9 shows the physical model and coordinate system. Additionally, in the momentum balance it is assumed that, while gravity and surface tension forces are considered in the radial direction, only the gravity force is present in the circumferantial direction where the curvature of the liquid surface changes little. In the energy equation, only conduction normal to the fin flank is considered. The momentum, energy, and mass balances are then given by:

$$\mu\frac{\partial^2 u}{\partial z^2} + \rho g\cos\phi + \frac{\partial P}{\partial x} = 0 \qquad (5\text{-}54)$$

$$\mu\frac{\partial^2 w}{\partial z^2} + \rho g\sin\phi = 0 \qquad (5\text{-}55)$$

$$\frac{\partial^2 T}{\partial z^2} = 0 \qquad (5\text{-}56)$$

$$\left(\frac{1}{R_0 - x}\right)\frac{\partial}{\partial\phi}\int_0^\delta w\,dz + \frac{\partial}{\partial x}\int_0^\delta u\,dz = \frac{k}{h_{fg}\rho}\left[\frac{\partial T}{\partial z}\right]_{z=\delta} \qquad (5\text{-}57)$$

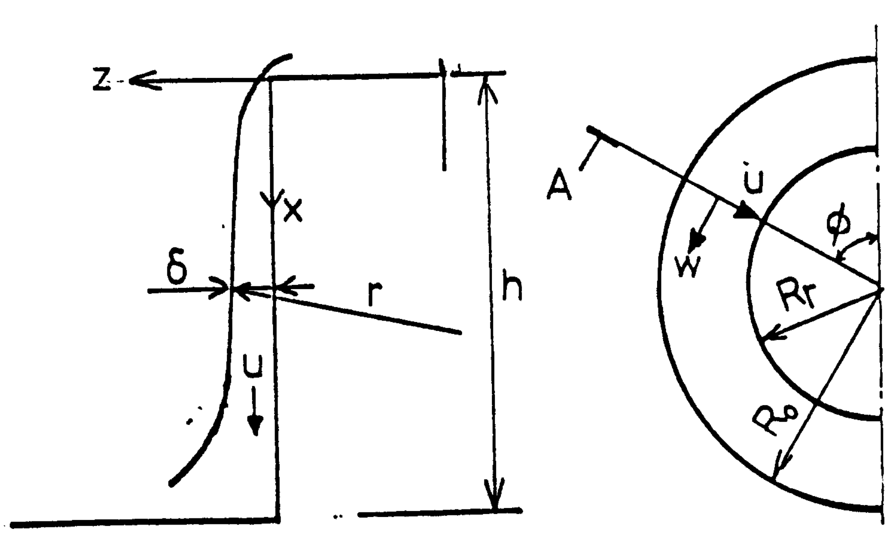

Fig.5-9 Physical model and coordinate system for theoretical analysis on motion of condensate on the fin flank

with the boundary conditions;

$$u=0\ ,\ w=0 \text{ and } T=T_w \text{ at } z=0 \qquad (5\text{-}58)$$

$$\frac{\partial u}{\partial z}=0,\ \frac{\partial w}{\partial z}=0 \text{ and } T=T_s \text{ at } z=\delta \qquad (5\text{-}59)$$

The pressure difference across the liquid-vapour interface at a point x is given by:

$$P-P_s=-\frac{\sigma}{r} \qquad (5\text{-}60)$$

where the curvature of condensate surface is found by:

$$r^{-1}=-(\partial^2 y/\partial x^2)/(1+(\partial y/\partial x)^2)^{3/2}$$

The velocity profile across the film at position x is calculated as follows:-

Integration of eq.(5-54) gives:

$$\frac{\partial u}{\partial z}=(-\frac{\rho g\cos\phi}{\mu}-\frac{1}{\mu}\frac{\partial P}{\partial x})z+C_1$$

The constant C_1 is found using the boundary condition (5-58) as:

$$C_1=(\frac{\rho g\cos\phi}{\mu}+\frac{1}{\mu}\frac{\partial P}{\partial x})\delta$$

Integrating again, we have:

$$u=(-\frac{\rho g\cos}{\mu}-\frac{1}{\mu}\frac{\partial P}{\partial x})\frac{1}{2}z^2+C_1z+C_2$$

C_2 is zero according to the boundary condition (5-59). Eventualy, the velocity profile in radial direction is given by:

$$u=-\frac{1}{2}(\frac{\rho g\cos\phi}{\mu}+\frac{1}{\mu}\frac{\partial P}{\partial x})(z^2-2\delta z) \qquad (5\text{-}61)$$

Then,

$$\int_0^\delta u\,dz = -\frac{1}{2}\left(\frac{\rho g\cos\phi}{\mu} + \frac{1}{\mu}\frac{\partial P}{\partial x}\right)\int_0^\delta (z^2 - 2z\delta)\,dz$$

$$= \frac{1}{3}\left(\frac{\rho g\cos\phi}{\mu} + \frac{1}{\mu}\frac{\partial P}{\partial x}\right)\delta^3 \qquad (5\text{-}62)$$

where

$$\frac{\partial P}{\partial x} = -\sigma\frac{\partial (r^{-1})}{\partial x} \qquad (5\text{-}63)$$

Hence,

$$\frac{\partial}{\partial x}\int_0^\delta u\,dz = \frac{1}{3}\left[\frac{\rho g\cos\phi}{\mu}\frac{\partial \delta^3}{\partial x} - \frac{\sigma}{\mu}\frac{\partial}{\partial x}\left\{\delta^3\frac{\partial (r^{-1})}{\partial x}\right\}\right] \qquad (5\text{-}64)$$

Integration of eq.(5-55) gives:

$$\frac{\partial w}{\partial z} = -\frac{\rho g}{\mu}\sin\phi\ z + C_1$$

The boundary condition (5-58) gives:

$$C_1 = \frac{\rho g}{\mu}\sin\phi\ \delta$$

Integrating again, we have:

$$w = -\frac{\rho g}{\mu}\sin\phi\cdot\frac{1}{2}z^2 + \frac{\rho g}{\mu}\sin\phi\cdot\delta z + C_2$$

The boundary condition (5-59) gives:

$$C_2 = 0$$

Therefore, the velocity profile in circumferential direction is given by:

$$w = -\frac{1}{2}\frac{\rho g}{\mu}\sin\phi(z^2 - 2\delta z) \qquad (5\text{-}65)$$

So that,

$$\int_0^\delta w\,dz = -\frac{1}{2}\frac{\rho g}{\mu}\sin\phi\int_0^\delta (z^2 - 2z)\,dz$$

$$= \frac{\rho g}{3\mu}\sin\phi\cdot\delta^3 \qquad (5\text{-}66)$$

Hence,

$$\frac{\partial}{\partial\phi}\int_0^\delta w\,dz = \frac{\rho g}{3\mu}\frac{\partial\delta^3\sin\phi}{\partial\phi} \qquad (5\text{-}67)$$

As in the Nusselt theory, the temperature distribution in the condensate film may be assumed linear, since the film is thin and laminar, so that:

$$\left[\frac{\partial T}{\partial z}\right]_{z=\delta} = \frac{T_v - T_w}{\delta} \qquad (5\text{-}68)$$

Eq.(5-57) may be rearranged using eqs.(5-64), (5-67) and (5-68) to give the differential equation for the condensate film thickness over the fin flank:

$$\frac{\rho g}{3\mu(R_0 - x)} \frac{\partial \delta^3 \sin\phi}{\partial \phi} + \frac{1}{3}\left[\frac{\rho g \cos\phi}{\mu} \frac{\partial \delta^3}{\partial x} - \frac{\sigma \partial}{\mu \partial x}\left\{\delta^3 \frac{\partial (r^{-1})}{\partial x}\right\}\right] = \frac{k(T_v - T_w)}{\rho h_{fg} \delta} \qquad (5\text{-}69)$$

It may be noted that, in a simpler approach by Honda et al [49], the first term in the left hand side, i.e. arrising from the circumferantial flow, was not included.

(b) <u>Differential equation for the film thickeness on the tube surface between fins</u>

Fig.5-10 shows the physical model and coordinate system. It is also assumed that both of gravity and surface tension forces are considered in the horizontal direction, and only gravity is considered in the circumferantial direction in the momentum balance. Only radial conduction is taken account for energy equation. The momentum, energy and mass balances are then given by:

$$\mu\frac{\partial^2 w}{\partial z^2} + \rho g \sin\phi = 0 \qquad (5\text{-}70)$$

$$\mu\frac{\partial^2 v}{\partial z^2} + \frac{\partial P}{\partial x} = 0 \qquad (5\text{-}71)$$

$$\frac{\partial^2 T}{\partial z^2} = 0 \qquad (5\text{-}72)$$

$$\frac{1}{R_r}\frac{\partial}{\partial \phi}\int_0^{\delta} w\,dz + \frac{\partial}{\partial}\int_0^{\delta} v\,dz = \frac{k}{h_{fg}\rho}\left[\frac{\partial T}{\partial z}\right]_{z=\delta} \qquad (5\text{-}73)$$

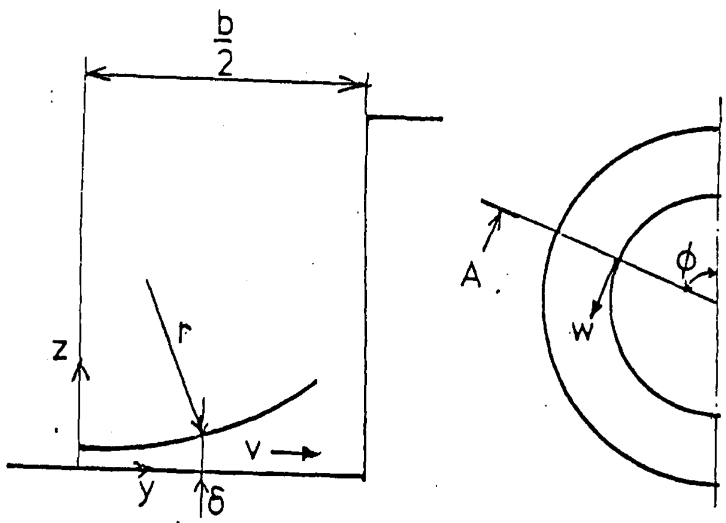

Fig.5-10 Physical model and coordinate system for theoretical analysis on motion of condensate on the tube surface between fins.

The boundary conditions are:

$$w=0,\ v=0 \text{ and } T=T_w \text{ at } z=0 \qquad (5\text{-}74)$$

$$\frac{\partial w}{\partial z}=0,\ \frac{\partial v}{\partial z}=0 \text{ and } T=T_v \text{ at } z=\delta \qquad (5\text{-}75)$$

The same procedure as descibed in (a) above gives:

$$w=-\frac{1}{2}\frac{\rho\ g}{\mu}\sin\phi\ (z^2-2\delta z) \qquad (5\text{-}76)$$

$$v=-\frac{1}{2}\ \frac{\sigma}{\mu}\frac{\partial(r^{-1})}{\partial x}(z^2-2\delta z) \qquad (5\text{-}77)$$

Eqs.(5-76) and (5-77) are substituted into eq.(5-73). The mass balance then gives the required equation:

$$\frac{\rho g}{3\mu R_r}\frac{\partial(\delta^3\sin\phi)}{\partial\phi} - \frac{\sigma}{3\mu}\frac{\partial}{\partial x}\{\delta^3\frac{\partial(r^{-1})}{\partial x}\} = \frac{k(T_v-T_w)}{\rho h_{fg}\delta} \qquad (5\text{-}78)$$

(c) Differential equation for the film thickness on the fin top

Eq.(5-78) also describes the film profile on the fin top except that R_r in the first term is replaced by R_o, i.e:

$$\frac{\rho g}{3\mu R_o}\frac{\partial(\delta^3 \sin\phi)}{\partial\phi}-\frac{\sigma}{3\mu}\frac{\partial}{\partial x}\{\delta^3\frac{\partial(r^{-1})}{\partial x}\}=\frac{k(T_v-T_w)}{h_{fg}\rho\delta} \qquad (5\text{-}79)$$

(2) Approximations and solutions

Eqs.(5-69), (5-78) and (5-79) are the fourth order differential equations for the film thickness, which require numerical solution with appropriate boundary conditions. Honda et al. [49] solved eq.(5-69) numerically but without circumferantial flow for fin flanks as described in Chapter 2. However, the solution is not entirely satisfactory and some points are questioned by the present author:-

1) The choice of the boundary condition for the angle of the tangent to the film surface at the fin-tube interface is not explained.

2) The fin profile mentioned in [49] had a given fin radius. It is not clear how to treat the sharp-

edge fin used in the present work.

Moreover, in [49] the approximate equations for heat transfer on the fin were based on an arbitrary combination of the surface tension effect given from numerical solution and the gravity effect given by the Beatty and Katz analysis [29]. Also the heat transfer on the tube surface in the interfin space is not taken into account.

Rather than attempting detailed numerical solution using arbitrary assumptions for uncertain boundary conditions, we shall proceed here in a simpler approximation in order to obtain a relatively simple equation.

(a) Approximations for "unflooded" region

(Surface tension driven condensate flow on the fin flank and tube surface between fins)

Karkhu and Borovkov [44], Borovkov [46] and Rudy and Webb [47] employed the simplification that the radial pressure gradient was uniform along the fin flank. In their models, only radial flow was concerned and it was assumed that flow was governed by surface tension forces. Therefore eq.(5-69) may be reduced to:

$$-\frac{1}{3}\frac{\sigma}{\mu}\frac{\partial}{\partial x}\delta^{3}\frac{\partial(r^{-1})}{\partial x}=\frac{k(T_v-T_w)}{\rho h_{fg}\delta} \qquad (5\text{-}80)$$

Further, in their models, the pressure in the condensate film given by eq.(5-60) was approximated to change linearly. The pressure drop over distance Δx with radii of r_1 at the begining and r_2 at the end is given by:

$$\Delta P=\sigma\left(\frac{1}{r_1}-\frac{1}{r_2}\right)$$

The pressure gradient (taken to be constant) over Δx is then given by:

$$\frac{\Delta p}{\Delta x}=\frac{\sigma}{\Delta x}\left(\frac{1}{r_1}-\frac{1}{r_2}\right) \qquad (5\text{-}81)$$

Karkhu and Borovkov [44] and Borovkov [46] took $r_1=t/2$ and $r_2 \to \infty$. The effective length of fin flank Δx was taken as the fin flank side minus the film thickness in the interfin space (see Chapter 2). Rudy and webb [47], on the other hand, took $r_1=t/2$ and $r_2=b/2$ and $\Delta x=h$. Honda's [49] analysis suggested constant radius over the fin top with an approximate value, based on the numerical solution, $r_1=t/2$.

At the moment, there is no conclusive support for the above approximaion. According to Honda's analysis, the linear approximation (eq.(5-81)) might be valid for a relatively low height fin but he gives no criterion for this.

As a matter of expediency we shall here adopt eq.(5-81) and take $r_1=t/2$ and r_2 given by eq.(5-30) or (5-38) in static condensate configuration analysis (section 5.2). The active distance along the fin flank is taken as $h-h_o$, where h_o is given by eq.(5-18). For the interfin space, r_2 is given by eq.(5-31) or (5-38) and a radius at the middle of spacing is $r_3 \rightarrow \infty$(note this is not strictly valid for the relatively small region between C and D as seen in Fig.5-1). Fig.5-11 shows parameters. The mass balances given by (5-80) are then approximated by:-

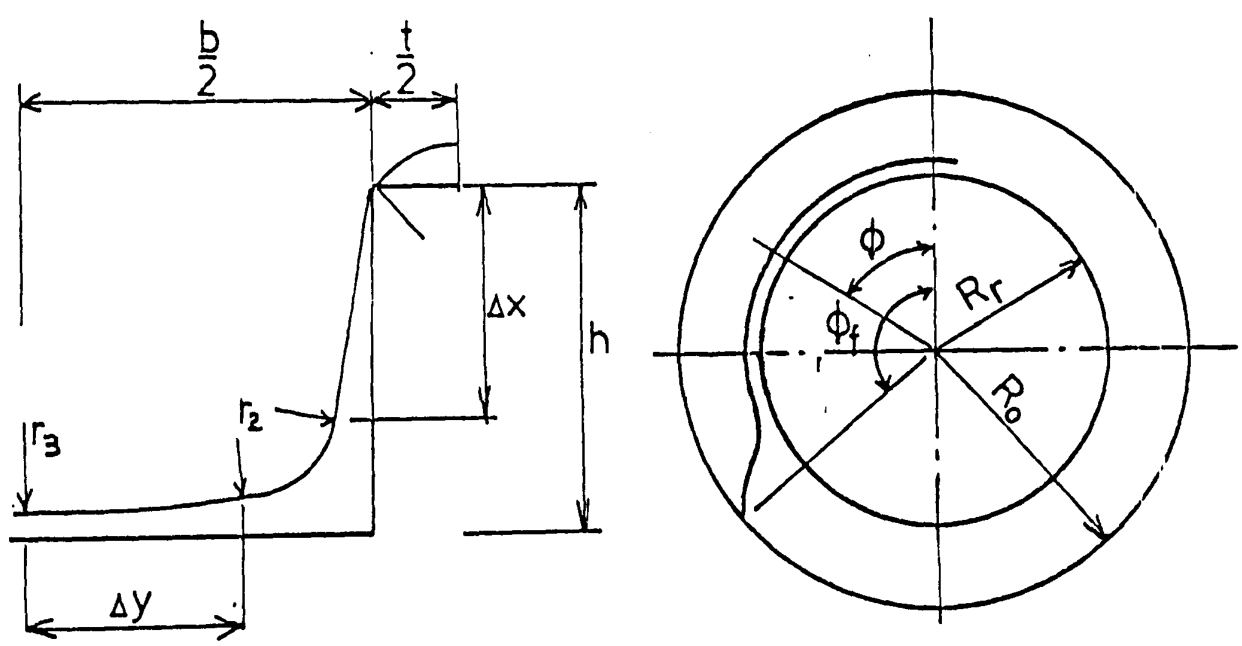

Fig.5-11 Parameters for approximations of theoretical expression for "unflooded" region

for fin flank:

$$\frac{1}{3} S_f \frac{d\delta^3}{dx} = \frac{1}{\delta} \tag{5-82}$$

$$S_f = \frac{\sigma \rho h_{fg}}{k\mu(T_v - T_w)} \frac{1}{h - h_o} \left(\frac{2}{t} + \frac{1}{r}\right) \tag{5-83}$$

for interfin space:

$$\frac{1}{3} S_b \frac{d\delta^3}{dx} = \frac{1}{\delta} \tag{5-84}$$

$$S_b = \frac{\sigma \rho h_{fg}}{k\mu(T_v - T_w)} \frac{1}{(b/2 - X_e)} \frac{1}{r} \tag{5-85}$$

Eq.(5-82) may be written:

$$S_f \delta^3 \frac{d\delta}{dx} = 1$$

Integrating, we have:

$$\frac{S_f}{4} \delta^4 = x + C$$

It is now assumed that $\delta = 0$ at $x=0$, i.e. at fin tip. So that,

$$\delta_f = \left(\frac{4}{S_f} x\right)^{1/4} \tag{5-86}$$

Following the same procedure and employing the assumption of $\delta = 0$ at the middle of interfin space leads to:

$$\delta_b = \left(\frac{4}{S_b} x\right)^{1/4} \tag{5-87}$$

The average film thickness is given by:

$$\delta_f = \frac{4}{5} \left(\frac{4}{S_f}\right)^{1/4} (h - h_o)^{1/4} \tag{5-88}$$

$$\delta_b = \frac{4}{5} \left(\frac{4}{S_b}\right)^{1/4} \left(\frac{b}{2} - X_e\right)^{1/4} \tag{5-89}$$

The corresponding average heat-transfer coefficients are given by:

$$\alpha_f = \frac{k}{\delta_f} = 0.884\left(\frac{S_f}{h-h_o}\right)^{1/4} \qquad (5\text{-}90)$$

$$\alpha_b = \frac{k}{\delta_b} = 0.884\left(\frac{S_b}{b/2-X_e}\right)^{1/4} \qquad (5\text{-}91)$$

The h_o and X_e are both taken as the mean "wedge" radius r in eq.(5-51), as described in the former section. Note that this procedure neglect any heat transfer across the retained liquid "wedge".

(b) <u>Approximation for "flooded" region</u>

(Surface tension driven condensate flow on fin top)

Owen et al. [42] and Rudy and Webb [47] analysed heat transfer in the flooded region as a conduction problem with parallel path composed of fins and condensate as described in Chapter 2. Honda et al. [49] on the other hand considered the surface tension forces on the heat transfer also in the unflooded region. Eq.(5-79) was used for the top of fin in horizontal direction but no detailed results were given in [49]. However their approximate equation for heat transfer in the flooded region based on their numerical analysis, indicated the same form as eq.(5-87) and (5-88) in which the approximation of uniform pressure gradient due to surface tension forces is used. (again no explanation were given in [49]) The following expression which took account only of heat transfer on the fin top was proposed:

$$\alpha = 0.9\left\{\frac{\sigma \rho h_{fg} k^3}{\mu(T_v-T_w)} \frac{1}{(0.8t/2)^2 r_{om}}\right\}^{1/4} \qquad (5\text{-}92)$$

where r_{om} is the radius of curvature of condensate film at the fin tip which was assumed to contact smoothly the curvature of condensate film between fins (see Fig.5-12). The average value of r_{om} is given by:

$$r_{om}=\frac{t(r_t+r_b)}{(p-t)}+r_t \qquad (5\text{-}93)$$

where p is pitch, r_t is the radius of fin tip, and r_b is the average radius of condensate surface in interfin space. The local radius r_b (radius of curvature assumed constant) is given by eq.(5-1), i.e:

$$r_b=\frac{\sigma}{\rho g z} \qquad (5\text{-}94)$$

where z is given for low-finned tube by:

$$z \simeq R_o(1-\cos\phi)$$

The average value of r_b is given by substitution of the average value of z in eq.(5-96):

$$\bar{z}=\frac{1}{\pi-\phi}\int_{\phi}^{\pi} R_o(1+\cos\phi)\,d\phi \qquad (5\text{-}95)$$

$$=R_o\left(1-\frac{\sin\phi}{\pi-\phi}\right)$$

so that, the average value of r_b is given by:

$$r_b=\frac{\sigma}{\rho g\bar{z}}=\frac{\sigma}{\rho g R_o\left(1-\frac{\sin\phi}{\pi-\phi}\right)} \qquad (5\text{-}96)$$

The assumption of uniform pressure gradient is again adopted, i.e. taken $r_t\rightarrow\infty$ (middle of top of fin where film is thin so that the radius of curvature of film surface is much larger than that of liquid surface between fins) and $r_2' = r_b$, thus:

$$\frac{\Delta P}{\Delta x} = \sigma \frac{2}{t} \frac{1}{r_b} \qquad (5\text{-}97)$$

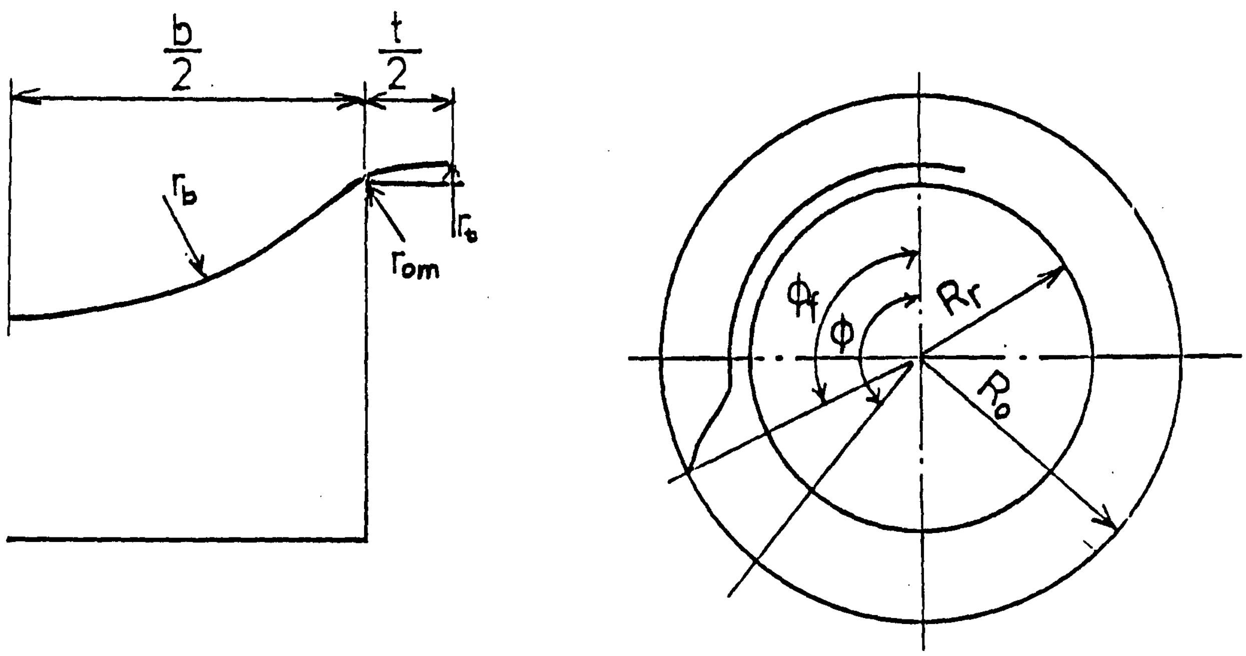

Fig.5-12 Parameters for approximations of theoretical expression for "flooded" region

It may be noted that since in the flooded region that static configuration indicates the two approximately uniform radii of curvature are directly connected (i.e. there is no intermediate region of low curvature as on the fin flank and in the interfin space for the unflooded region). The adoption of the uniform-pressure gradient approximation is probably more valid for the flooded region.

Since all of the condensate on the fin top flows horizontally into the interfin spaces, i.e. no account is taken of circumferantial flow on the fin top, the film thickness at the middle of fin top is taken to be zero. The same procedure as that between eqs.(5-82) and (5-91) leads to:

$$\delta_t = \frac{4}{5}\left(\frac{4}{S_f}\right)^{\frac{1}{4}}\left(\frac{t}{2}\right)^{\frac{1}{4}} \tag{5-98}$$

where

$$S_t = \frac{\sigma \rho h_{fg}}{k\ (T_v - T_w)}\ \frac{2}{t}\ \frac{1}{r_b} \tag{5-99}$$

Hence the average heat-transfer coefficient is given by:

$$\alpha_t = \frac{k}{\delta_t} = 1.25\left\{\frac{\sigma \rho h_{fg} k^3}{\mu (T_v - T_w)}\ \frac{1}{t^2}\ \frac{1}{r_b}\right\}^{\frac{1}{4}} \tag{5-100}$$

(c) <u>Approximate expression of heat transfer for whole tube</u>

Eqs.(5-90) and (5-91) give the average heat-transfer coefficient for fin flank and interfin space for the unflooded region and eq.(5-100) gives the heat-transfer coefficient for the flooded region. The total heat-transfer rate for the whole tube is then given by:

$$Q_{fin} = (A_f\alpha_f + A_b\alpha_b)\frac{\phi_f}{\pi} + A_t\alpha_t(1-\frac{\phi_f}{\pi}) \qquad (5\text{-}101)$$

Note that no heat transfer on the fin top in the unflooded region is included and only heat transfer on the fin top in the flooded region is considered.

The effective areas, for the whole circumferece over one pitch (i.e. over A B C D E as seen in Fig.5-13), are given by:-

for fin flank:

$$A_f = 2\frac{\pi}{4}\{(d_r+2h)^2-(d_r+2\bar{r})^2\} \qquad (5\text{-}102)$$
$$\simeq 2\pi d_r(h-\bar{r})$$

for interfin spacing:

$$A_b = \pi d_r(b-2\bar{r}) \qquad (5\text{-}103)$$

for fin top:

$$A_t = \pi t(d_r+2h) \qquad (5\text{-}104)$$

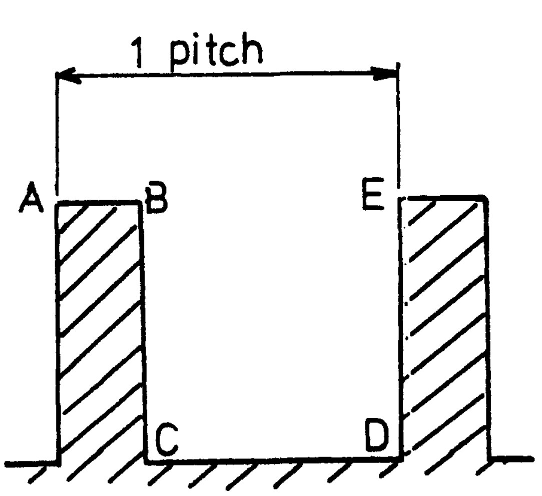

Fig.5-13 Definition of one pitch of fin

Then, the enhancement ratio of heat transfer on the finned tube to that of the plain tube may now be found. Here, the Nusselt equation is used for the plain tube. (Note that we have neglected effect of vapour velocity in the treatment for the finned tube.) The enhancement ratio for the same vapour-side temperature difference is given by:

$$E = \frac{Q_{fin}}{Q_{plain}} = E_u + E_f \qquad (5\text{-}105)$$

$$E_u = \left[\frac{0.884}{0.728}\left\{\frac{\sigma}{\rho\, g}\frac{d_r}{(h-h_o)^2}\left(\frac{2}{t}+\frac{1}{\bar{\bar{r}}}\right)\right\}^{\frac{1}{4}}\left(\frac{2(h-\bar{r})}{b+t}\right)\right.$$

$$\left.+\frac{0.884}{0.728}\left\{\frac{\sigma}{\rho\, g}\frac{d_r}{(b/2-h_o)^2}\frac{1}{\bar{\bar{r}}}\right\}^{\frac{1}{4}}\left(\frac{b-2\bar{r}}{b+t}\right)\right]\frac{\phi_f}{\pi}$$

$$E_f = \frac{1.25}{0.728}\left(\frac{\sigma}{\rho\, g}\frac{d_r}{t^2}\frac{1}{\bar{\bar{r}}}\right)^{\frac{1}{4}}\left(\frac{d_r+2h}{d_r}\right)\left(\frac{t}{b+t}\right)\left(1-\frac{\phi_f}{\pi}\right)$$

Result and comparison

Comparisons with the present experimental data are shown in Fig.5-14 where ratios of enhancement in unflooded region and flooded region are also shown seperately. $E=E_u+E_f$, where E_u is ratio for the unflooded region and E_f is that for the flooded region. It may be seen that eq.(5-105) overpredicts for all cases. For ethylene glycol with b=0.25 mm and for steam with b=0.25 mm and 0.5 mm the tubes were completely flooded, i.e.$\phi_f=0$, so that $E=E_f$, and prediction overestimates by a factor of around 2.2. For all three fluids and for values of b such that complete flooding does not occur, E_u alone overestimates the total enhancement except for b=0.5 mm for ethylene glyccl. The following reasons may account for these discrepancies:-

a) The assumption of uniform pressure gradient due to surface tension forces may not be adequate for all cases.

b) Approximations used lead significant errors during simplifying procedure, e.g. using inadequate average values.

(3) Ajustment of constants

For the second reason mentioned above, it might be possible empirically to compensate for errors by adjusting the constant coefficients, i.e. replacing the theoretical numberes, 0.884/0.728 and 1.25/0.728, by constants selected to give the "best" overall fit to the experimental data. $E_u{*}=C_1E_u$ and $E_f{*}=C_2E_f$ where C_1 and C_2 are constants, i.e. $E=C_1E_u+C_2E_f$, so that if eq.(5-105) were perfect correct, $C_1=C_2=1$.

Minimization of the sum of squares of relative residuals $\Sigma(E_{cal}/E_{obs}-1)^2$ using the least squares method and the data as described in section 5.4.2 gave $C_1=0.675$ and $C_2=0.44$. Results are shown in Fig.5-15. As may be seen, the modified equation underestimated the enhancement for R-113 and ethylene glycol and overestimated for steam. This modified equation predicts enhancement ratios by between 2 % and 24 % for R-113, between 5 % and 22 % for ethylene glycol and between 7 % and 35 % for steam. Table

5-10 shows numerical results for this case.

In an attempt further to improve the agreement between theory and expression, we next investigate empirical constants in the terms giving the heat transfer for the fin flanks and interfin spaces seperately. Thus we write E_u in eq.(5-105) as:

$$E_u=[C_{11}\ 1.214\{\frac{\sigma}{\rho\ g}\ \frac{d_r}{(h-\bar{r})^2}(\frac{2}{t}+\frac{1}{\bar{r}})\}^{\frac{1}{4}}\frac{2(h-\bar{r})}{b+t} \qquad (5\text{-}106)$$

$$+C_{12}\ 1.214\{\frac{\sigma}{\rho\ g}\ \frac{d_r}{(b/2-\bar{r})^2}\ \frac{1}{r}\}^{\frac{1}{4}}\frac{b-2\bar{r}}{b+t}]\ \frac{\phi_f}{\pi}$$

"Best" values for C_{11}, C_{12} and C_2 were again determined as indicated above. The values obtained were C_{11}=0.55, C_{12}=0.99 and C_2=0.45. Results are superimposed on Fig. 5-15 and Table 5-11 shows numerical comparisons. The fit was marginaly improved. The fact that for the interfin space the constant C_{12} was very close to its theoretical value might be taken to infer that the uniform pressure gradient due to surface tension forces might be adequate in the interfin space but less satisfactory for the fin flank.

(4) <u>Alternative approach using gravity condensate flow for the unflooded region</u>

(a) <u>"Beatty and Katz type" approach</u>

We now assume that a gravity overwhelms the effects of surface tension forces. This is essentially a Beatty and Katz [29] approach but allow for the presence of the liquid "wedge" (assumed adiabatic) at the fin roots in determining the effective heat-transfer area.

As Fig.5-16 shows, the fin surface at the fin root is covered by relatively thick film, so-called "wedge". Therefore the average fin vertical height L is obtained as:

$$L = \frac{A_{fu}}{X_f} \qquad (5\text{-}107)$$

where Afu is area of fin flank subtracting the "wedge" part given by:

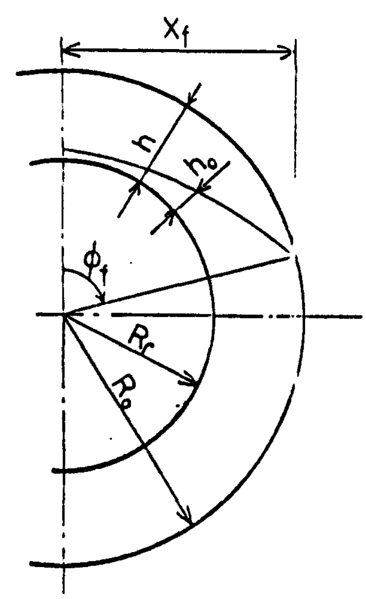

Fig.5-16 Physical model for modifying Beatty and Katz model using theoretical analysis of static configuration of retained liquid in unflooded region.

$$A_f = \int_0^{\phi_f} (h-h_0) R_0 \, d\phi \qquad (5\text{-}108)$$

$$= hR_0\phi_f - \frac{\sigma}{\rho g}\int_0^{\phi} \frac{R_0 \, d\phi}{(R_0+R_r\cos\phi)}$$

For low fin, Ro=Rr, so that:

$$A_f \simeq hR_0\phi_f - \frac{\sigma}{\rho g}\tan\frac{\pi}{2} \qquad (5\text{-}109)$$

and Xf is maximum base length

$$X_f = R_0 \qquad \text{for } \phi_f > \pi/2$$

$$= R_0\sin\phi_f \qquad \text{for } \phi_f < \pi/2$$

$$(5\text{-}110)$$

For the fin flank, the average heat-transfer coefficient is then given by:

$$\alpha_f = 0.943\left(\frac{k^3\rho^2 g h_{fg}}{\mu \Delta T L}\right)^{\frac{1}{4}} \tag{5-111}$$

For the interfin space, the average heat-transfer coefficient is given by:

$$\alpha_b = 0.728\left(\frac{k^3\rho^2 g h_{fg}}{\mu \Delta T d_r}\right)^{\frac{1}{4}} \tag{5-112}$$

Thus, the enhancement ratio is given by:

$$E = [C_{11}\ 1.295\left(\frac{d_r}{L}\right)^{\frac{1}{4}} \frac{2(h-\bar{r})}{b+t} + C_{12}\frac{b-2\bar{r}}{b+t}]\frac{\phi_f}{\pi} \tag{5-113}$$

$$+ C_2[1.717\left(\frac{\sigma}{\rho\ g}\frac{d_r}{t^2}\frac{1}{\bar{r}}\right)^{\frac{1}{4}}\left(\frac{d_r+2b}{d_r}\right)\left(\frac{t}{b+t}\right)](1-\frac{\phi_f}{\pi})$$

Results after ajusting constants by curve fitting procedure are shown numerically in Table 5-12 and graphically in Fig.5-17. As shown in table, the following constants appear:

C_{11}=1.54 C_{12}=4.27 C_2=0.446

The follows comments may be made in relation to the above. In comparison with the former case (i.e. flow driven by only surface tension forces);

(a) The overall fit is better, i.e. the standard deviation is smaller.

(b) The lines are closer to the data points for R-113 and steam, but the fit became marginally worse for ethylene glycol. The rate of fall of enhancement ratios with increasing spacing becomes smaller.

(c) The constant found for the fin spacing term, i.e. $C_{12}=4.27$ is of moderate magnitude but slightly lower than the "expected" value of unity.

(b) "Hybrid" approach

Finally, in view of the unsatisfactorily large value of C_{12} above and of the fact that, for the surface tension driven model, the constants for the interfin space was close to unity, and for the sake of completeness, we consider a model using gravity only for the fin flank and surface tension only for interfin space. As in all cases above, the surface tension model is used for the flooded region.

Thus:

$$E = \left[C_{11}\, 1.295\left(\frac{d_r}{L}\right)^{1/4} \frac{2(h-\bar{r})}{b+t} + C_{12}\, 1.214\left\{\frac{\sigma}{\rho g} \frac{d_r}{(b/2-\bar{r})^2} \frac{1}{r}\right\}^{1/4} \frac{b-2\bar{r}}{b+t} \right] \frac{\phi_f}{\pi} + C_2\left[1.717\left(\frac{\sigma}{\rho g} \frac{d_r}{t^2} \frac{1}{\bar{r}}\right)^{1/4} \left(\frac{d_r+2b}{d_r}\right)\left(\frac{t}{b+t}\right)\right]\left(1-\frac{\phi_f}{\pi}\right) \qquad (5\text{-}114)$$

Results are shown in Table 5-13 and illustrated in Fig.5-17. Constants found by fitting procedure are as follows:

$C_{11}=1.29 \quad C_{12}=0.94 \quad C_2=0.444$

In relation to the above, the following may be noted:-

(a) The lines are closer to the data points for R-113 and steam in comparison with surface tension model but discrepancies become slightly larger in comparison with the "Beatty and Katz type" model. For ethylene glycol the results for all three cases are very similar. For steam the result of the hybrid model falls between the other two cases.

(b) The constants found for fin flank and interfin space are reasonable, i.e. both are close to the "expected value" of unity.

(5) Effect of experimental errors in relation to the curve fitting procedures

Note that when finding disposable constants, both in the dimensional analysis based equation and in the theoretically based equation, we have taken no account of experimental errors and have treated all data equally, i.e. we have not used weighting functions. (Note that in Appendix C we conclude that on the basis of non-uniformity of wall temperature the uncertainties on vapour-side heat-transfer coefficient are greatest for steam and least for R-113) In view of this it is possible that minimization of absolute residuals of E which would give maximum weight to the large values, i.e. the data for R-113, might be a better procedure to have adopted. Results based on minimization of absolute residuals have been found for the case of eqs.(5-53), (5-113) and eq.(5-114). Fig.5-18 shows results and numerical comparisons are listed in Table 5-14. As seen in Table 5-14, constants are not greatly different to those found when minimizing relative residuals. The equations appear to represent the data more closely in comparison with results seen in Figs.5-8 and 5-17 for dimensional analysis based equation and for theoretically based equations. This, however, is natural since the absolute deviations of the points for the lines have been minimized.

(6) Concluding remarks

The important aspect of the present theoretical model is considered to be the recognition of the insulating effect of the condensate "wedge" retained at the fin roots in the unflooded region. This has not been included in earlier works, and explains the deleterious effect of surface tension for the unflooded region suggested by the study of the present experimental data using dimensional analysis. Earlier theoretical investigations have concentrated on the enhancing effect of surface tension through its effect on the condensate flow. The present study, on the contrary, seems to suggest that this may be of less importance.

Several somewhat different theoretical approaches have been used. These all have the common feature that the static configuration of the liquid in the unflooded region was used to estimate the surface area (both on the fin flanks and in the interfin space) "blanked" by the condensate "wedge". In general, agreement between theory and experiment was sufficientlly good to give confidence in the general method of approach. On the basis of the present experimental data, for the unflooded region it appears that the "Beatty and Katz" approach (gravity only) is probably the best. An unsatisfacory feature is the fact that, in all cases, and as a matter of expediency, the same surface tension driven flow model was used for the flooded region. This is a subject for future theoretical investigation. It may be significant that the constant for the flooded region obtained by the curve fitting procedure took closely similar values for all approaches. A similar result was found when fitting the data using equations based on dimensional analysis.

5.4.4 Comparison with other experimental data and other prediction

Comparisons are made for various expressions obtained both by dimensional analysis (see section 5.4.2) and by theory (see section 5.4.3).

From dimensional analysis:

$$E_1=[C_{11}\frac{2(h-\bar{r})}{b+t}+C_{12}\frac{b-2\bar{r}}{b+t}]\frac{\phi_f}{\pi}+C_2\xi(1-\frac{\phi_f}{\pi}) \qquad (5\text{-}115)$$

where $C_{11}=2.93$ $C_{12}=3.51$ $C_2=0.473$ by minimization of relative residuals

$C_{11}=2.98$ $C_{12}=4.11$ $C_2=0.491$ by minimization of absolute residuals

This was the simplest of the equations and also appeared best to fit the present data.

From theoretical approach we first consider:

$$E_2=\{C_{11}[1.295(\frac{d_r}{L})^{\frac{1}{4}}\frac{2(h-\bar{r})}{b+t}]+C_{12}\frac{b-2\bar{r}}{b+t}\}\frac{\phi_f}{\pi} \qquad (5\text{-}116)$$

$$+C_2[1.717(\frac{\sigma}{\rho g}\frac{d_r}{t^2}\frac{1}{\bar{r}_b})^{\frac{1}{4}}(\frac{d_r+2h}{d_r})(\frac{t}{b+t})](1-\frac{\phi_f}{\pi})$$

where $C_{11}=1.54$ $C_{12}=4.27$ $C_2=0.446$ by minimization of relative residuals

$C_{11}=1.58$ $C_{12}=4.75$ $C_2=0.453$ by minimization of absolute residuals

This is based on the Beatty and Katz model for the unflooded region (i.e. flow driven by only gravity).

We also consider:

$$E_3=\{C_{11}[1.295(\frac{d_r}{L})^{\frac{1}{4}}\frac{2(h-\bar{r})}{b+t}]+C_{12}[1.214(\frac{\sigma}{\rho g}\frac{d_r}{(b/2-r)^2}\frac{1}{\bar{r}})^{\frac{1}{4}}\frac{b-2\bar{r}}{b+t}]\}\frac{\phi_f}{\pi}$$

$$+C_2[1.717(\frac{\sigma}{\rho g}\frac{d_r}{t^2}\frac{1}{\bar{r}_b})^{\frac{1}{4}}(\frac{d_r+2h}{d_r})\frac{t}{b+t}](1-\frac{\phi_f}{\pi}) \qquad (5\text{-}117)$$

where $C_{11}=1.29$ $C_{12}=0.94$ $C_2=0.444$ by minimization of relative residuals

$C_{11}=1.18$ $C_{12}=1.27$ $C_2=0.458$ by minimization of absolute residuals

This is so-called "hybrid" model and gives similar results to those of eq.(5-116). In this case the constants appeared to be closer to the theoretical values.

(1) <u>Comparison with recent experimental data</u>

In the available data listed in Appendix B, only in the case of Georgiadis steam data [40] the fin geometry (i.e. fin spacing, thickness and height) was systematically studied. The data of Honda et al. [34] are also considered. These data appear to be of good reliability. For the Georgiadis data, enhancement ratios were calculated, by the present author, using the same procedure as that described in section 4.1 and using the coolant-side heat-transfer correlation given in [40].

Considering first the steam data of Georgiadis [40], in Fig.5-19 to 5-21, comparisons are made with the tubes having (a) t=0.5 mm h=1.0 mm, (b) t=1.0 mm h=1.0 mm and (c) t=1.0 mm h=2.0 mm.

As Fig.5-19 shows, eq.(5-115) (dimensional analysis) gives reasonable general agreement with the experimental data. Little difference was found between results when using constants determined by minimization of relative and absolute residuals. For the case when b=0.5 mm (completely flooded) eq.(5-115) underpredicts the enhacement ratios. For the higher spacing, eq.(5-115) marginally overpredicts for tube with h=2.0 mm, and underestimates the enhancement for other cases.

As Fig.5-20 shows, eq.(5-116) (Beatty and Katz type) generally underpredicts the enhancement ratios. These theoretical predictions are the same when using the constants based on minimization of relative and absolute residuals.

As Fig.5-21 shows, eq.(5-117) ("hybrid") generally underpredicts (except for the completely flooded case b=0.5 mm) when using constants determined by minimization of relative residuals. This prediction is, however, significantly improved when using constants obtained by minimization of absolute residuals and appears to give the best representation of the Georgiadis data. As other models, enhancement ratio decreases, as incresing fin thickness.

In Fig.5-22 the predictions are compared with the Georgiadis data by plotting enhancement ratio again fin spacing for a particular fin spacing (b=1.0 mm). For the three cases (dimensional analysis, Beatty and Katz type and "hybrid") the constants found by minimization of absolute residuals have been used. The equations are in broadly agreement with the data, particuraly the dimensional analysis and "hybrid", but do not show a maximum in the experimental data of fin thickness.

Figs.5-23 to 5-25 show comparisons with the Honda et al. data for R-113 and methanol. Since no experimental data for a plain tube are given, comparison is made on the basis of the calculated to measured heat-transfer coefficinet, i.e. $\alpha_{cal}/\alpha_{obs}$. In their experiments, three different fins and tubes geometries were used:

(a) dr=17.09 mm, b=0.39 mm, t=0.11 mm, h=1.13 mm, θ=0 deg

(b) dr=15.8 mm, b=0.47 mm, t=0.51 mm, h=1.46 mm, θ=4.5 deg

(c) dr=17.05 mm, b=0.35 mm, t=0.29 mm, h=0.92 mm, θ=5.3 deg

where θ is the "half angle at the fin tip" (zero for rectangular cross section fin). In (b) and (c) the fin cross sections are trapezoidal. Note that the theoretical expression and the determination of the constants using the present experimental data all relate to the case of rectangular section fins. When comparing three equations with data for trapezidal fins arithematic mean values have been used for b and t.

Eq.(5-115) (dimensional analysis) is compared in Fig.5-23 with the data for both fluids. Good agreement may be seen, except for case C, for both liquid. Eq.(5-116) (Beatty and Katz type) also shows good agreement with the data (see Fig 5-24). In this case, except those for low temperature difference, which are less reliable, it predicted to within 20 %. Eq.(5-117) ("hybrid") is compared with the data in Fig.5-25. This predicted heat-transfer coefficient are somewhat higher than those given by the Beatty and Katz type equation but are again seen to be in good general agreement with the the data.

(2) <u>Comparison of earlier predictions with the recent experimental data</u>

It is of interest to make comparison of those data used above with earlier predictions (described in section 2.2.3 and section 4.5). The Beatty and Katz [29], Owen et al. [42] and Rudy et al. [47] predictions are compared with the data of Georgiadias [40] and Honda et al. [34].

Figs.5-26 to 5-28 show comparisons with the Georgiadias data. As seen in Figs.5-26 and 5-27, the equations of Beatty and Katz, and Owen et al. are clearly less satisfactory than the equations developed in the present work, while their expressions give the correct enhancement at particular fin spacings. The Rudy et al. equation (see Fig.5-28) predicts correct general behaviour . This model, however, predicts zero heat transfer for the case of complete flooding at fin spacings less than 0.5 mm.

Fig.5-29 compares the Rudy et al. equation with the Georgiadis data for dependence of enhancement on fin thickness. The general behaviour is seen to be somewhat similar to the present predictions.

Fig.5-30 shows comparisons with Honda et al. data for R-113 and methanol. As Fig.5-30 (a) shows, the Beatty and

Katz equation underpredicted heat-transfer coefficient 30 % for R-113 and overpredicted those for metha Fig.5-30 (b) compares Owen et al. equation with the d This equation made generally good agreement for meth but underpredicted heat-transfer coefficients for R-11 40 %. Fig.5-30 (c) shows comparisons between Rudy et prediction and the data. In the case of tube(c) for fluid and in the case of tube(b) for R-113 good agree was made. However, in other cases, discrepancies are to be larger than those with the Beatty and Katz, and et al. equations.

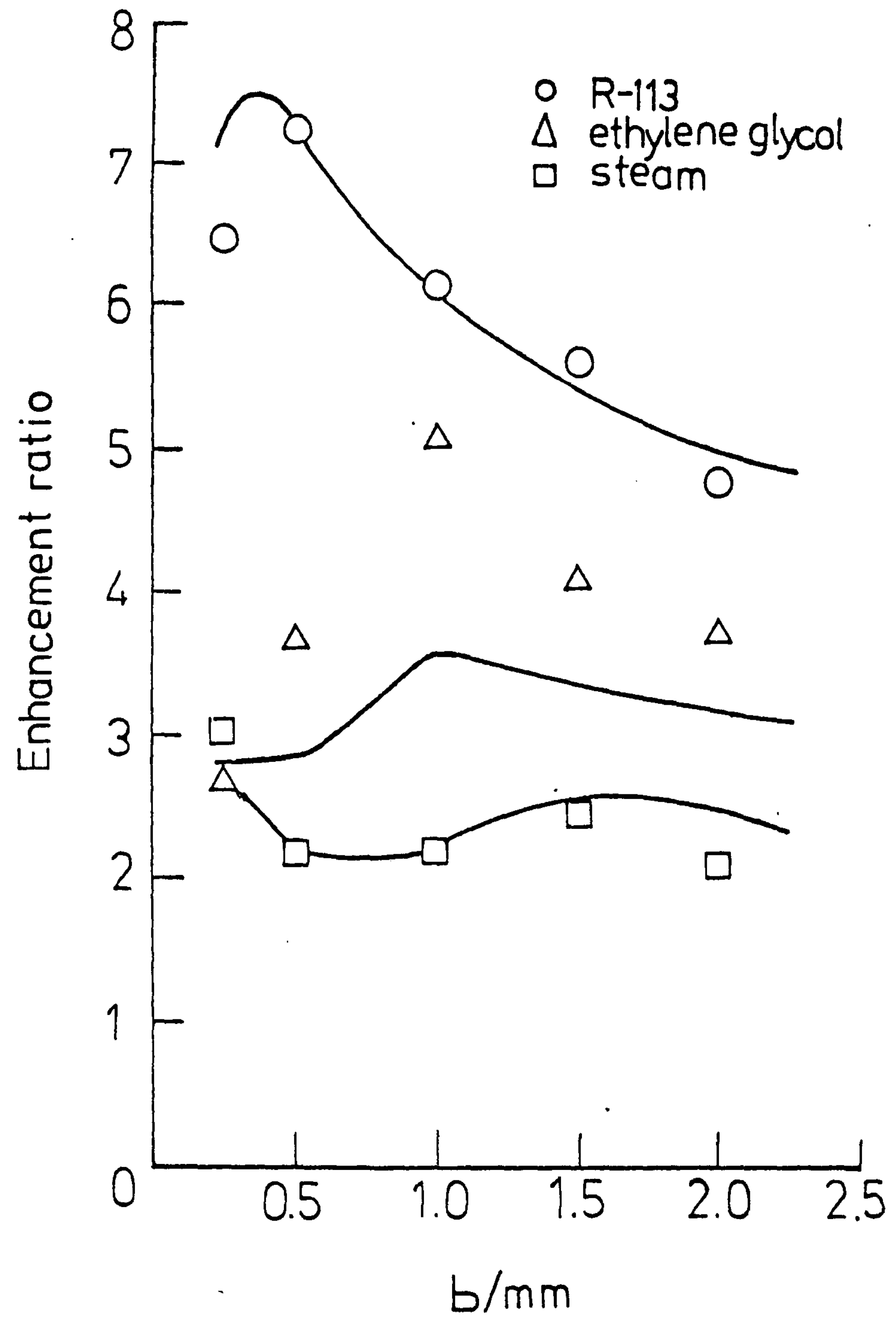

Fig.5-7 Comparison of eq.(5-48), using constan
$n=0$ $K_1=0$ $K_2=1.17$ $K_3=1.4$ $K_4=0.48$
(see Table 5-4), with the data.

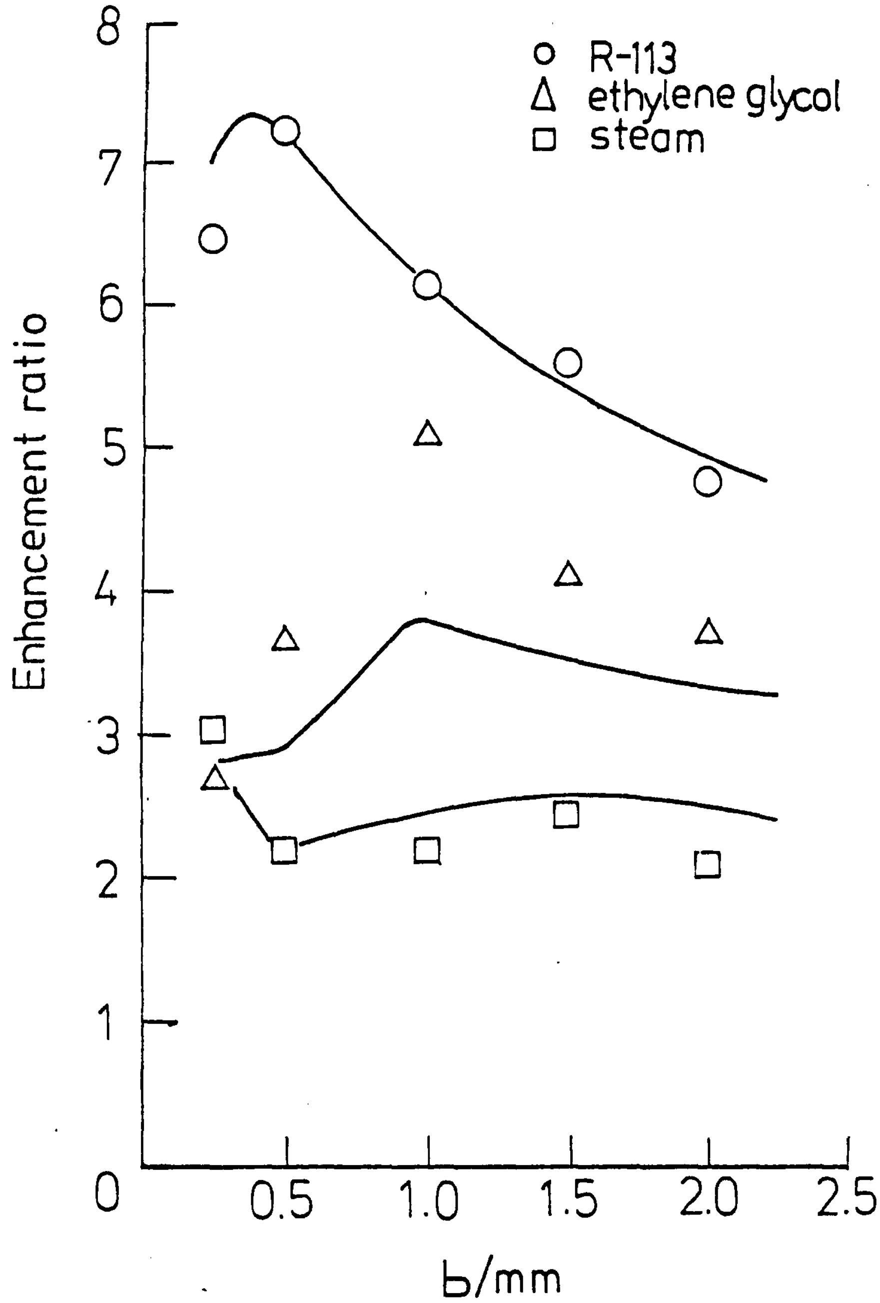

Fig.5-8 Comparison of eq.(5-52), using constar
$n=0$ $K_1=0$ $K_2=3.51$ $K_3=2.98$ $K_4=0.473$
(see Table 5-9), with the data.

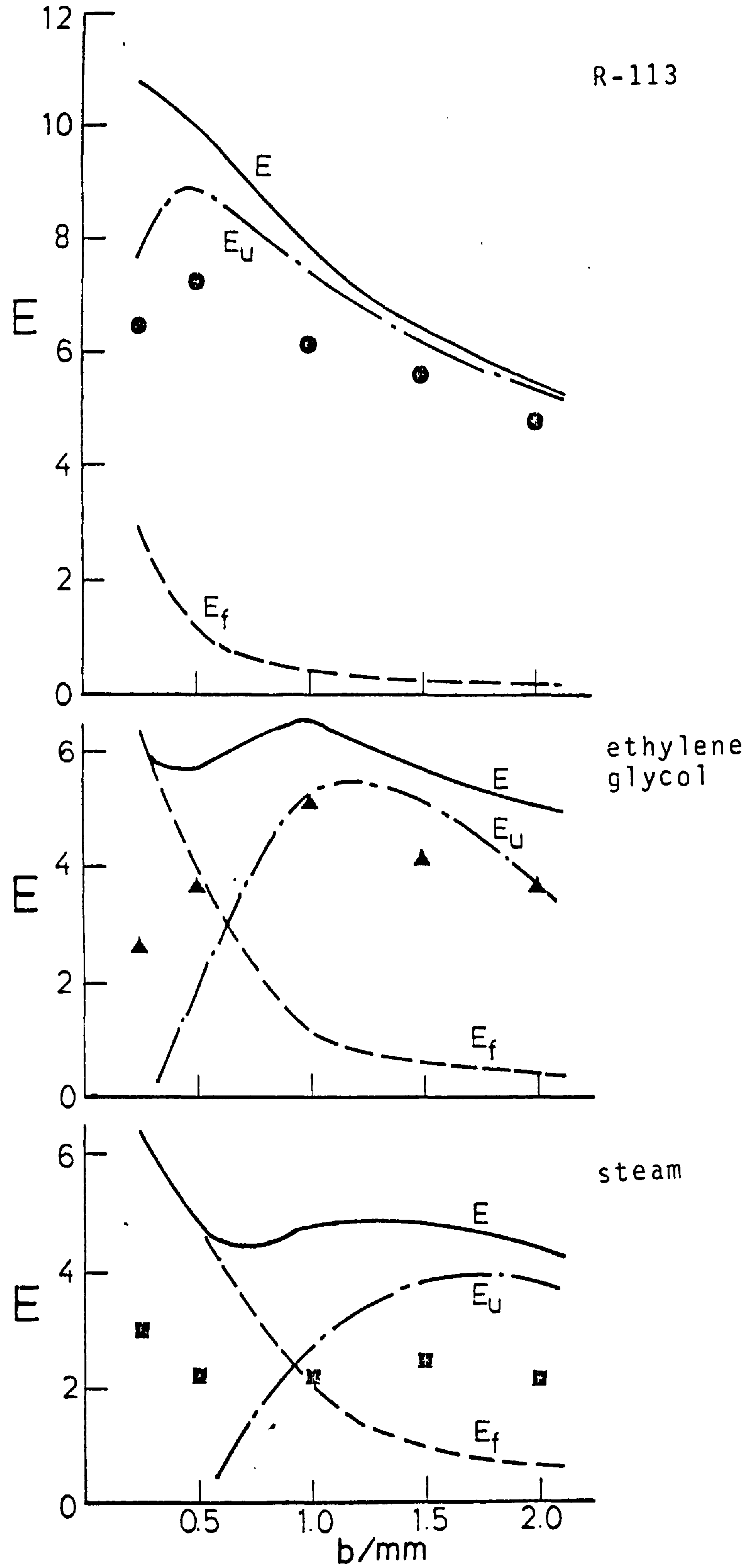

Fig.5-14 Comparison of theoretical equation (
with the data.

$E=E_u+E_f$

where E_u is portion of "unflooded"reg
and E_f is portion of "flooded" regio

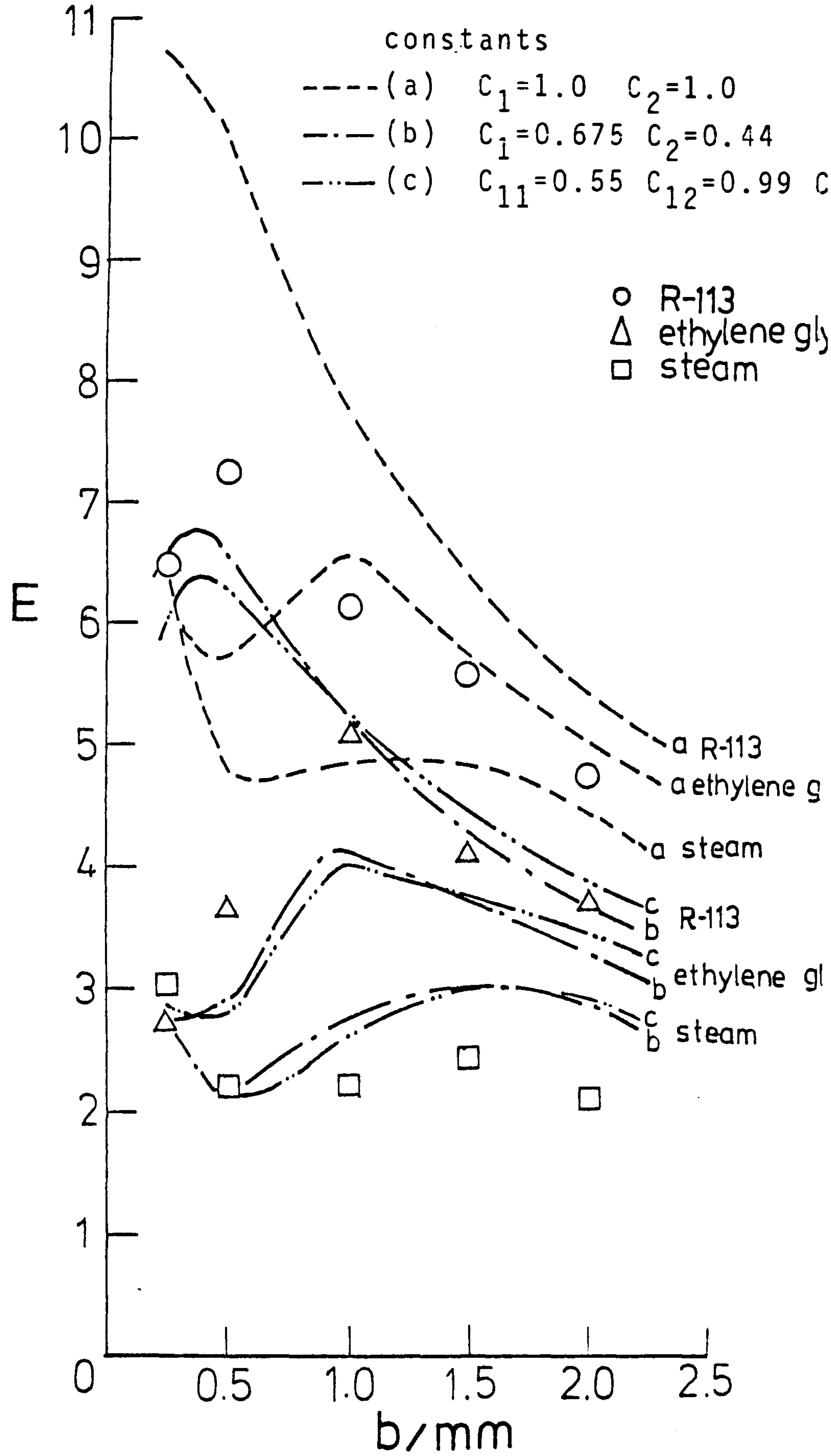

Fig.5-15 Comparison of theoretically-base equations with the data. Consta found by minimization of relativ residuals.

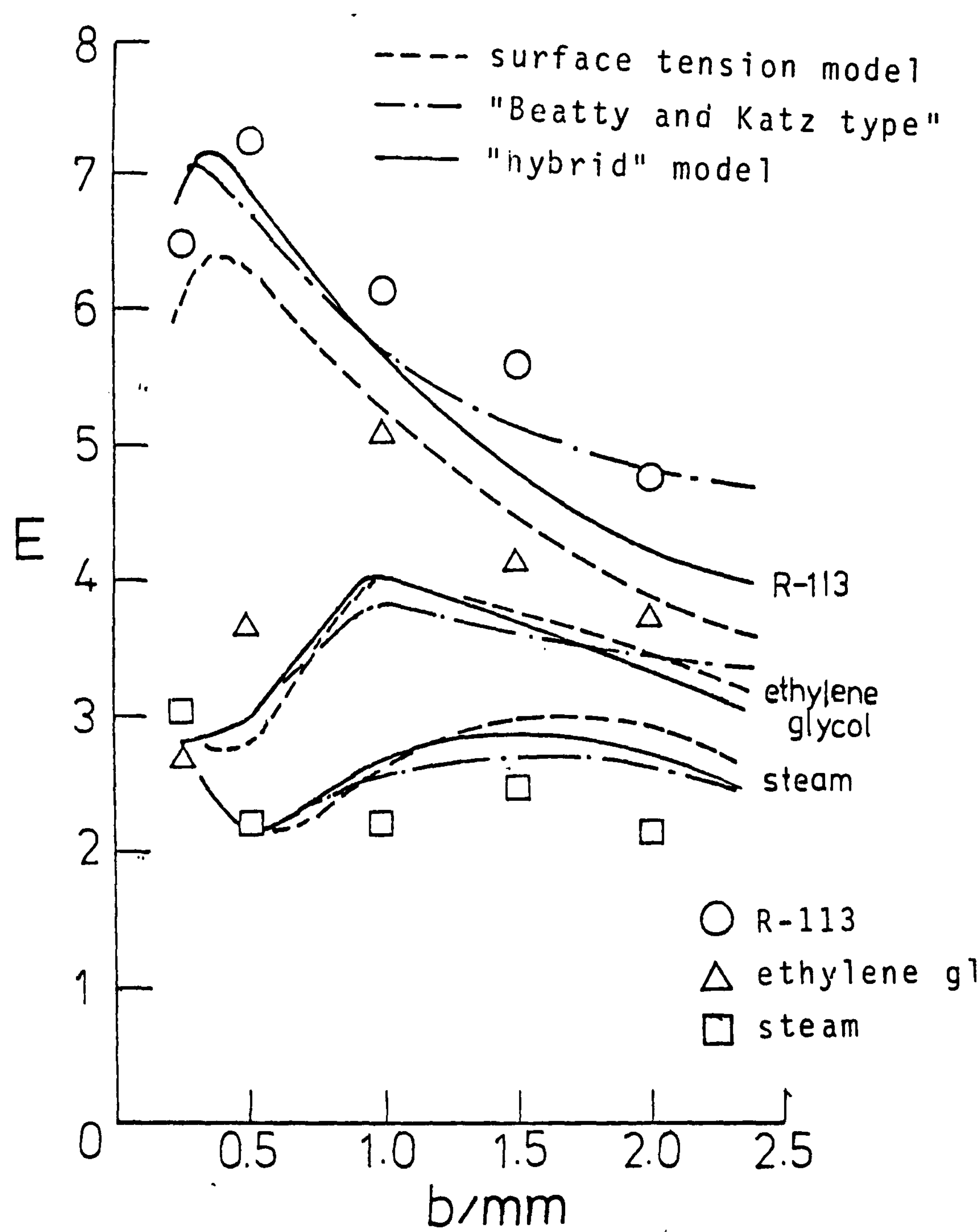

Fig.5-17 Comparison of the different theoretica models (constants found by minimizatio of relative residuals) with the data.

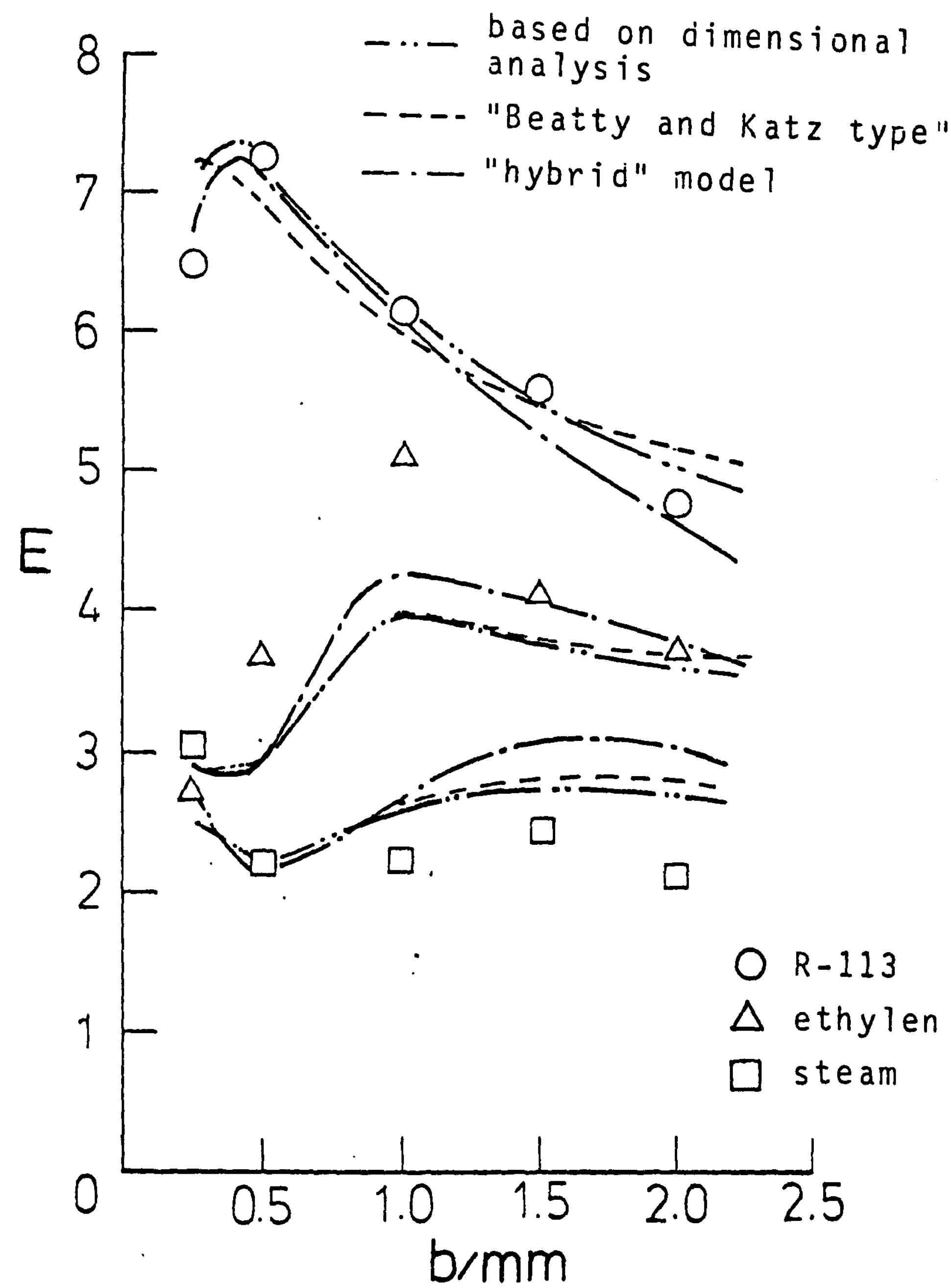

Fig.5-18 Comparisons of the different expres
(constants found by minimization of
absolute residuals) with the data.

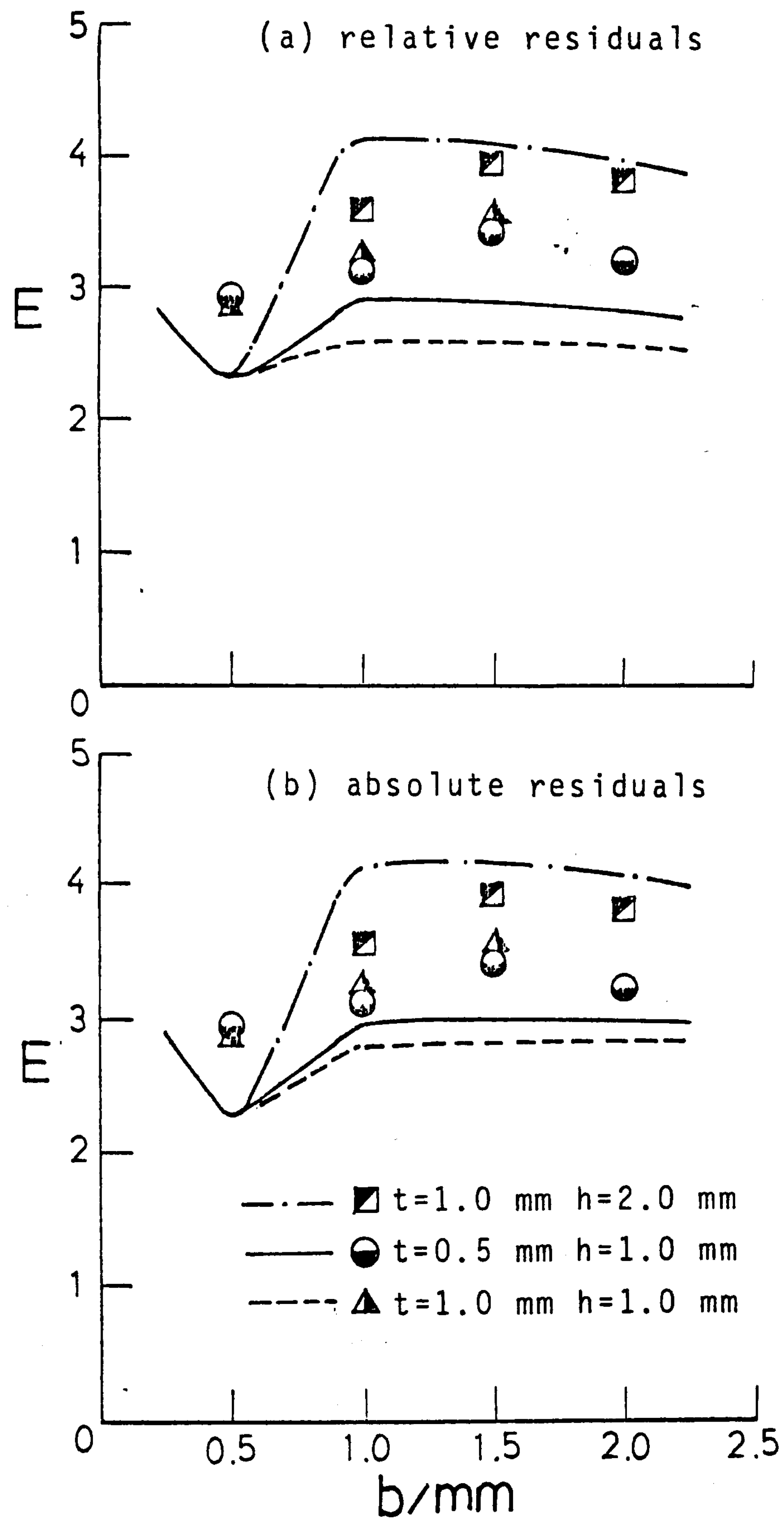

Fig.5-19 Comparison of eq.(5-115) (based on dimensional analysis) (constants found by minimization of (a) relat and (b) absolute residuals) with t data of Georgiadis [40] for steam.

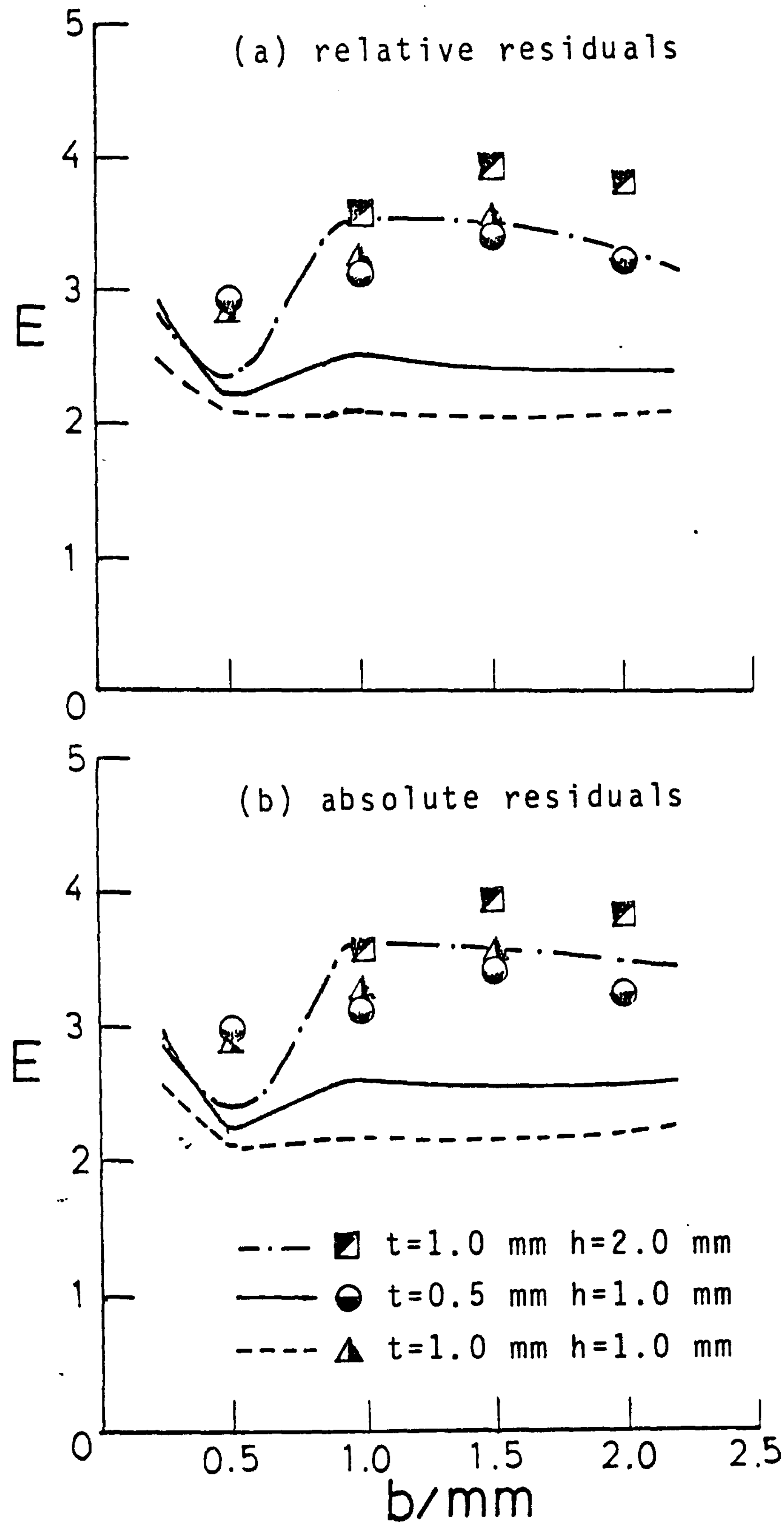

Fig.5-20 Comparison of eq.(5-116) ("Beatty a Katz type" model) (constants found minimization of (a) relative and (b) absolute residuals) with the data of Georgiadis [40] for steam.

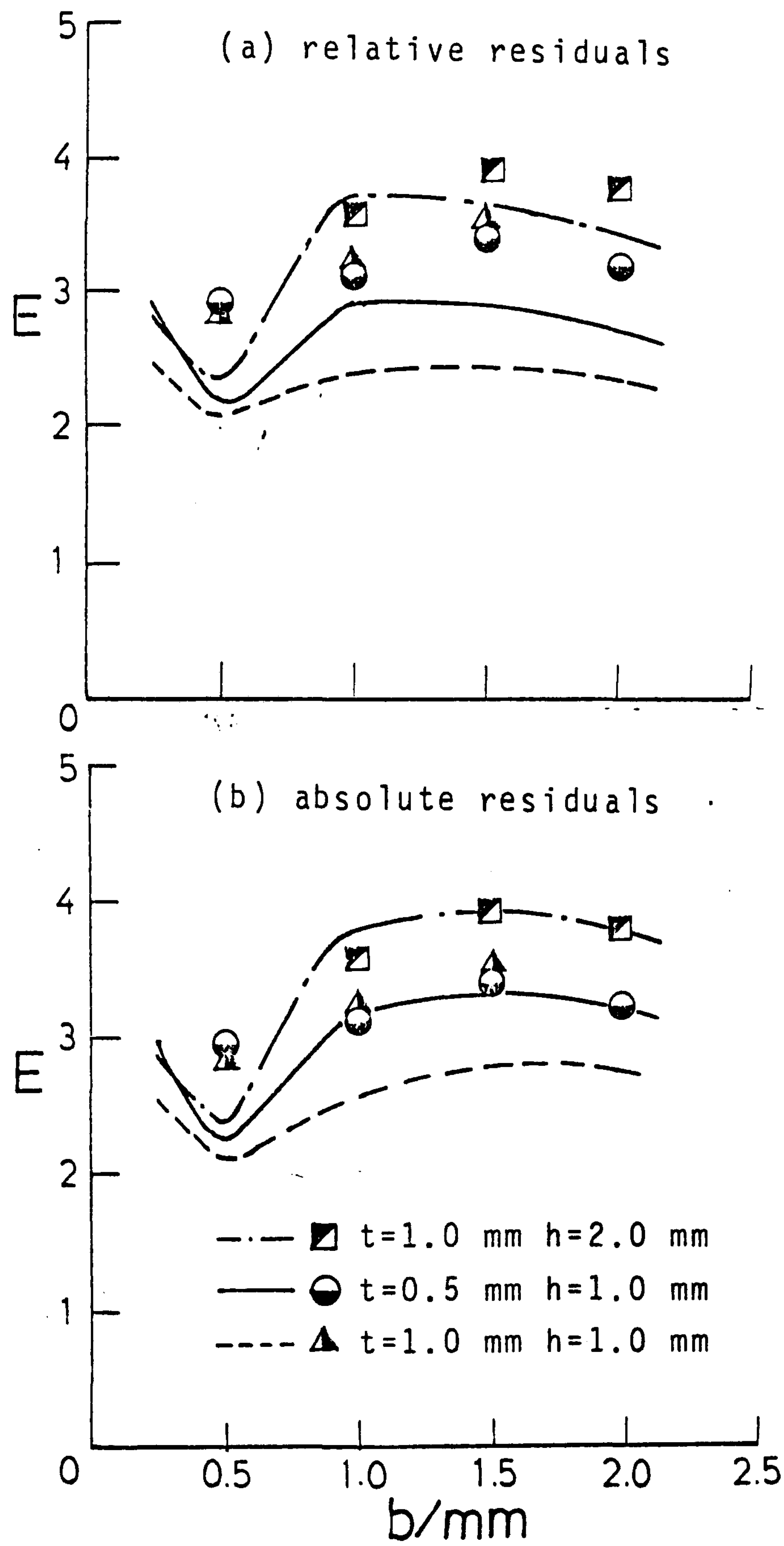

Fig.5-21 Comparisons of eq.(5-117) ("hybrid" model) with the data of Georgiadis [40] . Constants found by minimiza zation of (a) relative and (b) absolute residuals.

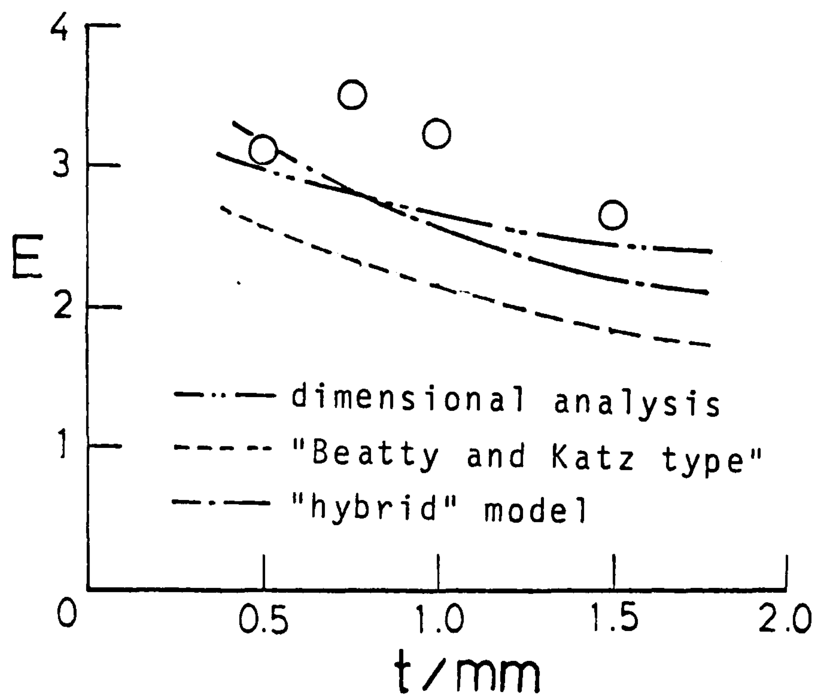

Fig.5-22 Comparisons of eq.(5-115) (based on dimensional analysis), eq.(5-116) ("Beatty and Katz type" model) and ("hybrid" model) (constants in all cases obtained by minimization of absolute residuals) with the steam data of Georgiadis [40] . Dependence of enhancement on fin thickness.

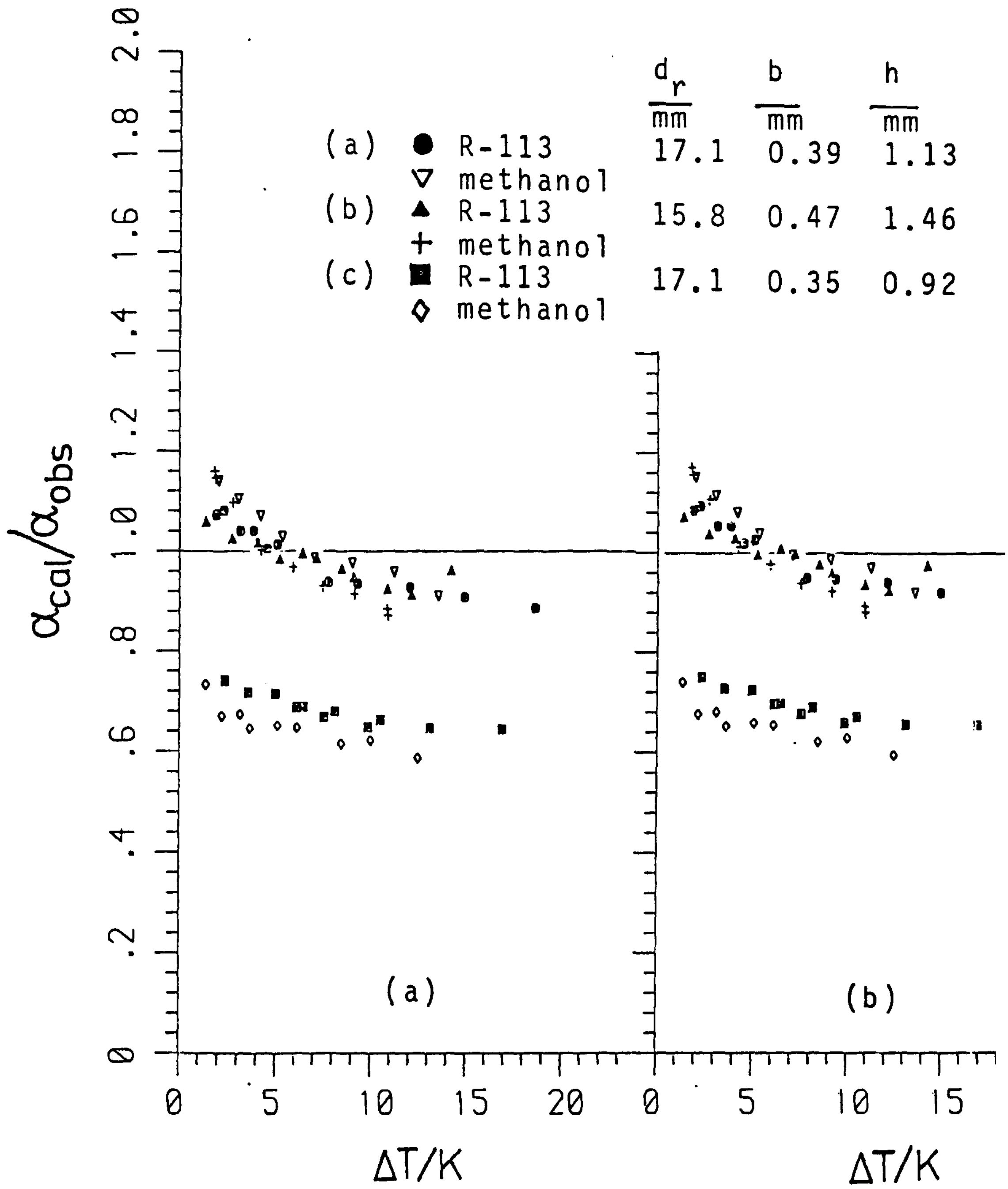

Fig.5-23 Comparisons of eq.(5-115) (based on dimensional analysis) (constants found by minimization of (a) relative and (b) absolute residuals) with the data of Honda et al. [52] for R-113 and methanol.

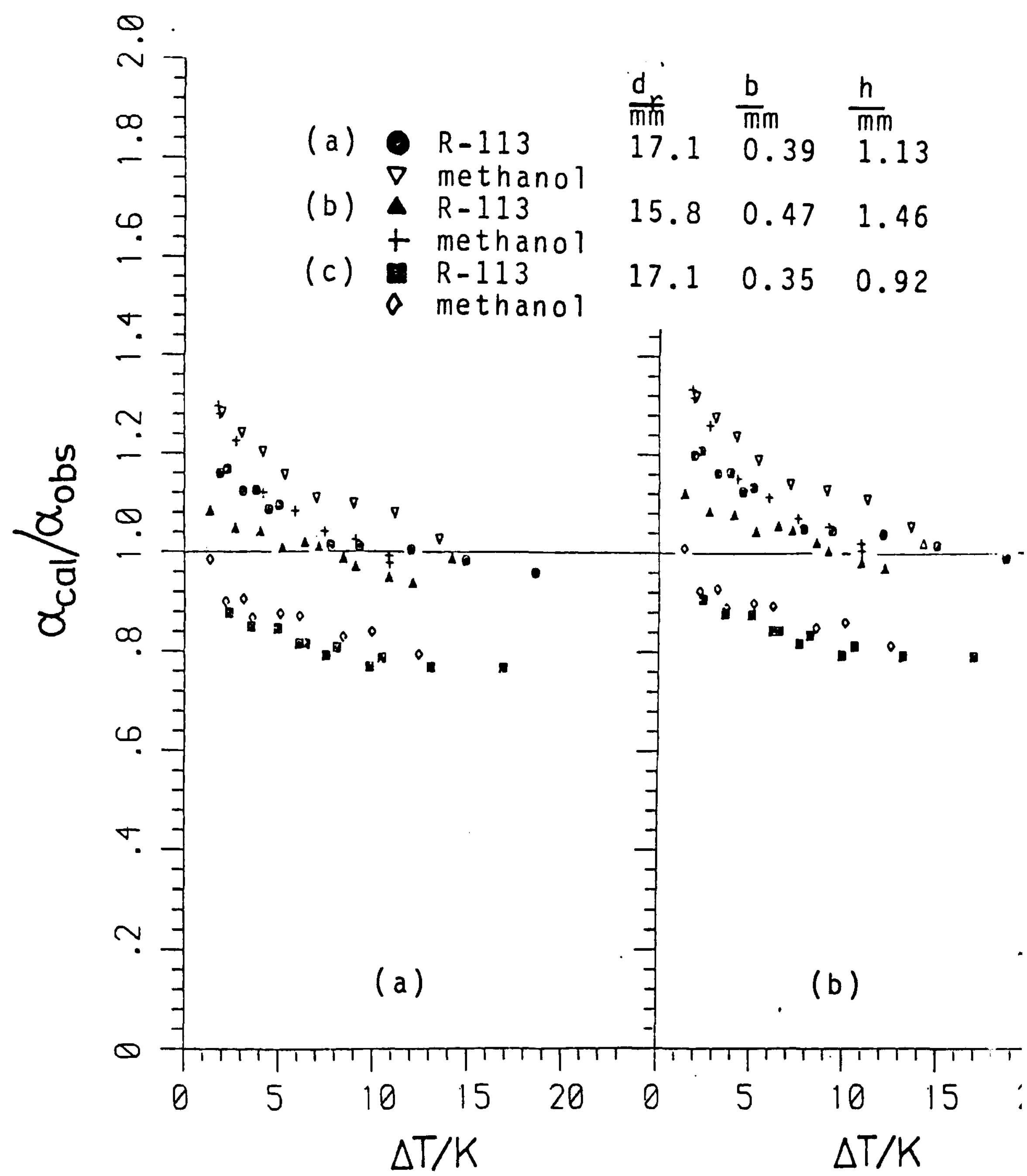

Fig.5-24 Comparisons of eq.(5-116) ("Beatty and Katz type" model) (constants found by minimization of (a) relative and (b) absolute residuals) with the data of Honda et al. [52] for R-113 and methanol

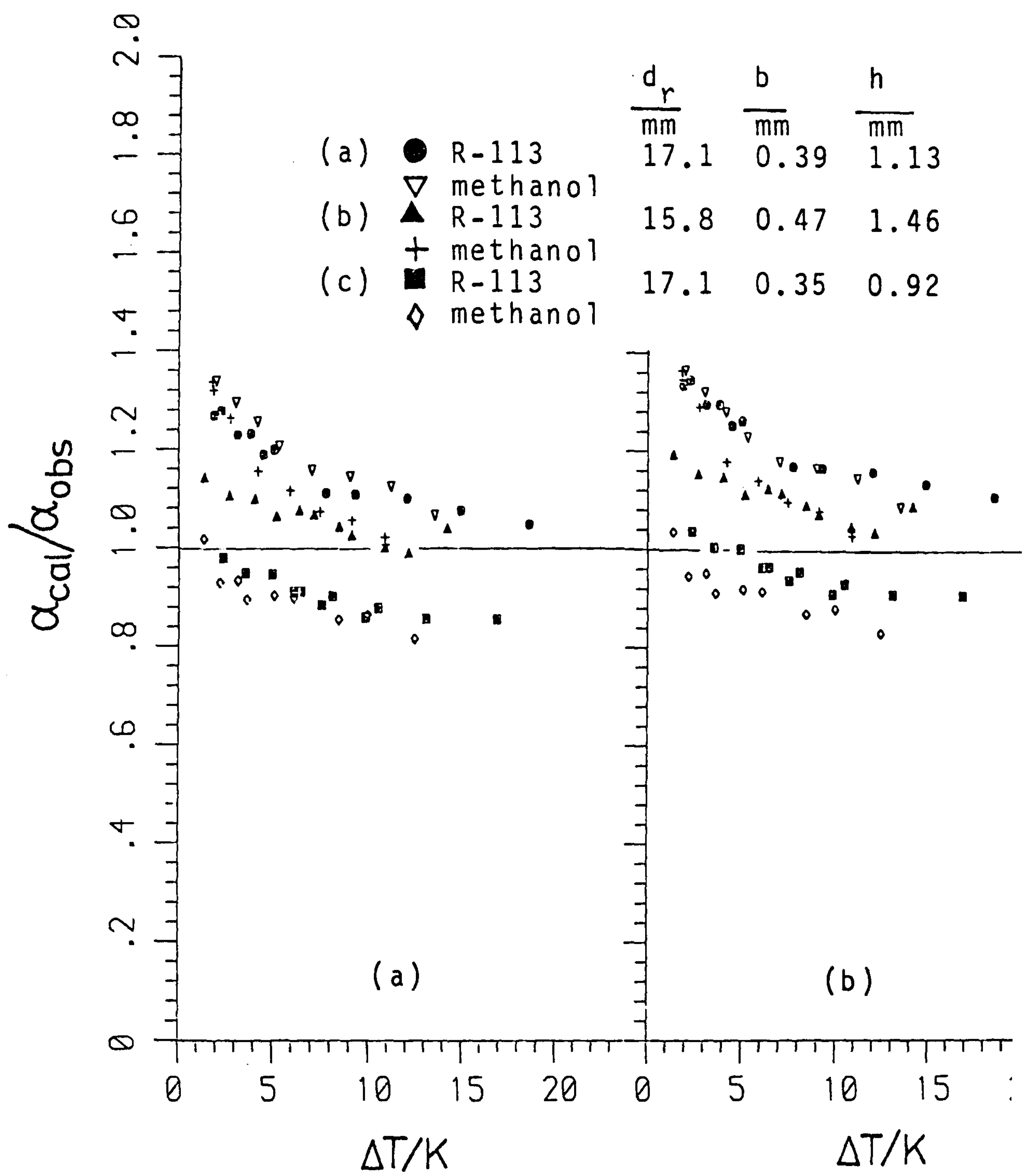

Fig.5-25 Comparison of eq.(5-117) ("hybrid" mode (constants found by minimization of (a) relative and (b) absolute residuals) w the data of Honda et al. [52] for R-11 and methanol.

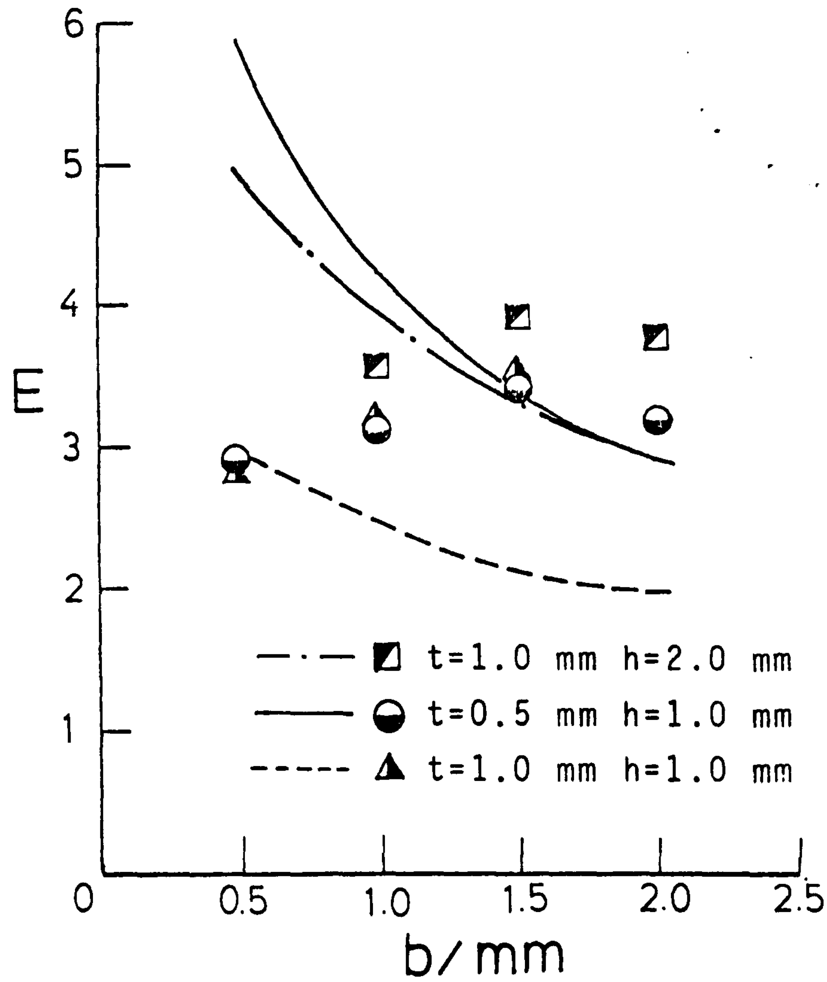

Fig.5-26 Comparisons of Beatty and Kat [29] model with the steam dat of Georgiadis [40]

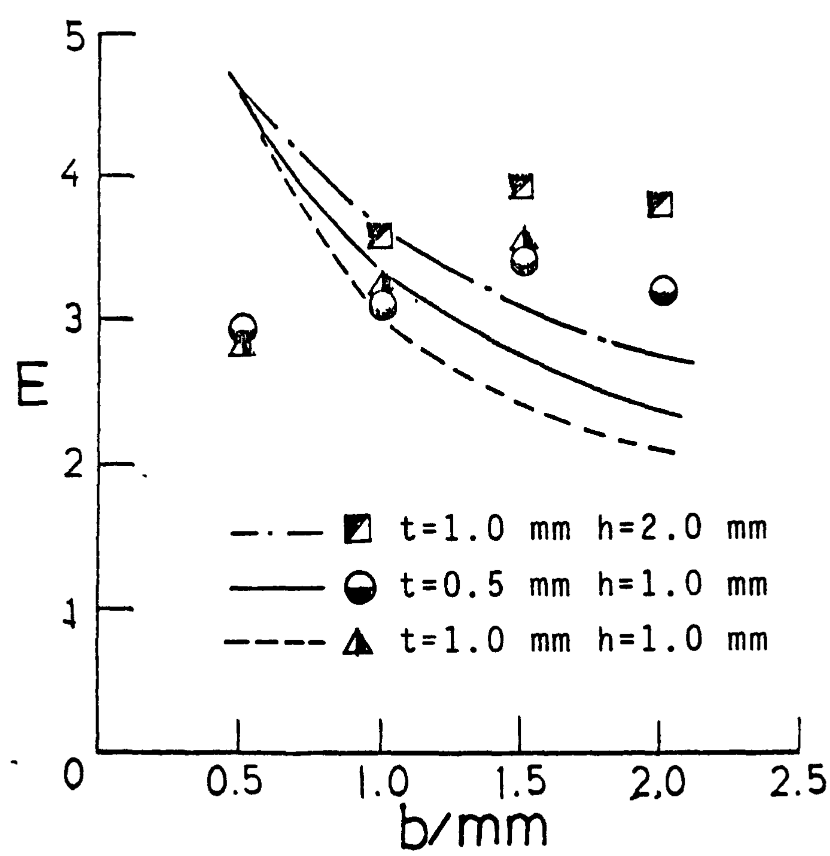

Fig.5-27 Comparisons of Owen et al. [4 model with the steam data of Georgiadis [40]

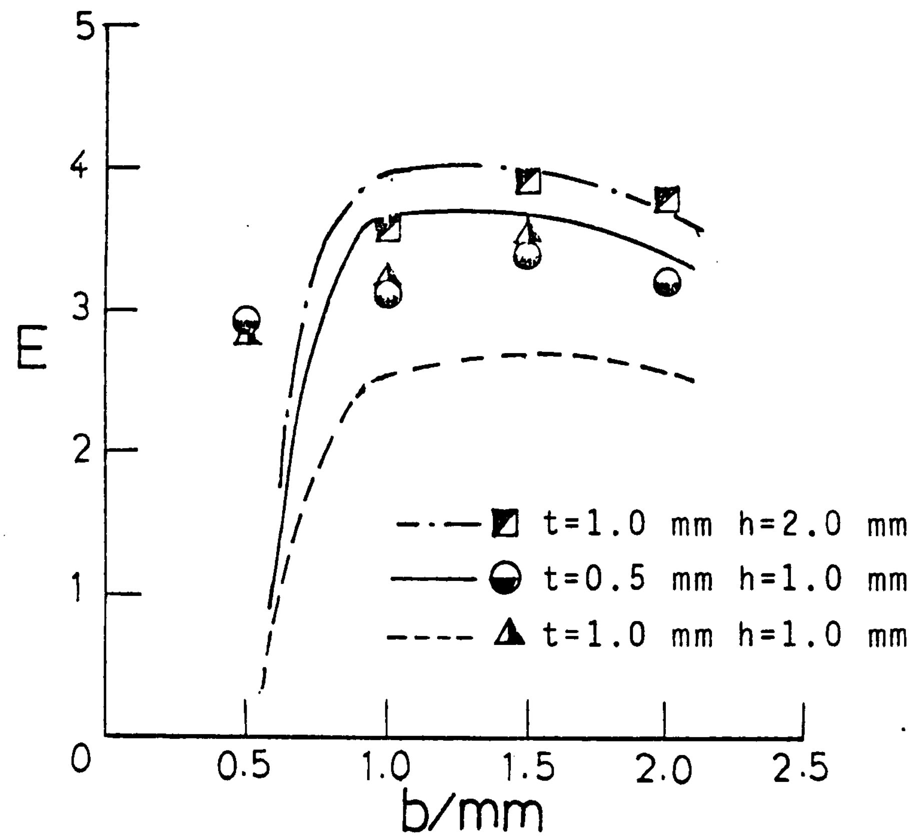

Fig.5-28 Comparisons of Rudy et al. [47] model with the steam data of Georgiadis [40] .

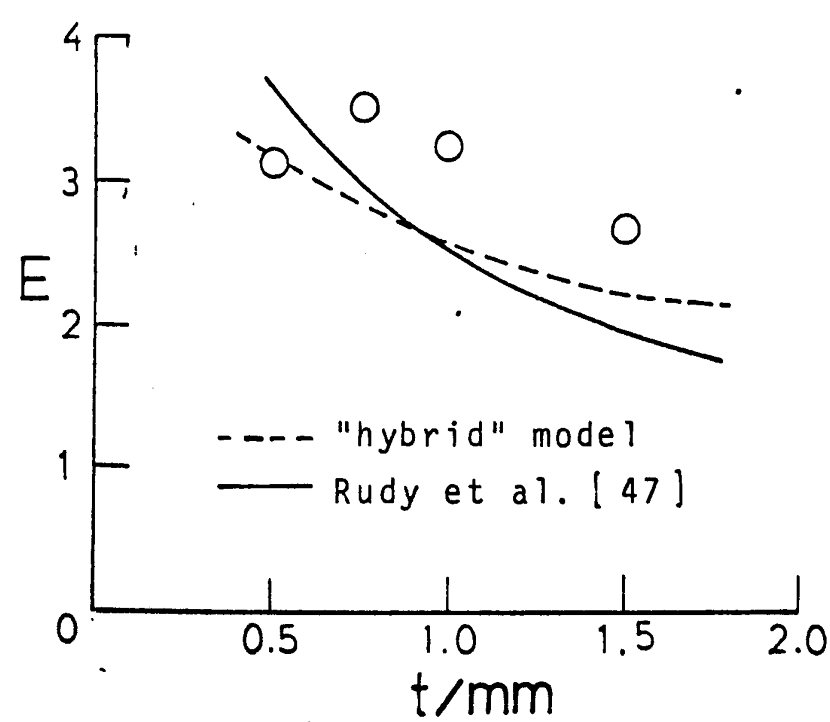

Fig.5-29 Comparison of Rudy et al. [47] model with the steam data of Georgiadis [40]. Dependence

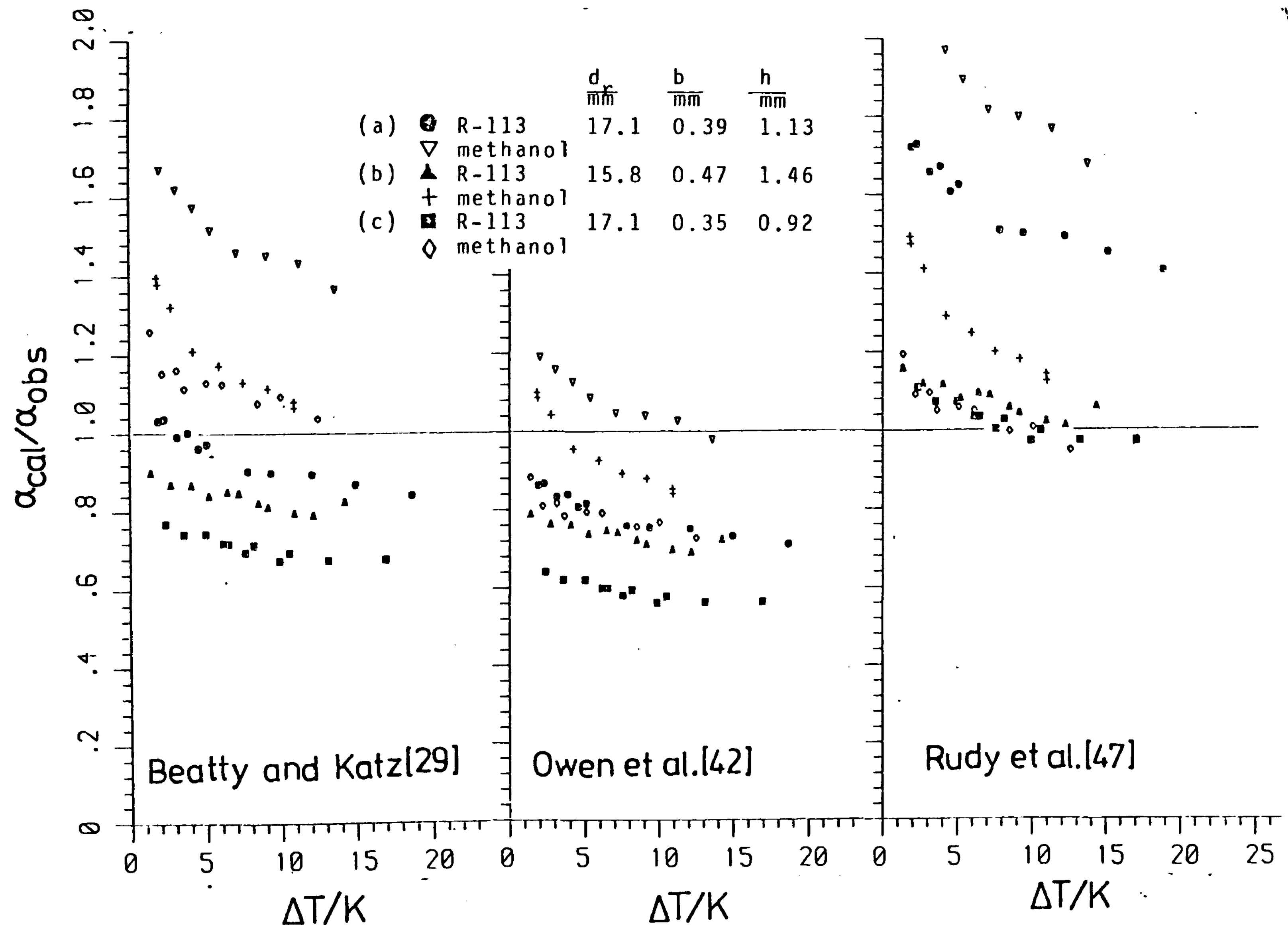

Fig.5-30 Comparison of Beatty and Katz [29], Owen et al.[42],

Table 5-1 Measurements of "retention" angle [55]

Liquid	Fin spacing mm	Liquid temperature ℃	ϕ_f/π
R-113	0.5	0.59	0.651
	1.0	3.0	0.712
	1.5	1.55	0.784
	2.0	1.35	0.790
	4.0	0.88	0.906
	6.0	1.13	0.906
	8.0	2.40	0.940
ethylene glycol	0.5	22.5	0.072
	1.0	22.0	0.498
	1.5	21.5	0.594
	2.0	21.5	0.649
	4.0	22.0	0.732
	6.0	21.5	0.745
	8.0	22.0	0.743
	110.0	19.0	0.759
	12.0	19.0	0.776
	14.0	20.0	0.769
	16.0	20.0	0.785
	18.0	20.0	0.787
	20.0	20.0	0.772
water	0.5	12.5	0
	1.0	12.5	0.181
	1.5	12.8	0.436
	2.0	13.0	0.525
	4.0	13.0	0.685
	6.0	12.0	0.721
	8.0	12.5	0.755
	10.0	12.0	0.697
	12.0	12.5	0.780
	14.0	12.5	0.769
	16.0	12.5	0.704
	18.0	12.0	0.757
	20.0	12.0	0.725

Table 5-2 Calculated values of enhancement ratio from experimental data and "retention" angle for eq.(5-35).

	b mm	E	φ deg
R-113	0.25	6.46	80
	0.5	7.25	115
	1.0	6.14	135
	1.5	5.62	144
	2.0	4.79	149
ethylene glycol	0.25	2.68	0
	0.5	3.69	23
	1.0	5.10	92
	1.5	4.13	111
	2.0	3.74	121
steam	0.25	3.02	0
	0.5	2.21	0
	1.0	2.18	58
	1.5	2.43	85
	2.0	2.12	100

Table 5-3 Computed results for eq.(5-48) (based on dimensional analysis) by minimization of relative residuals (no constrained parameters)

SD=0.16299 , n =-0.0023
K_1=-2606
K_2=1.84
K_3=245
K_4=0.484

	$\frac{b}{mm}$	$\frac{E_{cal}}{E_{obs}}$		$\frac{b}{mm}$	$\frac{E_{cal}}{E_{obs}}$		$\frac{b}{mm}$	$\frac{E_{cal}}{E_{obs}}$
R-113	0.25	1.1200	ethylene glycol	0.25	1.0685	steam	0.25	0.9482
	0.5	1.0259		0.5	0.7680		0.5	1.0222
	1.0	1.0268		1.0	0.7051		1.0	1.1110
	1.5	0.9752		1.5	0.8292		1.5	1.0590
	2.0	1.0220		2.0	0.8627		2.0	1.1905

Table 5-4 Computed results for eq.(5-48) (based on dimensional analysis) by minimization of relative residuals (K_1=0, fixed)

SD=0.15996, n =-0.275
K_1=0
K_2=1.168
K_3=1.401
K_4=0.479

	$\frac{b}{mm}$	$\frac{E_{cal}}{E_{obs}}$		$\frac{b}{mm}$	$\frac{E_{cal}}{E_{obs}}$		$\frac{b}{mm}$	$\frac{E_{cal}}{E_{obs}}$
R-113	0.25	1.1257	ethylene glycol	0.25	1.0586	steam	0.25	0.9394
	0.5	1.0036		0.5	0.7817		0.5	1.0126
	1.0	0.9940		1.0	0.7058		1.0	1.1491
	1.5	0.9632		1.5	0.8173		1.5	1.0746
	2.0	1.0437		2.0	0.8537		2.0	1.1956

Table 5-5 Computed results for eq.(5-48) (based on dimensional analysis) by minimization of relative residuals (K_1=0, n=0.25 fixed)

SD=0.32803, n =0.25
K_1=0.
K_2=-2.443
K_3=2.831
K_4=0.439

	$\frac{b}{mm}$	$\frac{E_{cal}}{E_{obs}}$		$\frac{b}{mm}$	$\frac{E_{cal}}{E_{obs}}$		$\frac{b}{mm}$	$\frac{E_{cal}}{E_{obs}}$
R-113	0.25	1.0531	ethylene glycol	0.25	0.9702	steam	0.25	0.8609
	0.5	0.8427		0.5	0.8766		0.5	0.9281
	1.0	0.6838		1.0	0.8321		1.0	1.494
	1.5	0.5519		1.5	0.8321		1.5	1.331
	2.0	0.5046		2.0	0.7468		2.0	1.3082

Table 5-6 Computed results for eq.(5-52) (based on dimensional analysis) by minimization of relative residuals (no constrained parameters)

SD=0.06691, n =0.1332
K_1=-121.69
K_2=5.86
K_3=14.85
K_4=0.479

	$\frac{b}{mm}$	$\frac{E_{cal}}{E_{obs}}$		$\frac{b}{mm}$	$\frac{E_{cal}}{E_{obs}}$		$\frac{b}{mm}$	$\frac{E_{cal}}{E_{obs}}$
R-113	0.25	1.0114	ethylene	0.25	1.0586	steam	0.25	0.9394
	0.5	0.9789	glycol	0.5	0.8862		0.5	1.0127
	1.0	1.0262		1.0	0.9383		1.0	1.1137
	1.5	0.9749		1.5	1.0460		1.5	0.9502
	2.0	1.0162		2.0	1.0285		2.0	0.9716

Table 5-7 Computed results of eq.(5-52) (based on dimensional analysis) by minimization of relative residuals (K_1=0, fixed)

SD=0.1389, n =-0.0494
K_1=0
K_2=2.300
K_3=1.696
K_4=0.4799

	$\frac{b}{mm}$	$\frac{E_{cal}}{E_{obs}}$		$\frac{b}{mm}$	$\frac{E_{cal}}{E_{obs}}$		$\frac{b}{mm}$	$\frac{E_{cal}}{E_{obs}}$
R-113	0.25	1.0964	ethylene	0.25	1.0600	steam	0.25	0.9406
	0.5	0.9963	glycol	0.5	0.7926		0.5	1.0140
	1.0	1.0078		1.0	0.7400		1.0	1.1308
	1.5	0.9730		1.5	0.862		1.5	1.0579
	2.0	1.0388		2.0	0.8967		2.0	1.1805

Table 5-8 Computed results for eq.(5-52) (based on dimensional analysis) by minimization of relative residuals (K_1=0, n=0.25 fixed)

SD=0.2170 , n =0.25
K_1=0
K_2=3.27
K_3=1.33
K_4=0.4697

	b / mm	E_{cal}/E_{obs}		b / mm	E_{cal}/E_{obs}		b / mm	E_{cal}/E_{obs}
R-113	0.25	0.8704	ethylene glycol	0.25	1.0375	steam	0.25	0.9207
	0.5	0.8455		0.5	0.7575		0.5	0.9925
	1.0	0.8623		1.0	0.7992		1.0	1.2099
	1.5	0.8004		1.5	0.9490		1.5	1.246
	2.0	0.8137		2.0	0.9663		2.0	1.4109

Table 5-9 Computed results for eq.(5-52) (based on dimensional analysis) by minimization of relative residuals (K_1=0, n=0 fixed)

SD=0.1455 , n =0
K_1=0
K_2=3.51
K_3=2.985
K_4=0.473

	b / mm	E_{cal}/E_{obs}		b / mm	E_{cal}/E_{obs}		b / mm	E_{cal}/E_{obs}
R-113	0.25	1.0856	ethylene glycol	0.25	1.0450	steam	0.25	0.9274
	0.5	0.9689		0.5	0.8021		0.5	0.9997
	1.0	0.9654		1.0	0.7557		1.0	1.1685
	1.5	0.9317		1.5	0.8764		1.5	1.0979
	2.0	1.0007		2.0	0.9143		2.0	1.2279

Table 5-10 Computed results for ajustment of constants in eq.(5-105) (surface tension model) by minimization of relative residuals.

SD=0.2069, C_1=0.675
C_2=0.44

	$\frac{b}{mm}$	$\frac{E_{cal}}{E_{obs}}$		$\frac{b}{mm}$	$\frac{E_{cal}}{E_{obs}}$		$\frac{b}{mm}$	$\frac{E_{cal}}{E_{obs}}$
R-113	0.25	1.012	ethylene glycol	0.25	0.999	steam	0.25	1.042
	0.5	0.901		0.5	0.771		0.5	0.909
	1.0	0.852		1.0	0.808		1.0	1.258
	1.5	0.766		1.5	0.907		1.5	1.250
	2.0	0.766		2.0	0.893		2.0	1.352

Table 5-11 Computed results for eq.(5-106) (surface tension model) by minimization of relative residuals

SD=0.2125, C_{11}=0.55
C_{12}=0.99
C_2 =0.45

	$\frac{b}{mm}$	$\frac{E_{cal}}{E_{obs}}$		$\frac{b}{mm}$	$\frac{E_{cal}}{E_{obs}}$		$\frac{b}{mm}$	$\frac{E_{cal}}{E_{obs}}$
R-113	0.25	0.9395	ethylene glycol	0.25	1.0819	steam	0.25	0.9601
	0.5	0.8640		0.5	0.7972		0.5	0.9840
	1.0	0.8592		1.0	0.7509		1.0	1.132
	1.5	0.7970		1.5	0.8720		1.5	1.052
	2.0	0.8148		2.0	0.9109		2.0	1.181

Table 5-12 Computed results for eq.(5-113) ("Beatty and Katz type" model) by minimization of relative residuals.

SD=0.15156, C_{11}=1.54
C_{12}=4.27
C_2 =0.446

	$\frac{b}{mm}$	$\frac{E_{cal}}{E_{obs}}$		$\frac{b}{mm}$	$\frac{E_{cal}}{E_{obs}}$		$\frac{b}{mm}$	$\frac{E_{cal}}{E_{obs}}$
R-113	0.25	1.0879	ethylene	0.25	1.0676	steam	0.25	0.9474
	0.5	0.9204	glycol	0.5	0.8143		0.5	0.9710
	1.0	0.9275		1.0	0.7533		1.0	1.1727
	1.5	0.9181		1.5	0.8750		1.5	1.1063
	2.0	1.0099		2.0	0.9285		2.0	1.2473

Table 5-13 Computed results for eq.(5-114) ("hybrid" model) by minimization of relative residuals

SD=0.1728 C_{11}=1.295
C_{12}=0.94
C_2 =0.444

	$\frac{b}{mm}$	$\frac{E_{cal}}{E_{obs}}$		$\frac{b}{mm}$	$\frac{E_{cal}}{E_{obs}}$		$\frac{b}{mm}$	$\frac{E_{cal}}{E_{obs}}$
R-113	0.25	1.0644	ethylene	0.25	1.0621	steam	0.25	0.9425
	0.5	0.9481	glycol	0.5	0.7849		0.5	0.9660
	1.0	0.9257		1.0	0.7933		1.0	1.2008
	1.5	0.8519		1.5	0.8986		1.5	1.1804
	2.0	0.8659		2.0	0.8986		2.0	1.2880

Table 5-14 Computed results by minimization of absolute residuals.

(a) eq.(5-53) based on dimensional analysis
(b) eq.(5-113) "Beatty and Katz type" model
(c) eq.(5-114) " hybrid" model)

(a) SD=0.5344, C_{11}=2.965
C_{12}=4.108
C_2 =0.4915

	$\frac{b}{mm}$	$\frac{E_{cal}}{E_{obs}}$		$\frac{b}{mm}$	$\frac{E_{cal}}{E_{obs}}$		$\frac{b}{mm}$	$\frac{E_{cal}}{E_{obs}}$
R-113	0.25	1.093	ethylene glycol	0.25	1.086	steam	0.25	0.964
	0.5	0.982		0.5	0.821		0.5	1.041
	1.0	0.997		1.0	0.775		1.0	1.193
	1.5	0.979		1.5	0.913		1.5	1.136
	2.0	1.065		2.0	0.965		2.0	1.290

(b) SD=0.5613, C_{11}=1.58
C_{12}=4.75
C_2 =0.453

	$\frac{b}{mm}$	$\frac{E_{cal}}{E_{obs}}$		$\frac{b}{mm}$	$\frac{E_{cal}}{E_{obs}}$		$\frac{b}{mm}$	$\frac{E_{cal}}{E_{obs}}$
R-113	0.25	1.1189	ethylene glycol	0.25	1.0840	steam	0.25	0.9679
	0.5	0.9545		0.5	0.8314		0.5	0.9860
	1.0	0.9743		1.0	0.7827		1.0	1.2050
	1.5	1.0272		1.5	0.9203		1.5	1.1535
	2.0	1.0681		2.0	0.9856		2.0	1.3156

(c) SD=0.5411, C_{11}=1.18
C_{12}=1.27
C_2 =0.458

	$\frac{b}{mm}$	$\frac{E_{cal}}{E_{obs}}$		$\frac{b}{mm}$	$\frac{E_{cal}}{E_{obs}}$		$\frac{b}{mm}$	$\frac{E_{cal}}{E_{obs}}$
R-113	0.25	1.059	ethylene glycol	0.25	1.097	steam	0.25	0.974
	0.5	0.982		0.5	0.786		0.5	0.995
	1.0	0.998		1.0	0.839		1.0	1.228
	1.5	0.941		1.5	0.985		1.5	1.272
	2.0	0.971		2.0	1.011		2.0	1.439

CHAPTER 6 CONCLUDING REMARKS

6. Concluding remarks

The main objective of the research described in this thesis was to obtain reliable experimental data under well-defined conditions, and with systematic change of some of the important variables, so as to obtain improved predictions of the heat-transfer performance of horizontal finned tubes.

Experiments have been made using two different fluids, i.e. R-113 and ethylene glycol, and fourteen finned tubes (having the same tube diameter and geometry of fin, but different fin spacings) to investigate the effect of fin spacing and liquid properties, especially surface tension, on heat-transfer enhancement.

It has been found that the vapour-side data for all tubes and both fluids, together with earlier data for steam [35,36,37], may be represented satifactorily by an equation of the form:

$$Q=C\Delta T^{3/4} \qquad (6\text{-}1)$$

so that the enhancement ratios $Q_{fin\ tube}/Q_{plain\ tube}$, for the same ΔT, ($=\alpha_{fin\ tube}/\alpha_{plain\ tube}$) are independent of ΔT and are given by $C_{fin\ tube}/C_{plain\ tube}$. Evidently, for the same Q, the heat-transfer coefficient enhancement ratio is given by $(C_{fin\ tube}/C_{plain\ tube})^{4/3}$.

The enhancement was highest for R-113 and lowest for steam, i.e. in reverse order of surface tension. It was found that there exist optimum fin spacings for all three fluids; this was lowest for R-113 (0.5 mm) and highest for steam (1.5 mm). For ethylene glycol the optimum fin spacing was 1.0 mm. The maximum enhancement ratios obtained (for the same ΔT) were 7.5, 5.2 and 3.0 for R-113, ethylene glycol and steam, respectively.

Study of the data by dimensional analysis and "curve fitting" led to the conclusion that surface tension forces play an adverse role on heat transfer for the upper part of the tube. A detailed theoretical study of the static configuration of retained liquid on a finned tube has been made. This revealed the existence of a "wedge" of fluid at the fin root for the unflooded portion of the tube. This phenomenon has apparently not been recognised earlier and evidently explains the above-mentioned fact.

Several expressions for heat-transfer enhancement of finned tube to plain tube have been developed and investigated both by dimensional analysis and using an approximate theoretical approach. In both cases, expressions were obtained to best fit the data by adjusting constants. The equations found are considered to represent the data (i.e. present data plus that of Yau et al. [35,36,37] for steam using the same set of tubes) satisfactorily. Furthermore these equations, when compared with the recent data of Georgiadis [40] for steam and Honda et al. [34] for R-113 and methanol, with different tube diameter and fin geometries, showed quite good agreement. It is noteworthy that no earlier models are able to predict the data (present, Yau et al., Georgiadis and Honda et al.) with the same degree of success. Had time been available the present equations could have been further improved by including the data of Georgiadis and Honda et al. in the curve fitting procedure.

The following topics are suggested for future work to obtain improved expressions for heat transfer on low finned tubes:-

(a) Further measurements to obtain data using other fluids and other geometries of finned tube.

(b) Visual observation to verify the theoretical expression for the configuration of retained liquid on a finned tube.

(c) Further theoretical study of the condensate flow problem, particularly for the lower "flooded region" of the tube.

APPENDIX A Present experimental data

R-113

PITCH= 0.000mm

DATE OF EXPERIMENT 21-12-1983

ambiente temp = 19.50 C
atmospheric press = 29.368 inch
input power = 2.97 kW

Data no. 1 to 1

PITCH= 0.000mm

DATE OF EXPERIMENT 7- 3-1984

ambiente temp = 20.75 C
atmospheric press = 30.702 inch
input power = 3.10 kW

Data no. 2 to 7

PITCH= 0.000mm

DATE OF EXPERIMENT 15- 3-1984

ambiente temp = 18.95 C
atmospheric press = 30.000 inch
input power = 3.07 kW

Data no. 8 to 19

	flow rate	Tin	Tout	Tv	Twi	Two	$Qx10^{-6}$
	l/min			K			J/m^2s
1	3.00	296.23	296.69	319.87	301.84	301.94	0.023772
2	3.00	293.77	294.24	321.13	299.71	299.81	0.024489
3	2.60	293.74	294.32	321.03	300.72	300.83	0.025691
4	2.20	293.74	294.39	321.01	301.36	301.47	0.024573
5	1.80	293.72	294.47	321.01	302.16	302.26	0.023198
6	1.40	293.69	294.62	321.03	303.57	303.66	0.022251
7	1.00	293.67	294.84	321.03	305.36	305.45	0.020187
8	4.00	294.01	294.44	320.36	299.62	299.74	0.029207
9	3.00	294.01	294.51	320.38	300.24	300.35	0.025770
10	2.40	293.99	294.59	320.36	301.13	301.23	0.024738
11	2.00	293.99	294.70	320.41	302.15	302.25	0.024479
12	1.80	293.99	294.74	320.41	302.40	302.50	0.023190
13	1.60	294.01	294.86	320.47	303.30	303.40	0.023360
14	1.40	293.99	294.94	320.50	304.08	304.18	0.022844
15	1.20	293.96	295.01	320.50	304.78	304.87	0.021641
16	1.00	293.96	295.19	320.54	306.09	306.18	0.021037
17	0.80	293.89	295.31	320.59	307.36	307.45	0.019577
18	0.60	293.79	295.49	320.57	308.95	309.02	0.017515
19	0.40	293.72	295.84	320.57	311.15	311.21	0.014594

R-113

PITCH= 0.750mm

DATE OF EXPERIMENT 22- 1-1985

ambiente temp = 16.00 C
atmospheric press = 29.260 inch
input power = 3.69 kW

Data no. 1 to 14

	flow rate	Tin	Tout	Tv	Twi	Two	Qx10^{-6}
	l/min			K			J/m^{2}s
1	23.00	291.26	291.69	319.89	299.37	300.08	0.168521
2	20.00	291.26	291.74	319.94	300.06	300.75	0.163774
3	15.00	291.26	291.86	319.99	301.72	302.37	0.155143
4	12.00	291.26	291.99	320.01	303.29	303.92	0.149960
5	9.00	291.26	292.09	320.01	304.17	304.71	0.127975
6	7.00	291.26	292.27	320.06	306.07	306.58	0.120637
7	5.00	291.26	292.47	320.10	307.82	308.25	0.103390
8	4.00	291.26	292.64	320.08	309.35	309.74	0.094764
9	3.00	291.29	292.84	320.08	310.50	310.83	0.080107
10	2.40	291.39	293.14	320.13	312.04	312.34	0.072337
11	1.80	291.41	293.47	320.10	314.14	314.41	0.063540
12	1.40	291.39	293.72	320.13	315.83	316.07	0.056041
13	1.20	291.41	293.92	320.13	316.84	317.06	0.051644
14	1.00	291.39	294.12	320.15	318.06	318.26	0.046905

R-113

PITCH= 1.000mm

DATE OF EXPERIMENT 12-12-1983

ambiente temp = 18.75 C
atmospheric press = 30.011 inch
input power = 3.05 kW

Data no. 1 to 9

PITCH= 1.000mm

DATE OF EXPERIMENT 1-10-1984

ambiente temp = 18.85 C
atmospheric press = 30.146 inch
input power = 2.94 kW

Data no. 10 to 17

PITCH= 1.000mm

DATE OF EXPERIMENT 9- 3-1984

ambiente temp = 19.00 C
atmospheric press = 30.788 inch
input power = 3.08 kW

Data no. 18 to 29

	flow rate	Tin	Tout	Tv	Twi	Two	$Qx10^{-6}$
	1/min			K			J/m^2s
1	24.50	294.82	295.22	320.41	303.62	304.33	0.168204
2	20.00	294.84	295.29	320.41	304.34	304.99	0.154463
3	15.00	294.85	295.39	320.39	305.54	306.12	0.138364
4	12.00	294.88	295.50	320.41	306.72	307.26	0.128700
5	9.00	294.89	295.64	320.38	308.26	308.75	0.115819
6	7.00	294.93	295.80	320.41	309.71	310.15	0.105082
7	5.00	294.94	296.01	320.41	311.84	312.23	0.092202
8	4.00	294.94	296.16	320.41	313.30	313.66	0.084046
9	3.00	294.94	296.36	320.41	315.04	315.35	0.073317
10	20.00	292.74	293.19	320.71	302.50	303.15	0.154871
11	15.00	292.76	293.31	320.68	303.98	304.58	0.141952
12	12.00	292.76	293.41	320.68	305.40	305.96	0.134201
13	9.00	292.81	293.61	320.71	307.41	307.93	0.123859
14	7.00	292.84	293.77	320.68	309.05	309.52	0.112879
15	5.00	292.86	294.02	320.71	311.54	311.96	0.099961
16	4.00	292.88	294.24	320.71	313.53	313.92	0.092854
17	3.00	292.88	294.44	320.68	315.19	315.52	0.079948
18	25.00	293.13	293.55	321.31	302.71	303.48	0.182747
19	20.00	293.18	293.68	321.26	303.93	304.65	0.171978
20	15.00	293.23	293.85	321.31	305.84	306.52	0.161207
21	12.00	293.25	293.98	321.33	307.20	307.83	0.149587
22	9.00	293.28	294.15	321.31	309.09	309.66	0.135385
23	7.00	293.25	294.20	321.26	309.58	310.06	0.114323
24	5.00	293.25	294.43	321.29	312.03	312.45	0.100986
25	4.00	293.25	294.55	321.29	313.08	313.46	0.089376
26	3.00	293.28	294.73	321.31	314.12	314.43	0.074758
27	2.40	293.25	294.85	321.22	315.21	315.49	0.065989
28	1.80	293.25	295.08	321.20	316.83	317.07	0.056444
29	1.20	293.20	295.43	321.38	319.58	319.77	0.045868

R-113

PITCH= 1.500mm

DATE OF EXPERIMENT 12- 1-1984

ambiente temp = 18.00 C
atmospheric press = 29.723 inch
input power = 2.89 kW

Data no. 1 to 8

PITCH= 1.500mm

DATE OF EXPERIMENT 9- 3-1984

ambiente temp = 19.80 C
atmospheric press = 30.754 inch
input power = 3.07 kW

Data no. 9 to 19

	flow rate	Tin	Tout	Tv	Twi	Two	$Q \times 10^{-6}$
	l/min			K			J/m^2s
1	20.00	293.25	293.68	320.89	302.02	302.63	0.146175
2	15.00	293.28	293.83	320.89	303.94	304.53	0.141860
3	12.00	293.30	293.93	320.94	304.86	305.40	0.128954
4	9.00	293.33	294.08	320.92	306.38	306.86	0.116046
5	7.00	293.35	294.28	320.89	308.57	309.04	0.111303
6	5.00	293.35	294.50	320.92	310.95	311.36	0.098827
7	4.00	293.35	294.65	320.92	312.32	312.69	0.089365
8	3.00	293.37	294.93	320.92	314.61	314.95	0.079899
9	20.00	293.45	293.87	321.24	302.20	302.81	0.146139
10	15.00	293.50	294.05	321.22	304.13	304.72	0.141821
11	12.00	293.50	294.12	321.24	305.03	305.57	0.123922
12	9.00	293.57	294.32	321.24	306.58	307.07	0.116011
13	7.00	293.57	294.47	321.15	308.36	308.81	0.103266
14	5.00	293.57	294.65	321.20	310.03	310.41	0.092360
15	4.00	293.55	294.80	321.24	311.78	312.14	0.085910
16	3.00	293.57	294.97	321.29	312.82	313.12	0.072155
17	2.40	293.55	295.07	321.10	313.58	313.84	0.062875
18	1.80	293.55	295.32	321.24	315.48	315.71	0.054879
19	1.20	293.52	295.67	321.29	317.92	318.10	0.044306

R-113

PITCH= 2.000mm

DATE OF EXPERIMENT 12- 1-1984

ambiente temp = 18.25 C
atmospheric press = 29.700 inch
input power = 2.97 kW

Data no. 1 to 7

PITCH= 2.000mm

DATE OF EXPERIMENT 9- 3-1984

ambiente temp = 20.30 C
atmospheric press = 30.733 inch
input power = 3.07 kW

Data no. 8 to 20

PITCH= 2.000mm

DATE OF EXPERIMENT 19- 3-1984

ambiente temp = 18.15 C
atmospheric press = 30.108 inch
input power = 3.10 kW

Data no. 21 to 35

	flow rate	Tin	Tout	Tv	Twi	Two	$Qx10^{-6}$
	l/min			K			J/m^2s
1	15.00	293.18	293.65	320.94	302.62	303.13	0.122537
2	12.00	293.20	293.75	320.89	303.63	304.11	0.113499
3	9.00	293.25	293.95	320.92	305.71	306.16	0.108323
4	7.00	293.25	294.10	320.89	307.57	308.00	0.102296
5	5.00	293.25	294.33	320.92	310.08	310.47	0.092397
6	4.00	293.28	294.53	320.92	311.91	312.27	0.085939
7	3.00	293.28	294.73	320.94	313.61	313.93	0.074758
8	20.00	293.84	294.24	321.22	302.20	302.78	0.137477
9	15.00	293.89	294.41	321.29	304.19	304.76	0.135311
10	12.00	293.84	294.47	321.38	305.54	306.08	0.128867
11	9.00	293.77	294.52	321.15	306.99	307.48	0.115982
12	7.00	293.64	294.54	321.24	308.70	309.15	0.108257
13	5.00	293.59	294.70	321.31	310.73	311.12	0.094504
14	4.00	293.50	294.72	321.26	311.73	312.08	0.084198
15	3.00	293.50	294.90	321.15	313.12	313.42	0.072162
16	2.40	293.57	295.10	321.17	313.97	314.24	0.062873
17	2.00	293.62	295.27	321.24	314.86	315.10	0.056681
18	1.80	293.64	295.49	321.29	316.84	317.08	0.057188
19	1.20	293.59	295.67	321.31	317.61	317.78	0.042759
20	1.00	293.55	295.80	321.29	318.62	318.78	0.038636
21	15.00	293.79	294.27	320.64	303.16	303.67	0.122443
22	12.00	293.84	294.42	320.66	304.64	305.13	0.118561
23	9.00	293.86	294.56	320.66	306.23	306.68	0.108240
24	7.00	293.82	294.64	320.54	307.63	308.05	0.099218
25	5.00	293.69	294.69	320.57	309.32	309.68	0.085907
26	4.00	293.64	294.79	320.66	310.78	311.11	0.079032
27	3.00	293.64	294.92	320.73	311.57	311.85	0.065712
28	2.40	293.64	295.09	320.87	313.08	313.33	0.059779
29	2.00	293.62	295.17	320.92	313.64	313.87	0.053249
30	1.80	293.62	295.27	320.96	314.46	314.67	0.051013
31	1.60	293.62	295.37	321.03	315.17	315.38	0.048090
32	1.40	293.57	295.47	321.03	316.31	316.50	0.045684
33	1.20	293.57	295.62	321.08	317.32	317.49	0.042246
34	1.00	293.50	295.67	321.08	317.80	317.96	0.037352
35	0.80	293.42	295.82	321.08	319.04	319.18	0.032971

R-113

PITCH= 2.500mm

DATE OF EXPERIMENT 7-11-1983

ambiente temp = 19.80 C
atmospheric press = 29.986 inch
input power = 2.99 kW

Data no. 1 to 7

PITCH= 2.500mm

DATE OF EXPERIMENT 12-12-1983

ambiente temp = 19.00 C
atmospheric press = 30.077 inch
input power = 3.07 kW

Data no. 8 to 14

PITCH= 2.500mm

DATE OF EXPERIMENT 21-12-1983

ambiente temp = 21.00 C
atmospheric press = 29.368 inch
input power = 2.97 kW

Data no. 15 to 21

PITCH= 2.500mm

DATE OF EXPERIMENT 11- 1-1984

ambiente temp = 20.15 C
atmospheric press = 29.759 inch
input power = 2.96 kW

Data no. 22 to 28

PITCH= 2.500mm

DATE OF EXPERIMENT 11- 3-1984

ambiente temp = 19.50 C
atmospheric press = 30.240 inch
input power = 3.12 kW

Data no. 29 to 42

PITCH= 2.500mm

DATE OF EXPERIMENT 15- 3-1984

ambiente temp = 18.15 C
atmospheric press = 29.999 inch
input power = 2.82 kW

Data no. 43 to 57

	flow rate	Tin	Tout	Tv	Twi	Two	$Qx10^{-6}$
	l/min	K					J/m^2s
1	15.00	295.26	295.68	320.45	303.47	303.93	0.109356
2	12.00	295.28	295.78	320.45	304.50	304.94	0.102916
3	9.00	295.31	295.91	320.45	305.73	306.12	0.092616
4	7.00	295.31	296.03	320.47	307.24	307.61	0.087035
5	5.00	295.28	296.16	320.45	308.72	309.03	0.075025
6	4.00	295.26	296.28	320.47	310.26	310.55	0.070305
7	3.00	295.23	296.41	320.47	311.44	311.70	0.060442
8	15.00	295.70	296.15	320.52	304.34	304.82	0.115724
9	12.00	295.70	296.22	320.52	305.32	305.77	0.108004
10	9.00	295.70	296.30	320.53	306.07	306.45	0.092570
11	7.00	295.71	296.47	320.52	308.18	308.56	0.091489
12	5.00	295.70	296.67	320.52	310.52	310.87	0.083551
13	4.00	295.71	296.82	320.52	311.84	312.16	0.076260
14	3.00	295.68	297.00	320.52	313.60	313.88	0.067471
15	15.00	296.23	296.63	319.81	303.88	304.31	0.102800
16	12.00	296.24	296.72	319.80	304.91	305.32	0.097654
17	9.00	296.27	296.84	319.80	306.15	306.52	0.088651
18	7.00	296.28	296.98	319.80	307.68	308.03	0.083933
19	5.00	296.31	297.20	319.81	309.94	310.26	0.077069
20	4.00	296.31	297.33	319.80	311.12	311.41	0.070213
21	3.00	296.31	297.52	319.81	312.79	313.06	0.062286
22	15.00	292.91	293.36	320.36	301.86	302.35	0.116128
23	12.00	292.93	293.46	320.41	302.90	303.35	0.108378
24	9.00	293.03	293.68	320.59	304.62	305.04	0.100617
25	7.00	293.03	293.83	320.66	306.53	306.94	0.095308
26	5.00	293.08	294.11	320.71	309.14	309.51	0.088121
27	4.00	293.08	294.26	320.71	310.63	310.97	0.080806
28	3.00	293.10	294.51	320.71	312.75	313.05	0.072197
29	15.00	293.35	293.78	320.80	301.77	302.23	0.109618
30	12.00	293.37	293.87	320.80	302.83	303.26	0.103162
31	9.00	293.42	294.07	320.80	304.95	305.38	0.100567
32	7.00	293.42	294.17	320.80	306.05	306.43	0.090247
33	5.00	293.42	294.37	320.78	308.30	308.64	0.081642
34	4.00	293.40	294.50	320.71	309.82	310.14	0.075622
35	3.00	293.40	294.62	320.68	310.65	310.91	0.063156
36	2.40	293.40	294.80	320.71	312.19	312.43	0.057737
37	2.00	293.40	294.95	320.73	313.41	313.63	0.053264
38	1.80	293.37	295.03	320.80	314.20	314.41	0.051029
39	1.60	293.37	295.13	320.87	314.92	315.12	0.048105
40	1.40	293.35	295.20	320.92	315.51	315.70	0.044496
41	1.20	293.33	295.30	320.94	316.24	316.41	0.040714
42	1.00	293.30	295.45	321.01	317.32	317.47	0.035932
43	15.00	294.35	294.75	320.47	302.19	302.62	0.103042
44	12.00	294.38	294.85	320.54	303.25	303.66	0.097882
45	9.00	294.38	295.00	320.54	305.35	305.75	0.095585
46	7.00	294.38	295.08	320.45	306.05	306.40	0.084133
47	5.00	294.40	295.30	320.54	308.36	308.68	0.077253
48	4.00	294.38	295.38	320.52	309.19	309.48	0.063667
49	3.00	294.40	295.58	320.38	310.78	311.03	0.060504
50	2.40	294.38	295.70	320.38	312.00	312.23	0.054579
51	2.00	294.38	295.85	320.45	313.24	313.46	0.050627
52	1.80	294.35	295.90	320.50	313.75	313.95	0.047880
53	1.60	294.33	295.95	320.57	314.19	314.38	0.044619
54	1.40	294.33	296.13	320.71	315.67	315.86	0.043242
55	1.20	294.30	296.20	320.71	316.15	316.31	0.039122
56	1.00	294.28	296.33	320.80	316.98	317.13	0.035173
57	0.80	294.28	296.58	320.85	318.57	318.70	0.031565

R-113

PITCH= 4.500mm

DATE OF EXPERIMENT 12- 1-1984

ambiente temp = 18.25 C
atmospheric press = 29.765 inch
input power = 2.97 kW

Data no. 1 to 6

PITCH= 4.500mm

DATE OF EXPERIMENT 11- 3-1984

ambiente temp = 19.50 C
atmospheric press = 30.266 inch
input power = 3.05 kW

Data no. 7 to 19

	flow rate	Tin	Tout	Tv	Twi	Two	$Qx10^{-6}$
	1/min			K			J/m^2s
1	12.00	293.42	293.84	320.58	301.72	302.08	0.085108
2	9.00	293.42	293.92	320.66	302.90	303.22	0.077367
3	7.00	293.47	294.10	320.78	304.68	304.99	0.075207
4	5.00	293.50	294.30	320.82	306.84	307.13	0.068751
5	4.00	293.50	294.45	320.86	308.58	308.86	0.065308
6	3.00	293.52	294.67	320.89	310.68	310.92	0.059283
7	9.00	293.91	294.36	320.82	302.41	302.70	0.069589
8	7.00	293.94	294.49	320.66	303.78	304.06	0.066147
9	5.00	293.94	294.64	320.68	305.60	305.86	0.060128
10	4.00	293.94	294.76	320.78	307.04	307.28	0.056688
11	3.00	293.91	294.89	320.82	308.50	308.71	0.050243
12	2.40	293.89	295.01	320.87	309.94	310.13	0.046375
13	2.00	293.89	295.19	320.92	311.69	311.88	0.044653
14	1.80	293.86	295.24	320.94	312.29	312.46	0.042505
15	1.60	293.86	295.31	320.96	312.82	312.99	0.039841
16	1.40	293.82	295.39	320.96	313.83	313.99	0.037866
17	1.20	293.72	295.42	320.99	314.66	314.80	0.035034
18	1.00	293.64	295.49	321.01	315.60	315.73	0.031771
19	0.80	293.64	295.77	321.06	317.65	317.77	0.029190

R-113

PITCH= 6.500mm

DATE OF EXPERIMENT 20-10-1983

ambiente temp = 20.45 C
atmospheric press = 30.460 inch
input power = 3.03 kW

Data no. 1 to 5

PITCH= 6.500mm

DATE OF EXPERIMENT 12- 1-1984

ambiente temp = 18.00 C
atmospheric press = 29.819 inch
input power = 2.96 kW

Data no. 6 to 11

PITCH= 6.500mm

DATE OF EXPERIMENT 11- 3-1984

ambiente temp = 18.85 C
atmospheric press = 30.282 inch
input power = 3.10 kW

Data no. 12 to 25

	flow rate	Tin	Tout	Tv	Twi	Two	$Qx10^{-6}$
	l/min			K			J/m^2s
1	9.00	294.89	295.29	321.22	302.69	302.95	0.061783
2	7.00	294.82	295.29	321.22	303.61	303.85	0.057066
3	5.00	294.77	295.37	321.22	305.13	305.34	0.051488
4	4.00	294.72	295.44	321.24	306.65	306.86	0.049771
5	3.00	294.72	295.62	321.26	308.64	308.84	0.046333
6	12.00	293.57	293.97	320.92	301.95	302.29	0.082514
7	9.00	293.59	294.07	320.89	302.97	303.27	0.073484
8	7.00	293.62	294.19	320.89	304.37	304.66	0.069180
9	5.00	293.64	294.42	320.94	307.09	307.37	0.066592
10	4.00	293.67	294.57	320.96	308.55	308.81	0.061859
11	3.00	293.67	294.74	320.96	310.38	310.62	0.055409
12	9.00	294.04	294.44	320.85	301.92	302.18	0.061850
13	7.00	293.99	294.49	320.87	303.33	303.58	0.060132
14	5.00	293.96	294.61	320.92	305.27	305.50	0.055833
15	4.00	293.91	294.69	320.92	306.77	306.99	0.053255
16	3.00	293.91	294.84	320.99	308.35	308.55	0.047668
17	2.40	293.91	294.94	320.99	309.19	309.37	0.042254
18	2.00	293.94	295.11	321.03	310.76	310.93	0.040360
19	1.80	293.94	295.24	321.10	312.10	312.27	0.040185
20	1.60	293.89	295.26	321.10	312.64	312.80	0.037781
21	1.40	293.89	295.36	321.15	313.45	313.59	0.035461
22	1.20	293.84	295.42	321.13	314.08	314.22	0.032455
23	1.00	293.79	295.57	321.17	315.71	315.84	0.030479
24	0.80	293.72	295.69	321.17	317.01	317.12	0.027130
25	0.60	293.62	295.84	321.15	318.37	318.46	0.022922

R-113

PITCH= 8.500mm

DATE OF EXPERIMENT 20-10-1983

ambiente temp = 21.45 C
atmospheric press = 30.447 inch
input power = 3.10 kW

Data no. 1 to 4

PITCH= 8.500mm

DATE OF EXPERIMENT 7-11-1983

ambiente temp = 21.50 C
atmospheric press = 29.950 inch
input power = 3.05 kW

Data no. 5 to 8

PITCH= 8.500mm

DATE OF EXPERIMENT 13-12-1983

ambiente temp = 19.30 C
atmospheric press = 30.130 inch
input power = 2.98 kW

Data no. 9 to 13

PITCH= 8.500mm

DATE OF EXPERIMENT 21-12-1983

ambiente temp = 21.00 C
atmospheric press = 29.374 inch
input power = 2.94 kW

Data no. 14 to 17

PITCH= 8.500mm

DATE OF EXPERIMENT 12- 3-1984

ambiente temp = 18.95 C
atmospheric press = 30.286 inch
input power = 3.05 kW

Data no. 18 to 32

	flow rate (l/min)	Tin (K)	Tout (K)	Tv (K)	Twi (K)	Two (K)	Qx10^{-6} (J/m^{2}s)
1	7.00	296.06	296.46	321.03	303.15	303.35	0.047983
2	5.00	296.04	296.54	321.03	304.31	304.49	0.042841
3	4.00	295.99	296.61	321.06	305.84	306.02	0.042840
4	3.00	295.96	296.71	321.08	307.11	307.27	0.038555
5	7.00	296.11	296.54	320.45	303.63	303.84	0.050979
6	5.00	296.14	296.68	320.43	305.20	305.39	0.047118
7	4.00	296.09	296.74	320.43	306.31	306.50	0.044548
8	3.00	296.04	296.81	320.41	307.53	307.69	0.039835
9	9.00	295.04	295.44	320.24	302.57	302.83	0.061772
10	7.00	295.01	295.49	320.25	303.51	303.75	0.057053
11	5.00	294.96	295.59	320.25	305.38	305.60	0.053619
12	4.00	294.93	295.66	320.25	306.65	306.86	0.050615
13	3.00	294.90	295.80	320.25	308.36	308.55	0.046323
14	7.00	296.38	296.78	319.79	303.44	303.64	0.047964
15	5.00	296.38	296.92	319.79	305.21	305.41	0.046033
16	4.00	296.38	297.03	319.78	306.57	306.75	0.044532
17	3.00	296.38	297.18	319.78	308.18	308.35	0.041102
18	9.00	293.77	294.19	320.89	301.89	302.17	0.065735
19	7.00	293.77	294.27	320.89	302.84	303.0[illegible]	0.060143
20	5.00	293.74	294.39	320.85	304.72	304.96	0.055843
21	4.00	293.74	294.52	320.80	306.22	306.44	0.053267
22	3.00	293.79	294.67	320.80	307.07	307.26	0.045099
23	2.60	293.82	294.79	320.80	308.16	308.34	0.043549
24	2.40	293.86	294.89	320.82	308.68	308.85	0.042257
25	2.20	293.89	294.94	320.82	308.80	308.97	0.039678
26	2.00	293.86	294.99	320.89	309.52	309.68	0.038647
27	1.80	293.86	295.06	320.94	310.19	310.34	0.037099
28	1.60	293.84	295.17	320.96	311.40	311.55	0.036411
29	1.40	293.82	295.24	320.96	312.18	312.32	0.034263
30	1.20	293.82	295.37	321.01	313.15	313.28	0.031942
31	1.00	293.77	295.49	321.01	314.46	314.59	0.0296[illegible]2
32	0.80	293.69	295.64	320.99	316.02	316.13	0.026787

R-113

R-113

PITCH=10.500mm

DATE OF EXPERIMENT 12- 1-1984

ambiente temp = 17.50 C
atmospheric press = 29.856 inch
input power = 2.99 kW

Data no. 1 to 5

PITCH=10.500mm

DATE OF EXPERIMENT 12- 3-1984

ambiente temp = 19.50 C
atmospheric press = 30.239 inch
input power = 3.10 kW

Data no. 6 to 20

	flow rate (l/min)	Tin (K)	Tout (K)	Tv (K)	Twi (K)	Two (K)	$Q \times 10^{-6}$ ($J/m^2 s$)
1	9.00	293.59	294.02	320.99	301.89	302.17	0.065750
2	7.00	293.62	294.14	321.01	303.33	303.59	0.063166
3	5.00	293.62	294.29	320.99	305.24	305.48	0.058004
4	4.00	293.62	294.39	320.99	306.35	306.57	0.053275
5	3.00	293.64	294.59	320.96	308.31	308.51	0.048972
6	9.00	294.16	294.56	320.80	301.92	302.18	0.061840
7	7.00	294.18	294.66	320.68	302.93	303.17	0.057112
8	5.00	294.16	294.76	320.66	304.46	304.67	0.051527
9	4.00	294.13	294.86	320.68	306.00	306.20	0.049807
10	3.00	294.13	294.98	320.73	307.23	307.42	0.043793
11	2.40	294.13	295.11	320.80	308.47	308.64	0.040183
12	2.20	294.13	295.16	320.85	308.93	309.09	0.038722
13	2.00	294.16	295.26	320.99	309.71	309.86	0.037775
14	1.80	294.11	295.31	321.01	310.69	310.84	0.037068
15	1.60	294.11	295.38	321.01	311.29	311.44	0.035026
16	1.40	294.06	295.46	321.01	312.39	312.53	0.033652
17	1.20	294.04	295.56	321.01	313.37	313.50	0.031418
18	1.00	293.96	295.64	320.99	314.41	314.53	0.028757
19	0.80	293.89	295.81	321.01	316.29	316.40	0.026438
20	0.60	293.84	296.06	321.01	318.21	318.30	0.022916

R-113

PITCH=12.500mm

DATE OF EXPERIMENT 12- 3-1984

ambiente temp = 19.40 C
atmospheric press = 30.218 inch
input power = 3.10 kW

Data no. 1 to 13

	flow rate	Tin	Tout	Tv	Twi	Two	$Q\times10^{-6}$
	l/min			K			J/m^2s
1	7.00	294.38	294.83	320.75	302.22	302.44	0.054094
2	5.00	294.38	294.95	320.78	303.71	303.92	0.049367
3	4.00	294.35	295.03	320.82	304.81	305.01	0.046361
4	3.00	294.38	295.15	320.87	305.70	305.87	0.039918
5	2.40	294.35	295.25	320.87	306.90	307.06	0.037084
6	2.00	294.35	295.40	320.89	308.42	308.57	0.036050
7	1.80	294.35	295.48	320.92	309.09	309.23	0.034761
8	1.60	294.33	295.50	320.94	309.36	309.50	0.032272
9	1.40	294.35	295.68	320.96	310.80	310.93	0.031839
10	1.20	294.30	295.75	320.96	311.73	311.86	0.029365
11	1.00	294.28	295.88	320.99	312.79	312.90	0.027460
12	0.80	294.26	296.11	321.01	314.65	314.75	0.025397
13	0.60	294.21	296.36	321.01	316.51	316.61	0.022134

R-113

PITCH=14.500mm

DATE OF EXPERIMENT 21-10-1983

ambiente temp = 21.75 C
atmospheric press = 30.646 inch
input power = 3.07 kW

Data no. 1 to 3

PITCH=14.500mm

DATE OF EXPERIMENT 10- 1-1984

ambiente temp = 19.05 C
atmospheric press = 30.156 inch
input power = 2.97 kW

Data no. 4 to 6

PITCH=14.500mm

DATE OF EXPERIMENT 13- 3-1984

ambiente temp = 19.50 C
atmospheric press = 30.208 inch
input power = 3.12 kW

Data no. 7 to 18

	flow rate	Tin	Tout	Tv	Twi	Two	$Q\times10^{-6}$
	l/min			K			J/m²s
1	5.00	295.94	296.38	321.36	302.28	302.43	0.037492
2	4.00	295.94	296.46	321.36	303.20	303.35	0.035990
3	3.00	295.94	296.59	321.36	304.41	304.55	0.033417
4	5.00	292.81	293.31	320.71	300.33	300.51	0.043014
5	4.00	292.86	293.49	320.71	301.81	301.99	0.043008
6	3.00	292.88	293.64	320.73	303.00	303.16	0.038703
7	5.00	293.96	294.44	320.61	301.01	301.18	0.040805
8	4.00	293.94	294.51	320.64	302.08	302.24	0.039516
9	3.00	293.96	294.66	320.68	303.30	303.45	0.036076
10	2.40	293.96	294.79	320.78	304.46	304.60	0.034012
11	2.00	293.94	294.89	320.78	305.57	305.70	0.032636
12	1.80	293.96	294.99	320.82	306.23	306.36	0.031689
13	1.60	293.94	295.06	320.85	307.07	307.20	0.030915
14	1.40	293.91	295.14	320.87	307.82	307.94	0.029454
15	1.20	293.89	295.21	320.89	308.46	308.58	0.027306
16	1.00	293.89	295.39	320.92	309.75	309.86	0.025758
17	0.80	293.84	295.59	320.99	311.49	311.59	0.024039
18	0.60	293.82	295.92	321.06	313.72	313.81	0.021631

R-113

R-113

PITCH=16.500mm

DATE OF EXPERIMENT 21-10-1983

ambiente temp = 21.25 C
atmospheric press = 30.652 inch
input power = 3.06 kW

Data no. 1 to 3

PITCH=16.500mm

DATE OF EXPERIMENT 12- 1-1984

ambiente temp = 18.40 C
atmospheric press = 29.783 inch
input power = 2.94 kW

Data no. 4 to 7

PITCH=16.500mm

DATE OF EXPERIMENT 13- 3-1984

ambiente temp = 20.65 C
atmospheric press = 30.192 inch
input power = 3.12 kW

Data no. 8 to 19

	flow rate	Tin	Tout	Tv	Twi	Two	$Qx10^{-6}$
	l/min			K			$J/m^2.s$
1	5.00	296.72	297.14	321.26	303.51	303.66	0.036386
2	4.00	296.57	297.09	321.29	304.40	304.54	0.035106
3	3.00	296.45	297.09	321.24	305.63	305.77	0.032754
4	7.00	293.55	293.95	320.85	300.65	300.85	0.048135
5	5.00	293.57	294.12	320.85	302.65	302.85	0.047269
6	4.00	293.59	294.27	320.85	304.21	304.41	0.046405
7	3.00	293.59	294.40	320.85	305.45	305.62	0.041246
8	5.00	294.65	295.10	320.80	302.01	302.18	0.038625
9	4.00	294.60	295.15	320.80	303.19	303.35	0.037767
10	3.00	294.62	295.30	320.82	304.55	304.70	0.034759
11	2.40	294.62	295.42	320.87	305.84	305.98	0.032954
12	2.00	294.60	295.52	320.89	307.08	307.21	0.031751
13	1.80	294.62	295.60	320.92	307.49	307.62	0.030119
14	1.60	294.60	295.67	320.94	308.43	308.55	0.029517
15	1.40	294.60	295.77	320.99	309.29	309.41	0.028228
16	1.20	294.57	295.87	320.99	310.31	310.42	0.026769
17	1.00	294.55	296.02	321.01	311.72	311.82	0.025308
18	0.80	294.55	296.27	321.03	313.67	313.77	0.023674
19	0.60	294.48	296.55	321.06	316.09	316.18	0.021356

R-113

PITCH=18.500mm

DATE OF EXPERIMENT 21-10-1983

ambiente temp = 20.60 C
atmospheric press = 30.659 inch
input power = 3.13 kW

Data no. 1 to 3

PITCH=18.500mm

DATE OF EXPERIMENT 11- 1-1984

ambiente temp = 20.10 C
atmospheric press = 29.709 inch
input power = 2.96 kW

Data no. 4 to 6

PITCH=18.500mm

DATE OF EXPERIMENT 13- 3-1984

ambiente temp = 20.65 C
atmospheric press = 30.173 inch
input power = 3.10 kW

Data no. 7 to 18

	flow rate	Tin	Tout	Tv	Twi	Two	$Qx10^{-6}$
	l/min			K			J/m^2s
1	5.00	296.45	296.85	321.26	302.19	302.33	0.034257
2	4.00	296.48	296.96	321.29	303.15	303.29	0.033398
3	3.00	296.52	297.14	321.33	304.42	304.55	0.031467
4	5.00	293.25	293.75	320.59	300.69	300.87	0.042991
5	4.00	293.25	293.85	320.57	301.77	301.94	0.041268
6	3.00	293.28	294.03	320.59	303.29	303.46	0.038684
7	5.00	294.94	295.36	320.66	301.15	301.30	0.036467
8	4.00	294.94	295.46	320.75	302.26	302.41	0.036035
9	3.00	294.96	295.61	320.89	303.50	303.64	0.033458
10	2.40	294.94	295.71	320.96	304.65	304.78	0.031912
11	2.00	294.92	295.82	321.03	305.77	305.90	0.030881
12	1.80	294.92	295.87	321.01	306.13	306.25	0.029336
13	1.60	294.99	296.04	321.03	307.06	307.18	0.028817
14	1.40	294.92	296.06	321.03	307.78	307.89	0.027617
15	1.20	294.92	296.21	321.08	308.98	309.09	0.026757
16	1.00	294.89	296.34	321.08	309.99	310.10	0.024869
17	0.80	294.87	296.57	321.08	311.74	311.84	0.023322
18	0.60	294.72	296.72	321.08	313.44	313.53	0.020579

R-113

PITCH=20.500mm

DATE OF EXPERIMENT 13- 3-1984

ambiente temp = 20.50 C
atmospheric press = 30.166 inch
input power = 3.12 kW

Data no. 1 to 12

	flow rate	Tin	Tout	Tv	Twi	Two	$Qx10^{-6}$
	l/min			K			J/m^2s
1	5.00	294.96	295.39	320.96	301.45	301.60	0.036465
2	4.00	294.94	295.46	320.99	302.59	302.74	0.036035
3	3.00	294.92	295.57	320.99	303.84	303.98	0.033460
4	2.40	294.92	295.67	320.96	304.75	304.88	0.030884
5	2.00	294.89	295.77	320.96	305.92	306.05	0.030025
6	1.80	294.89	295.83	320.92	306.46	306.58	0.028951
7	1.60	294.89	295.89	320.87	306.93	307.05	0.027449
8	1.40	294.89	295.99	320.87	307.76	307.88	0.026418
9	1.20	294.89	296.12	320.89	308.76	308.87	0.025215
10	1.00	294.84	296.22	320.92	309.84	309.93	0.023585
11	0.80	294.84	296.42	320.99	311.23	311.32	0.021610
12	0.60	294.82	296.72	321.03	313.40	313.48	0.019549

ethylene glycol

PITCH= 0.000mm

DATE OF EXPERIMENT 31- 8-1984

ambiente temp = 23.40 C
atmospheric press = 30.069 inch
input power = 8.87 kW

Data no. 1 to 9

	flow rate	Tin	Tout	Tv	Twi	Two	Qx10^{-6}
	l/min			K			J/m^{2}s
1	23.50	298.54	299.29	471.63	315.80	317.06	0.301040
2	22.00	298.59	299.41	471.67	317.25	318.55	0.309975
3	20.00	298.64	299.54	471.71	318.54	319.82	0.307[illegible]80
4	18.00	298.64	299.66	471.59	320.71	322.03	0.315041
5	16.00	298.69	299.83	471.63	322.74	324.06	0.314144
6	14.00	298.69	299.96	471.63	324.55	325.82	0.304730
7	12.00	298.78	300.30	471.63	328.47	329.78	0.312[illegible]27
8	10.00	298.78	300.55	471.63	331.85	333.12	0.302894
9	8.00	298.83	301.02	471.71	337.53	338.79	0.300239

ethylene glycol

PITCH= 0.750mm

DATE OF EXPERIMENT 5- 2-1985

ambiente temp = 20.00 C
atmospheric press = 29.990 inch
input power = 7.68 kW

Data no. 1 to 14

	flow rate	Tin	Tout	Tv	Twi	Two	$Qx10^{-6}$
	l/min			K			J/m^2s
1	22.00	294.43	296.40	465.61	338.58	341.70	0.745402
2	20.00	294.48	296.62	465.65	341.33	344.42	0.737558
3	18.00	294.55	296.95	465.75	345.30	348.41	0.740806
4	16.00	294.60	297.27	465.75	349.37	352.45	0.733778
5	14.00	294.62	297.59	465.79	353.45	356.44	0.713909
6	12.00	294.67	298.04	465.79	358.71	361.62	0.693984
7	10.00	294.70	298.54	465.83	364.39	367.15	0.659501
8	9.00	294.74	298.84	465.77	367.04	369.68	0.631958
9	8.00	294.79	299.26	465.83	371.25	373.82	0.612940
10	7.00	294.82	299.76	465.77	376.42	378.90	0.593060
11	6.00	294.82	300.43	465.81	383.65	386.07	0.577417
12	5.00	294.84	301.60	465.81	395.97	398.40	0.579130
13	4.00	294.87	303.44	465.75	414.29	416.75	0.587433
14	3.00	294.89	305.69	465.81	433.34	435.67	0.555063

ethylene glycol

PITCH= 1.000mm

DATE OF EXPERIMENT 27- 8-1984

ambiente temp = 22.70 C
atmospheric press = 30.204 inch
input power = 8.93 kW

Data no. 1 to 14

	flow rate	Tin	Tout	Tv	Twi	Two	$Qx10^{-6}$
	l/min			K			J/m^2s
1	23.50	296.60	299.14	471.06	351.59	355.88	1.024893
2	22.00	296.65	299.36	470.96	354.31	358.60	1.025149
3	20.00	296.72	299.69	470.88	358.01	362.27	1.017205
4	18.00	296.77	300.01	470.88	361.84	366.03	0.999831
5	16.00	296.84	300.43	470.90	366.60	370.73	0.984198
6	14.00	296.84	300.83	470.90	371.66	375.66	0.956625
7	12.00	296.89	301.37	470.88	377.65	381.51	0.922123
8	11.00	296.96	301.80	470.82	381.85	385.67	0.910746
9	10.00	296.94	302.17	470.90	386.46	390.21	0.896044
10	9.00	297.01	302.74	470.94	392.10	395.80	0.882894
11	8.00	297.01	303.48	470.82	400.65	404.37	0.886754
12	7.00	297.08	304.62	470.82	412.60	416.38	0.903560
--	6.00	297.08	305.86	470.82	425.32	429.09	0.901598
	5.00	297.11	307.75	470.82	443.49	447.30	0.909900

ethylene glycol

PITCH= 1.500mm

DATE OF EXPERIMENT 27- 8-1984

ambiente temp = 21.80 C
atmospheric press = 30.204 inch
input power = 8.87 kW

Data no. 1 to 14

	flow rate l/min	Tin	Tout	Tv K	Twi	Two	$Qx10^{-6}$ J/m^2s
1	23.50	296.14	299.20	470.76	361.49	366.67	1.236216
2	22.00	296.16	299.38	470.84	363.54	368.63	1.213615
3	20.00	296.18	299.65	470.82	366.97	371.95	1.188594
4	18.00	296.26	299.97	470.84	370.11	374.91	1.146414
5	16.00	296.31	300.34	470.86	374.16	378.80	1.107656
6	14.00	296.33	300.72	470.86	378.13	382.53	1.052700
7	12.00	296.40	301.34	470.90	384.63	388.88	1.014670
8	11.00	296.38	301.86	470.86	391.68	396.01	1.033145
9	10.00	296.43	302.41	470.80	397.49	401.78	1.024232
10	9.00	296.45	303.05	470.80	404.56	408.83	1.017412
11	8.00	296.50	304.09	470.84	416.03	420.39	1.040178
12	7.00	296.52	305.23	470.84	427.92	432.29	1.043595
13	6.00	296.52	306.65	470.82	442.02	446.37	1.039387
14	5.00	296.57	308.97	470.80	463.98	468.42	1.060403

ethylene glycol

PITCH= 2.000mm

DATE OF EXPERIMENT 27- 8-1984

ambiente temp = 23.80 C
atmospheric press = 30.181 inch
input power = 8.87 kW

Data no. 1 to 14

	flow rate l/min	Tin	Tout	Tv K	Twi	Two	$Qx10^{-6}$ J/m^2s
1	23.50	297.06	299.75	470.96	354.67	359.22	1.084456
2	22.00	297.08	299.98	470.92	357.78	362.35	1.090272
3	20.00	297.13	300.25	471.00	360.91	365.38	1.067845
4	18.00	297.16	300.52	470.96	364.19	368.54	1.037755
5	16.00	297.16	300.87	470.96	368.83	373.10	1.017893
6	14.00	297.21	301.29	470.88	373.39	377.50	0.980036
7	12.00	297.23	301.84	470.96	379.68	383.65	0.947264
8	11.00	297.33	302.21	470.82	382.68	386.53	0.919690
9	10.00	297.28	302.51	470.92	386.50	390.25	0.895665
10	9.00	297.33	303.23	470.84	394.64	398.45	0.909311
11	8.00	297.35	304.00	470.76	403.07	406.88	0.910147
12	7.00	297.38	304.99	470.88	413.56	417.38	0.912135
13	6.00	297.40	305.48	470.72	416.52	420.00	0.830111
14	5.00	297.42	308.36	470.76	446.86	450.77	0.934877

ethylene glycol

PITCH= 2.500mm

DATE OF EXPERIMENT 27- 8-1984

ambiente temp = 24.50 C
atmospheric press = 30.060 inch
input power = 8.87 kW

Data no. 1 to 14

	flow rate l/min	Tin	Tout	Tv K	Twi	Two	Qx10^{-6} J/m^{2}s
1	23.50	297.28	299.82	470.88	351.88	356.17	1.024023
2	22.00	297.33	299.99	470.82	353.64	357.85	1.005515
3	20.00	297.35	300.24	470.82	356.87	361.02	0.990826
4	18.00	297.40	300.59	470.82	361.17	365.29	0.983753
5	16.00	297.42	300.91	470.82	365.06	369.06	0.956222
6	14.00	297.47	301.38	470.82	370.58	374.51	0.937993
7	12.00	297.50	301.88	470.82	376.20	379.97	0.901004
8	11.00	297.52	302.15	470.72	378.88	382.53	0.872689
9	10.00	297.57	302.60	470.78	383.56	387.17	0.861337
10	9.00	297.57	303.00	470.72	387.83	391.33	0.836402
11	8.00	297.59	303.64	470.86	394.78	398.25	0.828388
12	7.00	297.64	304.68	470.82	405.98	409.51	0.843591
13	6.00	297.67	305.85	470.86	417.75	421.27	0.839998
14	5.00	297.64	307.68	470.88	436.37	439.96	0.858623

ethylene glycol

PITCH= 2.500mm

DATE OF EXPERIMENT 23- 8-1984

ambiente temp = 24.90 C
atmospheric press = 29.816 inch
input power = 8.96 kW

Data no. 1 to 15

	flow rate l/min	Tin	Tout	Tv K	Twi	Two	Qx10^{-6} J/m^{2}s
1	23.50	297.42	300.14	470.44	355.30	359.88	1.093983
2	22.00	297.50	300.39	470.36	357.94	362.50	1.089711
3	20.00	297.52	300.64	470.40	361.05	365.52	1.067328
4	18.00	297.57	300.91	470.42	363.88	368.19	1.029554
5	16.00	297.59	301.28	470.44	368.53	372.76	1.010526
6	14.00	297.64	301.70	470.38	373.09	377.17	0.973545
7	12.00	297.67	302.20	470.46	378.59	382.49	0.931438
8	10.00	297.69	302.82	470.58	385.07	388.75	0.878207
9	9.00	297.72	303.29	470.44	390.01	393.61	0.859188
10	8.00	297.77	304.03	470.36	397.91	401.51	0.858771
11	7.00	297.79	304.90	470.36	406.97	410.54	0.852341
12	6.00	297.79	306.09	470.44	419.30	422.87	0.852571
13	5.00	297.84	307.97	470.42	437.49	441.12	0.866863
14	4.00	297.86	310.47	470.38	459.60	463.21	0.862135
15	3.00	297.89	314.54	470.34	492.30	495.87	0.853215

ethylene glycol

PITCH= 4.500mm

DATE OF EXPERIMENT 23- 8-1984

ambiente temp = 23.90 C
atmospheric press = 29.834 inch
input power = 8.74 kW

Data no. 1 to 14

	flow rate	Tin	Tout	Tv	Twi	Two	$Qx10^{-6}$
	l/min			K			J/m^2s
1	23.50	297.28	299.37	470.44	343.07	346.60	0.843545
2	22.00	297.28	299.50	470.40	344.97	348.48	0.836644
3	20.00	297.30	299.70	470.38	347.51	350.94	0.820294
4	18.00	297.35	299.99	470.40	351.21	354.62	0.814993
5	16.00	297.38	300.29	470.36	355.01	358.36	0.799458
6	14.00	297.40	300.64	470.44	359.24	362.50	0.777073
7	12.00	297.45	301.11	470.46	364.57	367.73	0.752922
8	10.00	297.47	301.66	470.38	370.64	373.65	0.716817
9	8.00	297.50	302.48	470.42	379.54	382.40	0.682330
10	7.00	297.52	303.10	470.48	386.03	388.83	0.668419
11	6.00	297.52	303.99	470.30	395.65	398.43	0.664644
12	5.00	297.55	305.43	470.48	410.38	413.21	0.674691
13	4.00	297.57	307.56	470.40	430.60	433.47	0.683580
14	3.00	297.62	310.43	470.44	453.95	456.70	0.656901

ethylene glycol

PITCH= 6.500mm

DATE OF EXPERIMENT 23- 8-1984

ambiente temp = 21.85 C
atmospheric press = 28.860 inch
input power = 8.87 kW

Data no. 1 to 14

	flow rate	Tin	Tout	Tv	Twi	Two	$Qx10^{-6}$
	l/min			K			J/m^2s
1	23.60	296.72	298.62	470.36	338.80	342.01	0.767084
2	22.00	296.72	298.74	470.36	340.76	343.95	0.762065
3	20.00	296.72	298.91	470.40	343.40	346.56	0.752576
4	18.00	296.77	299.16	470.36	346.32	349.41	0.738757
5	16.00	296.82	299.46	470.44	349.86	352.89	0.724922
6	14.00	296.82	299.76	470.36	353.86	356.82	0.705985
7	12.00	296.84	300.18	470.36	359.03	361.91	0.686993
8	10.00	296.89	300.75	470.36	365.42	368.19	0.661961
9	8.00	296.94	301.60	470.36	374.70	377.38	0.638548
10	6.00	296.96	302.89	470.36	388.31	390.86	0.609031
11	5.00	296.99	304.25	470.36	402.66	405.26	0.622149
12	4.00	296.96	305.99	470.40	419.58	422.17	0.618092
13	3.00	296.99	308.91	470.38	444.91	447.47	0.611880
14	2.00	297.08	313.20	470.42	474.76	477.07	0.550912

ethylene glycol

PITCH= 8.500mm

DATE OF EXPERIMENT 29- 8-1984

ambiente temp = 22.00 C
atmospheric press = 30.156 inch
input power = 8.87 kW

Data no. 1 to 14

	flow rate l/min	Tin	Tout	Tv K	Twi	Two	$Qx10^{-6}$ J/m^2s
1	23.50	297.47	299.02	471.63	332.05	334.66	0.622675
2	22.00	297.47	299.12	471.69	333.67	336.27	0.620500
3	20.00	297.50	299.29	471.63	336.03	338.61	0.615297
4	18.00	297.52	299.47	471.69	338.20	340.71	0.599842
5	16.00	297.55	299.74	471.69	342.00	344.52	0.601440
6	14.00	297.55	300.01	471.69	345.85	348.33	0.591943
7	12.00	297.57	300.39	471.69	350.53	352.96	0.578989
8	10.00	297.55	300.79	471.43	355.72	358.05	0.554951
9	8.00	297.57	301.46	471.33	363.38	365.61	0.532526
10	7.00	297.62	302.05	471.47	369.86	372.08	0.531462
11	6.00	297.64	302.67	471.49	376.25	378.41	0.516755
12	5.00	297.69	303.86	471.39	388.79	391.00	0.528292
13	4.00	297.72	305.47	471.37	404.65	406.87	0.531168
14	3.00	297.72	308.05	471.31	427.92	430.14	0.530332

ethylene glycol

PITCH= 8.500mm

DATE OF EXPERIMENT 29- 8-1984

ambiente temp = 22.00 C
atmospheric press = 30.159 inch
input power = 8.87 kW

Data no. 1 to 14

	flow rate l/min	Tin	Tout	Tv K	Twi	Two	$Qx10^{-6}$ J/m^2s
1	23.50	297.08	298.68	471.55	332.84	335.54	0.643054
2	22.00	297.16	298.85	471.65	334.49	337.17	0.639536
3	20.00	297.18	299.03	471.59	336.83	339.48	0.632619
4	18.00	297.21	299.20	471.57	338.98	341.56	0.615446
5	16.00	297.23	299.47	471.73	342.76	345.33	0.615333
6	14.00	297.30	299.77	471.75	345.74	348.22	0.592123
7	12.00	297.42	300.24	471.81	350.47	352.89	0.579095
8	10.00	297.35	300.69	471.63	357.25	359.65	0.572130
9	8.00	297.38	301.36	471.63	364.82	367.11	0.546279
10	7.00	297.40	301.86	471.67	370.16	372.39	0.534585
11	6.00	297.47	302.58	471.89	377.23	379.43	0.524517
12	5.00	297.45	303.62	471.49	388.76	390.97	0.528451
13	4.00	297.47	305.18	471.51	404.05	406.26	0.527938
14	3.00	297.50	307.83	471.55	427.95	430.18	0.530475

ethylene glycol

PITCH=10.500mm

DATE OF EXPERIMENT 29- 8-1984

ambiente temp = 22.85 C
atmospheric press = 30.142 inch
input power = 8.90 kW

Data no. 1 to 14

	flow rate	Tin	Tout	Tv	Twi	Two	$Qx10^{-6}$
	l/min			K			J/m^2s
1	23.50	297.62	299.02	471.65	329.03	331.39	0.562366
2	22.00	297.67	299.16	471.61	330.74	333.10	0.564006
3	20.00	297.72	299.36	471.53	333.19	335.56	0.563920
4	18.00	297.77	299.58	471.53	335.94	338.29	0.561263
5	16.00	297.79	299.83	471.45	339.35	341.70	0.560315
6	14.00	297.84	300.16	471.37	343.34	345.66	0.555917
7	12.00	297.89	300.55	471.43	348.13	350.43	0.548081
8	10.00	297.91	301.05	471.43	354.27	356.52	0.537665
9	8.00	297.91	301.75	471.51	362.75	364.95	0.525492
10	7.00	297.96	302.24	471.47	367.80	369.95	0.513377
11	6.00	298.01	302.96	471.43	375.30	377.44	0.508874
12	5.00	298.03	304.05	471.47	386.91	389.07	0.515340
13	4.00	298.08	305.54	471.59	401.10	403.24	0.510601
14	3.00	298.10	307.67	471.45	419.57	421.62	0.490806

ethylene glycol

PITCH=12.500mm

DATE OF EXPERIMENT 29- 8-1984

ambiente temp = 23.50 C
atmospheric press = 30.124 inch
input power = 8.82 kW

Data no. 1 to 14

	flow rate	Tin	Tout	Tv	Twi	Two	$Qx10^{-6}$
	l/min			K			J/m^2s
1	23.50	297.91	299.16	471.57	326.08	328.18	0.501976
2	22.00	297.96	299.31	471.57	327.85	329.97	0.507468
3	20.00	298.01	299.48	471.49	329.88	331.99	0.503981
4	18.00	298.06	299.68	471.45	332.24	334.34	0.499634
5	16.00	298.08	299.90	471.53	335.32	337.41	0.498704
6	14.00	298.08	300.15	471.43	338.98	341.06	0.496067
7	12.00	298.10	300.50	471.41	343.53	345.59	0.491685
8	10.00	298.13	300.92	471.51	348.69	350.69	0.477896
9	8.00	298.25	301.66	471.43	356.45	358.40	0.467407
10	7.00	298.25	302.08	471.43	361.36	363.29	0.459611
11	6.00	298.30	302.78	471.45	368.83	370.76	0.460254
12	5.00	298.30	303.77	471.15	379.85	381.82	0.468493
13	4.00	298.32	305.04	471.53	392.13	394.06	0.459612
14	3.00	298.30	307.44	471.53	414.95	416.92	0.469143

ethylene glycol

PITCH=14.500mm

DATE OF EXPERIMENT 30- 8-1984

ambiente temp = 22.05 C
atmospheric press = 30.050 inch
input power = 8.87 kW

Data no. 1 to 14

	flow rate l/min	Tin	Tout	Tv K	Twi	Two	$Qx10^{-6}$ J/m^2s
1	23.50	297.64	298.96	471.08	327.48	329.71	0.532247
2	22.00	297.67	299.06	471.08	328.69	330.89	0.526438
3	20.00	297.69	299.19	471.04	330.18	332.33	0.512717
4	18.00	297.72	299.39	471.04	333.01	335.17	0.515210
5	16.00	297.74	299.61	470.96	336.06	338.21	0.512569
6	14.00	297.74	299.86	470.94	339.70	341.83	0.508220
7	12.00	297.79	300.21	470.92	343.80	345.88	0.496995
8	10.00	297.79	300.63	470.92	349.35	351.39	0.486621
9	8.00	297.86	301.37	470.94	357.82	359.83	0.481257
10	7.00	297.89	301.82	470.86	362.70	364.67	0.471734
11	6.00	297.91	302.39	470.86	368.72	370.65	0.460476
12	5.00	297.89	303.29	470.88	378.79	380.72	0.462362
13	4.00	297.91	304.75	470.82	393.60	395.56	0.468327
14	3.00	297.91	306.91	470.88	413.34	415.27	0.461757

ethylene glycol

PITCH=16.500mm

DATE OF EXPERIMENT 30- 8-1984

ambiente temp = 22.15 C
atmospheric press = 30.048 inch
input power = 8.87 kW

Data no. 1 to 14

	flow rate l/min	Tin	Tout	Tv K	Twi	Two	$Qx10^{-6}$ J/m^2s
1	23.50	297.69	298.76	470.80	322.21	324.02	0.431863
2	22.00	297.77	298.91	470.88	323.55	325.36	0.432445
3	20.00	297.81	299.08	470.88	325.70	327.53	0.435804
4	18.00	297.86	299.26	470.84	327.70	329.50	0.430618
5	16.00	297.89	299.48	470.92	330.93	332.77	0.437386
6	14.00	297.93	299.75	470.92	334.34	336.17	0.436445
7	12.00	297.96	300.08	470.88	338.67	340.49	0.435498
8	10.00	297.98	300.47	470.94	343.67	345.46	0.426849
9	8.00	298.01	301.10	470.94	351.35	353.12	0.423266
10	7.00	298.03	301.52	470.96	356.11	357.86	0.418031
11	6.00	298.06	302.09	470.96	362.44	364.18	0.414467
12	5.00	298.10	303.03	471.02	372.57	374.34	0.421836
13	4.00	298.15	304.37	470.96	386.02	387.80	0.425735
14	3.00	298.15	306.36	470.94	404.52	406.29	0.421016

ethylene glycol

PITCH=18.500mm

DATE OF EXPERIMENT 30- 8-1984

ambiente temp = 22.90 C
atmospheric press = 30.032 inch
input power = 8.87 kW

Data no. 1 to 14

	flow rate	Tin	Tout	Tv	Twi	Two	$Qx10^{-6}$
	l/min			K			J/m^2s
1	23.50	297.93	298.96	470.92	321.31	323.04	0.411664
2	22.00	297.98	299.08	470.92	322.65	324.38	0.413543
3	20.00	298.03	299.25	470.96	324.83	326.58	0.418612
4	18.00	298.08	299.45	470.96	327.35	329.12	0.422819
5	16.00	298.13	299.70	470.98	330.61	332.41	0.430428
6	14.00	298.15	299.95	470.96	334.01	335.82	0.430356
7	12.00	298.18	300.27	470.92	338.35	340.16	0.430264
8	10.00	298.20	300.69	470.92	343.78	345.57	0.426732
9	8.00	298.25	301.36	470.96	351.84	353.63	0.426544
10	7.00	298.27	301.81	470.94	356.95	358.73	0.423862
11	6.00	298.30	302.33	470.94	362.53	364.26	0.414342
12	5.00	298.32	303.30	470.96	373.30	375.08	0.426019
13	4.00	298.35	304.52	470.96	385.44	387.21	0.422290
14	3.00	298.35	306.72	470.90	406.46	408.26	0.429798

ethylene glycol

PITCH=20.500mm

DATE OF EXPERIMENT 30- 8-1984

ambiente temp = 23.35 C
atmospheric press = 30.016 inch
input power = 8.90 kW

Data no. 1 to 14

	flow rate	Tin	Tout	Tv	Twi	Two	$Qx10^{-6}$
	l/min			K			J/m^2s
1	23.50	298.20	299.22	471.04	321.51	323.23	0.411527
2	22.00	298.25	299.37	470.78	323.37	325.14	0.422794
3	20.00	298.27	299.50	470.78	325.00	326.75	0.418485
4	18.00	298.32	299.69	470.82	327.51	329.28	0.422691
5	16.00	298.35	299.89	470.84	330.27	332.05	0.423487
6	14.00	298.37	300.14	470.80	333.69	335.46	0.424270
7	12.00	298.40	300.46	470.80	338.04	339.82	0.425033
8	10.00	298.42	300.89	470.84	343.48	345.25	0.422357
9	8.00	298.47	301.51	470.94	350.78	352.52	0.416213
10	7.00	298.52	301.93	470.92	355.20	356.91	0.408845
11	6.00	298.52	302.50	470.94	361.90	363.61	0.409128
12	5.00	298.57	303.37	470.94	371.04	372.76	0.411028
13	4.00	298.59	304.76	470.94	385.48	387.25	0.422163
14	3.00	298.61	306.47	470.94	400.64	402.33	0.4030[illegible]1

APPENDIX B Recent experimental data of Yau et al. [35,36,37], Georgiadis [40] and Honda [52]

Symbols

ALF	vapour-side heat-transfer coefficient obtained by experiments
ALN	vapour-side heat-transfer coefficient obtained by Nuuselt equation
AR	area ratio of finned tube to plain tube
D	diameter at the fins of finned tube outer tube diameter of plain tube
DT	vapour-side temperature difference
h	fin height
Pitch	fin pitch
PSI	"retention" angle calculated by eq.(5-35)
Q	heat flux
t	fin thickness
T_w	outside wall temperature
T_s	vapour temperature
θ	a half angle og fin tip

Steam data of Yau et al. [35,36,37]

QMC
WATER

----- TUBE DIMENSION -----

D	Pitch	h	t	θ	AR
12.700	0.000	1.585	0.000	0.000	1.000

V=0.52 M/S

----- DATA TABLE -----

	Ts/K	Tw/K	Q /J/m2s
1	372.98	352.81	0.303600E+06
2	372.98	345.38	0.340300E+06
3	372.98	341.03	0.375500E+06
4	373.00	336.91	0.396800E+06
5	373.00	334.16	0.420000E+06
6	372.98	331.92	0.440700E+06
7	372.98	329.35	0.449600E+06
8	372.98	328.09	0.470600E+06
9	372.85	347.16	0.311300E+06
10	372.86	342.29	0.349900E+06
11	372.86	338.18	0.376800E+06
12	372.85	335.25	0.402100E+06
13	372.85	333.21	0.428200E+06
14	372.85	330.81	0.442500E+06
15	372.85	329.15	0.460200E+06
16	372.85	327.54	0.473700E+06
17	372.38	351.06	0.295900E+06
18	372.42	344.03	0.333700E+06
19	372.41	339.56	0.366800E+06
20	372.38	336.73	0.399900E+06
21	372.42	333.74	0.420800E+06
22	372.44	331.24	0.438300E+06
23	372.44	329.42	0.457600E+06
24	372.40	327.63	0.471500E+06
25	372.44	347.21	0.316100E+06
26	372.42	341.45	0.349500E+06
27	372.44	337.68	0.380300E+06
28	372.42	334.96	0.408600E+06
29	372.40	332.43	0.429600E+06
30	372.42	330.25	0.447400E+06
31	372.42	328.57	0.465600E+06
32	372.44	327.23	0.483700E+06

CALCULATION RESULTS

CASE	DT K	ALF J/m2s	ALN J/m2s	ALF/ALN	PSI deg
1	20.170	15052.1	12098.6	1.244	0.000
2	27.600	12329.7	11000.4	1.121	0.000
3	31.950	11752.7	10495.9	1.120	0.000
4	36.090	10994.7	10078.0	1.091	0.000
5	38.840	10813.6	9825.5	1.101	0.000
6	41.060	10733.1	9633.3	1.114	0.000
7	43.630	10304.8	9423.4	1.094	0.000
8	44.890	10483.4	9324.7	1.124	0.000
9	25.690	12117.6	11244.3	1.078	0.000
10	30.570	11445.9	10643.6	1.075	0.000
11	34.680	10865.1	10210.0	1.064	0.000
12	37.600	10694.1	9931.9	1.077	0.000
13	39.640	10802.2	9750.1	1.108	0.000
14	42.040	10525.7	9547.3	1.102	0.000
15	43.700	10530.9	9413.3	1.119	0.000
16	45.310	10454.6	9287.8	1.126	0.000
17	21.320	13879.0	11880.5	1.168	0.000
18	28.390	11754.1	10883.0	1.080	0.000
19	32.850	11165.9	10380.4	1.076	0.000
20	35.650	11217.4	10098.3	1.111	0.000
21	38.680	10879.0	9819.3	1.108	0.000
22	41.200	10638.3	9602.5	1.108	0.000
23	43.020	10636.9	9453.1	1.125	0.000
24	44.770	10531.6	9313.4	1.131	0.000
25	25.230	12528.7	11292.6	1.109	0.000
26	30.970	11285.1	10583.3	1.066	0.000
27	34.760	10940.7	10187.3	1.074	0.000
28	37.460	10907.6	9929.5	1.099	0.000
29	39.970	10748.1	9705.6	1.107	0.000
30	42.170	10609.4	9521.4	1.114	0.000
31	43.850	10618.0	9386.2	1.131	0.000
32	45.210	10699.0	9280.9	1.153	0.000

QMC
WATER

----- TUBE DIMENSION -----

D	Pitch	h	t	θ	AR
12.700	0.750	1.585	0.500	0.000	5.920

V=0.52 M/S

----- DATA TABLE -----

	Ts/K	Tw/K	Q /J/m2s
1	373.22	350.42	0.974474E+06
2	373.20	350.84	0.948125E+06
3	373.22	351.19	0.920147E+06
4	373.24	352.46	0.906790E+06
5	373.26	352.70	0.874516E+06
6	373.31	353.86	0.855063E+06
7	373.33	354.91	0.832227E+06
8	373.37	355.89	0.805881E+06
9	373.39	356.78	0.776081E+06
10	373.43	357.56	0.742856E+06
11	373.48	358.20	0.706271E+06
12	373.52	359.11	0.670991E+06
13	373.50	360.30	0.635630E+06
14	373.52	361.65	0.599041E+06
15	373.46	362.35	0.553025E+06
16	373.48	364.26	0.513857E+06

CALCULATION RESULTS

CASE	DT K	ALF J/m2s	ALN J/m2s	ALF/ALN	PSI deg
1	22.805	42730.7	11673.4	3.661	0.000
2	22.363	42397.0	11741.5	3.611	0.000
3	22.035	41758.4	11794.2	3.541	0.000
4	20.782	43633.4	12001.9	3.636	0.000
5	20.561	42532.8	12040.6	3.532	0.000
6	19.448	43966.6	12240.3	3.592	0.000
7	18.419	45183.1	12435.9	3.633	0.000
8	17.480	46103.0	12626.4	3.651	0.000
9	16.612	46718.1	12812.3	3.646	0.000
10	15.875	46794.1	12980.0	3.605	0.000
11	15.281	46218.9	13122.1	3.522	0.000
12	14.408	46570.7	13342.0	3.491	0.000
13	13.198	48161.1	13670.7	3.523	0.000
14	11.869	50471.1	14076.7	3.585	0.000
15	11.102	49813.1	14333.2	3.475	0.000
16	9.215	55763.1	15073.3	3.699	0.000

QMC
WATER

----- TUBE DIMENSION -----

D	Pitch	h	t	θ	AR
12.700	1.000	1.585	0.500	0.000	4.690

V=0.52 M/S

----- DATA TABLE -----

	Ts/K	Tw/K	Q /J/m2s
1	372.85	359.90	0.441900E+06
2	372.86	356.84	0.508300E+06
3	372.85	354.78	0.571000E+06
4	372.87	351.36	0.607300E+06
5	372.85	349.16	0.647700E+06
6	372.85	347.03	0.681000E+06
7	372.85	345.82	0.721600E+06
8	372.87	362.18	0.407300E+06
9	372.86	358.17	0.475000E+06
10	372.87	355.52	0.537700E+06
11	372.87	353.51	0.595400E+06
12	372.87	350.91	0.636400E+06
13	372.85	348.76	0.674100E+06
14	372.85	347.47	0.717200E+06
15	372.87	345.93	0.751200E+06

CALCULATION RESULTS

CASE	DT / K	ALF / J/m2s	ALN / J/m2s	ALF/ALN	PSI / deg
1	12.950	34123.6	13718.1	2.487	0.000
2	16.020	31729.1	12925.6	2.455	0.000
3	18.070	31599.3	12487.5	2.530	0.000
4	21.510	28233.4	11866.7	2.379	0.000
5	23.690	27340.7	11526.9	2.372	0.000
6	25.820	26374.9	11226.8	2.349	0.000
7	27.030	26696.3	11068.0	2.412	0.000
8	10.690	38101.0	14458.4	2.635	0.000
9	14.690	32334.9	13245.4	2.441	0.000
10	17.350	30991.4	12635.2	2.453	0.000
11	19.360	30754.1	12240.7	2.512	0.000
12	21.960	28980.0	11793.7	2.457	0.000
13	24.090	27982.6	11468.3	2.440	0.000
14	25.380	28258.5	11286.5	2.504	0.000
15	26.940	27884.2	11080.3	2.517	0.000

QMC
WATER

----- TUBE DIMENSION -----

D	Pitch	h	t	θ	AR
12.700	1.500	1.585	0.500	0.000	3.460

V=0.52 M/S

----- DATA TABLE -----

	Ts/K	Tw/K	Q /J/m2s
1	372.52	357.80	0.428100E+06
2	372.52	354.99	0.494200E+06
3	372.49	352.82	0.553700E+06
4	372.52	351.08	0.608400E+06
5	372.52	348.63	0.645700E+06
6	372.51	347.21	0.689300E+06
7	372.51	346.25	0.734900E+06
8	372.50	360.15	0.395600E+06
9	372.50	356.15	0.461000E+06
10	372.52	353.79	0.524200E+06
11	372.52	351.69	0.579000E+06
12	372.50	349.46	0.623000E+06
13	372.50	347.97	0.668700E+06
14	372.51	346.66	0.711100E+06
15	372.50	344.85	0.740000E+06

CALCULATION RESULTS

CASE	DT / K	ALF / J/m2s	ALN / J/m2s	ALF/ALN	PSI / deg
1	14.720	29082.9	13225.1	2.199	51.787
2	17.530	28191.7	12585.0	2.240	51.250
3	19.670	28149.5	12170.3	2.313	50.831
4	21.440	28376.9	11865.7	2.392	50.501
5	23.890	27028.0	11485.7	2.353	50.030
6	25.300	27245.1	11285.4	2.414	49.755
7	26.260	27985.5	11156.1	2.509	49.570
8	12.350	32032.4	13885.3	2.307	52.233
9	16.350	28195.7	12837.6	2.196	51.470
10	18.730	27987.2	12346.5	2.267	51.020
11	20.830	27796.4	11967.8	2.323	50.618
12	23.040	27039.9	11611.8	2.329	50.188
13	24.530	27260.5	11392.7	2.393	49.901
14	25.850	27508.7	11210.7	2.454	49.649
15	27.650	26763.1	10977.1	2.438	49.299

QMC
WATER

----- TUBE DIMENSION -----

D	Pitch	h	t	θ	AR
12.700	2.000	1.585	0.500	0.000	2.845

V=0.52 M/S

----- DATA TABLE -----

	Ts/K	Tw/K	Q /J/m2s
1	372.66	360.25	0.449300E+06
2	372.66	357.40	0.519600E+06
3	372.68	355.57	0.586900E+06
4	372.63	353.28	0.639400E+06
5	372.66	350.92	0.681400E+06
6	372.67	349.59	0.729700E+06
7	372.63	348.47	0.775900E+06
8	372.62	363.08	0.417500E+06
9	372.63	358.30	0.481800E+06
10	372.68	356.69	0.556500E+06
11	372.68	354.07	0.610200E+06
12	372.68	352.17	0.662300E+06
13	372.68	350.54	0.710100E+06
14	372.68	349.06	0.753800E+06
15	372.66	347.83	0.795900E+06

CALCULATION RESULTS

CASE	DT / K	ALF / J/m2s	ALN / J/m2s	ALF/ALN	PSI / deg
1	12.410	36204.7	13872.9	2.610	85.719
2	15.260	34049.8	13096.9	2.600	85.432
3	17.110	34301.6	12678.8	2.705	85.250
4	19.350	33043.9	12233.9	2.701	85.019
5	21.740	31343.1	11821.7	2.651	84.786
6	23.080	31616.1	11611.8	2.723	84.655
7	24.160	32115.1	11450.4	2.805	84.543
8	9.540	43763.1	14899.8	2.937	86.003
9	14.330	33621.8	13329.1	2.522	85.521
10	15.990	34803.0	12925.8	2.693	85.362
11	18.610	32788.8	12375.4	2.650	85.101
12	20.510	32291.6	12028.4	2.685	84.911
13	22.140	32073.2	11758.2	2.728	84.750
14	23.620	31913.6	11531.1	2.768	84.603
15	24.830	32054.0	11356.0	2.823	84.481

QMC
WATER

----- TUBE DIMENSION -----

D	Pitch	h	t	θ	AR
12.700	2.500	1.585	0.500	0.000	2.476

V=0.52 M/S

----- DATA TABLE -----

	Ts/K	Tw/K	Q /J/m2s
1	372.30	355.39	0.415100E+06
2	372.30	352.62	0.479200E+06
3	372.31	350.30	0.535100E+06
4	372.30	347.99	0.580700E+06
5	372.31	345.62	0.616700E+06
6	372.33	343.60	0.649200E+06
7	372.31	342.28	0.685800E+06
8	372.29	357.50	0.382100E+06
9	372.31	353.46	0.444300E+06
10	372.31	350.92	0.503100E+06
11	372.30	348.66	0.553600E+06
12	372.30	346.05	0.590200E+06
13	372.29	344.41	0.631100E+06
14	372.31	342.72	0.664800E+06
15	372.29	341.29	0.696700E+06

CALCULATION RESULTS

CASE	DT K	ALF J/m2s	ALN J/m2s	ALF/ALN	PSI deg
1	16.910	24547.6	12707.5	1.932	100.802
2	19.680	24349.6	12161.6	2.002	100.592
3	22.010	24311.7	11765.6	2.066	100.418
4	24.310	23887.3	11417.0	2.092	100.244
5	26.690	23106.0	11092.7	2.083	100.068
6	28.730	22596.6	10838.8	2.085	99.918
7	30.030	22837.2	10685.5	2.137	99.820
8	14.790	25835.0	13198.9	1.957	100.962
9	18.850	23570.3	12315.9	1.914	100.656
10	21.390	23520.3	11866.3	1.982	100.464
11	23.640	23417.9	11514.6	2.034	100.294
12	26.250	22483.8	11149.9	2.016	100.099
13	27.880	22636.3	10941.0	2.069	99.977
14	29.590	22467.0	10736.4	2.093	99.852
15	31.000	22474.2	10575.4	2.125	99.746

QMC
WATER

----- TUBE DIMENSION -----

D	Pitch	h	t	θ	AR
12.700	0.000	1.585	0.000	0.000	1.000

V=0.73 M/S

----- DATA TABLE -----

	Ts/K	Tw/K	Q /J/m2s
1	373.00	353.65	0.309000E+06
2	373.00	345.71	0.343400E+06
3	373.00	341.39	0.379400E+06
4	373.00	337.53	0.403900E+06
5	373.00	335.04	0.431000E+06
6	373.00	332.33	0.447100E+06
7	373.00	333.03	0.460500E+06
8	372.99	328.52	0.478800E+06
9	372.95	348.39	0.321900E+06
10	372.98	343.40	0.362300E+06
11	372.98	339.11	0.390200E+06
12	372.98	336.23	0.418000E+06
13	372.98	333.76	0.440700E+06
14	372.98	331.38	0.456800E+06
15	372.98	329.47	0.472400E+06
16	373.00	327.87	0.487200E+06
17	372.42	352.45	0.304400E+06
18	372.38	344.76	0.339700E+06
19	372.39	340.36	0.374500E+06
20	372.38	337.57	0.409300E+06
21	372.40	334.85	0.434700E+06
22	372.38	332.40	0.454300E+06
23	372.40	330.38	0.472000E+06
24	372.40	328.88	0.491700E+06
25	372.38	347.73	0.320000E+06
26	372.40	342.44	0.358000E+06
27	372.41	338.75	0.390900E+06
28	372.40	335.60	0.416200E+06
29	372.40	333.34	0.441600E+06
30	372.42	330.95	0.457600E+06
31	372.41	329.57	0.480800E+06
32	372.42	328.24	0.500700E+06

CALCULATION RESULTS

CASE	DT K	ALF J/m2s	ALN J/m2s	ALF/ALN	PSI deg
1	19.350	15969.0	12247.3	1.304	0.000
2	27.290	12583.4	11040.2	1.140	0.000
3	31.610	12002.5	10533.4	1.139	0.000
4	35.470	11387.1	10137.6	1.123	0.000
5	37.960	11354.1	9904.4	1.146	0.000
6	40.670	10993.4	9666.9	1.137	0.000
7	39.970	11521.1	9726.8	1.184	0.000
8	44.470	10766.8	9357.7	1.151	0.000
9	24.560	13106.7	11404.5	1.149	0.000
10	29.580	12248.1	10761.2	1.138	0.000
11	33.870	11520.5	10295.4	1.119	0.000
12	36.750	11374.1	10015.0	1.136	0.000
13	39.220	11236.6	9791.3	1.148	0.000
14	41.600	10980.8	9588.2	1.145	0.000
15	43.510	10857.3	9433.0	1.151	0.000
16	45.130	10795.5	9306.9	1.160	0.000
17	19.970	15242.9	12113.8	1.258	0.000
18	27.620	12299.1	10976.6	1.120	0.000
19	32.030	11692.2	10466.5	1.117	0.000
20	34.810	11758.1	10180.2	1.155	0.000
21	37.550	11576.6	9920.6	1.167	0.000
22	39.980	11363.2	9704.0	1.171	0.000
23	42.020	11232.7	9533.0	1.178	0.000
24	43.520	11298.3	9411.6	1.200	0.000
25	24.650	12981.7	11371.4	1.142	0.000
26	29.960	11949.3	10696.7	1.117	0.000
27	33.660	11613.2	10296.7	1.128	0.000
28	36.800	11309.8	9989.9	1.132	0.000
29	39.060	11305.7	9784.9	1.155	0.000
30	41.470	11034.5	9579.2	1.152	0.000
31	42.840	11223.2	9466.5	1.186	0.000
32	44.180	11333.2	9360.2	1.211	0.000

QMC
WATER

----- TUBE DIMENSION -----

D	Pitch	h	t	θ	AR
12.700	0.750	1.585	0.500	0.000	5.920

V=0.73 M/S

----- DATA TABLE -----

	Ts/K	Tw/K	Qr/J/m2s
1	373.48	352.20	0.992451E+06
2	373.48	352.57	0.965355E+06
3	373.48	352.93	0.936484E+06
4	373.48	353.71	0.914103E+06
5	373.50	354.44	0.889121E+06
6	373.50	355.57	0.868853E+06
7	373.46	356.14	0.838320E+06
8	373.48	357.10	0.811593E+06
9	373.46	357.51	0.775487E+06
10	373.43	358.26	0.742355E+06
11	373.46	359.77	0.716054E+06
12	373.50	360.26	0.675209E+06
13	373.50	361.41	0.639523E+06
14	373.50	362.36	0.598674E+06
15	373.50	363.44	0.556128E+06
16	373.46	364.97	0.513574E+06

CALCULATION RESULTS

CASE	DT / K	ALF / J/m2s	ALN / J/m2s	ALF/ALN	PSI / deg
1	21.281	46635.5	11926.2	3.910	0.000
2	20.902	46184.8	11989.8	3.852	0.000
3	20.547	45577.7	12050.6	3.782	0.000
4	19.766	46246.2	12188.5	3.794	0.000
5	19.061	46646.1	12319.1	3.786	0.000
6	17.930	48458.1	12539.0	3.865	0.000
7	17.317	48410.2	12663.4	3.823	0.000
8	16.372	49572.0	12868.6	3.852	0.000
9	15.949	48622.9	12963.7	3.751	0.000
10	15.169	48939.0	13147.7	3.722	0.000
11	13.686	52320.2	13532.2	3.866	0.000
12	13.239	51001.5	13659.0	3.734	0.000
13	12.088	52905.6	14005.5	3.777	0.000
14	11.140	53740.9	14321.5	3.752	0.000
15	10.055	55308.6	14724.7	3.756	0.000
16	8.488	60505.9	15407.1	3.927	0.000

QMC
WATER

----- TUBE DIMENSION -----

D	Pitch	h	t	θ	AR
12.700	1.000	1.585	0.500	0.000	4.690

V=0.73 M/S

----- DATA TABLE -----

	Ts/K	Tw/K	Qr/J/m2s
1	372.91	360.58	0.448000E+06
2	372.90	356.96	0.510500E+06
3	372.87	354.89	0.573700E+06
4	372.87	352.14	0.618500E+06
5	372.87	350.20	0.663800E+06
6	372.87	347.88	0.695700E+06
7	372.87	346.45	0.734000E+06
8	372.87	361.37	0.402600E+06
9	372.87	358.25	0.477100E+06
10	372.89	354.97	0.534000E+06
11	372.89	353.83	0.600800E+06
12	372.88	350.33	0.631100E+06
13	372.87	348.87	0.678000E+06
14	372.86	347.09	0.714000E+06
15	372.86	345.80	0.751700E+06

CALCULATION RESULTS

CASE	DT / K	ALF / J/m2s	ALN / J/m2s	ALF/ALN	PSI / deg
1	12.330	36334.1	13907.2	2.613	0.000
2	15.940	32026.3	12945.4	2.474	0.000
3	17.980	31907.7	12506.2	2.551	0.000
4	20.730	29836.0	11997.4	2.487	0.000
5	22.670	29281.0	11681.8	2.507	0.000
6	24.990	27839.1	11341.1	2.455	0.000
7	26.420	27782.0	11147.8	2.492	0.000
8	11.500	35008.7	14173.8	2.470	0.000
9	14.620	32633.4	13263.5	2.460	0.000
10	17.920	29799.1	12519.0	2.380	0.000
11	19.060	31521.5	12297.3	2.563	0.000
12	22.550	27986.7	11700.8	2.392	0.000
13	24.000	28250.0	11482.1	2.460	0.000
14	25.770	27706.6	11233.9	2.466	0.000
15	27.060	27779.0	11064.5	2.511	0.000

QMC
WATER

----- TUBE DIMENSION -----

D:	Pitch	h	t	θ	AR
12.700	1.500	1.585	0.500	0.000	3.460

V=0.73 M/S

----- DATA TABLE -----

	Ts/K	Tw/K	Qr/J/m2s
1	372.54	358.66	0.435700E+06
2	372.56	355.10	0.496400E+06
3	372.53	353.14	0.558700E+06
4	372.53	350.96	0.608900E+06
5	372.55	349.44	0.658800E+06
6	372.55	347.81	0.700500E+06
7	372.53	346.14	0.735300E+06
8	372.55	360.80	0.400900E+06
9	372.55	356.45	0.464600E+06
10	372.55	354.11	0.528700E+06
11	372.55	352.03	0.584400E+06
12	372.54	350.51	0.638100E+06
13	372.54	348.34	0.675900E+06
14	372.54	347.03	0.719100E+06
15	372.54	345.98	0.761500E+06

CALCULATION RESULTS

CASE	DT K	ALF J/m2s	ALN J/m2s	ALF/ALN	PSI deg
1	13.880	31390.5	13445.0	2.335	51.953
2	17.460	28430.7	12601.0	2.256	51.275
3	19.390	28813.8	12222.9	2.357	50.897
4	21.570	28229.0	11844.7	2.383	50.479
5	23.110	28507.1	11602.9	2.457	50.188
6	24.740	28314.5	11364.8	2.491	49.875
7	26.390	27862.8	11139.7	2.501	49.551
8	11.750	34119.1	14078.4	2.424	52.362
9	16.100	28857.1	12895.8	2.238	51.532
10	18.440	28671.4	12403.6	2.312	51.084
11	20.520	28479.5	12022.0	2.369	50.686
12	22.030	28965.0	11770.7	2.461	50.393
13	24.200	27929.8	11441.4	2.441	49.976
14	25.510	28188.9	11257.8	2.504	49.724
15	26.560	28670.9	11117.8	2.579	49.521

QMC
WATER

----- TUBE DIMENSION -----

D	Pitch	h	t	θ	AR
12.700	2.000	1.585	0.500	0.000	2.845

V=0.73 M/S

----- DATA TABLE -----

	Ts/K	Tw/K	Qr/J/m2s
1	372.66	361.16	0.456900E+06
2	372.61	358.14	0.527400E+06
3	372.67	356.14	0.594200E+06
4	372.63	353.64	0.645300E+06
5	372.62	352.22	0.700800E+06
6	372.63	350.20	0.740900E+06
7	372.67	349.62	0.796300E+06
8	372.66	363.94	0.424100E+06
9	372.65	358.42	0.483800E+06
10	372.62	356.40	0.554700E+06
11	372.63	354.65	0.618100E+06
12	372.66	352.79	0.671400E+06
13	372.66	350.70	0.713900E+06
14	372.66	349.98	0.769300E+06
15	372.66	348.77	0.813000E+06

CALCULATION RESULTS

CASE	DT K	ALF J/m2s	ALN J/m2s	ALF/ALN	PSI deg
1	11.500	39730.4	14165.7	2.805	85.811
2	14.470	36447.8	13292.1	2.742	85.504
3	16.530	35946.8	12803.9	2.807	85.307
4	18.990	33981.0	12301.1	2.762	85.055
5	20.400	34352.9	12045.3	2.852	84.913
6	22.430	33031.7	11710.6	2.821	84.714
7	23.050	34546.6	11616.3	2.974	84.658
8	8.720	48635.3	15264.6	3.186	86.092
9	14.230	33998.6	13356.0	2.546	85.534
10	16.220	34198.5	12871.2	2.657	85.330
11	17.980	34377.1	12497.5	2.751	85.156
12	19.870	33789.6	12140.4	2.783	84.972
13	21.960	32509.1	11786.2	2.758	84.765
14	22.680	33919.8	11672.7	2.906	84.693
15	23.890	34031.0	11490.7	2.962	84.574

QMC
WATER

----- TUBE DIMENSION -----

D	Pitch	h	t	θ	AR
12.700	2.500	1.585	0.500	0.000	2.476

V=0.73 M/S

----- DATA TABLE -----

	Ts/K	Tw/K	Qr/J/m2s
1	372.30	356.31	0.422600E+06
2	372.30	353.60	0.488800E+06
3	372.29	351.77	0.551500E+06
4	372.29	349.53	0.600100E+06
5	372.28	347.47	0.642200E+06
6	372.29	345.53	0.677900E+06
7	372.28	344.54	0.721900E+06
8	372.30	358.78	0.390900E+06
9	372.30	354.85	0.456100E+06
10	372.29	352.18	0.515800E+06
11	372.30	350.43	0.573800E+06
12	372.29	348.60	0.622600E+06
13	372.29	346.33	0.658100E+06
14	372.30	345.21	0.702600E+06
15	372.29	343.86	0.738800E+06

CALCULATION RESULTS

CASE	DT K	ALF J/m2s	ALN J/m2s	ALF/ALN	PSI deg
1	15.990	26429.0	12911.7	2.047	100.872
2	18.700	26139.0	12344.2	2.118	100.666
3	20.520	26876.2	12012.6	2.237	100.528
4	22.760	26366.4	11647.1	2.264	100.359
5	24.810	25884.7	11345.3	2.282	100.204
6	26.760	25332.6	11082.9	2.286	100.060
7	27.740	26023.8	10958.1	2.375	99.986
8	13.520	28912.7	13534.5	2.136	101.060
9	17.450	26137.5	12593.5	2.075	100.761
10	20.110	25648.9	12084.3	2.123	100.559
11	21.870	26236.9	11787.7	2.226	100.427
12	23.690	26281.1	11506.8	2.284	100.289
13	25.960	25350.5	11188.1	2.266	100.120
14	27.090	25935.8	11040.8	2.349	100.037
15	28.430	25986.6	10873.6	2.390	99.936

QMC
WATER

----- TUBE DIMENSION -----

D	Pitch	h	t	θ	AR
12.700	0.000	1.585	0.000	0.000	1.000

V=1.1 M/S

----- DATA TABLE -----

	Ts/K	Tw/K	Qr/J/m2s
1	372.74	354.04	0.314000E+06
2	372.73	346.49	0.353100E+06
3	372.80	342.19	0.391800E+06
4	372.78	339.08	0.425700E+06
5	372.78	336.43	0.454000E+06
6	372.76	333.78	0.475300E+06
7	372.75	332.06	0.497400E+06
8	372.80	330.67	0.519900E+06
9	372.83	349.41	0.331500E+06
10	372.83	344.06	0.371600E+06
11	372.80	340.47	0.407800E+06
12	372.85	337.66	0.439100E+06
13	372.80	334.96	0.462400E+06
14	372.83	333.40	0.491500E+06
15	372.85	331.32	0.507600E+06
16	372.85	330.34	0.534600E+06
17	372.99	355.37	0.319700E+06
18	372.99	348.39	0.364200E+06
19	372.99	343.61	0.400400E+06
20	373.00	339.87	0.429600E+06
21	372.99	336.30	0.447800E+06
22	372.98	333.63	0.466400E+06
23	372.98	331.65	0.485900E+06
24	372.98	329.95	0.503100E+06
25	372.98	349.83	0.332200E+06
26	372.95	344.93	0.376000E+06
27	372.98	340.32	0.403000E+06
28	372.96	337.48	0.433400E+06
29	372.95	335.05	0.458700E+06
30	372.95	332.72	0.477300E+06
31	372.94	331.44	0.499200E+06
32	372.93	329.34	0.512700E+06

CALCULATION RESULTS

CASE	DT K	ALF J/m2s	ALN J/m2s	ALF/ALN	PSI deg
1	18.700	16791.4	12360.2	1.359	0.000
2	26.240	13456.6	11166.5	1.205	0.000
3	30.610	12799.7	10637.0	1.203	0.000
4	33.700	12632.0	10305.6	1.226	0.000
5	36.350	12489.7	10045.6	1.243	0.000
6	38.980	12193.4	9804.7	1.244	0.000
7	40.690	12224.1	9656.4	1.266	0.000
8	42.130	12340.4	9538.1	1.294	0.000
9	23.420	14154.6	11566.3	1.224	0.000
10	28.770	12916.2	10851.7	1.190	0.000
11	32.330	12613.7	10449.0	1.207	0.000
12	35.190	12478.0	10159.5	1.228	0.000
13	37.840	12219.9	9908.2	1.233	0.000
14	39.430	12465.1	9767.6	1.276	0.000
15	41.530	12222.5	9589.4	1.275	0.000
16	42.510	12575.9	9508.9	1.323	0.000
17	17.620	18144.2	12583.7	1.442	0.000
18	24.600	14804.9	11400.2	1.299	0.000
19	29.380	13628.3	10784.9	1.264	0.000
20	33.130	12967.1	10372.0	1.250	0.000
21	36.690	12205.0	10021.0	1.218	0.000
22	39.350	11852.6	9779.9	1.212	0.000
23	41.330	11756.6	9610.7	1.223	0.000
24	43.030	11691.8	9471.4	1.234	0.000
25	23.150	14349.9	11612.2	1.236	0.000
26	28.020	13419.0	10947.1	1.226	0.000
27	32.660	12339.3	10420.4	1.184	0.000
28	35.480	12215.3	10135.2	1.205	0.000
29	37.900	12102.9	9908.1	1.222	0.000
30	40.230	11864.3	9702.7	1.223	0.000
31	41.500	12028.9	9595.1	1.254	0.000
32	43.590	11761.9	9424.9	1.248	0.000

QMC
WATER

----- TUBE DIMENSION -----

D	Pitch	h	t	θ	AR
12.700	0.750	1.585	0.500	0.000	5.920

V=1.1 M/S

----- DATA TABLE -----

	Ts/K	Tw/K	Qr/J/m2s
1	373.33	352.42	0.991479E+06
2	373.35	352.80	0.964409E+06
3	373.37	354.12	0.952733E+06
4	373.41	354.90	0.929458E+06
5	373.43	355.13	0.895933E+06
6	373.48	356.24	0.875256E+06
7	373.46	356.81	0.844300E+06
8	373.48	357.74	0.817221E+06
9	373.46	358.14	0.780698E+06
10	373.43	358.89	0.747147E+06
11	373.46	359.93	0.715332E+06
12	373.48	360.83	0.679256E+06
13	373.50	361.97	0.643136E+06
14	373.50	362.49	0.598089E+06
15	373.46	363.98	0.558937E+06
16	373.48	365.47	0.516018E+06

CALCULATION RESULTS

CASE	DT / K	ALF / J/m2s	ALN / J/m2s	ALF/ALN	PSI / deg
1	20.906	47425.6	11983.8	3.957	0.000
2	20.551	46927.6	12045.3	3.896	0.000
3	19.247	49500.3	12279.7	4.031	0.000
4	18.512	50208.4	12420.9	4.042	0.000
5	18.306	48942.0	12461.9	3.927	0.000
6	17.236	50780.7	12681.2	4.004	0.000
7	16.649	50711.8	12806.5	3.960	0.000
8	15.738	51926.6	13013.5	3.990	0.000
9	15.320	50959.4	13111.9	3.887	0.000
10	14.548	51357.4	13302.8	3.861	0.000
11	13.521	52905.3	13577.8	3.896	0.000
12	12.650	53696.1	13830.9	3.882	0.000
13	11.526	55798.7	14189.2	3.932	0.000
14	11.006	54342.1	14368.7	3.782	0.000
15	9.478	58972.0	14959.1	3.942	0.000
16	8.010	64421.7	15647.3	4.117	0.000

QMC
WATER

----- TUBE DIMENSION -----

D·	Pitch	h	t	θ	AR
12.700	1.000	1.585	0.500	0.000	4.690

V=1.1 M/S

----- DATA TABLE -----

	Ts/K	Tw/K	Qr/J/m2s
1	372.85	363.00	0.469400E+06
2	372.85	358.93	0.532200E+06
3	372.87	356.76	0.597800E+06
4	372.87	353.87	0.644200E+06
5	372.85	352.21	0.696600E+06
6	372.89	350.20	0.736200E+06
7	372.87	348.10	0.767300E+06
8	372.88	363.70	0.421000E+06
9	372.90	359.79	0.493000E+06
10	372.90	356.84	0.555800E+06
11	372.89	355.33	0.621900E+06
12	372.91	352.80	0.667300E+06
13	372.89	350.27	0.702500E+06
14	372.91	348.76	0.745400E+06
15	372.91	347.80	0.790600E+06

CALCULATION RESULTS

CASE	DT / K	ALF / J/m2s	ALN / J/m2s	ALF/ALN	PSI / deg
1	9.850	47654.8	14781.2	3.224	0.000
2	13.920	38232.8	13445.9	2.843	0.000
3	16.110	37107.4	12905.4	2.875	0.000
4	19.000	33905.3	12307.9	2.755	0.000
5	20.640	33750.0	12012.1	2.810	0.000
6	22.690	32446.0	11679.4	2.778	0.000
7	24.770	30977.0	11371.9	2.724	0.000
8	9.180	45860.6	15064.9	3.044	0.000
9	13.110	37604.9	13673.5	2.750	0.000
10	16.060	34607.7	12917.9	2.679	0.000
11	17.560	35415.7	12592.4	2.812	0.000
12	20.110	33182.5	12106.7	2.741	0.000
13	22.620	31056.6	11690.3	2.657	0.000
14	24.150	30865.4	11461.8	2.693	0.000
15	25.110	31485.5	11325.9	2.780	0.000

QMC
WATER

----- TUBE DIMENSION -----

D	Pitch	h	t	θ	AR
12.700	1.500	1.585	0.500	0.000	3.460

V=1.1 M/S

----- DATA TABLE -----

	Ts/K	Tw/K	Qr/J/m2s
1	372.57	361.00	0.455200E+06
2	372.57	357.39	0.519600E+06
3	372.56	355.78	0.589200E+06
4	372.56	353.72	0.644900E+06
5	372.56	351.14	0.684600E+06
6	372.57	349.57	0.729800E+06
7	372.55	348.69	0.780100E+06
8	372.57	362.89	0.416400E+06
9	372.54	358.29	0.481900E+06
10	372.57	355.86	0.548100E+06
11	372.56	353.87	0.607600E+06
12	372.57	351.96	0.659200E+06
13	372.56	351.03	0.716700E+06
14	372.55	348.83	0.750000E+06
15	372.56	348.11	0.799900E+06

CALCULATION RESULTS

CASE	DT K	ALF J/m2s	ALN J/m2s	ALF/ALN	PSI deg
1	11.570	39343.1	14138.7	2.783	52.402
2	15.180	34229.2	13113.0	2.610	51.713
3	16.780	35113.2	12745.2	2.755	51.405
4	18.840	34230.4	12326.9	2.777	51.011
5	21.420	31960.8	11870.4	2.692	50.516
6	23.000	31730.4	11620.4	2.731	50.215
7	23.860	32694.9	11491.2	2.845	50.044
8	9.680	43016.5	14839.5	2.899	52.762
9	14.250	33817.5	13346.6	2.534	51.882
10	16.710	32800.7	12760.8	2.570	51.421
11	18.690	32509.4	12355.6	2.631	51.039
12	20.610	31984.5	12007.2	2.664	50.674
13	21.530	33288.4	11852.3	2.809	50.495
14	23.720	31618.9	11511.7	2.747	50.071
15	24.450	32715.7	11406.2	2.868	49.934

QMC
WATER

----- TUBE DIMENSION -----

D	Pitch	h	t	θ	AR
12.700	2.000	1.585	0.500	0.000	2.845

V=1.1 M/S

----- DATA TABLE -----

	Ts/K	Tw/K	Qr/J/m2s
1	372.68	364.23	0.482600E+06
2	372.70	358.34	0.532200E+06
3	372.70	356.77	0.604600E+06
4	372.68	354.30	0.657400E+06
5	372.69	352.44	0.708400E+06
6	372.69	351.65	0.767300E+06
7	372.70	350.09	0.809800E+06
8	372.73	365.10	0.433400E+06
9	372.72	359.46	0.494600E+06
10	372.72	357.27	0.566100E+06
11	372.70	355.56	0.631600E+06
12	372.72	353.27	0.681200E+06
13	372.72	353.09	0.752000E+06
14	372.73	351.45	0.797100E+06
15	372.73	349.80	0.835300E+06

CALCULATION RESULTS

CASE	DT / K	ALF / J/m2s	ALN / J/m2s	ALF/ALN	PSI / deg
1	8.450	57112.4	15394.1	3.710	86.122
2	14.360	37061.3	13323.9	2.782	85.529
3	15.930	37953.5	12940.3	2.933	85.371
4	18.380	35767.1	12420.1	2.880	85.123
5	20.250	34982.7	12074.1	2.897	84.939
6	21.040	36468.6	11938.4	3.055	84.860
7	22.610	35816.0	11685.0	3.065	84.706
8	7.630	56802.1	15819.4	3.591	86.213
9	13.260	37300.2	13623.7	2.738	85.642
10	15.450	36640.8	13053.5	2.807	85.422
11	17.140	36849.5	12673.1	2.908	85.250
12	19.450	35023.1	12218.8	2.866	85.023
13	19.630	38308.7	12185.9	3.144	85.005
14	21.280	37457.7	11899.7	3.148	84.842
15	22.930	36428.3	11636.8	3.130	84.679

QMC
WATER

----- TUBE DIMENSION -----

D	Pitch	h	t	θ	AR
12.700	2.500	1.585	0.500	0.000	2.476

V=1.1 M/S

----- DATA TABLE -----

	Ts/K	Tw/K	Qr/J/m2s
1	372.31	359.15	0.444900E+06
2	372.29	355.99	0.511800E+06
3	372.31	354.32	0.579500E+06
4	372.35	352.66	0.638600E+06
5	372.30	349.76	0.674100E+06
6	372.34	348.64	0.724800E+06
7	372.33	347.76	0.774200E+06
8	372.34	360.60	0.403700E+06
9	372.36	357.19	0.476500E+06
10	372.33	354.87	0.543400E+06
11	372.36	352.82	0.601800E+06
12	372.34	351.09	0.655300E+06
13	372.36	349.16	0.698700E+06
14	372.33	348.14	0.748400E+06
15	372.36	346.87	0.789700E+06

CALCULATION RESULTS

CASE	DT K	ALF J/m2s	ALN J/m2s	ALF/ALN	PSI deg
1	13.160	33807.0	13636.7	2.479	101.089
2	16.300	31398.8	12841.0	2.445	100.847
3	17.990	32212.3	12483.7	2.580	100.721
4	19.690	32432.7	12161.6	2.667	100.597
5	22.540	29906.8	11681.6	2.560	100.377
6	23.700	30582.3	11507.2	2.658	100.294
7	24.570	31510.0	11381.0	2.769	100.228
8	11.740	34386.7	14073.5	2.443	101.202
9	15.170	31410.7	13107.6	2.396	100.941
10	17.460	31122.6	12592.5	2.472	100.764
11	19.540	30798.4	12189.2	2.527	100.609
12	21.250	30837.6	11890.6	2.593	100.478
13	23.200	30116.4	11582.5	2.600	100.334
14	24.190	30938.4	11435.3	2.706	100.256
15	25.490	30980.8	11254.1	2.753	100.163

Steam data of Georgiadis [40]

AMERICA
WATER

----- TUBE DIMENSION -----

D	Pitch	h	t	θ	AR
18.000	0.000	0.000	0.000	0.000	1.000

SIA111

----- DATA TABLE -----

	Ts/K	Tw/K	Qr/J/m2s
1	373.03	320.11	0.559688E+06
2	372.94	319.98	0.556595E+06
3	373.18	321.47	0.542495E+06
4	373.38	321.46	0.542497E+06
5	373.07	323.09	0.522547E+06
6	373.14	323.10	0.522545E+06
7	373.01	326.80	0.493725E+06
8	372.86	326.80	0.493725E+06
9	372.93	330.04	0.464928E+06
10	372.97	330.13	0.466311E+06
11	372.91	334.47	0.434417E+06
12	372.88	334.47	0.434417E+06
13	372.77	338.43	0.407173E+06
14	372.85	338.51	0.407984E+06
15	373.24	324.47	0.518579E+06
16	373.11	324.36	0.516437E+06
17	373.23	320.23	0.558375E+06
18	373.15	320.23	0.558375E+06

CALCULATION RESULTS

CASE	DT / K	ALF / J/m2s	ALN / J/m2s	ALF/ALN	PSI / deg
1	52.924	10575.3	8019.1	1.319	0.000
2	52.957	10510.3	8014.1	1.311	0.000
3	51.709	10491.3	8099.3	1.295	0.000
4	51.917	10449.3	8092.8	1.291	0.000
5	49.980	10455.1	8205.4	1.274	0.000
6	50.043	10441.9	8203.6	1.273	0.000
7	46.215	10683.2	8454.4	1.264	0.000
8	46.065	10718.0	8459.9	1.267	0.000
9	42.893	10839.3	8689.0	1.247	0.000
10	42.838	10885.5	8694.4	1.252	0.000
11	38.445	11299.7	9034.4	1.251	0.000
12	38.415	11308.5	9035.9	1.252	0.000
13	34.344	11855.7	9385.2	1.263	0.000
14	34.340	11880.7	9388.2	1.265	0.000
15	48.767	10633.8	8289.9	1.283	0.000
16	48.749	10593.8	8286.9	1.278	0.000
17	53.003	10534.8	8020.8	1.313	0.000
18	52.923	10550.7	8023.1	1.315	0.000

AMERICA
WATER

----- TUBE DIMENSION -----

D	Pitch	h	t	θ	AR
18.000	2.500	1.000	1.250	0.000	1.900

F5T125A172

----- DATA TABLE -----

	Ts/K	Tw/K	Qr/J/m2s
1	373.33	344.98	0.114338E+07
2	373.62	345.22	0.114954E+07
3	373.50	347.04	0.109991E+07
4	373.42	346.93	0.109721E+07
5	373.23	348.82	0.103613E+07
6	373.24	348.93	0.103846E+07
7	372.88	351.93	0.917487E+06
8	372.62	351.83	0.915734E+06
9	373.04	355.14	0.829145E+06
10	373.15	355.23	0.830518E+06
11	373.32	358.83	0.732804E+06
12	373.35	358.91	0.733841E+06
13	372.86	361.39	0.648202E+06
14	372.78	361.32	0.647387E+06
15	373.56	350.35	0.101127E+07
16	373.54	350.35	0.101127E+07
17	373.11	345.50	0.115567E+07
18	372.84	345.38	0.115259E+07

CALCULATION RESULTS

CASE	DT / K	ALF / J/m2s	ALN / J/m2s	ALF/ALN	PSI / deg
1	28.352	40328.0	10008.0	4.030	87.256
2	28.401	40475.3	10011.8	4.043	87.292
3	26.461	41567.2	10232.4	4.062	87.456
4	26.495	41412.0	10225.7	4.050	87.442
5	24.408	42450.4	10481.1	4.050	87.610
6	24.311	42715.6	10494.2	4.070	87.621
7	20.955	43783.7	10960.9	3.995	87.886
8	20.790	44046.8	10978.0	4.012	87.864
9	17.901	46318.4	11482.2	4.034	88.197
10	17.924	46335.5	11481.6	4.036	88.211
11	14.486	50537.0	12202.8	4.146	88.562
12	14.438	50827.1	12215.1	4.161	88.571
13	11.471	56507.9	12998.9	4.347	88.785
14	11.458	56500.9	13000.1	4.346	88.774
15	23.208	43574.2	10653.4	4.090	87.770
16	23.188	43611.8	10655.5	4.093	87.769
17	27.613	41852.4	10084.6	4.150	87.294
18	27.464	41967.3	10093.0	4.158	87.270

AMERICA
WATER

----- TUBE DIMENSION -----

D	Pitch	h	t	θ	AR
18.000	2.500	1.000	1.500	0.000	1.911

F25T15A160

----- DATA TABLE -----

	Ts/K	Tw/K	Qr/J/m2s
1	373.00	343.21	0.110983E+07
2	373.36	343.47	0.111599E+07
3	373.04	345.14	0.106511E+07
4	372.77	345.03	0.106241E+07
5	373.00	347.16	0.100856E+07
6	373.10	347.27	0.101088E+07
7	372.96	350.70	0.903798E+06
8	372.96	350.70	0.903798E+06
9	372.96	353.86	0.817020E+06
10	372.91	353.95	0.818400E+06
11	373.42	357.84	0.723657E+06
12	373.55	357.84	0.723653E+06
13	372.94	360.33	0.639426E+06
14	372.60	360.11	0.636990E+06
15	373.16	348.79	0.985933E+06
16	373.12	348.58	0.981669E+06
17	373.24	344.30	0.113439E+07
18	373.04	344.18	0.113131E+07

CALCULATION RESULTS

CASE	DT K	ALF J/m2s	ALN J/m2s	ALF/ALN	PSI deg
1	29.786	37260.1	9841.4	3.786	71.714
2	29.891	37335.3	9841.8	3.794	71.767
3	27.897	38180.1	10049.9	3.799	71.952
4	27.742	38296.1	10058.8	3.807	71.922
5	25.837	39035.5	10292.2	3.793	72.197
6	25.830	39135.9	10296.3	3.801	72.217
7	22.265	40592.8	10767.4	3.770	72.629
8	22.265	40592.8	10767.4	3.770	72.629
9	19.096	42784.9	11266.6	3.797	73.020
10	18.958	43169.1	11288.8	3.824	73.028
11	15.582	46441.9	11958.6	3.884	73.541
12	15.707	46072.0	11936.0	3.860	73.549
13	12.614	50691.8	12667.4	4.002	73.820
14	12.491	50995.9	12689.7	4.019	73.772
15	24.374	40450.2	10483.3	3.859	72.406
16	24.543	39997.9	10459.9	3.824	72.378
17	28.939	39199.4	9940.3	3.943	71.962
18	28.860	39199.9	9942.5	3.943	71.835

AMERICA
WATER

----- TUBE DIMENSION -----

D	Pitch	h	t	θ	AR
18.000	5.000	2.000	1.000	0.000	1.933

F05E2A139

----- DATA TABLE -----

	Ts/K	Tw/K	Qr/J/m2s
1	373.09	344.16	0.112814E+07
2	372.88	344.04	0.112507E+07
3	372.79	345.66	0.107309E+07
4	372.84	347.50	0.101311E+07
5	372.90	347.71	0.101776E+07
6	372.98	351.10	0.907146E+06
7	372.94	351.21	0.908895E+06
8	373.25	354.46	0.825257E+06
9	373.16	354.29	0.822492E+06
10	373.27	357.89	0.723621E+06
11	373.16	357.82	0.722585E+06
12	373.08	360.76	0.643446E+06
13	373.05	360.76	0.643446E+06
14	372.51	348.60	0.981652E+06
15	372.39	348.39	0.977388E+06
16	372.82	344.20	0.113129E+07
17	372.84	344.33	0.113437E+07

CALCULATION RESULTS

CASE	DT K	ALF J/m2s	ALN J/m2s	ALF/ALN	PSI deg
1	28.926	39000.9	9936.8	3.925	134.578
2	28.843	39006.7	9939.2	3.925	134.569
3	27.128	39556.5	10130.4	3.905	134.628
4	25.338	39983.8	10349.1	3.864	134.697
5	25.195	40395.3	10369.1	3.896	134.706
6	21.877	41465.7	10824.8	3.831	134.835
7	21.735	41817.1	10844.5	3.856	134.838
8	18.789	43922.3	11329.5	3.877	134.967
9	18.869	43589.6	11312.5	3.853	134.959
10	15.376	47061.7	11998.5	3.922	135.099
11	15.345	47089.3	12001.6	3.924	135.094
12	12.323	52215.0	12753.9	4.094	135.205
13	12.293	52342.5	12761.4	4.102	135.205
14	23.909	41057.8	10523.8	3.901	134.732
15	23.998	40727.9	10507.9	3.876	134.722
16	28.621	39526.6	9961.7	3.968	134.574
17	28.514	39782.9	9974.2	3.989	134.579

AMERICA
WATER

----- TUBE DIMENSION -----

D	Pitch	h	t	θ	AR
18.000	3.000	2.000	1.000	0.000	2.556

F03E2A140

----- DATA TABLE -----

	Ts/K	Tw/K	Qr/J/m2s
1	373.44	348.62	0.123890E+07
2	372.97	348.49	0.123583E+07
3	372.55	349.72	0.116754E+07
4	372.59	349.71	0.116755E+07
5	373.40	352.00	0.111060E+07
6	373.48	352.00	0.111060E+07
7	373.09	354.93	0.977251E+06
8	373.03	354.93	0.977251E+06
9	373.07	357.69	0.876336E+06
10	373.03	357.69	0.876336E+06
11	373.40	361.26	0.768198E+06
12	373.51	361.41	0.770274E+06
13	373.21	363.88	0.679196E+06
14	373.13	363.81	0.678384E+06
15	373.07	352.83	0.106907E+07
16	373.10	352.93	0.107120E+07
17	373.49	348.99	0.125450E+07
18	373.56	349.11	0.125758E+07

CALCULATION RESULTS

CASE	DT / K	ALF / J/m2s	ALN / J/m2s	ALF/ALN	PSI / deg
1	24.820	49915.4	10434.4	4.784	114.082
2	24.482	50479.1	10463.0	4.825	114.060
3	22.830	51140.6	10673.3	4.791	114.120
4	22.876	51038.2	10668.1	4.784	114.121
5	21.397	51904.5	10910.3	4.757	114.278
6	21.477	51711.1	10900.8	4.744	114.281
7	18.160	53813.4	11436.4	4.705	114.442
8	18.100	53991.8	11445.3	4.717	114.440
9	15.380	56978.9	11990.8	4.752	114.605
10	15.340	57127.5	11998.3	4.761	114.604
11	12.138	63288.7	12818.2	4.937	114.828
12	12.096	63680.1	12834.2	4.962	114.841
13	9.330	72797.0	13759.1	5.291	114.980
14	9.322	72772.4	13759.4	5.289	114.974
15	20.243	52811.8	11079.6	4.767	114.317
16	20.175	53095.4	11091.5	4.787	114.324
17	24.496	51212.4	10478.0	4.888	114.105
18	24.446	51443.2	10486.8	4.905	114.114

AMERICA
WATER

----- TUBE DIMENSION -----

D	Pitch	h	t	θ	AR
18.000	2.500	2.000	1.000	0.000	2.867

F25E2A128

----- DATA TABLE -----

	Ts/K	Tw/K	Qr/J/m2s
1	373.13	348.75	0.125473E+07
2	373.02	348.64	0.125164E+07
3	373.16	350.26	0.118947E+07
4	373.41	350.39	0.119216E+07
5	373.10	352.19	0.112009E+07
6	373.18	352.19	0.112009E+07
7	372.88	355.19	0.988356E+06
8	372.74	355.09	0.986596E+06
9	372.99	357.96	0.883361E+06
10	373.04	358.14	0.886118E+06
11	373.30	361.52	0.773475E+06
12	373.18	361.44	0.772439E+06
13	372.72	363.87	0.680060E+06
14	372.58	363.66	0.677624E+06
15	373.40	353.71	0.108829E+07
16	373.56	353.81	0.109042E+07
17	372.73	349.22	0.126067E+07
18	372.68	349.22	0.126067E+07

CALCULATION RESULTS

CASE	DT / K	ALF / J/m2s	ALN / J/m2s	ALF/ALN	PSI / deg
1	24.380	51465.5	10481.6	4.910	102.163
2	24.384	51330.4	10477.5	4.899	102.150
3	22.900	51941.9	10683.4	4.862	102.273
4	23.025	51776.8	10674.0	4.851	102.292
5	20.915	53554.4	10974.4	4.880	102.412
6	20.995	53350.3	10964.6	4.866	102.415
7	17.692	55864.6	11515.7	4.851	102.624
8	17.647	55907.3	11519.5	4.853	102.612
9	15.028	58781.0	12066.5	4.871	102.833
10	14.899	59475.0	12097.5	4.916	102.848
11	11.783	65643.3	12919.4	5.081	103.109
12	11.742	65784.3	12927.5	5.089	103.098
13	8.850	76842.9	13937.1	5.514	103.263
14	8.925	75924.3	13900.5	5.462	103.242
15	19.690	55271.2	11180.8	4.943	102.534
16	19.753	55202.8	11175.7	4.940	102.547
17	23.508	53627.3	10585.2	5.066	102.182
18	23.458	53741.6	10590.4	5.075	102.181

AMERICA
WATER

----- TUBE DIMENSION -----

D	Pitch	h	t	θ	AR
18.000	2.000	2.000	1.000	0.000	3.333

F02E2A137

----- DATA TABLE -----

	Ts/K	Tw/K	Qr/J/m2s
1	373.05	347.11	0.120520E+07
2	372.99	347.12	0.120519E+07
3	373.04	348.74	0.114600E+07
4	373.13	348.87	0.114869E+07
5	372.99	350.56	0.107806E+07
6	372.99	350.66	0.108038E+07
7	373.25	354.08	0.959648E+06
8	373.32	354.08	0.959644E+06
9	372.93	356.79	0.859670E+06
10	373.00	356.80	0.859663E+06
11	373.32	360.25	0.752544E+06
12	373.25	360.17	0.751508E+06
13	372.90	362.85	0.665277E+06
14	373.01	362.92	0.666089E+06
15	373.18	352.15	0.104968E+07
16	373.24	352.05	0.104754E+07
17	373.01	347.72	0.121422E+07
18	372.90	347.84	0.121730E+07

CALCULATION RESULTS

CASE	DT K	ALF J/m2s	ALN J/m2s	ALF/ALN	PSI deg
1	25.939	46462.9	10281.2	4.519	79.217
2	25.873	46581.0	10287.4	4.528	79.215
3	24.298	47164.4	10489.4	4.496	79.393
4	24.263	47343.3	10497.0	4.510	79.412
5	22.434	48054.7	10744.0	4.473	79.587
6	22.327	48388.9	10759.4	4.497	79.599
7	19.172	50054.7	11263.2	4.444	79.985
8	19.236	49887.9	11254.6	4.433	79.989
9	16.145	53246.8	11822.5	4.504	80.262
10	16.205	53049.2	11812.5	4.491	80.268
11	13.073	57564.8	12556.1	4.585	80.665
12	13.081	57450.3	12551.6	4.577	80.653
13	10.049	66203.3	13475.9	4.913	80.930
14	10.087	66034.4	13466.1	4.904	80.944
15	21.035	49901.6	10958.4	4.554	79.770
16	21.187	49442.6	10937.0	4.521	79.763
17	25.288	48015.7	10360.9	4.634	79.281
18	25.064	48567.7	10385.7	4.676	79.288

AMERICA
WATER

----- TUBE DIMENSION -----

D	Pitch	h	t	θ	AR
18.000	2.500	1.000	0.500	0.000	1.867

F250IA108

----- DATA TABLE -----

	Ts/K	Tw/K	Qr/J/m2s
1	373.28	344.52	0.116549E+07
2	373.15	344.53	0.116548E+07
3	372.98	346.23	0.111184E+07
4	373.05	346.12	0.110913E+07
5	373.01	348.06	0.104713E+07
6	372.93	347.95	0.104480E+07
7	373.27	351.71	0.936002E+06
8	373.34	351.82	0.937758E+06
9	373.31	354.86	0.843724E+06
10	373.33	354.86	0.843724E+06
11	373.15	358.23	0.737538E+06
12	373.15	358.16	0.736498E+06
13	373.32	361.24	0.656842E+06
14	373.03	361.10	0.655214E+06
15	373.19	349.10	0.100894E+07
16	373.27	349.40	0.101537E+07
17	373.25	344.95	0.117152E+07
18	373.16	344.95	0.117151E+07

CALCULATION RESULTS

CASE	DT K	ALF J/m2s	ALN J/m2s	ALF/ALN	PSI deg
1	28.756	40530.3	9961.6	4.069	110.157
2	28.620	40722.6	9972.4	4.084	110.153
3	26.746	41570.3	10181.6	4.083	110.254
4	26.932	41182.6	10161.8	4.053	110.249
5	24.952	41965.8	10403.6	4.034	110.368
6	24.981	41823.8	10397.3	4.023	110.359
7	21.556	43421.9	10882.1	3.990	110.605
8	21.524	43568.0	10889.2	4.001	110.614
9	18.454	45720.4	11390.7	4.014	110.805
10	18.474	45670.9	11387.8	4.011	110.805
11	14.916	49446.1	12097.4	4.087	111.014
12	14.991	49129.3	12080.3	4.067	111.010
13	12.085	54351.8	12830.8	4.236	111.212
14	11.935	54898.5	12864.6	4.267	111.194
15	24.091	41880.4	10521.7	3.980	110.439
16	23.868	42541.1	10554.0	4.031	110.460
17	28.303	41392.1	10010.9	4.135	110.182
18	28.207	41532.6	10018.7	4.145	110.180

AMERICA
WATER

----- TUBE DIMENSION -----

D	Pitch	h	t	θ	AR
18.000	2.000	1.000	0.500	0.000	2.083

F202IA107

----- DATA TABLE -----

	Ts/K	Tw/K	Qr/J/m2s
1	373.46	345.85	0.120267E+07
2	373.60	345.97	0.120576E+07
3	372.99	347.24	0.113905E+07
4	372.75	347.24	0.113905E+07
5	372.95	349.32	0.107754E+07
6	373.01	349.32	0.107754E+07
7	373.22	352.71	0.957259E+06
8	373.29	352.81	0.959020E+06
9	372.99	355.65	0.859046E+06
10	373.11	355.65	0.859043E+06
11	373.16	359.28	0.757271E+06
12	373.16	359.20	0.756223E+06
13	373.22	362.14	0.669143E+06
14	373.21	362.14	0.669140E+06
15	372.85	350.51	0.104339E+07
16	372.98	350.61	0.104553E+07
17	373.21	346.37	0.121500E+07
18	373.22	346.37	0.121500E+07

CALCULATION RESULTS

CASE	DT / K	ALF / J/m2s	ALN / J/m2s	ALF/ALN	PSI / deg
1	27.614	43552.9	10095.7	4.314	97.356
2	27.632	43636.4	10098.1	4.321	97.371
3	25.752	44231.5	10302.3	4.293	97.447
4	25.512	44647.6	10324.3	4.324	97.437
5	23.634	45592.8	10575.2	4.311	97.609
6	23.694	45477.3	10569.0	4.303	97.611
7	20.512	46668.2	11041.5	4.227	97.888
8	20.485	46815.7	11048.1	4.237	97.898
9	17.341	49538.4	11585.9	4.276	98.113
10	17.456	49211.9	11568.0	4.254	98.118
11	13.885	54538.8	12342.5	4.419	98.410
12	13.960	54170.7	12323.9	4.396	98.404
13	11.080	60392.0	13135.2	4.598	98.644
14	11.066	60468.1	13139.4	4.602	98.644
15	22.341	46702.9	10752.8	4.343	97.699
16	22.366	46746.4	10753.5	4.347	97.712
17	26.842	45264.9	10177.6	4.447	97.387
18	26.852	45248.0	10176.8	4.446	97.387

AMERICA
WATER

----- TUBE DIMENSION -----

D	Pitch	h	t	θ	AR
18.000	1.500	1.000	0.500	0.000	2.444

F150IA109

----- DATA TABLE -----

	Ts/K	Tw/K	Qr/J/m2s
1	373.42	343.81	0.115013E+07
2	373.50	343.93	0.115321E+07
3	373.31	345.55	0.109837E+07
4	373.21	345.55	0.109837E+07
5	373.29	347.63	0.104022E+07
6	373.36	347.64	0.104021E+07
7	373.07	350.93	0.923754E+06
8	373.05	350.93	0.923754E+06
9	373.12	354.03	0.832751E+06
10	373.20	354.13	0.834129E+06
11	373.01	357.61	0.734241E+06
12	373.03	357.68	0.735285E+06
13	373.26	360.99	0.655280E+06
14	373.33	360.98	0.655283E+06
15	373.00	348.82	0.100694E+07
16	372.80	348.72	0.100479E+07
17	373.14	344.39	0.116241E+07
18	373.26	344.51	0.116550E+07

CALCULATION RESULTS

CASE	DT / K	ALF / J/m2s	ALN / J/m2s	ALF/ALN	PSI / deg
1	29.614	38837.4	9873.2	3.934	71.812
2	29.566	39004.6	9880.9	3.947	71.833
3	27.759	39568.1	10074.3	3.928	72.019
4	27.659	39711.1	10082.5	3.939	72.013
5	25.660	40538.6	10323.4	3.927	72.272
6	25.725	40435.8	10317.6	3.919	72.277
7	22.144	41715.8	10788.6	3.867	72.664
8	22.124	41753.5	10790.8	3.869	72.663
9	19.086	43631.5	11273.7	3.870	73.051
10	19.072	43735.8	11278.7	3.878	73.067
11	15.405	47662.5	11983.3	3.977	73.486
12	15.346	47913.8	11996.9	3.994	73.497
13	12.275	53383.3	12773.9	4.179	73.922
14	12.350	53059.4	12755.0	4.160	73.926
15	24.185	41634.9	10503.0	3.964	72.400
16	24.084	41720.2	10509.9	3.970	72.376
17	28.750	40431.7	9957.8	4.060	71.867
18	28.748	40542.0	9961.8	4.070	71.889

AMERICA
WATER

----- TUBE DIMENSION -----

D	Pitch	h	t	θ	AR
18.000	1.000	1.000	0.500	0.000	3.167

F100IA112

----- DATA TABLE -----

	Ts/K	Tw/K	Qr/J/m2s
1	373.32	342.73	0.111275E+07
2	373.43	342.86	0.111584E+07
3	373.41	344.35	0.106012E+07
4	373.31	344.47	0.106283E+07
5	372.99	346.18	0.100031E+07
6	372.84	346.08	0.997981E+06
7	372.80	349.65	0.893556E+06
8	372.83	349.65	0.893556E+06
9	373.11	352.99	0.810397E+06
10	373.08	352.92	0.809008E+06
11	373.19	356.57	0.712493E+06
12	373.27	356.65	0.713530E+06
13	373-.04	359.58	0.6355583E+06
14	373.08	359.65	0.636395E+06
15	372.97	347.56	0.972387E+06
16	372.91	347.55	0.972391E+06
17	373.36	343.11	0.111626E+07
18	373.39	343.23	0.111934E+07

CALCULATION RESULTS

CASE	DT / K	ALF / J/m2s	ALN / J/m2s	ALF/ALN	PSI / deg
1	30.588	36378.6	9767.8	3.724	0.000
2	30.569	36502.3	9773.3	3.735	0.000
3	29.065	36474.1	9932.0	3.672	0.000
4	28.843	36848.8	9953.0	3.702	0.000
5	26.812	37308.3	10174.1	3.667	0.000
6	26.765	37286.8	10174.8	3.665	0.000
7	23.151	38596.9	10636.6	3.629	0.000
8	23.181	38546.9	10633.4	3.625	0.000
9	20.116	40286.2	11101.4	3.629	0.000
10	20.164	40121.4	11092.6	3.617	0.000
11	16.618	42874.8	11734.6	3.654	0.000
12	16.618	42937.2	11737.2	3.658	0.000
13	13.460	47220.1	12445.4	3.794	0.000
14	13.427	47396.7	12455.3	3.805	0.000
15	25.415	38260.4	10343.6	3.699	0.000
16	25.361	38342.0	10348.5	3.705	0.000
17	30.249	36902.4	9804.3	3.764	0.000
18	30.163	37109.7	9814.2	3.781	0.000

AMERICA
WATER

----- TUBE DIMENSION -----

D	Pitch	h	t	θ	AR
18.000	2.750	1.000	0.750	0.000	1.798

F275IA98

----- DATA TABLE -----

	Ts/K	Tw/K	Qr/J/m2s
1	373.04	345.81	0.119313E+07
2	372.79	345.68	0.119005E+07
3	372.97	347.42	0.113610E+07
4	373.04	347.42	0.113610E+07
5	373.30	349.57	0.107733E+07
6	373.21	349.46	0.107500E+07
7	373.19	352.85	0.955317E+06
8	373.07	352.84	0.955321E+06
9	373.15	355.87	0.858885E+06
10	373.21	355.87	0.858885E+06
11	373.08	359.04	0.747904E+06
12	373.10	359.04	0.747900E+06
13	373.19	362.18	0.667402E+06
14	373.08	362.04	0.665774E+06
15	373.01	350.52	0.103893E+07
16	373.02	350.63	0.104107E+07
17	373.07	346.12	0.120244E+07
18	373.02	346.12	0.120244E+07

CALCULATION RESULTS

CASE	DT / K	ALF / J/m2s	ALN / J/m2s	ALF/ALN	PSI / deg
1	27.230	43816.7	10126.6	4.327	110.229
2	27.107	43901.9	10132.9	4.333	110.213
3	25.549	44467.5	10326.9	4.306	110.327
4	25.619	44346.0	10320.4	4.297	110.329
5	23.728	45403.3	10573.9	4.294	110.472
6	23.746	45270.8	10568.5	4.284	110.462
7	20.342	46962.8	11067.6	4.243	110.674
8	20.227	47230.0	11082.2	4.262	110.670
9	17.278	49709.7	11603.4	4.284	110.864
10	17.338	49537.7	11593.9	4.273	110.866
11	14.043	53258.1	12300.9	4.330	111.064
12	14.058	53201.0	12297.9	4.326	111.064
13	11.008	60628.8	13157.4	4.608	111.269
14	11.038	60316.5	13143.8	4.589	111.256
15	22.486	46203.4	10737.2	4.303	110.522
16	22.391	46495.0	10751.2	4.325	110.529
17	26.949	44619.1	10160.5	4.391	110.249
18	26.899	44702.0	10164.7	4.398	110.248

AMERICA
WATER

----- TUBE DIMENSION -----

D	Pitch	h	t	θ	AR
18.000	2.250	1.000	0.750	0.000	1.975

F225IA103

----- DATA TABLE -----

	Ts/K	Tw/K	Qr/J/m2s
1	373.34	346.56	0.121483E+07
2	373.37	346.69	0.121792E+07
3	372.95	347.94	0.114969E+07
4	372.95	347.94	0.114969E+07
5	372.99	349.88	0.108433E+07
6	373.00	349.99	0.108666E+07
7	372.82	353.05	0.958830E+06
8	372.78	353.06	0.958826E+06
9	373.05	356.17	0.863007E+06
10	373.08	356.17	0.863007E+06
11	373.41	359.72	0.756165E+06
12	373.32	359.65	0.755124E+06
13	372.90	362.26	0.667352E+06
14	373.01	362.40	0.668982E+06
15	373.34	351.34	0.105384E+07
16	373.23	351.23	0.105170E+07
17	373.18	346.82	0.121780E+07
18	373.08	346.94	0.122089E+07

CALCULATION RESULTS

CASE	DT / K	ALF / J/m2s	ALN / J/m2s	ALF/ALN	PSI / deg
1	26.780	45363.3	10189.2	4.452	97.407
2	26.683	45644.0	10201.7	4.474	97.418
3	25.011	45967.4	10394.1	4.422	97.500
4	25.006	45976.6	10394.7	4.423	97.501
5	23.111	46918.4	10648.3	4.406	97.655
6	23.013	47219.4	10662.3	4.429	97.663
7	19.768	48504.1	11148.8	4.351	97.899
8	19.722	48617.1	11155.1	4.358	97.898
9	16.883	51116.9	11677.0	4.378	98.156
10	16.913	51026.3	11672.1	4.372	98.158
11	13.687	55246.9	12400.5	4.455	98.456
12	13.671	55235.5	12401.4	4.454	98.447
13	10.637	62738.7	13270.1	4.728	98.641
14	10.612	63040.1	13282.5	4.746	98.656
15	22.004	47893.1	10817.9	4.427	97.784
16	21.998	47808.9	10815.2	4.421	97.771
17	26.358	46202.3	10234.5	4.514	97.421
18	26.137	46711.2	10258.0	4.554	97.427

AMERICA
WATER

----- TUBE DIMENSION -----

D	Pitch	h	t	θ	AR
18.000	1.750	1.000	0.750	0.000	2.254

F175IA104

----- DATA TABLE -----

	Ts/K	Tw/K	Qr/J/m2s
1	373.40	345.28	0.118081E+07
2	373.25	345.17	0.117771E+07
3	373.19	346.75	0.111983E+07
4	373.14	346.75	0.111982E+07
5	373.32	348.87	0.106098E+07
6	373.18	348.77	0.105865E+07
7	373.01	352.18	0.941156E+06
8	372.88	352.09	0.939392E+06
9	373.05	355.20	0.846371E+06
10	373.16	355.30	0.847745E+06
11	373.26	358.78	0.742625E+06
12	373.22	358.78	0.742625E+06
13	373.06	361.60	0.659190E+06
14	373.04	365.13	0.823124E+06
15	373.13	350.28	0.103023E+07
16	373.16	350.08	0.102595E+07
17	373.24	345.70	0.118684E+07
18	373.25	345.70	0.118684E+07

CALCULATION RESULTS

CASE	DT / K	ALF / J/m2s	ALN / J/m2s	ALF/ALN	PSI / deg
1	28.118	41994.8	10036.5	4.184	71.992
2	28.077	41945.7	10036.3	4.179	71.969
3	26.442	42350.4	10224.7	4.142	72.158
4	26.386	42439.9	10229.8	4.149	72.156
5	24.449	43395.6	10478.7	4.141	72.427
6	24.411	43367.7	10479.1	4.138	72.406
7	20.834	45174.0	10984.0	4.113	72.814
8	20.795	45173.9	10985.8	4.112	72.795
9	17.853	47407.8	11491.4	4.125	73.190
10	17.865	47452.8	11492.9	4.129	73.209
11	14.477	51296.9	12202.9	4.204	73.648
12	14.437	51439.0	12210.9	4.213	73.646
13	11.459	57526.0	13009.7	4.422	73.987
14	7.915	103995.5	14369.9	7.237	74.426
15	22.847	45092.6	10689.9	4.218	72.589
16	23.080	44451.9	10658.2	4.171	72.566
17	27.536	43101.4	10097.6	4.268	72.033
18	27.546	43085.7	10096.8	4.267	72.034

AMERICA
WATER

----- TUBE DIMENSION -----

D	Pitch	h	t	θ	AR
18.000	1.250	1.000	0.750	0.000	2.756

F125IA101

----- DATA TABLE -----

	Ts/K	Tw/K	Qr/J/m2s
1	373.02	343.06	0.111629E+07
2	373.32	343.22	0.112193E+07
3	373.32	344.74	0.106821E+07
4	373.29	344.95	0.107365E+07
5	373.03	346.72	0.101196E+07
6	372.98	346.62	0.100963E+07
7	373.26	350.40	0.907660E+06
8	373.35	350.49	0.909424E+06
9	373.31	353.47	0.818719E+06
10	373.44	353.47	0.818719E+06
11	373.04	356.96	0.718769E+06
12	372.97	356.80	0.716694E+06
13	372.76	359.64	0.637255E+06
14	372.80	359.79	0.638880E+06
15	372.95	348.18	0.987449E+06
16	373.03	348.28	0.989589E+06
17	373.17	343.86	0.114053E+07
18	373.30	343.75	0.113743E+07

CALCULATION RESULTS

CASE	DT / K	ALF / J/m2s	ALN / J/m2s	ALF/ALN	PSI / deg
1	29.958	37261.8	9823.8	3.793	0.000
2	30.105	37267.2	9818.0	3.796	0.000
3	28.580	37376.1	9982.3	3.744	0.000
4	28.337	37888.6	10008.4	3.786	0.000
5	26.308	38465.9	10235.7	3.758	0.000
6	26.361	38300.1	10227.6	3.745	0.000
7	22.860	39705.2	10692.3	3.713	0.000
8	22.859	39784.1	10695.3	3.720	0.000
9	19.838	41270.2	11153.4	3.700	0.000
10	19.968	41001.6	11136.4	3.682	0.000
11	16.077	44707.9	11840.4	3.776	0.000
12	16.166	44333.4	11819.5	3.751	0.000
13	13.119	48575.0	12524.5	3.878	0.000
14	13.013	49095.5	12554.1	3.911	0.000
15	24.775	39856.7	10424.4	3.823	0.000
16	24.750	39983.4	10430.2	3.833	0.000
17	29.308	38915.3	9898.0	3.932	0.000
18	29.554	38486.5	9875.7	3.897	0.000

AMERICA
WATER

----- TUBE DIMENSION -----

D	Pitch	h	t	θ	AR
18.000	2.500	1.000	1.000	0.000	1.889

F25IA118

----- DATA TABLE -----

	Ts/K	Tw/K	Qr/J/m2s
1	373.07	346.53	0.120251E+07
2	373.05	346.53	0.120251E+07
3	373.01	348.16	0.114670E+07
4	373.09	348.15	0.114671E+07
5	373.35	350.27	0.108643E+07
6	373.45	350.26	0.108644E+07
7	373.20	353.55	0.963947E+06
8	373.30	353.55	0.963951E+06
9	373.09	356.42	0.864266E+06
10	373.24	356.51	0.865647E+06
11	373.24	359.79	0.755029E+06
12	373.11	359.70	0.753999E+06
13	372.94	362.37	0.667284E+06
14	372.84	362.36	0.667290E+06
15	373.18	351.45	0.105375E+07
16	373.06	351.34	0.105161E+07
17	372.97	346.82	0.121461E+07
18	372.15	346.81	0.121462E+07

CALCULATION RESULTS

CASE	DT / K	ALF / J/m2s	ALN / J/m2s	ALF/ALN	PSI / deg
1	26.537	45314.5	10209.4	4.439	97.394
2	26.523	45338.4	10210.4	4.440	97.393
3	24.853	46139.3	10416.3	4.430	97.520
4	24.944	45971.4	10407.2	4.417	97.522
5	23.079	47074.4	10664.5	4.414	97.700
6	23.190	46849.5	10652.4	4.398	97.703
7	19.646	49065.8	11181.6	4.388	97.954
8	19.751	48805.2	11167.4	4.370	97.958
9	16.668	51851.8	11721.2	4.424	98.178
10	16.730	51742.2	11713.8	4.417	98.191
11	13.450	56136.0	12454.9	4.507	98.455
12	13.408	56235.0	12461.2	4.513	98.442
13	10.568	63141.9	13295.0	4.749	98.651
14	10.477	63690.9	13322.6	4.781	98.646
15	21.729	48495.1	10853.3	4.468	97.786
16	21.719	48418.9	10850.8	4.462	97.773
17	26.152	46444.2	10252.6	4.530	97.413
18	25.338	47936.7	10326.6	4.642	97.380

AMERICA
WATER

----- TUBE DIMENSION -----

D	Pitch	h	t	θ	AR
18.000	2.000	1.000	1.000	0.000	2.111

F02IA131

----- DATA TABLE -----

	Ts/K	Tw/K	Qr/J/m2s
1	373.35	345.09	0.116235E+07
2	373.43	345.23	0.116542E+07
3	373.21	346.79	0.110848E+07
4	373.21	346.58	0.110306E+07
5	373.17	348.72	0.104583E+07
6	373.20	348.72	0.104583E+07
7	373.40	352.39	0.937335E+06
8	373.41	352.40	0.937331E+06
9	372.79	354.90	0.835044E+06
10	372.70	354.90	0.835044E+06
11	373.17	358.57	0.734058E+06
12	372.87	358.42	0.731979E+06
13	373.02	361.46	0.652434E+06
14	373.18	361.60	0.654058E+06
15	373.40	350.35	0.101790E+07
16	373.36	350.35	0.101790E+07
17	373.08	345.91	0.117440E+07
18	372.99	346.02	0.117748E+07

CALCULATION RESULTS

CASE	DT K	ALF J/m2s	ALN J/m2s	ALF/ALN	PSI deg
1	28.258	41133.5	10019.1	4.105	71.965
2	28.205	41319.6	10027.7	4.121	71.986
3	26.417	41960.9	10228.3	4.102	72.165
4	26.635	41413.9	10202.2	4.059	72.138
5	24.446	42781.2	10474.2	4.084	72.399
6	24.476	42728.8	10471.3	4.081	72.401
7	21.011	44611.6	10969.3	4.067	72.865
8	21.015	44603.0	10969.0	4.066	72.866
9	17.895	46663.5	11475.0	4.067	73.137
10	17.805	46899.4	11488.6	4.082	73.131
11	14.599	50281.4	12171.2	4.131	73.616
12	14.447	50666.5	12196.6	4.154	73.579
13	11.564	56419.4	12975.9	4.348	73.966
14	11.580	56481.7	12976.7	4.353	73.994
15	23.046	44168.2	10670.7	4.139	72.614
16	23.006	44245.0	10675.0	4.145	72.612
17	27.172	43221.0	10134.6	4.265	72.049
18	26.968	43662.1	10155.6	4.299	72.057

AMERICA
WATER

----- TUBE DIMENSION -----

D	Pitch	h	t	θ	AR
18.000	1.500	1.000	1.000	0.000	2.481

F15IA113

----- DATA TABLE -----

	Ts/K	Tw/K	Qr/J/m2s
1	372.94	341.59	0.108498E+07
2	373.08	341.72	0.108807E+07
3	373.49	343.71	0.104662E+07
4	373.38	343.59	0.104391E+07
5	373.33	345.79	0.993367E+06
6	373.41	345.90	0.995697E+06
7	373.24	349.21	0.886548E+06
8	373.15	349.31	0.888305E+06
9	373.10	355.07	0.843576E+06
10	373.09	352.32	0.800762E+06
11	373.01	355.94	0.705276E+06
12	372.88	355.86	0.704239E+06
13	372.91	359.09	0.630736E+06
14	372.93	359.17	0.631548E+06
15	372.99	347.53	0.972408E+06
16	373.01	347.53	0.972408E+06
17	372.89	342.63	0.109749E+07
18	373.01	342.63	0.109749E+07

CALCULATION RESULTS

CASE	DT / K	ALF / J/m2s	ALN / J/m2s	ALF/ALN	PSI / deg
1	31.347	34611.9	9678.3	3.576	0.000
2	31.358	34698.3	9681.7	3.584	0.000
3	29.784	35140.3	9857.3	3.565	0.000
4	29.790	35042.3	9853.2	3.556	0.000
5	27.537	36073.9	10100.4	3.572	0.000
6	27.508	36196.6	10106.3	3.582	0.000
7	24.030	36893.4	10531.4	3.503	0.000
8	23.837	37265.8	10554.3	3.531	0.000
9	18.033	46779.6	11459.9	4.082	0.000
10	20.770	38553.8	10996.6	3.506	0.000
11	17.067	41324.0	11639.6	3.550	0.000
12	17.017	41384.4	11645.0	3.554	0.000
13	13.816	45652.6	12351.0	3.696	0.000
14	13.764	45884.0	12364.6	3.711	0.000
15	25.464	38187.6	10338.1	3.694	0.000
16	25.484	38157.6	10336.3	3.692	0.000
17	30.259	36269.9	9788.1	3.706	0.000
18	30.379	36126.6	9779.5	3.694	0.000

Data of Honda [52] for R-113 and methanol

HONDA
R113

----- TUBE DIMENSION -----

D	Pitch	h	t	θ	AR
17.090	0.500	1.130	0.110	0.000	5.480

----- DATA TABLE -----

	Ts/K	Tw/K	$Qr/J/m^2s$
1	327.68	318.36	0.137200E+06
2	325.01	317.22	0.119500E+06
3	326.28	321.76	0.745000E+05
4	322.09	318.25	0.635000E+05
5	321.23	319.33	0.364000E+05
6	323.74	321.46	0.415000E+05
7	327.45	324.30	0.551000E+05
8	334.96	320.03	0.201200E+06
9	328.35	316.30	0.167100E+06
10	343.25	324.63	0.244100E+06
11	324.76	319.70	0.803000E+05

CALCULATION RESULTS

CASE	DT/K	ALF/J/m^2s	ALN/J/m^2s	ALF/ALN	PSI/deg
1	9.320	14721.0	1407.8	10.457	114.399
2	7.790	15340.2	1474.7	10.402	114.087
3	4.520	16482.3	1687.8	9.765	114.741
4	3.840	16536.5	1762.7	9.381	114.034
5	1.900	19157.9	2102.6	9.111	114.115
6	2.280	18201.8	2005.8	9.075	114.542
7	3.150	17492.1	1845.4	9.478	115.142
8	14.930	13476.2	1245.7	10.818	115.076
9	12.050	13867.2	1319.9	10.506	114.182
10	18.620	13109.6	1171.6	11.189	116.217
11	5.060	15869.6	1642.6	9.661	114.384

HONDA
R113

----- TUBE DIMENSION -----

D	Pitch	h	t	θ	AR
17.050	0.640	0.920	0.290	5.300	3.680

----- DATA TABLE -----

	Ts/K	Tw/K	Q /J/m²s
1	325.46	318.98	0.872000E+05
2	327.90	320.34	0.100900E+06
3	331.49	321.64	0.126900E+06
4	330.22	317.12	0.156700E+06
5	327.11	316.61	0.129600E+06
6	324.09	315.96	0.104100E+06
7	324.56	318.45	0.834000E+05
8	331.66	314.75	0.189600E+06
9	328.48	324.93	0.536000E+05
10	326.11	323.75	0.382000E+05
11	326.43	321.46	0.690000E+05

LCULATION RESULTS

CASE	DT / K	ALF / J/m²s	ALN / J/m²s	ALF/ALN	PSI / deg
1	6.480	13456.8	1544.5	8.713	109.380
2	7.560	13346.6	1483.9	8.995	109.739
3	9.850	12883.2	1385.7	9.297	110.173
4	13.100	11961.8	1291.9	9.259	109.452
5	10.500	12342.9	1367.9	9.023	109.167
6	8.130	12804.4	1460.7	8.766	108.870
7	6.110	13649.8	1568.2	8.704	109.244
8	16.910	11212.3	1211.2	9.257	109.224
9	3.550	15098.6	1790.9	8.431	110.425
10	2.360	16186.4	1986.5	8.148	110.091
11	4.970	13883.3	1649.1	8.419	109.792

HONDA
R113

----- TUBE DIMENSION -----

D	Pitch	h	t	θ	AR
15.770	0.980	1.460	0.510	4.500	3.840

----- DATA TABLE -----

	Ts/K	Tw/K	Qr/J/m²s
1	322.30	310.17	0.120100E+06
2	324.37	313.50	0.109600E+06
3	326.71	317.60	0.940000E+05
4	329.37	320.90	0.877000E+05
5	324.84	318.42	0.690000E+05
6	321.70	314.53	0.754000E+05
7	324.77	319.56	0.597000E+05
8	325.22	323.83	0.207000E+05
9	327.10	324.38	0.354000E+05
10	324.36	320.31	0.479000E+05
11	328.78	314.57	0.128900E+06

CALCULATION RESULTS

CASE	DT / K	ALF / J/m²s	ALN / J/m²s	ALF/ALN	PSI / deg
1	12.130	9901.1	1348.9	7.340	118.611
2	10.870	10082.8	1385.0	7.280	119.093
3	9.110	10318.3	1445.5	7.138	119.683
4	8.470	10354.2	1469.3	7.047	120.211
5	6.420	10747.7	1579.2	6.806	119.670
6	7.170	10516.0	1539.0	6.833	119.059
7	5.210	11458.7	1663.8	6.887	119.795
8	1.390	14892.1	2313.5	6.437	120.309
9	2.720	13014.7	1953.7	6.662	120.482
10	4.050	11827.2	1772.2	6.674	119.857
11	14.210	9071.1	1292.1	7.020	119.458

HONDA
METHANOL

----- TUBE DIMENSION -----

D	Pitch	h	t	θ	AR
17.090	0.500	1.130	0.110	0.000	5.480

----- DATA TABLE -----

	Ts/K	Tw/K	Qr/J/m²s
1	344.46	330.91	0.328900E+06
2	344.45	333.25	0.272600E+06
3	344.44	335.41	0.229400E+06
4	344.46	337.41	0.189700E+06
5	344.62	339.29	0.148300E+06
6	344.44	340.26	0.119100E+06
7	344.46	341.40	0.917000E+05
8	344.51	342.49	0.652000E+05

CALCULATION RESULTS

CASE	DT / K	ALF / J/m²s	ALN / J/m²s	ALF/ALN	PSI / deg
1	13.550	24273.1	3525.4	6.885	68.560
2	11.200	24339.3	3705.0	6.569	68.979
3	9.030	25404.2	3917.2	6.485	69.367
4	7.050	26907.8	4174.4	6.446	69.729
5	5.330	27823.6	4483.8	6.205	70.083
6	4.180	28492.8	4768.6	5.975	70.242
7	3.060	29967.3	5160.2	5.807	70.450
8	2.020	32277.2	5730.0	5.633	70.652

HONDA
METHANOL

----- TUBE DIMENSION -----

D	Pitch	h	t	θ	AR
17.050	0.640	0.920	0.290	5.300	3.680

----- DATA TABLE -----

	Ts/K	Tw/K	Qr/J/m²s
1	344.53	320.02	0.308700E+06
2	344.36	334.37	0.218700E+06
3	344.35	338.24	0.147400E+06
4	344.35	341.21	0.869000E+05
5	344.26	342.89	0.431000E+05
6	344.91	332.45	0.271700E+06
7	344.32	335.86	0.196300E+06
8	344.61	339.23	0.161000E+06
9	344.31	339.23	0.128000E+06
10	344.63	341.00	0.101000E+06
11	344.44	342.25	0.669000E+05

CALCULATION RESULTS

CASE	DT / K	ALF / J/m²s	ALN / J/m²s	ALF/ALN	PSI / deg
1	24.510	12594.9	3011.6	4.182	54.013
2	9.990	21891.9	3818.4	5.733	57.273
3	6.110	24124.4	4332.1	5.569	58.149
4	3.140	27675.2	5129.3	5.396	58.822
5	1.370	31459.9	6320.0	4.978	59.193
6	12.460	21805.8	3607.0	6.045	56.899
7	8.460	23203.3	3985.5	5.822	57.606
8	5.380	29925.7	4475.7	6.686	58.403
9	5.080	25196.9	4540.5	5.549	58.369
10	3.630	27823.7	4945.7	5.626	58.806
11	2.190	30547.9	5617.6	5.438	59.068

HONDA
METHANOL

----- TUBE DIMENSION -----

D	Pitch	h	t	θ	AR
15.770	0.980	1.460	0.510	4.500	3.840

----- DATA TABLE -----

	Ts/K	Tw/K	Qr/ J/m²s
1	344.30	333.43	0.222500E+06
2	344.20	333.31	0.226000E+06
3	344.30	335.17	0.189600E+06
4	344.11	336.63	0.161100E+06
5	344.21	338.31	0.130100E+06
6	344.19	339.98	0.980000E+05
7	344.25	341.50	0.653000E+05
8	344.18	342.37	0.452000E+05
9	344.28	342.41	0.469000E+05

CALCULATION RESULTS

CASE	DT / K	ALF / J/m².s	ALN / J/m².s	ALF/ALN	PSI / deg
1	10.870	20469.2	3809.2	5.374	80.596
2	10.890	20753.0	3807.1	5.451	80.572
3	9.130	20766.7	3985.0	5.211	80.850
4	7.480	21537.4	4193.9	5.135	81.050
5	5.900	22050.8	4456.6	4.948	81.303
6	4.210	23277.9	4855.7	4.794	81.547
7	2.750	23745.5	5408.0	4.391	81.776
8	1.810	24972.4	6008.5	4.156	81.899
9	1.870	25080.2	5959.9	4.208	81.912

APPENDIX C Error analysis

APPENDIX C Error analysis

As indicated in [42], the probable uncertainty in a computated quatity is given by:

$$\Delta W=[(\frac{\partial W}{\partial X_1}\Delta W_1)^2+(\frac{\partial W}{\partial X_2}\Delta W_2)^2+\cdots+(\frac{\partial W}{\partial X_n}\Delta W_n)^2]^{\frac{1}{2}} \quad \text{(C-1)}$$

where W is the calculated result, i.e.

temperatures of vapour, coolant to-inlet and rise between to-inlet and from-outlet, coolant flow rate and potential across the heater terminal in the present work,

$X_1, X_2 \ldots X_n$ are measured quatities,

$\Delta W_1, \Delta W_2 \ldots \Delta W_n$ are uncertainties in measured quantities.

Thus we use eq.(C-1) to estimate the errors in Q, LMTD, U and v_v.

(1) Uncertainty of overall heat-transfer coefficient

The uncertainty of the overall heat-transfer coefficient given by eq.(3-17) is then determined by:

$$\frac{\Delta U}{U} = \{(\frac{\Delta Q}{Q})^2+(\frac{\Delta LMTD}{LMTD})\}^{\frac{1}{2}} \quad \text{(C-2)}$$

where

$$\frac{\Delta Q}{Q}=\{2(\frac{\Delta T_\varepsilon}{T_{out}-T_{in}})^2+(\frac{\Delta V}{V})^2\}^{\frac{1}{2}} \quad \text{(C-3)}$$

$$\frac{\Delta LMTD}{LMTD}=(A_1{}^2+A_2{}^2+A_3{}^2)^{\frac{1}{2}} \quad \text{(C-4)}$$

$$A_1=\Delta T_\varepsilon \frac{T_{in}-T_{out}}{\{(T_v-T_{in})(T_v-T_{out})\ln(\frac{T_v-T_{in}}{T_v-T_{out}})\}}$$

$$A_2=\Delta T\varepsilon \frac{1}{\{(T_v-T_{in})\ln(\frac{T_v-T_{in}}{T_v-T_{out}})\}}$$

$$A_3=\Delta T\varepsilon \frac{1}{\{(T_v-T_{out})\ln(\frac{T_v-T_{in}}{T_v-T_{out}})\}}$$

where ΔT_ε is dependent on the precision of digital voltmeter and estimated to be ±1 μV equivalent to a temperature difference of 0.025 K, and ΔV is dependent on the accuracy of the flow meter estimated to be ±1 %.

The uncertainty in the vapour velocity is calculated as follows. When assuming negligible error in measurement of dimensions of the test section and in properties equations, the uncertainty of the vapour velocity is given by:

$$\frac{\Delta v_v}{v_v} = \frac{\Delta m_v}{m_v} \qquad \text{(C-5)}$$

$$=\{(\frac{\Delta Q}{Q_h-Q_{loss}})^2 + (\frac{\Delta Q_{loss}}{Q_h-Q_{loss}})^2 + 2(\frac{c_{p_c}\Delta T_\varepsilon}{c_{p_c}\Delta T+h_{fg}})^2\}^{½}$$

The uncertainty of input power is estimated by:

$$\frac{\Delta Q_h}{Q_h} = 2n(\frac{\Delta V_{volt}}{V_{volt}}) \qquad \text{(C-6)}$$

where n is the number of heaters used, i.e. one for R-113 and three for ethylene glycol and we estimated ΔV_{volt} ±5 V. Eq.(3-15) was judged to give the thermal losses with an accuracy of 10 %. The thermal losses from the apparatus were about 4 % and 16 % for R-113 and ethylene glycol respectively of the total boiler input power so that the estimate of the error in Qloss is not a critical significance. The values of $\Delta Q_{loss}/(Q_h-Q_{loss})$ were in fact found to be 0.2 % and 1 % for R-113 and ethylene glycol respectively. The values of $\Delta Q_h/(Q_h-Q_{loss})$ were found to be 4 % and 14 % for R-113 and ethylene glycol respectively.

The value of the third term in the right hand side in eq.(C-5) is negligibly small in comaprison with other terms. Eventually, the uncertainties of vapour velocities were found to be around 6 % for R-113 and 15 % for ethylene glycol. These are probably upper limits.

Table C-1 shows the calculated consequential error estimates at a coolant velocity of around 4 m/s, except in the case of plain tube for R-113 in which errors were estimated at a coolant velocity of around 0.9 m/s, (data at higher coolant velocities were neglected as described in section 4.3). The table also includes results for Yau et al. [35,36] steam data for comparison.

(2) Uncertainty of vapour-side heat-tarnsfer coefficient

The calculation of the vapour-side coefficient from the overall coeffcient invokes the assumption of uniform radial conduction, i.e. concentrics isotherms, in the tube wall. Even for the case of the plain tube this cannot be valid since the vapour-side coefficient decreases as the condensate film thickens around the tube. For finned tube the phenomenon of condensate retention accenturates the variation of wall temperature. Thus a vapour-side coefficient defined as the mean heat flux devided by the mean wall temperature differs from that obtained by the subtracting wall and coolant resistances from the measured overall resistance. It is therefore not possible to obtain "true" estimates of "error" in the vapour-side coefficient.

We can infer that the vapour-side coefficients reported here (i.e. based on a "modified Wilson plot" method) will be less valiable when the error in the overall coefficient is large. However,as indicated above, this is not the only factor to be considered, since when the coolant-side resistance is small, the wall temperature is more uniform and the assumption underling the calculation is more valid. As a guide to the validity of the uniform wall temperature approximation, we may use the ratio of coolant-side temperature difference. When this quantity appears zero the approxiamtion becomes completely valid (since the coolant-side coefficient is essentially uniform over the tube). Thus we consider:

$$\Delta T_{coolant}/\Delta T_{overall} \simeq U/\alpha_c \qquad \text{(C-7)}$$

For the present data and those of Yau et al. [35,36] this "index of uncertainty" (small values are "good") was found to be between 0.35 and 0.5 for R-113, between 0.4 and 0.65

for ethylene glycol and between 0.7 and 0.85 for steam. On this basis, the uncertainty of vapour-side heat-transfer coefficients increases in the sequence steam, ethylene glycol and R-113. Since this is in reverse order of the estimated errors in the overall heat-transfer coefficients (see Table C-1), it could be the case that all of the data are of similar reliability although this cannot be said with certainty.

Table C-1 Estimation errors of parameters calculated directly from measured variables

		$(\frac{\Delta U}{U})\times100$	$(\frac{\Delta LMTD}{LMTD})\times100$	$(\frac{\Delta Q}{Q})\times100$	$(\frac{\Delta v_v}{v_v})\times100$
R-113	plain	12	8.3	8.4	4
	b≤2 mm	10	7.0	7.5	
ethylene glycol	plain	5.0	3.5	3.6	14
	b≤2 mm	2.0	1.2	1.6	
steam	plain	3.0	2.0	2.5	17
	b≤2 mm	2.0	1.4	1.7	

APPENDIX D Computer program for data processing

Appendix D Computer program for data processing

A. Program "ANA"

This program is written for calculations described in section 3.3, section 4.2 and section 4.3.

All data given from the experiments may be set in the data file or alternatively manual input is possible in this program. The data files should be written in the following form;-

```
INPUT FORM

list
fin pitch          ;  p/mm
date               :  day, month, year
number of heaters  :  1≤n≤4
conditions         :  no. of heater     ambient.    barometer
                      & potential/W  ,  temp./ C ,  reading/inHg

measurement

   flow                       temperature                          gage pressure
   rate    coolant   condensate   vapour   coolant                 in test section
           inlet     return                increase
   -----   ----------------------------------------               ---------------
   l/min                          μV                                cm liquid

                                  :
                              data  set
                                  :
```

Data set which give flow rate, temperature of coolant inlet and outlet, and vapour in μV or K are also avilable, e.g. Yau et al. [35,36,37] data and Georgiadis [40] data.

For run of this program, the following command may be required.

F(ANA,F=3.BMC+4.data file+7.out1+8.out2+9.out3)

where BMC is data file for Barrow meter correction.

Calculated parameters are written in out1, and optionally out2 is data file for graph drawing, Q vs Tv-Tw. Library source "CURV" can offer program for drawing graphs. The out3 is data for construction of data base "MULTI".

B. Data base "MULTI"

Configuration of finned tubes, temperature of vapour and tube wall, and heat flux are stored in this file for the following data;-

1) The present data for R-113 and ethylene glycol
2) Yau et al. [35,36,37] data for steam
3) Honda et al. [34] for R-113 and methanol
4) Georgiadis [40] for steam

C. Program "CALL"

This program is written for collecting parameters from the data of "MULTI" as follows;-

(1) For selected name of experimentors or liquid or both from the list shown on the screen, the vapour-side heat-transfer coefficient, Tv, Tw and Q, the retention angle and all properties are listed in the output file.

(2) The parameters for requirement are also listed in the other output file.

For run this program, the following command may be used;-

```
F(CALL,F=4.MULTI+7.filel+8.file2)
```

where filel stores results (1) and file2 stores (2).

Computer program "ANA"

```
C                     PROGRAM  ANA
C
C     This progrmme is for analysing the experimental data by using
C     the theory of least squares and for calculating theoretical
C     heat transfer coefficients on the base of experimental temparature
C     differens (Ts-Tw).
C
C     command for run:
C       F(ANA,F=3.BMC+4.datafile +7.out1+8.out2+9.out3)
C             BMC: barometer correction
C             7  : all output  8: Q-dT graph data  9: Tw,Ts and Q data
C
      COMMON/VALU/VOLU(100),PD(100),T(7,100),Q(100),UW(100),VOL(100),
     1             UV(100)
      COMMON/CCC/CPLC,VLC,VISC,KC,HFGC
      COMMON/PPP/CPV,CPL,VV,VL,VISV,VISL,KL,HFG
      COMMON/BMC/BARO(11,25)
      REAL KL,KC,KT
C
C-----------------------------------------------------
C          DIMENSIONS OF FINNED TUBE AND APARATUS
C-----------------------------------------------------
C
       DATA DI,DO,AL,KT/.009779,.0127,.1016,.3962/
C
C
      PI=4*ATAN(1.)
      DTS=.1143
      AS=PI*DTS**2/4
C
C-----------------------------------------------------
C                 CORELATION OF BAROMETER
C-----------------------------------------------------
C
       READ(3,*) ((BARO(I,J),I=1,11),J=1,25)
       DO 50 I=1,11
       DO 50 J=1,25
   50  BARO(I,J)=BARO(I,J)/1000.
C
   10 CONTINUE
C
C-----------------------------------------------------
C                   INITIALIZATION
C-----------------------------------------------------
       DO 100 I=1,100
       VOLU(I)=0.
       VOL(I) =0.
       UV(I)  =0.
  100  CONTINUE
C
C-----------------------------------------------------
C                     MAIN CALCULATION FLOW
C-----------------------------------------------------
C
        WRITE(6,1200)
        READ(5,*) ISD
        WRITE(6,1400)
        READ(5,*) LIQ
```

```
         IF(LIQ.EQ.1) WRITE(7,5100)
         IF(LIQ.EQ.2) WRITE(7,5200)
         IF(LIQ.EQ.3) WRITE(7,5300)
         IF(ISD.EQ.1) CALL INPUT1(N,AS,PI,DI,DO,AL,LIQ,PIT)
         IF(ISD.EQ.2) CALL INPUT2(N,PI,DI,DO,AL,PIT)
C
        WRITE(6,1500)
        READ(5,*) MET
        IF(MET.EQ.1) WRITE(6,2000)
        IF(MET.EQ.1) READ(5,*) COA,COB
        IF(MET.EQ.1) CALL COOL(N,DO,DI,KT,COA,COB)
        IF(MET.EQ.2) CALL LEAS(N,DO,DI,KT,LIQ)
C
         CALL THEOR(N,DO,LIQ)
C
         CALL UNCERN(N,DO,DI,KT,PI)
C
         DO 300 I=1,N
         VOLU(I)=VOL(I)*60000.
  300    CONTINUE
C
         WRITE(9,2400) N
         DO 400 I=1,N
         Q1000=Q(I)*1000.
         TS=T(3,I)
         TW=T(6,I)
         WRITE(9,2200) TS,TW,Q1000
  400    CONTINUE
        WRITE(6,1000)
        READ(5,*) IJK
        IF(IJK.EQ.2) GO TO 999
        GO TO 10
C
  999  WRITE(8,1600)
       STOP
 1000  FORMAT(/' IF INPUT NEXT DATA, YES=1 : NO=2')
 1200  FORMAT(/' DATA FORM: 5  TEMP DATA=1',
     1        /'           3           =2')
 1400  FORMAT(/' LIQUID CHOICE     WATER=1',
     1        /'                   R113 =2',
     2        /'                   ETHLEN=3')
 1500  FORMAT(/' Chose Analysis Method; Original=1',
     1        /'                          Wilson =2')
 1600  FORMAT('////')
 2000  FORMAT(/'  Give COA and COB (usualy COA=0.03 COB=0) ',
     1        /'                 (america COA=0.0635 COB=26.4)',
     2        /' for [COA]*RE**.8*PR**.33*(VIS/VISW)**.14+[COB]')
 2200  FORMAT(3E15.6)
 2400  FORMAT(I3)
 5100  FORMAT('   WATER')
 5200  FORMAT('   R-113')
 5300  FORMAT('  .ETHYLENE GLYCOL')
          END
C
C-----------------------------------------------------------
C                       SUBROUTINE PROGRAMME
C-----------------------------------------------------------
C
```

```
C
C                                   INPUT FORM
C-----------------------------------------------------------
C
      SUBROUTINE INPUT1(JN,AS,PI,DI,DO,AL,LIQ,PITCH)
C
      DIMENSION E1D(100),E2D(100),E3D(100),E4D(100)
      COMMON/VALU/VOLU(100),PD(100),T(7,100),Q(100),UW(100),VOL(100),
     1          UV(100)
      COMMON/CCC/CPLC,VCL,VISC,KC,HFGC
      COMMON/PPP/CPV,CPL,VV,VL,VISV,VISL,KL,HFG
      REAL KC,KL
C
      WRITE(6,3000)
      READ(5,*) MC
      IF(MC.EQ.1) GO TO 5
      WRITE(6,1000)
      WRITE(6,1100)
      READ(5,*) PITCH
      WRITE(7,1150) PITCH
    5 CONTINUE
      J=0
      JN=0
   10 CONTINUE
      IF(MC.EQ.1) GO TO 200
      WRITE(6,1200)
      READ(5,*) IDAY,IMON,IYEAR
      WRITE(6,1400)
      CALL POWER(QP,TA,PA,LIQ,5,IYEAR)
      WRITE(6,1600)
      READ(5,*) N
      GO TO 250
  200 CONTINUE
      READ(4,*) PITCH
      WRITE(7,1150) PITCH
      READ(4,*) IDAY,IMON,IYEAR
      CALL POWER(QP,TA,PA,LIQ,4,IYEAR)
      READ(4,*) N
  250 CONTINUE
      CALL PCOR(PA,TA,PAN)
      IF(LIQ.EQ.1) VLA=.01*(.099917+TA*(6.5E-6+3.83333E-7*TA))
      IF(LIQ.EQ.2) VLA=(.617+.000647*TA**1.1)*1.E-3
      IF(LIQ.EQ.3) VLA=9.24848E-4+6.2796E-7*(TA-65.)+9.2444E-10
     1                 *(TA-65.)**2+3.057E-12*(TA-65.)**3
C
      I=0
   15 I=I+1
      IF(MC.EQ.1) GO TO 300
      WRITE(6,1700)
      READ(5,*) VOLU(I)
      WRITE(6,1800)
      READ(5,*) E1D(I),E2D(I),E3D(I),E4D(I)
      WRITE(6,1900)
      READ(5,*) PD(I)
       GO TO 350
  300 READ(4,*) VOLU(I),E1D(I),E2D(I),E3D(I),E4D(I),PD(I)
  350 CONTINUE
C
```

```
      IF(I.LT.N) GO TO 15
C
   20 CONTINUE
      WRITE(6,2400) IDAY,IMON,IYEAR
      WRITE(6,1150) PITCH
       WRITE(6,2000)
       WRITE(6,2100) (I,VOLU(I),E1D(I),E2D(I),E3D(I),E4D(I),PD(I),
     1                I=1,N)
       WRITE(6,2200)
       READ(5,*) IC
       IF(IC.EQ.999) GO TO 25
      WRITE(6,2100)IC,VOLU(IC),E1D(IC),E2D(IC),E3D(IC),E4D(IC),PD(IC)
       WRITE(6,2300)
       READ(5,*) VOLU(IC),E1D(IC),E2D(IC),E3D(IC),E4D(IC),PD(IC)
       GO TO 20
C
   25 CONTINUE
          WRITE(7,2400) IDAY,IMON,IYEAR
       WRITE(7,2000)
       DO 50 I=1,N
       IJN=I+JN
      WRITE(7,2100) IJN,VOLU(I),E1D(I),E2D(I),E3D(I),E4D(I),PD(I)
   50 CONTINUE
C
      WRITE(7,2500)
C
      JO=J+1
      DO 100 I=1,N
       IF(E4D(I).LE.15.) GO TO 100
      J=J+1
      VOL(J)=VOLU(I)/60000
      UW(J)=VOL(J)/(PI*DI**2/4)
      E1=E1D(I)
      E2=E2D(I)
      E3=E3D(I)
      E4=E4D(I)
      P =PD(I)
      CALL TEMP(TIN,E1)
      CALL TEMP(TSUB,E2)
      CALL TEMP(TS,E3)
      E5=E1+E4/2
      DT=(2.5518416E-2-6.6119645E-7*E5+2.6750257E-11*3*E5**2)*E4
      TOUT=TIN+DT
      TM=(TIN+TOUT)/2
      CALL WATER(TM,TS)
C
      QCOOL=CPLC*VOL(J)*(TOUT-TIN)/(PI*DO*AL*VCL)
      PA=PAN+P/VLA/100*9.81183/1E+6
      CALL PROP(TS,TS,PS,LIQ)
      QLOS=8.328*(TS-TA-273.15)/1000
      U=(QP-QLOS)*VV/AS/(CPL*(TS-TSUB)+HFG)
C
      IF(LIQ.EQ.1) AMASS=18.015
      IF(LIQ.EQ.2) AMASS=187.38
      IF(LIQ.EQ.3) AMASS=62.07
      W=(PA-PS)/(PA-PS*(1.-AMASS/28.96))
      W=W*100.
      WRITE(7,2600) PA,PS,W,U
```

```
C
      T(1,J)=TIN
      T(2,J)=TOUT
      T(3,J)=TS
      T(4,J)=TSUB
      T(5,J)=TM
      Q(J)  =QCOOL
      UV(J) =U
  100 CONTINUE
C
      JN=J
      WRITE(7,2700)
      WRITE(7,2800) (I,(T(K,I),K=1,4),I=JO,JN)
      WRITE(6,2900)
      READ(5,*) III
      IF(III.EQ.1) GO TO 10
      RETURN
C
 1000 FORMAT(/' INPUT EXPERIMENTAL DATA')
 1100 FORMAT(/' PITCH ?')
 1150 FORMAT(/ ' PITCH=',F6.3,'mm')
 1200 FORMAT(/' DATE  DAY,MONTH,YEAR ?')
 1400 FORMAT(/' V LOSS(volt) Ambient Temp(c) Atmospheric Press(in)')
 1600 FORMAT(/' NUMBER OF TEST CASES')
 1700 FORMAT(/' FLOW RATE(l/min) ?')
 1800 FORMAT('Read of MicroVolt E1,E2,E3,E4 ?')
 1900 FORMAT('CHAMBER PRESS (cm liquid)')
 2000 FORMAT(/'CASE  VOL    COOLANT    LIQUID    TEST       DT',10X,'P'/
     1      '         L/MIN  INLET      RETURN     SECTION    (M. VOLT)')
 2100 FORMAT(1H ,I3,F6.2,4F10.2,4X,F6.2)
 2200 FORMAT(//'WHICH CASE WOULD YOU LIKE CHANGE? IF NO, INPUT 999')
 2300 FORMAT(1H ,'INPUT NEW VALUES')
 2400 FORMAT(/'  DATE OF EXPERIMENT',I3,'-',I2,'-',I4)
 2500 FORMAT(/9X,'    PA    PS(Mpa)  W(%)    U(m/s)')
 2600 FORMAT(9X,4F8.4)
 2700 FORMAT(/' CASE   TIN     TOUT     TS     TSUB')
 2800 FORMAT(2X,I3,4F8.2)
 2900 FORMAT(/' Any Other DATA ? YES=1 OR NEXT=999')
 3000 FORMAT(/' DATA FILE=1 or MANUAL INPUT=2')
C
       END
C
C-----------------------------------------------------
C              INPUT FORM FOR YAU'S AND AMERICAN DATA
C-----------------------------------------------------
C
      SUBROUTINE INPUT2(JN,PI,DI,DO,AL,PITCH)
      DIMENSION E1D(50),E2D(50),E3D(50)
      COMMON/VALU/VOLU(100),PD(100),T(7,100),Q(100),UW(100),
     1            VOL(100),UV(100)
      COMMON/CCC/CPLC,VCL,VISL,KC,HFGC
      REAL KC
C
      WRITE(6,3000)
      READ(5,*) MC
      IF(MC.EQ.1) WRITE(6,3100)
                  READ(5,*) ITD
      IF(ITD.EQ.1) WRITE(6,3200)
```

```
      IF(ITD.EQ.1) READ(5,*) IAME
      IF(MC.EQ.1) GO TO 5
      WRITE(6,1000)
      WRITE(6,1100)
      READ(5,*) PITCH
      WRITE(7,1200) PITCH
C
    5 CONTINUE
      J=0
      JN=0
   10 CONTINUE
      IF(MC.EQ.1) GO TO 200
      WRITE(6,1300)
      READ(5,*) IDAY,IMON,IYEAR
      WRITE(6,1400)
      READ(5,*) N
      GO TO 250
  200 CONTINUE
       READ(4,*) PITCH
      IF(IAME.NE.1) READ(4,*) IDAY,IMON,IYEAR
      READ(4,*) N
  250 CONTINUE
      I=0
   15 I=I+1
      IF(MC.EQ.1) GO TO 300
      WRITE(6,1600)
      READ(5,*) VOLU(I)
      WRITE(6,1800)
      READ(5,*) E1D(I),E2D(I),E3D(I)
      GO TO 350
  300 READ(4,*) VOLU(I),E1D(I),E2D(I),E3D(I)
  350 CONTINUE
C
      IF(I.LT.N) GO TO 15
   20 CONTINUE
      WRITE(6,2400) IDAY,IMON,IYEAR
      WRITE(6,1200) PITCH
      WRITE(6,2000)
      WRITE(6,2100)(I,VOLU(I),E1D(I),E2D(I),E3D(I),I=1,N)
      WRITE(6,2200)
      READ(5,*) IC
      IF(IC.EQ.999) GO TO 25
      WRITE(6,2100) IC,VOLU(IC),E1D(IC),E2D(IC),E3D(IC)
      WRITE(6,2300)
      READ(5,*) VOLU(IC),E1D(IC),E2D(IC),E3D(IC)
      GO TO 20
   25 CONTINUE
       WRITE(7,1200) PITCH
      WRITE(7,2400) IDAY,IMON,IYEAR
      WRITE(7,2000)
      DO 50 I=1,N
      IJN=I+JN
      WRITE(7,2100) IJN,VOLU(I),E1D(I),E2D(I),E3D(I)
   50 CONTINUE
      JO=J+1
      DO 100 I=1,N
      J=J+1
      IF(ITD.EQ.1) GO TO 120
```

```
      VOL(J)=VOLU(I)/60000
      UW(J)=VOL(J)/(PI*DI**2/4)
      E1=E1D(I)
      E2=E2D(I)
      E3=E3D(I)
      CALL TEMP(TIN,E1)
      CALL TEMP(TOUT,E2)
      CALL TEMP(TS,E3)
      GO TO 140
  120 CONTINUE
       IF(IAME.EQ.1) GO TO 160
       TABS=0.
       GO TO 180
  160  DI=0.0127
       DO=0.018
       AL=0.133
       TABS=273.16
  180 CONTINUE
                  UW(J)=VOLU(I)
                  VOL(J)=UW(J)*PI*DI**2/4.
                  VOLU(I)=VOL(J)*60000.
                  TIN=E1D(I)+TABS
                  TOUT=E2D(I)+TABS
                  TS=E3D(I)+TABS
  140 CONTINUE
      TM=(TIN+TOUT)/2
      CALL WATER(TM,TS)
      QCOOL=CPLC*VOL(J)*(TOUT-TIN)/(PI*DO*AL*VCL)
      T(1,J)=TIN
      T(2,J)=TOUT
      T(3,J)=TS
      T(5,J)=TM
      Q(J)  =QCOOL
      UV(J)=0.
  100 CONTINUE
      JN=J
      WRITE(7,2700)
      WRITE(7,2800)(I,(T(K,I),K=1,3),I=J0,JN)
      WRITE(6,2900)
      READ(5,*) III
      IF(III.EQ.1) GO TO 10
      RETURN
C
 1000 FORMAT(/' INPUT EXPERIMENTAL DATA')
 1100 FORMAT(/' PITCH (mm) ?')
 1200 FORMAT(/' PITCH=',F6.3,'mm')
 1300 FORMAT(/' DATE DAY,MONTH,YEAR ?')
 1400 FORMAT(/' NUMBER OF TEST CASES')
 1600 FORMAT(/' FLOW RATE (l/min)')
 1800 FORMAT(' READ OF MicroVolt E1,E2,E3')
 2000 FORMAT(/' CASE    VOL        COOLANT        TEAS',
     1       /'         l/min  inlet    outlet   SECTION(m.volt)')
 2100 FORMAT(2X,I3,F6.2,3F10.2)
 2200 FORMAT('Which would you like change? no. or 999 for next')
 2300 FORMAT('Change VALUES')
 2400 FORMAT(/'   DATE OF EXPERIMENT',I3,'-',I2,'-',I4)
 2700 FORMAT(/'   CASE   TIN      TOUT       TS')
 2800 FORMAT(2X,I3,2X,3F9.2)
```

```
 2900  FORMAT(/'Any other data? YES=1 or 999 for next')
 3000  FORMAT(/'  DATA FILE=1 or MANUAL INPUT=2')
 3100  FORMAT(/' If data witten in temp., input 1')
 3200  FORMAT(/' If american data, input 1')
       END
C
C
C-----------------------------------------------------------
C                                   ANALYSIS
C-----------------------------------------------------------
C
C                                   LEAST SQUEAR METHOD
C-----------------------------------------------------------
C
      SUBROUTINE LEAS(N,DO,DI,KT,LIQ)
      COMMON/VALU/VOLU(100),PD(100),T(7,100),Q(100),UW(100),VOL(100),
     1          UV(100)
      DIMENSION DT(100),C1(100),C2(100),C3(100)
      REAL KT
C
      EPS=.0005
      ALFO=1/.03
      BETO=1/.728**(4./3.)
C
      DO 100 I=1,N
      T(6,I)=(T(3,I)+T(5,I))/2
      T(7,I)=T(5,I)
  100 CONTINUE
C
   10 CONTINUE
      A=0.
      B=0.
      C=0.
      D=0.
      E=0.
      DO 200 I=1,N
      TWO=T(6,I)
      TWI=T(7,I)
      TS=T(3,I)
      TM=T(5,I)
      DTI=TS-TM
      DT(I)=DTI
      QC=Q(I)
      U =UW(I)
C
      CC3=QC*DO*ALOG(DO/DI)/(2*KT)
      C3(I)=CC3
      CALL NUSP(TM,TWI,U,DI,DO,QC,CC1)
      C1(I)=CC1
      CALL NUST(TS,TWO,DO,QC,CC2,LIQ)
      C2(I)=CC2
C
      A=A+CC1*CC1
      B=B+CC1*CC2
      C=C+(CC1*DTI-CC1*CC3)
      D=D+CC2*CC2
      E=E+(CC2*DTI-CC2*CC3)
  200 CONTINUE
C
      ALF=(C*D-B*E)/(A*D-B*B)
```

```
      BET=(A*E-B*C)/(A*D-B*B)
      DO 220 I=1,N
      T(7,I)=T(5,I)+ALF*C1(I)
  220 T(6,I)=T(7,I)+C3(I)
      IF(ABS((ALF-ALFO)/ALF).LT.EPS.AND.ABS((BET-BETO)/BET).LT.EPS)
     1   GO TO 250
         PRINT *,ALF,BET
        ALFO=ALF
        BETO=BET
      GO TO 10
  250 CONTINUE
C
      ALF=1/ALF
      BET=(1/BET)**(3./4.)
      WRITE(7,1000)
      WRITE(7,1200) ALF,BET
      WRITE(7,1400)
      WRITE(7,1600) (I,T(7,I),T(6,I),DT(I),I=1,N)
       RETURN
 1000 FORMAT(/' CALCULATING RESULTS')
 1200 FORMAT(/' a=',E12.4,' b=',E12.4)
 1400 FORMAT(/' CASE    TI      TO    Ts-Tm')
 1600 FORMAT(2X,I3,2F8.2,F8.3)
C
        END
C
C-------------------------------------------------------------
C                    THEORETIVAL CALCULATION FOR PLAIN TUBE
C-------------------------------------------------------------
C
      SUBROUTINE THEOR(N,DO,LIQ)
      COMMON/VALU/VOLU(100),PD(100),T(7,100),Q(100),UW(100),VOL(100),
     1            UV(100)
      COMMON/PPP/CPV,CPL,VV,VL,VISV,VISL,KL,HFG
      COMMON/CCC/CPLC,VC,VISC,KC,HFGC
      DIMENSION ALF(3),ARTH(3),QQ(3)
      REAL KL,KC
C
      DO 200 K=1,3
       ALF(K)=0.
       ARTH(K)=0.
       QQ(K) =0.
  200 CONTINUE
C
      WRITE(7,1000)
      DO 100 I=1,N
      TS=T(3,I)
      TO=T(6,I)
      TIN=T(1,I)
      TOUT=T(2,I)
      TML=(TOUT-TIN)/ALOG((TS-TIN)/(TS-TOUT))
      DT=TS-TO
      QC=Q(I)
      U =UV(I)
      IF(DT.LT.0.) WRITE(7,1400) I
      IF(DT.LT.0..) GO TO 100
      Q1000=QC*1000.
      WRITE(8,1600) DT,Q1000
```

```
C       OUV=Q1000/TML
C       WRITE(8,1600) UW(I),OUV
        IF((VOL(I)-VOL(I+1)).LT.0.) WRITE(8,1800)
        TSM=.6667*TO+.3333*TS
        CALL PROP(TSM,TS,PS,LIQ)
C
C       IF(LIQ.GE.2) GO TO 300
C
C       SL=(-.0003*(TSM-273.15)**2-.138*(TSM-273.15)+75.6)/1000.
C 300   CONTINUE
C
C       IF(LIQ.EQ.2) SL=(-.11*TSM+50.1)/1000.
C       IF(LIQ.EQ.3) SL=5.021E-2-8.9E-5*(TSM-273.15)
C       PRAN=VISL*CPL/KL
C       XX=SL*VL/9.81183
C       WRITE(9,2100) I,TS,TO,CPL,VL,VISL,KL,HFG,SL,XX,PRAN
C 350   CONTINUE
C
        ALEX=QC/DT
        EXNU=DO/KL*ALEX
         IF(U.EQ.0.) GO TO 49
         FF=9.81183*DO*VISL*HFG/(U**2*KL*DT)
        RE=U*DO/(VISL*VL)
         AREX=EXNU/RE**.5
   49   K=1
   50   CONTINUE
C
         IF(U.EQ.0.) FF=0.
         IF(U.EQ.0.) AREX=0.
         IF(K.EQ.1) GO TO 400
         IF(K.EQ.2) GO TO 420
C
C                           SHEKRILADZE EQATION
         CALL SHE(TS,TO,U,FNU,DO)
          GO TO 450
C
C                           FUJII EQATION
  420    CALL FUJI(TS,TO,U,FNU,DO)
          GO TO 450
C
C                           NUSSELT EQATION
  400    CALL NUSSEL(TS,TO,FNU,DO)
C
  450   CONTINUE
C
         ALF(K)=FNU*KL/DO
        QQ(K)=ALF(K)*DT
        IF(U.NE.0.) ARTH(K)=FNU/RE**.5
C
         IF(U.LE.0.) GO TO 60
         IF(K.EQ.3) GO TO 60
         K=K+1
         GO TO 50
   60    CONTINUE
C
        WRITE(7,1200) I,DT,ALEX,QC,ALF(1),QQ(1),ALF(2),QQ(2),
     1              ALF(3),QQ(3),FF,AREX,ARTH(1),ARTH(2),ARTH(3)
  100   CONTINUE
```

```
      WRITE(8,1800)
      RETURN
C
 1000 FORMAT(/10X,'EXPERIMENT',8X,'NUSSELT',7X,'FUJII',6X,'SHKLIRAZE'
     1      /8X,'DT',5X,'h',5X,'Q',6X,'h',5X,'Q',6X,'h',5X,'Q',5X,'h',
     2      5X,'Q'/' CASE',10X,'F',3X,'NU/RE',8X,'NU/RE',8X,'NU/RE',
     3      8X,'NU/RE')
 1200 FORMAT(2X,I3,F7.2,4(F6.2,F7.2)/11X,2F7.2,3(7X,F6.2))
 1400 FORMAT(/' (Ts-Tw) is negative at CASE=',I3)
 1600 FORMAT(F10.3,F14.3)
 1800 FORMAT('////')
C2000 FORMAT(//' CASE',4X,'Ts',5X,'Tw',5X,'Cp',10X,'v',9X,'U',
C    1          9X,'K',9X,'Hfg',6X,'Sigm',6X,'s/(p*g)',6X,'Pr'
C    2      /12X,'K',9X,'KJ/Kgk',5X,'m3/Kg',5X,'Kg/ms',5X,'KJ/msk',
C    3       5X,'KJ/Kg',5X,'N/S')
C2100 FORMAT(/2X,I3,2F7.2,7E10.3,E12.4)
C2200 FORMAT(2E12.4)
      END
C
C
C-----------------------------------------------------------------
C                              HEAT TRANSFER OF COOLANT SIDE
C-----------------------------------------------------------------
C
      SUBROUTINE COOL(N,DO,DI,KT,COA,COB)
       COMMON/VALU/VOLU(100),PD(100),T(7,100),Q(100),UW(100),
     1                   VOL(100),UV(100)
       COMMON/CCC/CPLC,VCL,VISC,KC,HFGC
       DIMENSION DT(100)
       REAL KC,KT
C
      DO 100 I=1,N
       QI=Q(I)*DO/DI
       TIN=T(1,I)
       TOUT=T(2,I)
       TIO=T(5,I)
  200  CALL NUSC(TIO,UW(I),DI,ANU,COA,COB)
       ALIN=ANU*KC/DI
       AA=ALIN*(TOUT-TIN)/QI
       BB=EXP(AA)
       TI=(BB*TOUT-TIN)/(BB-1)
       IF(ABS((TIO-TI)/TIO).LT.1.E-5) GO TO 250
       TIO=TI
       TM=TI-(TOUT-TIN)/ALOG((TI-TIN)/(TI-TOUT))
       CALL WATER(TM,TS)
       GO TO 200
  250  CONTINUE
C
       TO=TI+DO*ALOG(DO/DI)*Q(I)/(2.*KT)
       T(6,I)=TO
       T(7,I)=TI
       DT(I)=T(3,I)-T(5,I)
  100 CONTINUE
       WRITE(7,1000)
       WRITE(7,1400)
       WRITE(7,1600) (I,T(7,I),T(6,I),DT(I),I=1,N)
      RETURN
 1000 FORMAT(/' CALCULATING  RESULT')
```

```
 1400   FORMAT(/' CASE   TI       TO       Ts-Tm')
 1600   FORMAT(2X,I3,2F8.2,F8.3)
        END
C
C
        SUBROUTINE NUSP(TM,T1,U,DI,DO,Q,CC1)
        COMMON/CCC/CPC,VC,VIS,KC,HFGC
        REAL KC
        CALL WATER(TM,TS)
        VISW =.00002414*10**(247.8/(T1 -140))
        RE=U*DI/(VIS*VC)
        PR=CPC*VIS/KC
         ANU=RE**.8*PR**(1./3.)*(VIS/VISW)**.14
         CC1=Q*(DO/DI)*DI/(KC*ANU)
        RETURN
        END
C
C
            SUBROUTINE NUSC(TI,U,DI,ANU,A,B)
            COMMON/CCC/CPLC,VCL,VISC,KC,HFG
            REAL KC
            VISW=.00002414*10**(247.8/(TI-140.))
            RE=U*DI/(VISC*VCL)
            PR=CPLC*VISC/KC
            ANU=A*RE**.8*PR**(1./3.)*(VISC/VISW)**.14+B
            RETURN
            END
C
C-------------------------------------------------------------
C                             HEAT TRANSFER OF VAPOUR SIDE
C                             FOR WILSON METHOD
C-------------------------------------------------------------
C
        SUBROUTINE NUST(TS,TW,DO,Q,CC2,LIQ)
        COMMON/PPP/CPV,CPL,VV,VL,VISV,VISL,KL,HFG
        REAL KL
        TSM=.6667*TW+.3333*TS
        CALL PROP(TSM,TS,PS,LIQ)
        A=Q**4*VISL*DO*VL**2
        B=KL**3*9.81183*HFG
        CC2=(A/B)**(1./3.)
         RETURN
         END
C
C
C---------------------------------------------------
C                            THEORETCAL FORMURA
C---------------------------------------------------
        SUBROUTINE FUJI(TS,TO,U,FNU,DO)
        COMMON/PPP/CPV,CPL,VV,VL,VISV,VISL,KL,HFG
        REAL KL
        R=(VV*VISL/(VL*VISV))**.5
        H=KL*(TS-TO)/(VISL*HFG)
        FR=U**2/(9.81183*DO)
        RE=U*DO/(VISL*VL)
        X=.9*(1+1/(R*H))**.3333
        FNU=X*(1+.276/(X**4*FR*H))**.25*RE**.5
        RETURN
```

```
      END
C
      SUBROUTINE NUSSEL(TS,TO,TNU,DO)
      COMMON/PPP/CPV,CPL,VV,VL,VISV,VISL,KL,HFG
      REAL KL
      DT=TS-TO
      G=9.81183
       RP=G*DO**3*HFG/(KL*VISL*VL*VL*DT)
      TNU=.728*RP**.25
      RETURN
      END
C
       SUBROUTINE SHE(TS,TO,U,ANU,DO)
       COMMON/PPP/CPV,CPL,VV,VL,VISV,VISL,KL,HFG
       REAL KL
       RE=U*DO/(VISL*VL)
       AK=9.81182*DO*HFG*VISL/(KL*(TS-TO)*U*U)
       ANU=.64*SQRT(RE*(1+SQRT(1+1.69*AK)))
       RETURN
       END
C-----------------------------------------------------------
C                             TEMPARATURE CONVERT
C-----------------------------------------------------------
      SUBROUTINE TEMP(T,E)
      T=273.0995+2.5518496E-2*E-6.6119645E-7*E**2
     1  +2.6750257E-11*E**3
      RETURN
      END
C
C-----------------------------------------------------------
C                             PROPERTIES
C-----------------------------------------------------------
C
       SUBROUTINE PROP(T,TS,PS,LIQ)
       COMMON/PPP/CPV,CPL,VV,VL,VISV,VISL,KL,HFG
       COMMON/CCC/CP,V,VIS,KC,HFGC
       REAL KC,KL
       IF(LIQ.EQ.1) CALL STEAM(T,TS,PS)
       IF(LIQ.EQ.2) CALL REFRI(T,TS,PS)
       IF(LIQ.EQ.3) CALL ETYLEN(T,TS,PS)
       RETURN
       END
C
C----------------------- PROPERTIES OF WATER
       SUBROUTINE WATER(T,TS)
       COMMON/CCC/CP,V,VIS,KC,HFG
       REAL KC
       V=.01*(.099917+(T-273.15)*(6.5E-6+3.83333E-7*(T-273.15)))
       KC=-.92247+2.8395*(T/273.15)-1.8007*(T/273.15)**2+
     1 .52577*(T/273.15)**3-.07344*(T/273.15)**4
        KC=KC/1000
       Y=247.8/(T-140)
       VIS=.00002414*10**Y
       CP=4391.21-.7*T
        CP=CP/1000
      HFG=3468920.-TS*(5707.4-TS*(11.5562-.0133103*TS))
      HFG=HFG/1000.
       RETURN
```

```
      END
C
C---------------------------- PROPERTIES OF STAEM
      SUBROUTINE STEAM(T,TS,PS)
      COMMON/PPP/CPV,CPL,VV,VL,VISV,VISL,KL,HFG
      REAL KL
      CPL=4391.21-.7*T
      CPL=CPL/1000
      HFG=3468920.-TS*(5707.4-TS*(11.5562-.0133103*TS))
      HFG=HFG/1000
      PS=PSTE(TS)
      VL=.01*(.099917+(T-273.16)*(6.5E-6+3.83333E-7*(T-273.16)))
      R=461.51
      VV=R*TS/PS
      Y=247.8/(T-140.)
      VISL=0.00002414*10**Y
      VISV=-4.478415E-6+TS*(5.0216E-8-1.579E-11*T)
      TT=T/273.16
      KL=-.92247+2.8395*TT-1.8007*TT**2+.52577*TT**3-.07344*TT**4
      KL=KL/1000
      PS=PS/1.E+6
      RETURN
      END
C
      FUNCTION PSTE(TS)
      TP=TS/1000.
      A1=15.49217901
      A2=-5.6783717693
      A3=1.4597584637
      A4=13.877000608
      A5=-80.887673591
      A6=123.56883468
      A7=-188.31212064
      A8=660.91763485
      A9=-1382.4740091
      A10=1300.1040184
      A11=-449.39571976
      PSTE=1.E+6*EXP(A1+A2/TP+A3*ALOG(TP)+A4*TP+A5*TP**2+A6*TP**3
     1   +A7*TP**4+A8*TP**5+A9*TP**6+A10*TP**7+A11*TP**8)
      RETURN
      END
C
C------------------------ PROPERTIES OF REFREGERANT
      SUBROUTINE REFRI(T,TS,PS)
      COMMON/PPP/CPV,CPL,VV,VL,VISV,VISL,KL,HFG
      REAL KL,J,J1
      CPL=929+1.03*(T-273.15)
       CPL=CPL/1000
      HFG=(1.611-.0031*(TS-273.15))*1E+5
       HFG=HFG/1000
      TC=487.25
      J1=(TC-TS)/TS
      J=-J1*(2.8+.1*(1+185*J1**5.8)**.2)
      PS=10**J*3.413
C     VL=4.91E-4+2.72E-8*T+1.58E-9*T*T
      VL=(.617+.000647*(T-273.15)**1.1)*1.E-3
      R=44.372
      PC=3.413
```

```
      VV=R*TS/((1+.636*(PS/PC)**.816)*PS*1E+6)
      J=503/(T-2.15)
       VISL=1.34E-5*10**J
       VISV=(.92+.003*(TS-273.15))*1E-5
       KL=.0802-.000203*(T-273.15)
        KL=KL/1000
       RETURN
       END
C
C----------------------- PROPERTIES OF ETHYLENE GLYCOL
      SUBROUTINE ETYLEN(T,TS,PS)
      COMMON/PPP/CPV,CPL,VV,VL,VISV,VISL,KL,HFG
      REAL KL
      CPL=4186.8*(1.6884E-2+3.35083E-3*T-7.224E-6*T*T
     1    +7.61748E-9*T*T*T)
      CPL=CPL/1000.
      HFG=1.35234E+6-6.38263E+2*TS-0.747462*TS*TS
      HFG=HFG/1000.
      A=9.394685-3066.1/TS
      PS=133.32*10**A
      PS=PS/1.E+6
      TB=T-338.15
      VL=9.24848E-4+6.2796E-7*TB+9.2444E-10*TB*TB
     1   +3.057E-12*TB**3
      R=133.95
      VV=R*TS/(PS*1.E+6)
      VISL=EXP(-11.0179+1.744E+3/T-2.80335E+5/T**2
     1          +1.12661E+8/T**3)
      VISV=7.2E-5+2.5974E-7*(TS-273.15)
      KL=418.68E-6*(519.442+0.32092*T)
      KL=KL/1000.
      RETURN
      END
C
C-----------------------------------------------------
C                      BARROW METER CORRECTION
C-----------------------------------------------------
C
       SUBROUTINE PCOR(P,T,PA)
       COMMON/BMC/BARO(11,25)
C
       IP=INT(P)
       PO=(P-FLOAT(IP))*10.
       IF(PO.LT.5.) P1=FLOAT(IP)
       IF(PO.GE.5.) P1=FLOAT(IP)+.5
       IT=INT(T)
       TO=(T-FLOAT(IT))*10.
       IF(TO.LT.5.) T1=FLOAT(IT)
       IF(TO.GE.5.) T1=FLOAT(IT)+.5
       I=INT((P1-26.)/.5)+1
       J=INT((T1-16.)/.5)+1
       A=BARO(I,J)
       B=BARO(I+1,J)
       C=BARO(I,J+1)
       D=BARO(I+1,J+1)
       X1=A+(B-A)*(P-P1)/.5
       X2=C+(D-C)*(P-P1)/.5
       X =X1+(X2-X1)*(T-T1)/.5
```

```
C
          PA=(P-X)*0.0033864
          RETURN
          END
C
C-----------------------------------------------------
C                                POWER INPUT
C-----------------------------------------------------
        SUBROUTINE POWER(QP,TA,PA,LIQ,K,IY)
        DIMENSION NH(4),VH(4),R(4)
        R(1)=18.
        R(2)=17.
        R(3)=11.2
        R(4)=11.8
C
C        We changed the heaters after the experiments with R113 in 1984.
C
        IF(LIQ.EQ.2.AND.IY.LE.1984) GO TO 100
C
        READ(K,*) J
        READ(K,*) (NH(I),VH(I),I=1,J),TA,PA
        GO TO 200
  100   J=1
        READ(K,*) VH(1),TA,PA
  200   CONTINUE
C
        QP=0
        DO 300 I=1,J
        IF(LIQ.EQ.3.OR.LIQ.EQ.1) RES=R(NH(I))
        IF(LIQ.EQ.2) RES=18.6
        QP=VH(I)*VH(I)/(RES*1000.)+QP
  300   CONTINUE
        RETURN
        END
C
C-----------------------------------------------------
C                          ERROR ANALYSIS
C-----------------------------------------------------
C
              SUBROUTINE UNCERN(N,DO,DI,KT,PI)
       COMMON/CCC/CP,VCL,VISL,KL,HFG
       COMMON/VALU/VOLU(100),PD(100),T(7,100),Q(100),UW(100),VOL(100),
     1            UV(100)
       DIMENSION UN(100)
       REAL KL,KT
C                               uncertainty of temperature
                                UDT=0.025
        WRITE(7,1000)
C
       DO 100 I=1,N
          TS=T(3,I)
          TWO=T(6,I)
          TIN=T(1,I)
          TOUT=T(2,I)
          DTS=TS-TWO
          DTLM=(TOUT-TIN)/ALOG((TS-TIN)/(TS-TOUT))
          TC=(TIN+TOUT)/2.
          QC=Q(I)*1000.
```

```
         TWI=TWO-Q(I)*DO/(2*KT)*ALOG(DO/DI)
C
         W=VOL(I)
C                                  uncertainty of flow rate 2 %
                                   UDW=0.01*W
C        coolant properties
         CALL WATER(TC,TS)
              AR=1./VCL
              AK=KL
              AC=CP
              AM=VISL
C                                  uncertainty of properties
                                   TCD=TC+2*UDT
                                   CALL WATER(TCD,TS)
                                   BR=1./VCL
                                   BK=KL
                                   BC=CP
                                   BM=VISL
                                   UR=ABS(AR-BR)
                                   UK=ABS(AK-BK)
                                   UC=ABS(AC-BC)
                                   UM=ABS(AM-BM)
C        uncertainty of heat flux
         DQ=QC*(2*(UDT/(TOUT-TIN))**2+(UR/AR)**2+(UDW/W)**2
     1         +(UC/AC)**2)**.5
C
C        uncertainty of log mean temp difference
         A1=UDT*(TIN-TOUT)/((TS-TIN)*(TS-TOUT)*ALOG((TS-TIN)/(TS-TOUT)))
         A2=UDT/((TS-TIN)*ALOG((TS-TIN)/(TS-TOUT)))
         A3=UDT/((TS-TOUT)*ALOG((TS-TIN)/(TS-TOUT)))
         DL=DTLM*(A1**2+A2**2+A3**2)**.5
C
C        uncertainty of overall heat transfer coeff.
         UO=QC/DTLM
         DU=UO*((DQ/QC)**2+(DL/DTLM)**2)**.5
C
C        uncertainty of Reynolds and Prantle number
         RE=AR*W*4./(PI*DI*AM)
         DRE=RE*((UDW/W)**2+(UR/AR)**2+(UM/AM)**2)**.5
         PR=AM*AC/AK
         DPR=PR*((UM/AM)**2+(UC/AC)**2+(UK/AK)**2)**.5
C
C        uncertainty of coolant-side H-T-C
         HI=QC*(DO/DI)/(TWI-TC)
C        DHI=HI*((UK/AK)**2+(.8*DRE/RE)**2+(.25*DPR/PR)**2+
C    1       2*(.14*UM/AM)**2)**.5
         DHI=HI*((DQ/QC)**2+3*(UDT/(TWI-TC))**2)**.5
C
C        uncertainty of vapour-side H-T-C
         HO=QC/DTS
         DHO=HO*((DU/UO**2*HO)**2+(DO/DI*DHI/HI**2*HO)**2)**.5
C
C        % error
                DU=DU/UO*100.
                DQ=DQ/QC*100.
                DL=DL/DTLM*100.
                DHI=DHI/HI*100.
                DHO=DHO/HO*100.
```

```
C
      WRITE(7,1200) I,UO,DU,DTLM,DL,QC,DQ,HI,DHI,HO,DHO
            UN(I)=DHO
  100 CONTINUE
C
      SHO=0.
      DO 200 I=1,N
      SHO=SHO+UN(I)
  200 CONTINUE
      SHO=SHO/N
      WRITE(7,1400) SHO
C
       RETURN
C
 1000 FORMAT(/10X,'UO: overall H-T-C   LMTD: log-mean temp. difference',
     1        '   Q :  heat flux',/10X,'HI: coolant side H-T-C',
     2        '   HO:  vapourside H-T-C  %: % ERROR',
     3 //4X,'CASE',4X,'UO',9X,'%UO',4X,'LMTD',7X,'%L',8X,'Q',9X,'%Q',7X,
     4      'HI',8X,'%HI',8X,'HO',5X,'%HO')
 1200 FORMAT(5X,I3,5(E12.4,F6.2,' '))
 1400 FORMAT(/'    average of % HO =',F6.2)
      END
```

Computer program "CALL"

```
C                 PROGRAMME CALL
C  This Progrmme is for calling DATA form DATA BASE,  which stores
C  destinction of NAME , LIQUID , TEMPARATURE DATA and HEAT FLUX, and
C  the dimension of FINNED TUBES. The heat transfer coefficient based
C  on both experimental data and NUSSELT's theory are calculated. Add
C  to them, properties of liquid are predicted.
C
C-----------------------------------------------------------------------
C                MAIN PROGRAMME
C-----------------------------------------------------------------------
C
      DIMENSION A(100,5),B(100,40),P(100,100,3),D(40,6),LP(100),NT(100)
      DIMENSION NAME(100,6),ND(100),LIQ(10,6),MESAG(100,20)
      DIMENSION FL(50),FLO(50),LF(50),V(100),C(100,5)
      COMMON/PROP/ROW,HFG,AK,AMIU,SIGM,CP
C
C------------------------------------- DATA
      PI=4.*ATAN(1.)
      G =9.81183
      DATA IEND,INO,IYES/3HEND,2HNO,3HYES/
C------------------------------------- READING DATA
C                                      DIMENSION OF TUBE
      READ(4,*) N
      READ(4,*) (NN,(D(I,J),J=1,6),I=1,N)
C                                      LIQUID KINDS
      READ(4,*) NL
      READ(4,1250) (NN,(LIQ(I,J),J=1,4),I=1,NL)
C                                      EXPERIMENTAL DATA
      K=0
  100 CONTINUE
      K=K+1
      READ(4,1000) NAME(K,1),NAME(K,2)
      IF(NAME(K,1).EQ.IEND) GO TO 150
      READ(4,*) LP(K),NT(K),V(K)
      READ(4,1100) (MESAG(K,I),I=1,20)
      READ(4,*) ND(K)
      NN=ND(K)
      READ(4,*) ((P(K,I,J),J=1,3),I=1,NN)
      GO TO 100
  150 CONTINUE
      NO=K-1
      WRITE(6,2800)
      READ(5,*) JAMP
      IF(JAMP.EQ.1) GO TO 250
C------------------------------------- DATA OUTPUT
      J=JAMP
      WRITE(J,2000)
      DO 200 K=1,NO
      WRITE(J,1000) NAME(K,1),NAME(K,2)
      LL=LP(K)
      NN=NT(K)
      NS=ND(K)
      WRITE(J,1200) (LIQ(LL,JJ),JJ=1,4)
      WRITE(J,2200)
      WRITE(J,2300) (D(NN,JJ),JJ=1,6)
      WRITE(J,2400)
      WRITE(J,1100) (MESAG(K,JJ),JJ=1,20)
      WRITE(J,2500)
```

```
      WRITE(J,2600) (II,(P(K,II,JJ),JJ=1,3),II=1,NS)
  200 CONTINUE
  250 CONTINUE
C---------------------------------------- LEQUEST
      WRITE(6,2900)
      READ(5,1000) IG1,IG2
      WRITE(6,3550)
      IS=0
  330 IS=IS+1
      READ(5,*) LF(IS)
      IF(LF(IS).EQ.0) GO TO 340
      IF(LF(IS).EQ.99) GO TO 360
      GO TO 330
  360 IS=22
      DO 380 I=1,IS
  380 LF(I)=I
  340 CONTINUE
      IF(LF(IS).EQ.0) IS=IS-1
      WRITE(6,3370)
      READ(5,1150) N1,N2
  300 CONTINUE
      WRITE(6,3000)
      WRITE(6,3050)
      WRITE(6,1000) NAME(1,1),NAME(1,2)
      DO 320 K=2,NO
      IF(NAME(K,1).NE.NAME(K-1,1)) WRITE(6,1000) NAME(K,1),NAME(K,2)
  320 CONTINUE
      WRITE(6,3100)
      WRITE(6,1200)((LIQ(I,J),J=1,4),I=1,NL)
      WRITE(6,3200)
      READ(5,1000) NA,ME
      WRITE(6,3300)
      READ(5,1200) L1,L2,L3,L4
      WRITE(6,3350)
      READ(5,1000) M1,M2
      IF(M1.EQ.INO) GO TO 325
      WRITE(6,3360)
      READ(5,*) PITCH
      PITCH=PITCH/1000.
  325 CONTINUE
C---------------------------------------- SELECT DATA & CALCULATION
C
      IC=0
      DO 400 K=1,NO
      IF(NA.EQ.INO) GO TO 420
      IF((NAME(K,1)+NAME(K,2)).NE.(NA+ME)) GO TO 400
  420 CONTINUE
      LL=LP(K)
      NN=NT(K)
      NS=ND(K)
      IF(L1.EQ.INO) GO TO 440
      IF((LIQ(LL,1)+LIQ(LL,2)).NE.(L1+L2)) GO TO 400
  440 CONTINUE
      IF(M1.EQ.INO) GO TO 460
      IF(ABS(D(NN,2)-PITCH).GT.0.001E-3) GO TO 400
  460 CONTINUE
      IF(N1.EQ.INO) GO TO 480
      IF((MESAG(K,2)+MESAG(K,3)).NE.(N1+N2)) GO TO 400
```

```
  480 CONTINUE
      IC=1
      DR =D(NN,1)
      PIT=D(NN,2)
      HIG=D(NN,3)
      THI=D(NN,4)
      SPA=PIT-THI
      ANG=D(NN,5)
      ANG=ANG/180.*PI
      AR =D(NN,6)
      SUMP=0.
      SUMTS=0.
      SUMTW=0.
      SUMR=0.
      SUMK=0.
      SUMH=0.
      SUMM=0.
      SUMS=0.
      DO 600 I=1,NS
      TS=P(K,I,1)
      TW=P(K,I,2)
      Q =P(K,I,3)
      DT=TS-TW
      ALF=Q/DT
      CALL PROPR(LL,TS,TW)
      ALN=.728*(G*ROW**2*AK**3*HFG/(AMIU*DT*DR))**.25
C                             FLOODED POINT
          IF(PIT.EQ.0) GO TO 700
      FP=4.*SIGM*COS(ANG)/(ROW*G*(PIT-THI)*(DR+2.*HIG))-1
      IF(FP.GE.1) GO TO 700
      PSI=ATAN(SQRT(1./(FP*FP)-1))
      IF(FP.LT.0.) PSI=PI-PSI
      IF(PSI.LE.0.) PSI=0.
      GO TO 750
  700 PSI=0.
  750 PSI=PSI/PI*180.
C                             ARRENGEMENT OF DATA
      A(I,1)=DT
      A(I,2)=ALF
      A(I,3)=ALN
      A(I,4)=ALF/ALN
      A(I,5)=PSI
      B(I,1)=ROW
      B(I,2)=AK
      B(I,3)=AMIU
      B(I,4)=CP
      B(I,5)=HFG
      B(I,6)=SIGM
      B(I,7)=SIGM/(ROW*G)
      B(I,8)=V(K)
      C(I,1)=SPA
      SUMP=PSI+SUMP
      SUMTS=TS+SUMTS
      SUMTW=TW+SUMTW
      SUMR=ROW+SUMR
      SUMK=AK+SUMK
      SUMH=HFG+SUMH
      SUMM=AMIU+SUMM
```

```
      SUMS=SIGM+SUMS
  600 CONTINUE
C
      PSIM=SUMP/NS
      TSM =SUMTS/NS
      TWM =SUMTW/NS
      ROWM=SUMR/NS
      AKM =SUMK/NS
      HFGM=SUMH/NS
      AMIUM=SUMM/NS
      SIGMM=SUMS/NS
C
      IF(IS.LE.0) GO TO 880
      DO 800 I=1,NS
      DO 850 J=1,IS
      IF(LF(J).LT.7) FL(J)=D(NN,LF(J))
      IF(LF(J).GE.7.AND.LF(J).LT.10) FL(J)=P(K,I,LF(J)-6)
      IF(LF(J).GE.10.AND.LF(J).LT.15) FL(J)=A(I,LF(J)-9)
      IF(LF(J).GE.15.AND.LF(J).LT.23) FL(J)=B(I,LF(J)-14)
      IF(LF(J).GE.23) FL(J)=C(I,LF(J)-22)
C
  850 CONTINUE
  800 WRITE(8,5000) (FL(J),J=1,IS)
  880 CONTINUE
C----------------------------------------- FILING DATA
      DO 10 J=1,4
      D(NN,J)=D(NN,J)*1000.
   10 CONTINUE
      WRITE(7,1000) NAME(K,1),NAME(K,2)
      WRITE(7,1200) (LIQ(LL,J),J=1,4)
      WRITE(7,2200)
      WRITE(7,2300) (D(NN,J),J=1,6)
      WRITE(7,2400)
      WRITE(7,1100) (MESAG(K,I),I=1,20)
      WRITE(7,4800)
      WRITE(7,2500)
      WRITE(7,2600) (I,(P(K,I,J),J=1,3),I=1,NS)
      WRITE(7,4800)
      WRITE(7,4000)
      WRITE(7,4200) (I,(A(I,J),J=1,5),I=1,NS)
      WRITE(7,4800)
      WRITE(7,4400)
      WRITE(7,4600) (I,(B(I,J),J=1,7),I=1,NS)
C
      WRITE(7,4900)
      WRITE(7,4950) TSM,TWM,PSIM,ROWM,AKM,AMIUM,HFGM,SIGMM
      WRITE(7,4800)
C
      DO 20 J=1,4
      D(NN,J)=D(NN,J)/1000.
   20 CONTINUE
C
C-----------------------------------------------
      IF(IG1.NE.INO) WRITE(8,2950)
  400 CONTINUE
      DO 500 I=1,IS
      FLO(I)=0.
  500 CONTINUE
```

```
      IF(IC.EQ.0) WRITE(6,3400)
      IF(IC.EQ.1) WRITE(6,3500)
      WRITE(6,3600)
      READ(5,*) NC
      IF(NC.EQ.1) GO TO 300
      IF(IG1.NE.INO) WRITE(8,2950)
      IF(IG1.EQ.INO) WRITE(8,5000) (FLO(I),I=1,IS)
      STOP
C------------------------------------------------ FORMAT
C
 1000  FORMAT(2A4)
 1100  FORMAT(20A2)
 1150  FORMAT(2A2)
 1200  FORMAT(4A4)
 1250  FORMAT(I2,4A4)
 2000  FORMAT(1H ,'*********  DATA BASE ***********')
 2200  FORMAT(1H ,8X,'----- TUBE DIMENSION -----',
     1 /7X,'Dr mm',6X,'Pitch',7X,'h',9X,'t',9X,'O',9X,'AR',
     2 /6X,58('-'))
 2300  FORMAT(1H ,4X,F8.3,5(2X,F8.3))
 2400 FORMAT(6X,58('-'))
 2500  FORMAT(1H ,8X,'----- DATA TABLE -----',
     1 /14X,'Ts K',5X,'Tw K',5X,'Qr J/m2s',
     2 /'  ----------------------------------------')
 2600 FORMAT(1H ,6X,I3,2X,F7.2,2X,F7.2,2X,E14.6)
 2800  FORMAT(1H ,'Finishing READING DATA, DO YOU NEED REFERENCE?',
     1          /'          NO=1 or YES= 6 ON DISPLAY or 7 IN FILE')
 2900  FORMAT(/' DO YOU MAKE GRAPH DATA? YES OR NO')
 2950  FORMAT('////')
 3000 FORMAT(//' SELECT DATA FOR CALCULATION',/
     1         '          IF YOU DO ONT NEED LEQUEST, INPUT "NO"')
 3050 FORMAT(1H ,'-----VARIETY OF DATA NAME')
 3100 FORMAT(1H ,'-----VARIETY OF LIQUID')
 3200 FORMAT(1H ,' DATA NAME ?')
 3300 FORMAT(1H ,' LIQUID NAME ?')
 3350 FORMAT(//' DO YOU SELECT PITCH? YES OR NO')
 3360 FORMAT(/' PICTH=')
 3370 FORMAT(/' VAPOUR VELOCITY V=? NO or ANY NUMBER')
 3400 FORMAT(1H ,' NO DATA FOR YOUR REQUEST')
 3500 FORMAT(1H ,' NO MORE DATA')
 3550 FORMAT(//' LIQUEST FOR DATA FILE',/'1=DR 2=PITCH 3=HIGTH 4=THICK',
     1' 5=ANGLE 6=A.R',/'7=TS 8=TW 9=Q 10=DT 11=ALF 12=ALN 13=ALF/ALN',
     2' 14=PSI',/'15=ROW 16=K 17=MIU 18=Cp 19=Hfg 20=Sigm 21=S/(P*G)',
     3' 22=V 23=b', /' PUTIN NUMBER,or STOP=0 ALL=99')
 3600 FORMAT(1H ,' If you want to continue,type 1',
     1         /' otherwise any oter number.')
 4000 FORMAT(1H ,'          CALCULATION RESULTS',
     1 /3X,'CASE',5X,'DT',8X,'ALF',6X,'ALN',6X,'ALF/ALN',5X,'PSI',
     2 /12X,'K ',6X,'J/m2s',4X,'J/m2s',17X,'deg',/60('-'))
 4200 FORMAT(/(3X,I3,2X,F8.3,2(2X,F8.1),2(2X,F8.3)))
 4400 FORMAT(1H ,'            PROPERTIES',
     1 /'  CASE',7X,'P',10X,'K',12X,'U',12X,'Cp',11X,'Hfg',10X,'S',
     2  10X,'S/(P*G)',
     3  /12X,'Kg/m3',6X,' J/msk',7X,'Kg/ms',7X,' J/Kgk',7X,' J/Kg',9X,
     4   'Nm/s',9X,'m2')
 4600 FORMAT(/(2X,I3,7(2X,E11.4)))
 4800 FORMAT(//)
 4900 FORMAT(/'      MEAN VALUES',
```

```
    1        /4X,'TS',6X,'TW',6X,'PSI',6X,'ROW',8X,'AK',9X,'AMIU',
    2         6X,'HFG',9X,'SIGM')
 4950 FORMAT(3F8.2,5E11.4)
 5000 FORMAT(7E12.4)
C-----------------------------------------------------------------------
      END
C-----------------------------------------------------------------------
C                 SUBROUTINE PROGRAMME
C------------------------------------------------------------------------
      SUBROUTINE PROPR(L,TS,TW)
      COMMON/PROP/ROW,HFG,AK,AMIU,SIGM,CP
      TM=.6667*TW+.3333*TS
      IF(L.EQ.1) CALL WATER(TM,TS)
      IF(L.EQ.2) CALL REFRE(TM,TS)
      IF(L.EQ.3) CALL ETHYL(TM,TS)
      IF(L.EQ.4) CALL METAL(TM,TS)
      IF(L.EQ.5) CALL R11(TM,TS)
      IF(L.EQ.6) CALL R22(TM,TS)
      RETURN
      END
C---------------------------------- WATER
      SUBROUTINE WATER(T,TS)
      COMMON/PROP/R,H,AK,AM,S,CP
C
      V=.01*(.099917+(T-273.15)*(6.5E-6+3.83333E-7*(T-273.15)))
      R=1./V
      H=3468920.-TS*(5707.4-TS*(11.5562-.0133103*TS))
      AK=-.92247+2.8395*(T/273.15)-1.8007*(T/273.15)**2+
    1    .52577*(T/273.15)**3-.07344*(T/273.15)**4
      Y=247.8/(T-140)
      AM=.00002414*10**Y
      S=-.0003*(T-273.15)**2-.138*(T-273.15)+75.6
      S=S/1000.
      CP=4391.21-.7*T
      RETURN
      END
C
C-------------------------------- R113
      SUBROUTINE REFRE(T,TS)
      COMMON/PROP/R,H,AK,AM,S,CP
      REAL J
C
      V=(.617+.000647*(T-273.15)**1.1)*1.E-3
      R=1/V
      H=(1.611-.0031*(TS-273.15))*1.E+5
      AK=.0802-.000203*(T-273.15)
      J=503/(T-2.15)
      AM=1.34E-5*10**J
      IF((T-273.15).GE.20.) S=-1.1E-4*(T-273.15)+0.0217
      IF((T-273.15).LT.20.) S=-1.3E-4*(T-273.15)+0.0221
      CP=929+1.03*(T-273.15)
      RETURN
      END
C
C---------------------------------- ETYLENE GLYCOL
      SUBROUTINE ETHYL(T,TS)
      COMMON/PROP/R,H,AK,AM,S,CP
C
```

```
      TB=T-338.15
      V=9.24848E-4+6.2796E-7*TB+9.2444E-10*TB*TB+3.057E-12*TB**3
      R=1./V
      H=1.35234E+6-6.38263E+2*TS-.747462*TS*TS
      AK=418.68E-6*(519.442+.32092*T)
      AM=EXP(-11.0179+1.744E+3/T-2.80335E+5/T**2+1.12661E+8/T**3)
      S=5.021E-2-8.9E-5*(T-273.15)
      CP=4186.8*(1.6884E-2+3.35083E-3*T-7.224E-6*T**2
     1          +7.61748E-9*T**3)
      RETURN
      END
C
C----------------------------------- METHANOL
      SUBROUTINE METAL(T,TS)
      COMMON/PROP/R,H,AK,AM,S,CP
      R=-1.E-5*T**3+8.49E-3*T**2-3.29*T+1278.8
      H=1.107E-2*TS**3-21.61*TS**2+8.666E+3*TS+2.3E+5
      AK=(687.314-0.689519*T)*1.E-4
      AK=AK*4.187
      Y=-8.857+3.835E+3/T-9.593E+5/T**2+9.344E+7/T**3
      AM=10**Y
      S=-1.2E-9*T**3+1.163E-6*T**2-0.4606E-3*T+87.97E-3
      CP=(0.582485-3.75646E-4*T-1.67844E-6*T**2+1.06214E-8*T**3)*1E+3
      CP=CP*4.187
      RETURN
      END
C
C----------------------------- R11
      SUBROUTINE R11(T,TS)
      COMMON/PROP/R,H,AK,AM,S,CP
      R=-1.3021E-5*T**3+8.789E-3*T**2-4.142*T+2275.
      H=-8.594E-7*TS**3+6.445E-4*TS**2-.244*TS+81.17
      H=H*4.187E+3
      AK=-2.89E-4*(T-273.15)+.095
      Y=-6.169+1.593E+3/T-3.208E+5/T**2+2.781E+7/T**3
      AM=10**Y
      S=8.889E-8*T**2-0.1812E-3*T+0.06392
      CP=1.071E-3*T**2+1.829E-1*T+735.
      RETURN
      END
C
C----------------------------- R22
      SUBROUTINE R22(T,TS)
      COMMON/PROP/R,H,AK,AM,S,CP
      R=-7.639E-5*T**3+0.05367*T**2-15.588*T+3092.
      H=-5.625E-6*TS**3+3.844E-3*TS**2-1.032*TS+158.6
      H=H*4.187E+3
      AK=-5.75E-4*(T-273.15)+0.101
      Y=-10.5403+4.527E+3/T-1.0264E+6/T**2+8.277E+7/T**3
      AM=10**Y
      S=2.E-7*T**2-2.632E-4*T+0.0686
      CP=1.944E-2*T**2-7.864*T+1868.
      RETURN
      END
```

APPENDIX E Computer program for curve fitting

Appendix E Computer program for curve fitting

1. Linear equation

Consider the linear equation:

$$Y=K_1X_1+K_2X_2+\cdots+K_nX_n \tag{E-1}$$

If this equation is fitted to m sets of data, then, for the i'th set of data:

$$Y_i=K_1X_{i,1}+K_2X_{i,2}+\cdots+K_nX_{i,n}+\delta Y_i \tag{E-2}$$

where

Y_i and $X_{i,1}..X_{i,n}$	are measured values
K_1 to K_n	are n parameters to be calculated using the method of least squares and Gaussian elimination
δY_i	is the observational error in $\delta Y_i=Y_{i,obs}-Y_{i,cal}$

"Least squares" analysis produces the following set of n linear equations:

$$\begin{aligned}
a_{11}K_1+a_{12}K_2+\ldots+a_{1n}K_n&=b_1\\
a_{21}K_1+a_{22}K_2+\ldots+a_{2n}K_n&=b_2\\
&\vdots\\
a_{n1}K_1+a_{n2}K_2+\ldots+a_{nn}K_n&=b_n
\end{aligned} \tag{E-3}$$

where

$$a_{r,c}=\sum_{i=1}^{m}X_{i,r}X_{i,c} \qquad r=1 \text{ to } n \quad c=1 \text{ to } n$$

and

$$b_r=\sum_{i=1}^{m}X_{i,r}Y_i$$

To begin with, the function LESQ computes the value of all $a_{r,c}$, and b_r and then proceed to calculation the value of K_1 to K_n, from the resulting sets of n equations. During the calculation of the $a_{r,c}$, and b_r values, LESQ calls on a subroutine L(N,I,K), for eachset of data. This subroutine supplies the values of $X_{i,1}$ to $X_{i,n}$ and Y_i, when it is called for the i'th set of data. $X_{i,1}$ to $X_{i.n}$ are put into the variables K(1) to K(N-1) and Y_i is put into K(N), where N=n+1. When LESQ has finished its work, the parametars K_1 to K_n are held in variables K(1) to K(N-1) and the variables K(N) and LESQ each hold the quantity $\sum_i^m \delta Y_i^2$, which is the usual calcuation for "goodess of fit".

2 Non-linear equations

A nonlinear equation may be solved by a modified version of the previous method, if the equation can be expressed in the form:

$$\begin{aligned} Y = & K_1 f_1(X_1, X_2 \cdots X_n; v_1, v_2 \cdots v_s) \\ & + K_2 f_2(\quad \text{"} \quad) \\ & \vdots \\ & + K_n f_n(\quad \text{"} \quad) \end{aligned} \qquad \text{(E-4)}$$

where

X_1 to X_r are kown quantities determined from the data for each data set.

v_1 to v_s are unkown non-linear parameters

K_1 to K_n are unkown linear parameters.

When kown values for v_1 to v_s are introduced into the above equation, the functions f_1 to fn may be calculated, thus reducing the equation to a linear form. The routine LESQ may then be used to find the parameters K_1 to K_n, for the given set of values v_1 to v_s.

An iterative technique is required to determine the values of v_1 to v_s which minimize $\Sigma\delta Y_i^2$.

LEMINI is a routine which minimizes a function of one variable, with respect to that variable. More precisely, LEMINI varies the values of a variable VAR, between specified lower and upper limit LOW and UPP, until the given function, FUN(VAR), attains a mimimum value, the variable VAR being determined within the specified tolerance, TOL. A boolean variable, CUP, is set to TRUE or FALSE according to whether or not the minimization has been successful, i.e whether or not a minimum has been found in the specified range.

3 <u>Outline of method</u>

Consider the known values have been substituted in eq.(E-4) for the non-linear parameters $(v_1, v_2 \ldots v_s)$, An initial call on LEMINI will vary v_1 until a minimum has been found for the specified function, which is the function LESQ. Let this minimumvalues of LESQ or $\Sigma\delta Y_i^2$ be named lemi1. This initial call on LEMIN1, being involved with calls on LESQ, thereby also finds values for the linear parameters K_1 to K_n.

A second call on LEMINI will vary the second non-linear parameter V_2, in order to minimize the second specified function, which is lemi1. Let the minimum values of lemi1 be called lemi2. Every time that parameter 2 is given a new value, between the specified lower and upper limits, the initial call on LEMINI is invoked to find a new value for lemi1 and also for V_1 and K_1 to K_n.

Futher calls on LEMINI are necessary to optimize any other non-linear parameters, until at the end of this process of LEMINI calls within LEMINI calls, final optimum values will have been determined for all the parameters, linear and non-linear. At this stage, the quantity $\Sigma\delta Y_i^2$ will have its over all minimum values.

4 Note about Recursion

Recursion is not allowed in FORTRAN programs and so the non-linear problem e requires several copies to be made of LEMINI, one copy for each non-linear variable. Each copy must have a distinct name, which should be used throughout the body of the function. For example, names given to copies of LEMINI could be: LEMINI, LEMIN2, LEMIN3 etc.

-Meaning of variable names-

STDV standerd diviation= $(\sum_i \delta Y_i^2 /(m-n-s))^{\frac{1}{2}}$

n= number of linear parameters

s= number of non-linear parameters

(a) Variables in LESQ

K An array which eventually holds the values of the linear parameters K_1 to K_n, in K(1) to K(N-1). While in the process of solving for K_1 to K_n, the variables K(1) to K(N) are used to hold values of X_1 to X_n and Y, for each set of tata, in turn.

L The subroutine which calculates the values of X_1 to X_n and Y, for each set of data in turn. The values are put into K(1) to K(N) and returned to LESQ.

M Total number of sets of data or experimental points.

N Number of linear parameters plus 1; N=n+1

C Array for manipulating data, used inside LESQ.

IC Size of array C, equal to (N*N+N)/2

ESPLIN A numerical precosion as a result of FORTRAN compilation. It is the number which, if any smaller would not be destinguished from zero, by the computer, when added to 1.

(b) Variables in LEMINI

LOW(I)	Specified lower limit to the value of non-linear variable number I.
TOL(I)	Specified tolerance, or prcision, within which VAR(I) is determined.
UPP(I)	Specified upper limit to the value of parameter number I.
FUN	The function of non-linear parameter number I, which is to be optimized by LEMINI.
VAR(I)	The values of non-linear variable number I, which is to be optimuzed by LEMINI in order to mininize FUN.
CUP(I)	A logical (boolean) variable for parameter number I, the value of which is set ti TRUE or FALSE according to whether or not FUN has been successfully minimized.
MNREAL	The smallest positive number that a REAL variable can hold.
ESPLIN	see above.

```
      PROGRAM NONLN2
      IMPLICIT DOUBLE PRECISION (A-H,O-Z)
      DOUBLE PRECISION LOW(4),K(11),MNREAL,LEMINI
      LOGICAL CUP(4)
      EXTERNAL FUNC
      COMMON MNREAL,EPSILN,X(350,6),Y(350,2)
      COMMON/BLESQ/K,M,N,IC
      COMMON/BLEMI/NN,LOW,TOL(4),UPP(4),VAR(4),CUP
C
C    MNREAL is smallest positive number that can be held and EPSLIN is
C    largest number such that (1+EPSLIN)-1=0 (1+EPSLIN cannot be
C    distinguished from 1 by the computer).
C
      MNREAL=5.3976D-79
      EPSILN=2.2204D-16
C
C     READ OBSERVATIONAL DATA PRESENTED IN FREE-FORMAT MODE
C
      READ(4,*) M,(Y(I,1),X(I,1),X(I,2),X(I,3),X(I,4),X(I,5),X(I,6),
     1           Y(I,2),I=1,M)
C
C    NL is numbe of equation linear parameters; NN is number of non-linear
C    parameters.  Maximum values are 10 and 4 respectively.
C
      NL=4
      NN=2
C
C   IC is number of element of main array in 'linear least squareas' function

C   LESQ.
C
      N=NL+1
      IC=(N*N+N)/2
10    DO 20 I=1,NN
      WRITE(6,500) I
      READ (5,*) LOW(I),UPP(I)
      TOL(I)=0.1D0*(UPP(I)-LOW(I))
20    CONTINUE
500   FORMAT(/' Give LOW and UPP for non-linear parameter number ',I1)
      DX=M-NL-NN
      STDV=DSQRT(LEMINI(LOW(2),TOL(2),UPP(2),FUNC,VAR(2),CUP(2),MNREAL,
     1EPSILN)/DX)
C
C     PRINT RESULTS AT TERMINAL
C
      CALL SUMM1(6,STDV)
C
C     PRINT EQUATION AND DATA VALUES COMPARISON TABLE, IF REQUIRED
C
      WRITE(6,510)
510   FORMAT(1H /'Do you want a results table?  0=No, 1=Yes')
      READ(5,*) IYN
      IF (IYN.NE.1) GOTO 40
      WRITE(6,520)
520   FORMAT(1H /'Where should table be printed?  6=VDU, 7=Lineprinter')
      READ(5,*) NW
      CALL SUMM2(NW,STDV)
40    WRITE(6,530)
530   FORMAT(1H /'Type: 0=Stop, 1=Change values of LOW and UPP')
```

```
      READ(5,*) IGO
      IF (IGO.EQ.1) GOTO 10
      STOP
      END
C-----
      SUBROUTINE SUMM1(NW,S)
C
C     PRINT EQUATION SUMMARY AT TERMINAL NUMBER NW
C
      IMPLICIT DOUBLE PRECISION (A-H,O-Z)
      DOUBLE PRECISION LOW(4),K(11)
      LOGICAL CUP(4)
      COMMON/BLESQ/K,M,N,IC
      COMMON/BLEMI/NN,LOW,TOL(4),UPP(4),VAR(4),CUP
C
      WRITE(NW,100) S
100   FORMAT(1H /'Standard Deviation = ',D13.6)
      IF (NN.EQ.0) GOTO 10
      WRITE(NW,110)
110   FORMAT(1H /'  I        LOW(I)           TOL(I)           UPP(I)     ',
     1'      VAR(I)       CUP(I)',/)
      WRITE(NW,120) (I,LOW(I),TOL(I),UPP(I),VAR(I),CUP(I),I=1,NN)
120   FORMAT(1H ,(I3,2X,4(D13.6,2X),1X,L2))
10    NL=N-1
      WRITE(NW,130) (I,K(I),I=1,NL)
130   FORMAT(1H /'K(',I1,') = ',D13.6)
      RETURN
      END
C-----
      SUBROUTINE SUMM2(NW,S)
C
C     PRINT COMPARISON-TABLE OF EQUATION AND DATA VALUES AT TERMINAL NUMBER
      NW
C
      IMPLICIT DOUBLE PRECISION (A-H,O-Z)
      DOUBLE PRECISION K(11),LOW(4),MNREAL
      LOGICAL CUP(4)
      COMMON MNREAL,EPSILN,X(350,6),Y(350,2)
      COMMON/BLESQ/K,M,N,IC
      COMMON/BLEMI/NN,LOW,TOL(4),UPP(4),VAR(4),CUP
C
      IF (NW.EQ.7) CALL SUMM1(7,S)
      WRITE(NW,100)
100   FORMAT(1H /'Obs. no.   Yobs             Ycal              Ydif',
     1'          %Ydif',/)
      DO 10 I=1,M
      YCAL=K(1)*X(I,1)+K(2)*X(I,2)*X(I,6)**VAR(1)+K(3)*X(I,3)**VAR(1)
     1     *X(I,4)+
     2     K(4)*X(I,5)**VAR(2)*Y(I,2)
      YDIF=YCAL-Y(I,1)
      PYDIF=100.D0*(1.D0-Y(I,1)/YCAL)
10    WRITE(NW,110) I,Y(I,1),YCAL,YDIF,PYDIIF
110   FORMAT(1H ,I4,3(2X,D13.6),2X,F7.2)
      RETURN
      END
C-----
      SUBROUTINE L(N,I,K)
C
C  This routine calculates the variable part of each linear term and also
```

```
C   the variable Y-term of the equation.  These values are put in K(1) to
C   K(n). The routine is called by the function LESQ, for each observation
C   1 to M.
C
      IMPLICIT DOUBLE PRECISION (A-H,O-Z)
      DOUBLE PRECISION K(N),LOW(4),MNREAL
      LOGICAL CUP(4)
      COMMON MNREAL,EPSILN,X(350,6),Y(350,2)
      COMMON/BLEMI/NN,LOW,TOL(4),UPP(4),VAR(4),CUP
C
      K(1)=X(I,1)
      K(2)=X(I,2)*X(I,6)**VAR(1)
      K(3)=X(I,3)**VAR(1)*X(I,4)
      K(4)=Y(I,2)*X(I,5)**VAR(2)
      K(N)=Y(I,1)
      RETURN
      END
C-----
      FUNCTION FUNA(V)
C
C     THE VALUE OF FUN(V) IS MINIMISED BY LEMINI WITH RESPECT TO VARIABLE
C     VAR
C
      IMPLICIT DOUBLE PRECISION (A-H,O-Z)
      DOUBLE PRECISION K(11),LOW(4),LESQ,MNREAL
C
C     SIZE OF ARRAY C IS (NMAX*NMAX+NMAX)/2 :  (NMAX=11 HERE)
C
      DIMENSION C(66)
      LOGICAL CUP(4)
      EXTERNAL L
      COMMON MNREAL,EPSILN,X(350,6),Y(350,2)
      COMMON/BLESQ/K,M,N,IC
      COMMON/BLEMI/NN,LOW,TOL(4),UPP(4),VAR(4),CUP
C
      VAR(1)=V
      FUNA=LESQ(K,L,M,N,C,IC,EPSILN)
      RETURN
      END
C-----
      FUNCTION FUNC(V)
      IMPLICIT DOUBLE PRECISION (A-H,O-Z)
      DOUBLE PRECISION K(11),LOW(4),JEMINI,MNREAL
      LOGICAL CUP(4)
      EXTERNAL FUNA
      COMMON MNREAL,EPSILN,X(350,6),Y(350,2)
      COMMON/BLEMI/NN,LOW,TOL(4),UPP(4),VAR(4),CUP
C
      VAR(2)=V
      FUNC=JEMINI(LOW(1),TOL(1),UPP(1),FUNA,VAR(1),CUP(1),MNREAL,
     1EPSILN)
      RETURN
      END
C-----
      FUNCTION LESQ(K,L,M,N,C,IC,EPS)
C     SOLVES A SYSTEM OF M LINEAR EQUATIONS IN N-1 UNKNOWNS (M'GE'N-1)
C     OF THE FORM : F(N) = V(1)*F(1) + ...... + V(N-1)*F(N-1)  .
C     A CALL OF SUBROUTINE L(N,G,K) MUST PUT THE COEFFICIENTS OF THE G-TH
```

```
C     EQUATION INTO K(1) TO K(N) . EVENTUALLY : THE SOLUTION IS PUT IN
C     K(1) TO K(N-1) . THE SUM OF THE SQUARES OF RESIDUALS IS PUT IN K(N)
C     AND LESQ IS SET TO K(N).
C     THE REAL ARRAY C HAS ITS UPPER BOUND EQUAL TO IC = (N*(N+1))/2 .
C     SINCE THIS IS VARIABLE THE ACTUAL ARRAY FOR C MUST BE DECLARED IN
C     THE MAIN PROGRAM SEGMENT WITH UPPER BOUND EQUAL TO THE MAXIMUM
C     VALUE OF IC THAT MIGHT OCCUR.THE ACTUAL PARAMETER FOR IC MUST HAVE
C     ITS VALUE ASSIGNED IN THE MAIN SEGMENT EACH TIME THAT N IS
C     ALTERED.
C     SO THAT ARRAYS OF VALUES (1:M), READ-IN TO THE MAIN
C     PROGRAM SEGMENT CAN BE INTRODUCED TO THE SUBROUTINE L, IN ORDER
C     TO CALCULATE THE COEFFICIENTS (1:N) FOR EACH OF THE M EQUATIONS,
C     THE LATTER SUBROUTINE MUST INCLUDE A DECLARATION OF A COMMON BLOCK
C     ( ALSO DECLARED IN THE MAIN SEGMENT), THAT INCORPORATES A LIST OF
C     SUCH ARRAYS.
C
      IMPLICIT DOUBLE PRECISION (A-H,O-Z)
      DOUBLE PRECISION K(N),LESQ
      DIMENSION C(IC)
      INTEGER D,E,F,G,H,S,T
      LOGICAL O
      EXTERNAL L
C
      NN=0
    5 O=M.LE.N-1
      IF (O) N=M+1
      D = N
      F = 1
      IZ = (D*D+D)/2
      DO 10 I = 1,IZ
   10 C(I) = 0.0D0
      DO 20 G = 1,M
      CALL L(N,G,K)
      H = 0
      DO 20 I = 1,D
      DO 20 J = I,D
      H = H+1
   20 C(H) = C(H) + K(I)*K(J)
      P=C(H)
      Q=P*EPS/D
      DO 50 I = 1,N-1
      A=C(F)
      IF ( A.GT.Q .OR. N.LT.3 ) GOTO 25
      N=N-1
      NN=NN+1
      GOTO 5
   25 A=1.0D0/A
      C(F)=A
      E = F + D - I
      F = F + 1
      H = E + 1
      DO 40 S = F,E
      B = A*C(S)
      J = S - H
      G = E - J
      DO 30 T = H,G
   30 C(T) = C(T) - B*C(T+J)
   40 H = G + 1
```

```
   50 F = E + 1
      K(D) = C(F)
      B = K(D)
      IF ( O .OR. B.LT.0.0D0 ) B = 0.0D0
      IF ( P.LT.0.0D0 ) P = 0.0D0
      IF ( B.GT.0.0D0 .AND. P.GT.B ) GOTO 55
      K(D)=0.0D0
      GOTO 58
   55 B=B/P
      P=1.0D0+B
      IF ( .NOT.P.GT.1.0D0 ) K(D)=0.0D0
   58 DO 70 S = 1,N-1
      I = N - S
      H = F - 1
      E = H - D
      F = I + E
      IP1 = I + 1
      IF ( IP1.GT.N-1 ) GOTO 70
      DO 60 J = IP1,N - 1
   60 C(H) = C(H) - K(J)*C(J+E)
   70 K(I) = C(H)*C(F)
      IF ( O ) GOTO 80
      LESQ = K(D)
      GOTO 90
   80 LESQ = 0.0D0
   90 IF ( NN.EQ.0 ) RETURN
      DO 100 I=1,NN
      K(N+1)=K(N)
      K(N)=0.0D0
100   N=N+1
      RETURN
      END
C----
      FUNCTION LEMINI(LOW,TOL,UPP,FUN,VAR,CUP,MNREAL,EPSILN)
C
C   LEMINI MINIMIZES THE FUNCTION FUN(VAR) WITH RESPECT TO VAR. THE SPEC-
C   IFIED LOWER AND UPPER LIMITS ON VAR ARE LOW AND UPP RESPECTIVELY AND
C   TOL IS THE SPECIFIED TOLERANCE ON VAR WITHIN WHICH VAR IS CALCULATED.
C   FINALLY, VAR IS SET EQUAL TO ITS OPTIMUM VALUE AND LEMINI IS SET
C   EQUAL TO THE MINIMUM VALUE OF FUN(VAR). CUP IS A LOGICAL VARIABLE
C   THAT INDICATES WHETHER OR NOT THE MINIMIZATION HAS BEEN SUCCESSFUL
C   WITHIN THE LIMITS OF LOW AND UPP, SET ON VAR. CUP=TRUE AND CUP=FALSE
C   RESPECTIVELY INDICATE A SUCCESSFUL AND AN UNSUCCESSFUL ATTEMPT AT
C   MINIMIZATION.
C
      IMPLICIT DOUBLE PRECISION (A-H,O-Z)
      DOUBLE PRECISION J,K,L,M,N,LOW,LEMINI,MNREAL
      INTEGER G
      LOGICAL A,B,C,D,E,F,CUP
      EXTERNAL FUN
C
      IF (UPP.NE.LOW) GOTO 5
      VAR=UPP
      CUP=.TRUE.
      LEMINI=FUN(VAR)
      RETURN
5     M=16.0D0*MNREAL
      N= 8.0D0*EPSILN
```

```
      O=DABS(TOL)
      G=-1
      D=.TRUE.
      C=D
      VAR=-DMAX1(-LOW,-UPP)
      X=VAR
      U=FUN(VAR)
      B=.FALSE.
      CUP=B
      VAR=DMAX1(LOW,UPP)
      Z=VAR
      W=FUN(VAR)
      S=Z-X
      L=8.0D0*S
C TWO
   10 T=S/2.0D0
      R=S-T
      VAR=X+T
      Y=VAR
      V=FUN(VAR)
      IF (CUP) GOTO 30
      CUP=U.GT.V.AND.V.LT.W
      IF (CUP) GOTO 30
      X2=M+N*(DABS(X)+DABS(Z))
      IF (S.LE.DMAX1(O,X2)) GOTO 130
      IF (U.LT.W) GOTO 20
C YZ
      X=Y
      U=V
      S=R
      GOTO 10
C XY
   20 Z=Y
      W=V
      S=T
      GOTO 10
C TEST
   30 J=M+N*DABS(Y)
      K=M+N*DABS(V)
      P=W-V
      X2=J+N*DABS(Z)
      F=R.LT.DMAX1(O,X2).OR.P.LT.K+N*DABS(W)
      Q=U-V
      X2=J+N*DABS(X)
      A=T.LT.DMAX1(O,X2).OR.Q.LT.K+N*DABS(U)
      IF (A.AND.F) GOTO 130
      E=G.EQ.1
      IF (.NOT.(A.AND.F.OR..NOT.A.AND..NOT.F)) GOTO 160
      IF (R.EQ.T) GOTO 140
      A=R.GT.T
      GOTO 160
  140 IF (.NOT.((U.NE.W).OR.E)) GOTO 150
      A=W.GT.U
      GOTO 160
  150 A=G.EQ.0
  160 IF (C) GOTO 50
C SAFE
   40 IF (.NOT.A) GOTO 170
```

```
      Q=R
      GOTO 180
  170 Q=-T
  180 Q=Y+Q/2.0D0
      GOTO 70
C CONIC
   50 P=P/R
      Q=Q/T
      K=P-Q+(U-W)/S
      P=(P+Q)/S
      Q=K/(P+P)
      K=P
      P=V-Q*K*Q
      Q=Y-Q
      IF (E.AND.Y.NE.Q) GOTO 60
      K=(1.0D0-N)*DABS(K)
      J=M+2.0D0*N*DABS(P)
      IF (J.GE.K) GOTO 190
      GOTO 200
  190 IF (K*8.0D0/J.NE.0.0D0) GOTO 200
      K=N/M
      GOTO 210
  200 K=J/K
  210 X2=(M+N*DABS(Q)*2.0D0)/(1.0D0-N)
      K=(1.0D0-128.0D0*N)*DMAX1(DMAX1(0,X2),DSQRT(K))
      DG=G
      IF (.NOT.E) Q=Q+(1.0D0+2.0D0*DG)*K
      IF (Q.NE.Y) GOTO 60
      IF (.NOT.A) GOTO 220
      X2=R/2.0D0
      XQ=-DMAX1(-K,-X2)
      GOTO 230
  220 X2=T/2.0D0
      XQ=DMAX1(-K,-X2)
  230 Q=Q+XQ
C CHECK
   60 IF (Q.GE.Z.OR.Q.LE.X) GOTO 40
C SET
   70 IF (E) G=-1
      IF (.NOT.E) G=G+1
      D=.NOT.D
      IF (.NOT.(E.AND..NOT.D)) GOTO 80
      C=64.0D0*S.LT.L.OR..NOT.C
      L=S
C CALL
   80 VAR=Q
      P=FUN(VAR)
      A=Q.GT.Y
      B=P.GT.V
      IF (.NOT.B) GOTO 250
      IF (A) GOTO 120
      GOTO 110
  250 F=P.LT.V
      IF (A) GOTO 90
C XQY
      Z=Y
      W=V
      S=T
```

```
      R=Y-Q
      T=S-R
      IF (F) GOTO 100
      X=Q
      U=P
      S=R
      GOTO 10
C YQZ
   90 X=Y
      U=V
      S=R
      T=Q-Y
      R=S-T
      IF (F) GOTO 100
      Z=Q
      W=P
      S=T
      GOTO 10
C QQ
  100 Y=Q
      V=P
      GOTO 30
C QYZ
  110 X=Q
      U=P
      T=Y-X
      S=R+T
      GOTO 30
C XYQ
  120 Z=Q
      W=P
      R=Z-Y
      S=R+T
      GOTO 30
C EXIT
  130 VAR=Y
      IF (B) LEMINI=FUN(VAR)
      IF(.NOT.B) LEMINI=V
      RETURN
      END
C LEMINI OF 1967.05.04, AMENDED 1973.11.05, TRANSLATED INTO
C ALGOL 68-R 1977.10.10, TRANSLATED INTO FORTRAN IV 1979.10.11.
C----
      FUNCTION JEMINI(LOW,TOL,UPP,FUN,VAR,CUP,MNREAL,EPSILN)
C
C   JEMINI MINIMIZES THE FUNCTION FUN(VAR) WITH RESPECT TO VAR. THE SPEC-
C   IFIED LOWER AND UPPER LIMITS ON VAR ARE LOW AND UPP RESPECTIVELY AND
C   TOL IS THE SPECIFIED TOLERANCE ON VAR WITHIN WHICH VAR IS CALCULATED.
C   FINALLY, VAR IS SET EQUAL TO ITS OPTIMUM VALUE AND JEMINI IS SET
C   EQUAL TO THE MINIMUM VALUE OF FUN(VAR). CUP IS A LOGICAL VARIABLE
C   THAT INDICATES WHETHER OR NOT THE MINIMIZATION HAS BEEN SUCCESSFUL
C   WITHIN THE LIMITS OF LOW AND UPP, SET ON VAR. CUP=TRUE AND CUP=FALSE
C   RESPECTIVELY INDICATE A SUCCESSFUL AND AN UNSUCCESSFUL ATTEMPT AT
C   MINIMIZATION.
C
      IMPLICIT DOUBLE PRECISION (A-H,O-Z)
      DOUBLE PRECISION J,K,L,M,N,LOW,JEMINI,MNREAL
      INTEGER G
```

```
      LOGICAL A,B,C,D,E,F,CUP
      EXTERNAL FUN
C
      IF (UPP.NE.LOW) GOTO 5
      VAR=UPP
      CUP=.TRUE.
      JEMINI=FUN(VAR)
      RETURN
5     M=16.0D0*MNREAL
      N= 8.0D0*EPSILN
      O=DABS(TOL)
      G=-1
      D=.TRUE.
      C=D
      VAR=-DMAX1(-LOW,-UPP)
      X=VAR
      U=FUN(VAR)
      B=.FALSE.
      CUP=B
      VAR=DMAX1(LOW,UPP)
      Z=VAR
      W=FUN(VAR)
      S=Z-X
      L=8.0D0*S
C TWO
   10 T=S/2.0D0
      R=S-T
      VAR=X+T
      Y=VAR
      V=FUN(VAR)
      IF (CUP) GOTO 30
      CUP=U.GT.V.AND.V.LT.W
      IF (CUP) GOTO 30
      X2=M+N*(DABS(X)+DABS(Z))
      IF (S.LE.DMAX1(O,X2)) GOTO 130
      IF (U.LT.W) GOTO 20
C YZ
      X=Y
      U=V
      S=R
      GOTO 10
C XY
   20 Z=Y
      W=V
      S=T
      GOTO 10
C TEST
   30 J=M+N*DABS(Y)
      K=M+N*DABS(V)
      P=W-V
      X2=J+N*DABS(Z)
      F=R.LT.DMAX1(O,X2).OR.P.LT.K+N*DABS(W)
      Q=U-V
      X2=J+N*DABS(X)
      A=T.LT.DMAX1(O,X2).OR.Q.LT.K+N*DABS(U)
      IF (A.AND.F) GOTO 130
      E=G.EQ.1
      IF (.NOT.(A.AND.F.OR..NOT.A.AND..NOT.F)) GOTO 160
```

```
      IF (R.EQ.T) GOTO 140
      A=R.GT.T
      GOTO 160
  140 IF (.NOT.((U.NE.W).OR.E)) GOTO 150
      A=W.GT.U
      GOTO 160
  150 A=G.EQ.0
  160 IF (C) GOTO 50
C SAFE
   40 IF (.NOT.A) GOTO 170
      Q=R
      GOTO 180
  170 Q=-T
  180 Q=Y+Q/2.0D0
      GOTO 70
C CONIC
   50 P=P/R
      Q=Q/T
      K=P-Q+(U-W)/S
      P=(P+Q)/S
      Q=K/(P+P)
      K=P
      P=V-Q*K*Q
      Q=Y-Q
      IF (E.AND.Y.NE.Q) GOTO 60
      K=(1.0D0-N)*DABS(K)
      J=M+2.0D0*N*DABS(P)
      IF (J.GE.K) GOTO 190
      GOTO 200
  190 IF (K*8.0D0/J.NE.0.0D0) GOTO 200
      K=N/M
      GOTO 210
  200 K=J/K
  210 X2=(M+N*DABS(Q)*2.0D0)/(1.0D0-N)
      K=(1.0D0-128.0D0*N)*DMAX1(DMAX1(0,X2),DSQRT(K))
      DG=G
      IF (.NOT.E) Q=Q+(1.0D0+2.0D0*DG)*K
      IF (Q.NE.Y) GOTO 60
      IF (.NOT.A) GOTO 220
      X2=R/2.0D0
      XQ=-DMAX1(-K,-X2)
      GOTO 230
  220 X2=T/2.0D0
      XQ=DMAX1(-K,-X2)
  230 Q=Q+XQ
C CHECK
   60 IF (Q.GE.Z.OR.Q.LE.X) GOTO 40
C SET
   70 IF (E) G=-1
      IF (.NOT.E) G=G+1
      D=.NOT.D
      IF (.NOT.(E.AND..NOT.D)) GOTO 80
      C=64.0D0*S.LT.L.OR..NOT.C
      L=S
C CALL
   80 VAR=Q
      P=FUN(VAR)
      A=Q.GT.Y
```

```
      B=P.GT.V
      IF (.NOT.B) GOTO 250
      IF (A) GOTO 120
      GOTO 110
  250 F=P.LT.V
      IF (A) GOTO 90
C XQY
      Z=Y
      W=V
      S=T
      R=Y-Q
      T=S-R
      IF (F) GOTO 100
      X=Q
      U=P
      S=R
      GOTO 10
C YQZ
   90 X=Y
      U=V
      S=R
      T=Q-Y
      R=S-T
      IF (F) GOTO 100
      Z=Q
      W=P
      S=T
      GOTO 10
C QQ
  100 Y=Q
      V=P
      GOTO 30
C QYZ
  110 X=Q
      U=P
      T=Y-X
      S=R+T
      GOTO 30
C XYQ
  120 Z=Q
      W=P
      R=Z-Y
      S=R+T
      GOTO 30
C EXIT
  130 VAR=Y
      IF (B) JEMINI=FUN(VAR)
      IF(.NOT.B) JEMINI=V
      RETURN
      END
C JEMINI OF 1967.05.04, AMENDED 1973.11.05, TRANSLATED INTO
C ALGOL 68-R 1977.10.10, TRANSLATED INTO FORTRAN IV 1979.10.11.
```

APPENDIX F Tables and equations of fluid properties (R-113, ethylene glycol, water, methanol)

Table F-1 Thermophysical properties of water (reproduced from [54])

t °C	P Pa	ρ kg/m³	h_{fg}x10⁻⁶ J/kg	c_px10⁻³ J/kgK	μx10⁶ Ns/m²	kx10³ W/mK	σx10³ N/m
10	1227	999.78	2.4779	4.193	1308	582	74.22
20	2337	998.28	2.4543	4.182	1003	560	74.74
30	4242	995.71	2.4307	4.179	797	615	71.20
40	7375	992.25	2.4069	4.179	653	629	69.60
50	12335	988.03	2.3829	4.181	547	641	67.95
60	19920	983.15	2.3586	4.185	467	651	66.24
70	31162	977.66	2.3340	4.190	404	659	64.49
80	47360	971.64	2.3088	4.197	355	667	62.68
90	70109	965.11	2.2832	4.205	315	673	60.82
100	101325	958.12	2.2569	4.216	282	678	58.92
110	143270	950.69	2.2300	4.229	254	681	56.97
120	198540	942.84	2.2022	4.245	232	683	54.97
130	270130	934.56	2.1736	4.263	213	685	52.94
140	361380	925.87	2.1440	4.285	196	685	50.94
150	476000	916.78	2.1132	4.310	182	684	50.86

Correlations reproduced from [56]

$$t = T - 273.15$$

$$\upsilon = 0.01 \cdot (0.099917 + t(6.5\times10^{-6} + 3.83333\times10^{-7} t))$$

$$\rho = 1/\upsilon$$

$$k = -0.92247 + 2.8395(T/273.15) - 1.8007(T/273.15)^2 + 0.52577(T/273.15)^3 - 0.07344(T/273.15)^4$$

$$Y = 247.8/(T-140.0)$$

$$\mu = 0.00002414\times10^{Y}$$

$$\sigma = (-0.0003t^2 - 0.138t + 75.6)/1000.0$$

$$h_{fg} = 3468920. - T\times(5707.4 - T\times(11.5562 - 0.0133103T))$$

$$c_p = 4391.21 - 0.7T$$

Table F-2 Thermophysical properties of R-113 (reproduced from [54])

t	$Px10^{-5}$	ρ	$h_{fg}x10^{-3}$	$\mu x10^5$	k	σ
°C	Pa	kg/m^3	J/kg	Ns/m^2	W/mK	N/m
-50	0.01	1720	173.0	0.85	0.120	2.86
-30	0.03	1683	167.8	0.90	0.119	2.60
-20	0.05	1664	165.4	0.92	0.118	2.47
-10	0.09	1643	163.2	0.94	0.118	2.34
0	0.12	1621	160.6	0.97	0.117	2.21
10	0.19	1599	158.0	0.99	0.108	2.08
20	0.37	1576	155.2	1.02	0.098	1.96
30	0.55	1553	152.3	1.04	0.097	1.84
40	0.79	1529	149.2	1.07	0.095	1.73
50	1.11	1503	145.9	1.09	0.94	1.62
70	2.04	1452	139.4	1.13	0.091	1.40

Correlation reproduced from [56]

$t = T - 273.15$

$\upsilon = (0.617 + 0.000647t^{1.1})/1000$

$\rho = 1/\upsilon$

$k = 0.0802 - 0.000203\ t$

$Y = 503/(T - 2.15)$

$\mu = 1.34x10^{-5}10^{Y}$

$\sigma = -1.1x10^{-4}t + 0.0217$ $\quad t \geq 20$ °C $\quad$ (*)

$\quad -1.3x10^{-4}t + 0.0221$ $\quad t < 20$ °C

$h_{fg} = (1.611 - 0.0031t)x100$

$c_p = 929 + 1.03t$

(*) the equation for σ was correlated by the present author.

Table F-3 Thermophysical properties of ethylene glycol (reproduced from [56])

T	P	υx10^4	h_{fg}x10^{-6}	c_p	μx10^4	k	σ
K	Pa	m^3/kg	J/kg	J/kgK	Ns/m^2	W/mK	N/m
300	19.92	9.021	1.094	2418.5	158.15	0.258	0.048
310	42.55	9.078	1.083	2463.5	108.08	0.259	0.047
320	86.70	9.137	1.072	2508.0	76.93	0.260	0.046
330	169.19	9.198	1.060	2552.7	56.71	0.262	0.045
340	317.42	9.260	1.049	2597.8	43.09	0.263	0.044
350	574.51	9.324	1.037	2643.3	33.60	0.265	0.043
360	1006.09	9.390	1.026	2689.4	26.80	0.266	0.042
370	1709.32	9.459	1.014	2736.4	21.81	0.267	0.042
380	2824.20	9.530	1.002	2784.4	18.06	0.269	0.041
390	4547.63	9.603	0.990	2833.6	15.19	0.270	0.040
400	7150.40	9.679	0.977	2884.3	12.94	0.271	0.039
410	10997.34	9.759	0.965	2936.5	11.17	0.273	0.038
420	16570.75	9.841	0.952	2990.6	9.74	0.274	0.037
430	24497.13	9.927	0.940	3046.6	8.58	0.275	0.036
440	35577.15	10.016	0.927	3104.8	7.62	0.277	0.035
450	50818.84	10.109	0.914	3165.4	6.82	0.278	0.034
460	71473.58	10.206	0.901	3228.5	6.15	0.279	0.034
470	99074.82	10.307	0.857	3294.4	5.58	0.281	0.033
480	135479.00	10.413	0.874	3363.3	5.09	0.282	0.032

Correlations reproduced from[56]

$$T_b = T - 338.15$$

$$\upsilon = 9.24848\times10^{-4} + 6.2796\times10^{-7}T_b + 9.2444\times10^{-10}T_b^2 + 3.057\times10^{-12}T_b^3$$

$$\rho = 1/\upsilon$$

$$k = 418.68\times10^{-6}(519.442 + 0.3209\times T)$$

$$\mu = \exp(-11.0179 + 1.744\times10^3/T - 2.80335\times10^5/T^2 + 1.12661\times10^8/T^3)$$

$$\sigma = 5.021\times10^{-2} - 8.9\times10^{-5}(T - 273.15)$$

$$h_{fg} = 1.35234\times10^6 - 6.38263\times10^2T - 0.747462\,T^2$$

$$c_p = 4186.8(1.6884\times10^{-2} + 3.35083\times10^{-3}T - 7.224\times10^{-6}T^2 + 7.61748\times10^{-9}T^3)$$

Table F-4 Thermophysical prperties of methanol (reproduced from [58])

t	ρ	h_{fg}x10⁶	μx10³	σ
°C	kg/m³	J/kg	Ns/m²	N/m
0	810	1.210	0.817	24.5
10	800.8	1.2016	-	23.5
20	791.5	1.1911	0.578	22.6
30	782.5	1.1786	0.509	21.8
40	774.0	1.1639	0.446	20.9
50	765.0	1.1472	0.393	20.1
60	755.5	1.1304	0.347	19.3
70	746.0	1.1095	0.306	18.4
80	735.5	1.0844	0.271	17.5
90	725	1.0593	0.240	16.6
100	714	1.030	0.214	15.7
110	702	1.0006	0.19	14.7
120	690	0.9713	0.17	13.6
130	677	0.9399	0.152	12.6
140	644	0.9043	0.136	11.5
150	649.5	0.8667	0.121	10.4
160	634	0.829	0.109	9.3
170	616	0.7871	0.098	8.1
180	598.	0.7411	0.0883	6.9
190	577	0.6908	0.0794	5.7
200	553	0.6364	0.0716	4.5

(*) Equations for k and c_p are given in[59]

Coorelations obtained by least squares method

$$\rho = -1.0\text{x}10^{-5}T^3+8.49\text{x}10^{-3}T^2-3.29T+1278.8$$

$$\upsilon = 1/\rho$$

$$k = (687.314-0.680519T)\text{x}4.187\text{x}10^{-4} \quad (*)$$

$$Y=-8.857+3.835\text{x}10^3/T-9.593\text{x}10^5/T^2+9.344\text{x}10^7/T^3$$

$$\mu = 10^Y$$

$$\sigma = -1.2\text{x}10^{-9}T^3+1.163\text{x}10^{-6}T^2-0.4604\text{x}10^{-3}+87.97\text{x}10^{-3}$$

$$h_{fg}=1.107\text{x}10^{-2}T^3-21.61T^2+8.666\text{x}10^3T+2.3\text{x}10^5$$

$$c_p = (0.582485-3.75646\text{x}10^{-4}T-1.67844\text{x}10^{-6}T^2 + 1.06214\text{x}10^{-8}T^3)\text{x}4.187\text{x}10^3 \quad (*)$$

References

1. Brown,C.E. and Matin,S.A.
"Effect of finite metal conductivity on the condensation heat transfer to falling water rivulets on vertical heat-transfer surface", J of Heat Transfer ASME, vol 93, pp69-76, (1971)

2. Cary,J.D. and Mikic,B.B.
"The influence of thermocapillary force on heat transfer in film condensation", J of Heat Transfer ASME, vol 95, pp21-24, (1973)

3. Glicksman,L.R., Mikic,B.B. and Snow,D.F.
"Augmentation of film condensation on the outside of horizontal tube", AIchE J., vol 19 No 3, pp636-637, (1973)

4. Nicol,A.A. and Medwell,J.O.
"Surface roughness effects on condensing films", ASME paper 65-HT-43, (1965)

5. Webb,R.L.
"The use of enhancement surface geometries in condensers: An overview", Power Condenser Heat Transfer Technology computer modeling/ design/ fouling, edited by Marto,D.J. and Nunn,R.H., Heamisphere Publishing Corp., p294

6. Notaro,F

"Enhancement condensation heat transfer device and method", U.S. patent 4, 154, 294 (1979)

7. Gregorig,R
"Film condensation on surface with fine corrugations with condensation of surface tension", Math. Phys., vol 5, pp26-49, (1954)

8. Zener,C and Lavi,A
"Drainage system for condensation", J. of Engineering Power ASME, vol 96, pp209-215, (1974)

9. Webb,R.L.
"A generalized procedure for the design and optimization of fluted Gregorig condensing surface", J. of Heat Transfer ASME, vol 101, pp335-339, (1979)

10. Panchal,C.B. and Bell,K.J.
"Analysis of Nusselt-type condensation on a vertical fluted surface", Numerical Heat Transfer, vol 3, pp357-371, (1980)

11. Barner,C.G and Rohsenow,W.M.
"Vertical fluted tube condenser performance prediction", Int Heat Transfer conf, paper cs7, pp39-43, (1983)

12. Adamek,T.
"Bestimmung der kondensationgroBen auf feingenwallten

oberflachen zur auslegung optimaler wand profile", Warme und Stoffuubertragung, vol 15, pp225-270, (1981)

13. Honda,H. and Fujii,T.
"Semi-empirical equation for condensation heat transfer on vertical fluted tubes", submitted to J. of Heat Transfer ASME (1983)

14. Carnavos,T.C.
"Some recent development in augmentated haet exchange elements", Heat Exchangers: Design and Theory Sourcebook, edited by N. Afgan and E.U. Schlunder, Macgrow-Hill book, p443 (1974)

15. Cooper,J.R. and Rose,J.W.
"Condensation heat-transfer enhancement by vapour side surface geometry modification", HTFS RS402, pp647-672, (1981)

16. Combs,S.K.
"An experimental study of heat transfer enhancement for ammonia condensing on vertical fluted tubes", Report ORNL-5356, Oak Ridge National Laboratory, (1978)

17. Combs,S.K., Mailen,G.S. and Murphy,R.W.
"Condensation of refrigerants on vertical fluted tubes", Report ORNL/TM-5848, Oak Ridge National Laboratry, (1978)

18. Tomas,D.G.
"Enhancement of film condensation rate on vertical tubes by longitudinal fins", AIchE J., vol 14, No 4, pp644-649, (1968)

19. Rifert,V.G. and Leont'ev,G.G
"An analysis of heat transfer with steam condensing on avertical surface with wires to promote heat transfer", Terploenrgetika, vol 23 (4), pp58-61, (1976)

20. Tomas,A. et al.
"Performance tests of the 1 Mwt shell and tube exchangers for OTEC", proc. 6th OTEC conf, paper 3c, (1979)

21. Arai,N. et al.
"Heat transfer tube enhancing boiling and condensation in heat exchangers of a refrigerating machine", Trans. ASHRAE, vol 82 (2), pp58-70, (1977)

22. Webb,R.L. and Gee,B.L.
"Analytical prediction for a new concept spine-fin surface geometry", Trans. ASHRAE, vol 85 (2), pp274-283, (1979)

23. Webb,R.L., Keswani,S.T. and Rudy,T.M.
"Investigation of surface tension and gravity effect in film condensation", Int. Heat Transfer conf., paper cs28, pp175-180, (1983)

24. Nader,W.K.
"External surface heat transfer with condensation", Int. Heat Transfer conf., vol 2, pp407-412, (1978)

25. Patanker,S.V. and Sparrow,E.M.
"Condensation on an extended surface", J. of Heat Transfer ASME, vol 101, pp434-440, (1979)

26. Mori,Y., Hijikata,K., Hirasawa,S. and Nakayama,W.
"Effect of surface tension on laminar film condensation along a vertical plate with small leading radius", 6th Int. Heat Transfer conf., vol 2, pp413-418, (1978)

27. Mori,Y., Hijikata,K., Hiraswa,S. and Nakayama,W.
"Optimised performance of condensers with outside condensing surface", Condensing Heat Transfer, edited by D.J. Marto and D.G.Kroeger, pp56-62, (1979)

28. Mori,Y., Hijikata,K., Hirasawa,S. and Nakayama,W.
"Effect of surface tension on condensate motion in laminar film condensation (study of liquid film in a small trough)", J. Heat mass Transfer, vol 23, pp1471-1478, (1980)

29. Beatty,K.O. and Katz,D.L.
"Condensation of vapour on outside of finned tubes", Chem. Eng. Prog., vol 44 (1), pp55-70, (1948)

30. Katz,D.L., Geist,J.M. and Ann Arbop
"Condensation on six finned tubes in a vertical row", Trans. ASME, pp907-914, (1948)

31. Pearson,J.F. and Withers,J.G.
"New finned tube configuration improves refrigerant condensing", ASHRAE J., pp77-82, (1969)

32. Mills,A.F., Hubbard,G.L., Janes,R.K. and Tan,C.
"Experimental study of film condensation on horizontal grooved tube", Desalation, vol 16, No.2, pp121-133, (1975)

33. Carnavos,T.C.
"An Experimental study: Condensing R-11 on Augmente tubes", ASME paper 80-HT-54, 19th Nat. Heat Transfer conf., (1980)

34. Honda,H. and Nozu,S.
"Augmentation of condensation on horizontal finned tubes by attaching a porous drainage plate", ASME-JASME Tearmal Eng. conf., vol 3, (1983)

35. Yau,K.K
"Condensation Heat-Transfer enhancement by vapour-side geometry modification", Project Report Queen Mary College, (1982)

36. Yau,K,K, Cooper,J.P. and Rose,J,W
"Effect of fin spacing on the performance of horizontal

integral-fin condenser tube", submitted to J. of Heat Transfer ASME (1984)

37. Yau,K.K., Cooper,J.P. and Rose,J.W.
"Effect of drainage strips and fin spacing on heat transfer and condensate retention for horizontal finned and plain condenser tubes", J. of Heat Transfer ASME, pp151-156, (1985)

38. Wanniarachchi,A.S., Marto,P.J.and Rose,J.W.
"Filmwise condensatin of steam on experimentally-finned horizontal tubes", submitted to ASME (1984)

39. Wanniarchchi,A.S., Marto,P.J. and Rose,J.W.
"Film condensation of staem on horizontal integral-fin tubes with rectangulaly-shaped fins", Paper for Naval Poast Graduate School (private communication) (1984)

40. Georgiadis,I.V.
"Filmwise condensation on low integral-finned tubes", Thesis NPS-69-84-008, Naval Postgraduate School, (1984)

41. Rudy,T.M. and Webb,R.L.
"Condensation retention of horizontal integral fin tube", Advances in Rnhancement Heat Transfer ASME, HTD-18, pp35-41, (1981)

42. Sardesai,R.G., Owen,R.G. and Smith,R.A.

"Gravity controlled condensation on horizontal integral-fin tubes", Heat Transfer and Fluid Flow Service Research Symposium Series, HTFSRS 455, pp582-592, (1982)

43. Rudy,T.M., Kedzierski,M.A. and Webb,R.L.
"Investigation of integral-fin-type condenser tubes for process industry applications", IchemE symposium Series, No.86, pp633-647 (1984)

44. Karkhu,V.A. and V.P.Borovkov
"Film condenstion of vapour at finely-finned horizontal tubes", Heat-Transfer Soviet Research, vol 3, No.2, pp183-191, (1971)

45. Edwards,D.K., Gier,K.D., Ayyaswamy,P.S. and Catton,I.
"Evaporation and condensation circumferential groove on horizontal tubes", ASME paper 73-HT-25, (1973)

46. Borovkov,V.P.
"Refined method of calculating heat exchange in the condensation of staionary vapour on horizontal finned tubes", J. Eng. Phys., vol.39, No.4, pp1046-1051, (1980)

47. Rudy,T.M. and Webb,R.L
"Thermal model for condensation on horizontal, integral-fin tubes", Heat Transfer AIchE Symp. Ser., vol 79, No.225 (1983)

48. Flook,F.A.
"Film condensation of steam on externally finned horizontal tubes", Thesis Naval postgraduate School, Montarely Calif., (1985)

49. Honda,H. and Nozu,S.
"A prediction method for heat transfer during film condensation on horizontal low integral-fin tube", submitted to J. of Heat Transfer ASME, (1984)

50. Lee,W.C. and Rose,J.W.
"Forced convection film condensation of refrigerant-113 and ethanediol on a horizontal tube", Prc. 18th Nat. Heat Transfer Conf., (1983)

51. Lee,W.C.and Rose,J.W.
"Effect of vapour velocity on condensation on a horizontal tube", Harwell Report HTFS RS465 AREA R10561

52. Honda,H private communication

53. Nobbs,D.W.
"The effect of downward vapour velocity and inundation on the condensation rates on horizontal tubes and tube banks", PhD thesis, Univ. of Bristol, (1975)

54. Ueda,T
"Two phase flow - fluid dynamics anf heat transfer-",

published by Yokendo, p240, (1981)

55. Chivng,C.W.
"A study of liquid film on horizontal integral-fin tubes", Project paper, Queen Mary College, University of London, (1983)

56. Lee,W.C.
"Filmwise condensation on a horizontal tube in the presence of forced convection and non-condensing gas", Phd thesis, Department of Mechanical Engineering, Queen Mary College, University of London, (1982)

57. Michael,A.G.
"Forced convection condensation on a horizontal tube", Project paper, Queen Mary College, University of London, (1983)

58. Vargafitik,N.B.
"Tables on the thermophysical properties of liquid and gases", A HALSTED PRESS BOOK, J.Wiley and sons inc. (1975)

59. Toloukian,Y.S. et al.
"Thermophysical properties of matter-TPRC data series", LFI/PLENUM N.Y. (1970)